THE UNIVERSITY OF QUEENSLAND

AUSTRALIA

Antibody Discovery

for

Development of a Serotyping Dengue Virus NS1 Capture Assay

Kebaneilwe Lebani

Master of Biotechnology (Advanced)

A thesis submitted for the degree of Doctor of Philosophy at

The University of Queensland in 2014

Australian Institute for Bioengineering and Nanotechnology

A B S T R A C T

Dengue virus (DENV) infections are a significant public health burden in tropical and sub-tropical regions of the world. Infections are caused by four different but antigenically related viruses which result in four DENV serotypes. The multifaceted nature of DENV pathogenesis hinders the sensitivity of assays designed for the diagnosis of infection. Different markers can be optimally detected at different stages of infection. Of particular clinical importance is the identification of acute viremia during the febrile phase of infection which is pivotal for management of infection. Non-structural protein 1 (NS1) has been identified as a good early surrogate marker of infection with possible applications in epidemiological surveillance and the development of blood screening assays. This contribution is towards using serotype-specificity to achieve specific and more sensitive diagnostic detection of DENV NS1.

The general aim of this work is to isolate immune-reagents that can be used to develop an assay with improved sensitivity of DENV NS1 detection in a diagnostic setting. In this work, we sought to isolate serotype-specific antibodies that discern discreet antigenic differences in NS1 from each DENV serotype. Additionally, we also sought to isolate a pairing antibody that recognises NS1 from all four DENV serotypes (pan-reactive) for tandem capture of the DENV NS1. To achieve this, three naive, immunoglobulin gene libraries (a V_H domain, a scFv and a Fab library) were interrogated for binders to recombinant NS1 antigen from all four DENV serotypes using phage display technology and various biopanning approaches.

From biopanning experiments, four antibody fragments specific to NS1 from each DENV serotype as well as a panel of pan-reactive antibody fragments were isolated. The isolated antibody fragments were reformatted into fully assembled IgG1 antibodies for characterisation. In a sandwich ELISA, none of the pan-reactive antibodies were able to bind DENV NS1 in tandem with the serotype-specific antibodies. All four of the serotype-specific antibodies however, recognised

their serotype-respective recombinant and native DENV NS1. The serotype-specific immunoglobulins showed equilibrium dissociation constants that ranged from μM to nM. Used as capture reagents in a sandwich ELISA with a commercial pan-reactive antibody as the detection probe, three of the antibodies (9H2 anti DENV-1 NS1, 7G11 anti DENV-3 NS1 and 6A5 anti DENV-4 NS1) were able to achieve clinically relevant limits of DENV NS1 detection. 4C11, an antibody against DENV-2 NS1 had the poorest performance and was subjected to affinity maturation through targeted mutagenesis of V_H CDR3. A new variant A4, showed marginal 2-fold improvement in performance when incorporated into a limit of detection ELISA with the commercial pan-reactive antibody.

Our data suggests that the four serotype-specific antibodies, including the new variant, would be useful for inclusion in a sandwich ELISA that uses NS1 to serotype DENV infections. To develop a complete DENV NS1 serotyping assay however, the serotype-specific antibodies will need to be used in a new iteration of a biopanning campaign to isolate an appropriate pan-reactive pairing partner.

DECLARATION BY AUTHOR

This thesis is composed of my original work, and contains no material previously published or written by another person except where due reference has been made in the text. I have clearly stated the contribution by others to jointly-authored works that I have included in my thesis.

I have clearly stated the contribution of others to my thesis as a whole, including statistical assistance, survey design, data analysis, significant technical procedures, professional editorial advice, and any other original research work used or reported in my thesis. The content of my thesis is the result of work I have carried out since the commencement of my research higher degree candidature and does not include a substantial part of work that has been submitted to qualify for the award of any other degree or diploma in any university or other tertiary institution. I have clearly stated which parts of my thesis, if any, have been submitted to qualify for another award.

I acknowledge that an electronic copy of my thesis must be lodged with the University Library and, subject to the General Award Rules of The University of Queensland, immediately made available for research and study in accordance with the *Copyright Act 1968*.

I acknowledge that copyright of all material contained in my thesis resides with the copyright holder(s) of that material. Where appropriate I have obtained copyright permission from the copyright holder to reproduce material in this thesis.

PUBLICATIONS DURING CANDIDATURE

No publications

PUBLICATIONS INCLUDED IN THIS THESIS

No publications included

CONTRIBUTIONS BY OTHERS TO THE THESIS

Dr Daniel Watterson – technical assistance with Vero cell culture, virus infection and immunofluorescence.

STATEMENT OF PARTS OF THE THESIS SUBMITTED TO QUALIFY FOR THE AWARD OF ANOTHER DEGREE

None

ACKNOWLEDGEMENTS

My mum Nduka Jongman-Lebani, and my sisters; Tawana Lebani and Ame Lebani, I dedicate this thesis to you.

My friends, your support has been unwavering and invaluable. I could not have concluded this journey without you. There are too many of you to name individually but I genuinely thank you all for taking the ride of high highs and low lows with me.

Sumukh Kumble, thank you so much for the most awesome illustrations!

My sponsor, the Botswana International University of Science and Technology (BIUST) I am thankful for the opportunity to have embarked on this journey as your development fellow.

My enrolling institution, the Australian Institute for Bioengineering and Nanotechnology I am thankful for your funding and the opportunity to undertake my research in a world class institute.

The Schlumberger Foundation, I am grateful for the assistance with conference travel costs through the Fellowship for the Future Award.

My supervisors Steve and Martina, I am truly thankful for your guidance and patience. It has been a most humbling experience that has forced me to confront my weaknesses. I am still a work in progress. If I had to go through this journey again, I would still pick both of you. Whether you would pick me is a completely different story! I am heavily indebted to you both for having reached this juncture.

KEYWORDS

Antibodies, Phage Display, Dengue Virus, NS1, Diagnosis, Serotyping

AUSTRALIAN AND NEW ZEALAND STANDARD RESEARCH CLASSIFICATIONS (ANZSRC)

ANZSRC code: 110702, Applied Immunology (including Antibody Engineering, Xenotransplantation and T-cell Therapies), 40%

ANZSRC code: 110302, Clinical Chemistry (diagnostics), 40%

ANZSRC code: 110804, Medical Virology, 20%

FIELDS OF RESEARCH (FOR) CLASSIFICATION

FoR code: 1107, Immunology, 40%

FoR code: 1103, Clinical Sciences, 40%

FoR code: 1108, Medical microbiology, 20%

CONTENTS

FIGURES

TABLES

ABBREVIATIONS

ADCC – Antibody-Dependent Cellular Cytotoxicity

ADE – Antibody-Dependent Enhancement

BLI – Bio Layer Interferometry

CDR – Complementarity Determining Region

CHO-(S) Cells – Chinese Hamster Ovary Cells (Adapted for suspension culture)

dAb – Domain Antibody

DENV – Dengue Virus

DHF – Dengue Hemorrhagic Fever

DSS – Dengue Shock Syndrome

ECL Substrate – Enhanced Chemiluminescent Substrate

ELISA – Enzyme-Linked Immunosorbent Assay

E protein – Envelope Protein

ER – Endoplasmic Reticulum

Fab – Antigen Binding Fragment

Fc – Fragment Crystallizable

HRP – Horseradish Peroxidase

IFA – Immunofluorescence Assay

Ig (A/D/E/G/M) – Immunoglobulin (Class A/D/E/G/M)

JEV – Japanese Encephalitis Virus

k_a – Association Rate Constant

k_d – Dissociation Rate Constant

K_D – Equilibrium Dissociation Rate Constant

KUNV – Kunjin Virus

LB – Lysogeny Broth

mAb – Monoclonal Antibody

MHC – Major Histocompatibility Complex

NS1 – Non Structural Protein 1

PCR – Polymerase Chain Reaction

RDT – Rapid Diagnostic Test

RPM – Revolutions per Minute

RT-PCR – Reverse Transcription-Polymerase Chain Reaction

RU – Resonance Units

scFv – Single Chain Variable Fragment

SPR – Surface Plasmon Resonance

TBEV – Tick-Borne Encephalitis Virus

TCR – T Cell Receptor

TMB - 3,3',5,5' – Tetramethylbenzidine

UTR – Untranslated Region

V - Volts

V_H – Variable Region of the Immunoglobulin Heavy Chain

V_L – Variable Region of the Immunoglobulin Light Chain

V_λ – Lambda Isotype Variable Region of the Immunoglobulin Light Chain

V_κ – Kappa Isotype Variable Region of the Immunoglobulin Light Chain

WNV – West Nile Virus

YFV – Yellow Fever Virus

Chapter 1

A GENERAL INTRODUCTION TO ANTIBODIES PHAGE DISPLAY AND DENGUE VIRUS DIAGNOSIS

1.1 HUMORAL IMMUNE RESPONSE

Adaptive immunity is a branch of the immune system that involves two different classes of lymphocytes known as T and B cells. T cells are involved in cell-mediated responses and are not the focus of this current work. B cells on the other hand can be recruited for the elimination of foreign molecules in humoral responses which involve secretion of antibodies also referred to as immunoglobulins. Immunoglobulins A, D, E, G and M shown in Figure 1.1 are made of light and heavy chains. Light chains are of either κ or λ isotypes while the heavy chains α, δ, ε, γ and μ are what determine the antibody class. Antibodies consist of units which includes the antigen binding fragment (Fab) molecule, made up of V_L-V_H and C_L-C_H1 domains as well as a class-specific Fc (fragment crystallizable) region made up of C_H2 and C_H3 domains or C_H2, C_H3 and C_H4 in the case of IgE and IgM. The antibody molecule is stabilized by inter-chain and intra-chain disulphide bridges.

The variable regions on the Fab fragment are involved in antigen recognition. An antigen is "any entity—a cell, a macromolecular assembly, or a molecule—that may be bound by either a B-cell receptor or an antibody molecule" (87) while the specific region on the antigen that is bound is called a B-cell epitope or an antigenic determinant. The ability to bind antigen is determined by specific amino acid residues on the antibody (paratopes) and their complementarity to the B-cell epitope. These regions of hyper-variability known as complementarity determining regions (CDRs) are found within the variable light and variable heavy chains. The light chain loci is spread over two gene segments (**V**ariable-**J**oining) while the heavy chain loci is spread over three gene segments (**V**ariable-**D**iversity-**J**oining) (71, 79).

The Fc regions determine the effector function of the antibody. On binding to the B-cell epitope, the antibody-mediated response directed by the Fc region of the recruited antibody can result in inactivation of the pathogen by perturbing their ability to attach to host cells (65), marking of pathogens for destruction by recruiting phagocytic cells (108), cell-mediated cytotoxicity (92), complement activation (73) and mast cell binding (41). The majority (80%) of the immune response is dominated by IgG. Its sub-classes IgG1, IgG2, IgG3 and IgG4 are so named based on the order of their relative concentrations in serum. The main effector functions that are characteristic of IgG (except IgG4) are antibody-dependent cellular cytotoxicity (ADCC), complement activation and antigen opsonization for subsequent phagocytic uptake (43, 69, 107). Despite the dominance of IgG in circulation, other classes of antibodies can be recruited upon insult and these are antigen/pathogen dependent (46).

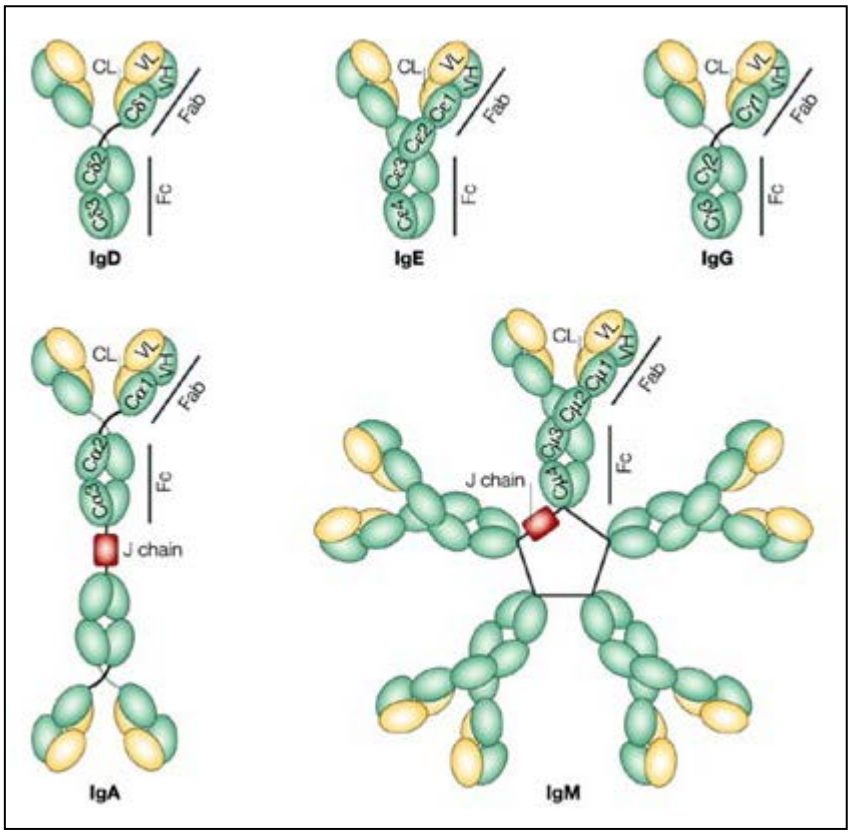

Figure 1.1 Structural representation of antibody classes (91). Shown are monomeric IgD, IgE and IgG as well as dimeric IgA and pentameric IgM. Antibody multimers are linked by J chains which promote polymerisation.

During an antigenic challenge, a genetically varied polyclonal response to different B-cell epitopes is mounted. Germinal centres (high cell density regions in secondary lymphoid organs) are the epicentre of clonal expansion and secondary diversification of immunoglobulin genes (42). Iterative rounds of selection and hypermutation facilitate selection of antibodies based on their affinity for the target antigen. The challenge widens an individual's immune repertoire by exposure of immune-competent B-cells to the antigen, leading to a maximally finite number of antibodies (10^{12}) being able to recognize an infinite number of antigens with varied specificities and associated affinities (60, 84). In most cases the effector function results in elimination of the foreign molecule and classically results in immunological memory.

Antibody responses shape the foundations of vaccination, antibody therapeutics and antibody diagnostics. Strategies that prevent infections are highly valued for improvement of public health. Vaccination relies on immunogenicity of pathogens. Immunogenicity of a molecule refers to its ability to evoke a potentially protective immune response. This aspect can be taken advantage of by artificially sensitize the immune system to an attenuated pathogen and thus generate memory B-cells. Priming of the immune system allows for swift clearance of the pathogen on a subsequent

encounter. Antibodies can be used to identify regions of the pathogen that contribute to immunogenicity and have these regions alone used as subunit vaccines. In the absence of an effective preventative strategy, therapeutic options are often explored as an infection management strategy. Monoclonal antibodies (mAbs) are regarded as a potential panacea for different disease states in the 21st century. The ability of a particular antibody to induce a therapeutic effect, firstly by its targeted antigen binding which is then followed by an appropriate effector function is highly valued. It is for this reason that antibodies against varying targets ranging from receptors to cytokines for management of chronic diseases such as cancer and inflammatory diseases dominate the biopharmaceutical market (17). The ability of antibodies to specifically bind target antigens also makes them desirable as diagnostic reagents. The use of immunoassays to analyze biomolecules for diagnostic purposes has grown immensely. Antibodies are improving diagnostic sensitivity and specificity by dedicating more focus on engineering highly refined antibody properties (12). To be able to carry out any of the aforementioned applications, a source of the antibodies is required.

Antibodies have historically been sourced from antisera. Serum contains circulating antibodies, the specificities of which can be shaped by an antigen used for immunization. The antigen-induced antibodies can then be harvested for use in different applications. The limitation in the amount of antibody that can be harvested and the invariable polyclonal nature of the serum is apparent. Due to these disadvantages, a progression to sourcing antibodies from hybridomas was developed. This involves somatic fusion of antigen-activated splenic B-cells and myeloma cells (62). Alternately, the Epstein-Barr Virus can be used to immortalize antigen-specific human B lymphocytes (104). Continuous culture of the polyclonal B-cells is followed by antigen-specific selection. The selection process allows for an antibody of a single idiotype (monoclonal) and with desired properties to be maintained in culture. Both antiserum and hybridomas however, heavily rely on antigen-driven production of B-cells and antibodies in immunized laboratory animals. Hurdles such as difficulty in expressing the target antigen to use in immunization and the need to perform immunization each time that antibodies are required for a particular target have necessitated the need to employ other techniques to source antibodies. Combinatorial immune repertoire libraries sourced from peripheral blood mononuclear cells (PBMCs) have gained popularity in recent times. The immune libraries are displayed as antibody fragments on different platforms, such as bacteriophage (phage), yeast, *E. coli*, ribosomes and mammalian cells. Phage display is deemed the more ancestral molecular display technology compared to others such as yeast and ribosomal display. The phage display technology has been shown to be robust and has had immense success. This body of work focuses on phage display of antibody fragment libraries.

Phage display technology links genotype with phenotype to screen and identify protein-ligand interactions. There are variations of phage display systems that exist. Detailed here are generic concepts that relate to a gIIIp phage display system that was used in this current work.

Phage display facilitates display of foreign polypeptides on the surface of a phage particle by splicing the genes encoding an array of polypeptides into a gene that encodes a phage coat structural protein (81, 85). The coat protein functions to anchor the displayed polypeptide via a peptide linker. The resultant fusion protein is engineered to affect neither the structure and assembly of the phage particle, nor the structure and function of the tethered polypeptide (13, 19). The phage particles encoding and displaying the polpeptides are used to identify specific ligands in screening assays referred to as biopanning.

Phage are a varied group of viruses that infect prokaryotic cells (13). Phage display applications typically employ the use of filamentous phage. Filamentous phage have a circular, single stranded DNA genome that is surrounded by a cylindrical protein coat Figure 1.2. The genome encodes 11 genes, five of which are responsible for the expression of structural coat proteins. The coat is mainly made up of 2 700 molecules of pVIII, the major coat protein that covers the length of the phage particle. The orientation of the genome is such that a capped 78 nucleotide hairpin structure that makes up the packaging signal, is on one end which also has five copies of pVII and pIX proteins (6, 80). The other end of the particle is capped by another pair of coat proteins pIII and pVI both of which also have five copies.

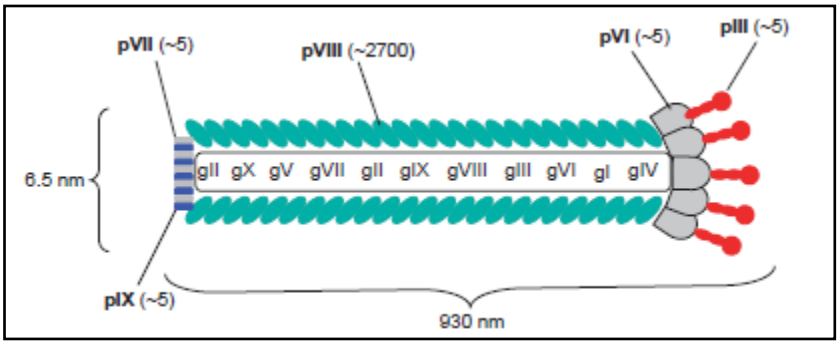

Figure 1.2 Structural architecture and dimensions of filamentous phage (76). The schematic shows cylindrically shaped bacteriophage and the different coat proteins that it has on its surface. In parentheses are the copy numbers of each coat protein.

In 1985, Smith (95) showed that foreign DNA stretches can be integrated into the genome of bacteriophage. Each of the coat proteins has been used for display of polypeptides (33, 58, 70). The

first display system published by Smith involved in-frame cloning DNA segments within the amino and carboxy terminal ends of the gene which codes for the minor protein pIII (gIIIp) of the bacteriophage. The result was the expression of a fusion protein which displayed the foreign protein tethered to the pIII coat. This landmark method allowed for the development of different variations of in vitro selection methods. In 1991 Hoogenboom demonstrated the ability to integrate more than one subunit within the gene III of bacteriophage (57). This advancement allowed the display of Fab on the distal pIII, generating an *in vitro* selection library of the immune repertoire. This technology took advantage of the domain architecture of antibodies allowing tethering of antibody fragments on the coat of filamentous bacteriophage. The modular design of immunoglobulins allows the deletion of individual domains of immunoglobulins to allow the use of 'fragments' in antigen driven selection.

The construction of a combinatorial phage display library involves cloning of recombinant antibody genes from B-cell cDNA of antigen immunized or antigen naive individuals into phagemid vectors. Phagemid vectors have a phage derived origin of replication (intergenic region) as well as their own plasmid origin of replication.The reverse transcribed B-cell mRNA is PCR amplified with germline-specific primers for variable regions. The variable fragment (Fv) region of antibodies as previously mentioned is responsible for antigen binding. This means that the Fc portion of antibodies can be excluded in display technologies. Smaller fragments lend themselves well to phage display as they can be produced in bacterial host systems without compromising protein folding. A fragment format is chosen for variable gene restriction cloning into the phagemid vector. The V_H and V_L domains are amplified and artificially shuffled in single chain variable fragments (scFv) and Fab formats to create added antibody repertoire diversity. scFv are the product of linked recombinant genes that encode V_H and V_L domains brought together with a short linker peptide such as 3 x (Glycine-Glycine-Glycine-Glycine-Serine). Construction of the Fab molecule involves two component polypeptides as it is made up of V_L-V_H and C_L-C_H1 domain interactions. The variable regions are cloned into a vector that already includes the constant domains. Each heavy and light chain can be designed to have its own ribosomal binding site allowing each chain to be independently translated for display on the surface of filamentous phage. The minimal V_H domains of human antibodies (dAb) are sufficient for antigen recognition and therefore can also be singly amplified and cloned into a phagemid vector.

Phage display libraries are used for selection of binders to target ligands. The selection protocol for an antibody library displayed on phage involves biopanning for antigen binders. A schematic of the typical process is shown in Figure 1.3. Often the antigen is immobilized on a surface, following which the library is then exposed to the antigen-coated surface. Different types of surfaces such as

nitrocellulose, polystyrene, magnetic beads and column matrices can be used. The displayed antibody fragments interact with the presented antigen during biopanning, functioning as probes to essentially self-select when exposed to an antigen to which they have binding specificity. Non-specific binders are washed away followed by elution of specific binders. The specific binders then need to be amplified in bacteria. Phage display takes advantage of the bacteriophage replication cycle to enrich selected binders. The N-terminal of pIII forms knob-like structures illustrated in Figure 1.2. pIII not displaying tethered polypeptide binds to the F-pilus for infection of bacteria. Adsorption of pIII to the bacterial host cell F-pilus is followed by delivery of the single stranded phage DNA into the bacterial cytoplasm. The phagemid vector includes an origin of replication that has both a cis-acting sequence for replication and also an optimal cis-acting signal sequence for packaging single stranded DNA into nascent viral filaments. The gIIIp while allowing for foreign antibody fragements to be displayed on the virion surface, the hybrid protein by itself cannot support phage assembly. Virus assembly requires helper phage in a process called phage rescue. Phagemids carry a filamentous phage origin of replication which is inactive until a bacterial cell is infected with helper phage. Trans-acting sequences on helper phage provide the supplementary genes required for phage assembly. Helper phage are also filamentous phage that rely on the expression of the F-pilus on bacteria for infectivity. Additionally, helper phage carry a selectable marker different to the phagemid, have gene sequences that code for production of coat proteins, have gene sequences that code for virus assembly and importantly have a defunct packaging signal (109). This results in the preferential assembly of phage particles with phagemid DNA when both phagemid and helper phage infect the same bacterium. The amplified phage population of binders is then subjected to more iterations of panning to enrich for specific binders.

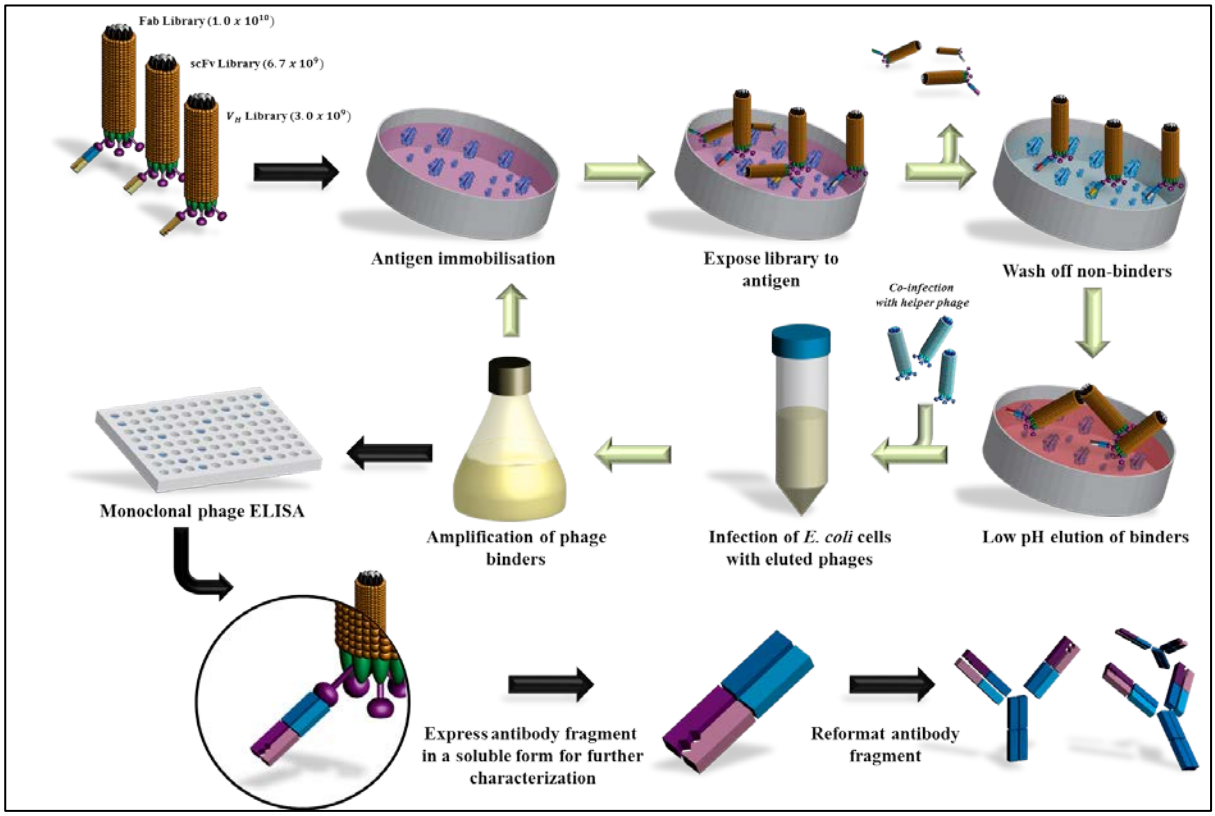

Figure 1.3 General overview of biopanning a phage library displaying antibody fragments. The target antigen is either adsorbed onto a solid surface or immobilized to a desired matrix. The phage-displayed antibody fragment library is then exposed to the antigen select for binders. Weak binders and non-binders are discarded during washing steps. pH shift elution is used to recover the target-specific binders which are rescued and amplified by infecting *E. coli* with the target-specific phage and helper phage. Bacterial replication allows replication of the phage which can be used in iterative rounds of biopanning. The biopanning protocol is repeated until sufficient enrichment is achieved. Individual phage are screened in a monoclonal ELISA to determine target-specificity. Positive binders from the screening are sequenced and characterized as phage-displayed antibody fragments, soluble antibody fragments of reformatted fully assembled antibodies.

1.3 AN OVERVIEW OF DENGUE VIRUS INFECTIONS

Infection with dengue virus (DENV) is an increasingly significant health problem that puts nearly 3.5 billion people in the tropics and sub-tropics at risk each year. 2010 population data and cartographic methods estimated the global dengue infection rate at 390 million infections annually, 96 million of which were symptomatic (9). The World Health Organization cites this viral disease as one which is pandemic-prone due to a 30-fold increase in incidence of dengue in the last 50 years. The global distribution of dengue has spread over the years and epidemics have been reported in many countries including Brazil, Columbia, Cuba, Peru, Venezuela, Lao People's Democratic Republic, Vietnam, Malaysia, Thailand and Vietnam (97). The spread of DENV has been attributed to factors such as urbanization which has led to the geographic spread of the principal mosquito vectors *Aedes aegypti* and *Aedes albopictus*, increased host densities caused by swelling populations within the same limited living areas, increased ease and frequency of global travel which allows establishment of transmission cycles in non-endemic regions, and the rescinding of vector control programs (7, 29). The lack of an approved dengue virus vaccine or a dengue virus specific therapeutic, both of which are the focus of many research efforts, means that there is a heavy reliance on the management of the dengue disease burden. Consequently, there are concerted efforts towards improvements in diagnostic acumen, vector control, public health measures and disease surveillance. The necessity for improved diagnostic acumen is exemplified by the DENFRAME project, a consortium of researchers from Asia, Europe and Latin America working towards reliable and rapid diagnosis including integration of progressive tools such as biosensor technology.

Dengue virus along with other insect-transmitted viruses such as West Nile virus (WNV), yellow fever virus (YFV), Japanese encephalitis virus (JEV) and tick-borne encephalitis virus (TBEV) belong to the flavivirus genus (5, 51, 97). Two or more flaviviruses often co-circulate in regions of hyper-endemicity such as parts of Asia where both DENV and JEV are commonly found (52). Dengue virus has four antigenically and phylogenetically distinct serotypes which can also co-circulate within the same regions (56). Within these four serotypes are further genotypic subtypes. The dengue virus serotypes have varied infectivity and virulence (28, 106). DENV infections evoke both an innate and an adaptive immune response. The humoral immune system response is involved in two ways; (i) Antibodies target major glycoproteins produced by the virus (ii) Antibodies can mediate infection of target cells and aid viral replication through a phenomenon called antibody dependent enhancement (ADE) in secondary DENV infections. In ADE, non-neutralising antibodies produced during primary infections are thought to form immune complexes with the

virus, inadvertently aiding virus attachment to the Fc-γ receptor which allows mediated infection of host cells (53, 86, 88, 97).

Dengue virus infections are generally self-limiting and result in a benign dengue fever (DF) which may be asymptomatic or lead to a wide spectrum of mild disease syndromes that share clinical characteristics with many other febrile illnesses (83). Serious infections such as Dengue Hemorrhagic Fever (DHF) or Dengue Shock Syndrome (DSS) however, are characterized by plasma leakage as a result of vascular permeability and haemostatic dysfunction (47, 52, 54). The development of DHF and DSS has been attributed to various factors such as host genetics, involvement of T-cells in immune response, and a second heterotypic infection subsequent to an initial priming infection (ADE) (32, 50, 55). It is the possibility of progression to serious disease and possible mortality in the absence of timely supportive treatment that highlights the need for improved diagnostic acumen. Mitigation of mortality governs current protocols for hospitalization of all individuals infected with dengue viruses (102). In 2005, the mean cost of a hospitalized DENV infection case in international dollars (I$) was I$ 1394 (98). This is a significant cost that brings into play the fact that beyond just improved diagnosis of infection, diagnostic assays in the future need to be prognostic of severe disease so as manage disease associated costs.

1.4 DENV STRUCTURE AND REPLICATION

DENV is a 50 nm spherical virus made up of a nucleocapsid core that encapsulates the DENV genome within a capsid coat. A host-derived viral envelope made up a lipid bilayer covers the nucleocapsid. 180 copies of envelope and membrane proteins are embedded in the viral envelope and are displayed in an icosahedral pattern on the virus surface. The embedded proteins offer both a protective function and mediation of virus entry into host cells. A schematic of the DENV structure is shown in Figure 1.4.

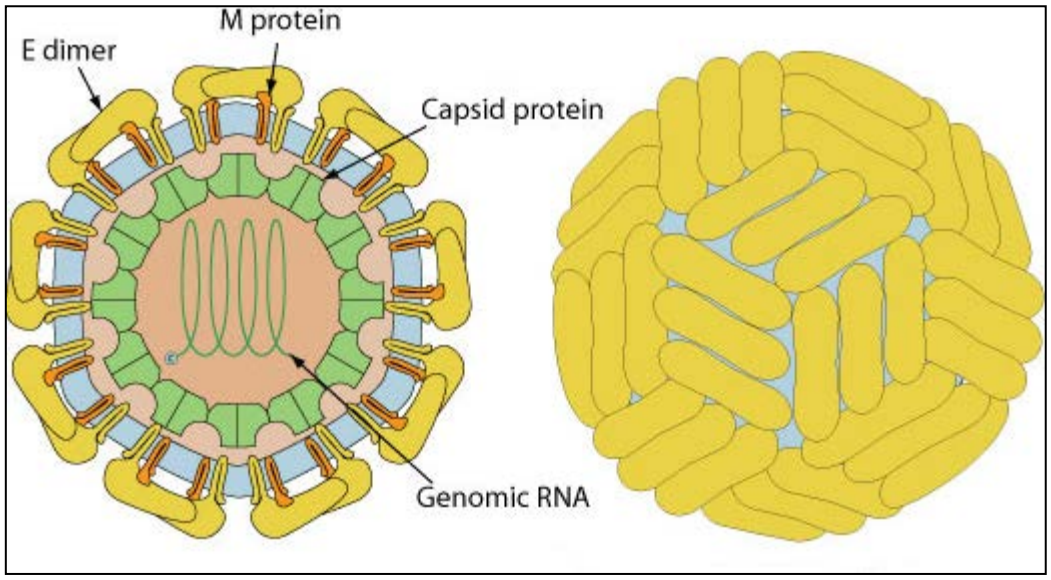

Figure 1.4 Schematic representation of the dengue virus structure (113). Shown, is the icosahedral-like symmetry of envelope (E) and membrane (M) proteins on the surface of spherical DENV. Mature virions display M proteins while immature virions display a membrane protein precursor (prM). Within the protective outer protein coat are the capsid proteins which encapsulate the virus genome.

The dengue virus has a tropism for dendritic cells, blood monocytes and tissue macrophages (22, 110). Infection is mediated by dendritic cells on the skin surface as these cells are used for replication of the viral genome and proteins so the newly synthesized dengue viruses can go on to infect other host cells. The dengue virus has an incubation period of about two weeks before the presence of virus in blood and the presentation of symptoms (100). Upon a blood meal by a DENV vector, the virus attaches and is internalized by Langerhans cells through endocytosis. Fusion with endosomal membranes allows for acid-dependent cytoplasmic release of the virus genome (Figure 1.5) (75). DENV is a single-stranded, positive sense, RNA virus of 11 kb. The 5’ end of the viral genome is made up of an untranslated region (UTR) of about 100 bp, while the 3’ UTR is about 450 bp. Between the UTR ends is an open reading frame that encodes a single polypeptide of about 3400 amino acids. The amino acids code for 3 structural proteins - capsid, membrane and envelope - and 7 non-structural (NS) proteins - NS1, NS2A, NS2B, NS3, NS4A, NS4B and NS5 (20). These proteins are produced following post-translational cleavage by viral and host proteins and all have various roles in the pathogenicity of DENV (101). These proteins are pivotal for replication at the surface of the endoplasmic reticulum (ER) where double stranded RNA is synthesized from the transcription of single stranded RNA provided be the virus genome. The structural proteins are included in the assembly of extracellular mature virus particles which also occurs in the ER.

Following assembly, the virions bud from the ER, are transported to the Golgi apparatus and then leave the host cell through the secretory pathway.

Even though the non-structural proteins are expressed within the infected host cell, they are not part of the virion and as such, their use as diagnostic antigens is attractive. The role of the non-structural proteins is in virus replication. Six of the seven non-structural proteins are incorporated into a scaffolded replication complex formed by NS2A, NS2B, NS3, NS4A, NS4B and NS5 on the cytoplasmic face of the ER (1). NS1 however is not part of the replication complex. NS1 is found within the ER lumen and associates with the replication complex through NS4B and possibly NS4A (77). Following different signals and post-translational modifications, some proportions of NS1 gets trafficked through the ER to the Golgi and then get secreted into circulation. The secretory characteristic of NS1 in measurable amounts makes it a good surrogate marker of infection and therefore an attractive diagnostic target (77, 111). Furthermore, the amount of DENV NS1 in circulation has also been found to be positively correlated with development of severe disease (66).

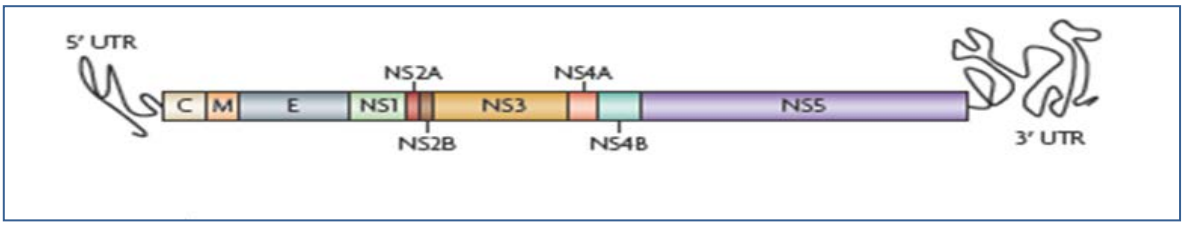

Figure 1.5 Representation of the RNA genome of DENV (48). 5' and 3' untranslated regions flank the single polypeptide that codes for dengue virus.

1.5 IMMUNE MODULATIONS IN DENV INFECTIONS

Dengue virus infections evoke complex innate and adaptive immune responses. The outcomes of the infection are governed by the interplay between the speed of viral replication, the spread of infection, the response to infection and pushback from immune evasion tactics employed by the virus.

Initial viral replication occurs in the Langerhans cells which are infected upon a blood meal by the viral vector. In their defense, the infected Langerhans cells initially produce interferons. This is a non-specific, innate response to infection that is encoded in the germline. Interferons – types I (α and β) and II (γ) result in a generalized antiviral state to minimize the effects of infection by inhibiting translation /replication of viral RNA and activating phagocytic cells respectively (27).

Furthermore the innate immune system responds by activating complement. Complement activation is important in; restraint of viral infectivity by mechanisms which lyse viral envelopes, recruitment and activation of phagocytic cells, promotion of viral clearance, and facilitation of antigen presentation to induce adaptive immune responses by B-cell and T-cell receptors.

Some of the infected dendritic cells drain to the lymph nodes in an attempt to sequester and clear the pathogen. This unfortunately leads to the spread of the virus as the lymphatic system aids dissemination of the virus and new rounds of viral replication occur which in turn increase viremia. High titre viremia which is Fc-γ receptor mediated occurs during the febrile period.

The engagement of the adaptive immune system involves B-cell antigen receptors – antibodies – which are produced to; neutralize the viral particles by direct receptor binding, complement mediated lysis of the infected cells or antibody-dependent cytotoxicity. The main targets of the antibodies are multiple domains of the E-protein, pre-membrane protein and NS1. The NS1 response in particular is associated with ADCC and complement-mediated cytolysis (36, 44). In this flurry of responses, cytotoxic T cells are also recruited to kill the infected cells in response to the proteins synthesized by the viral particles. T-cells, like B-cells express clonally distributed antigen-specific receptors that are generated by the same V-(D)-J gene rearrangement strategies. Peptides are displayed on surfaces of the host cells and these are recognized by the Major Histocompatibility Complex (MHC) which associates with the infected cells. This association flags the infected cells for killing by T-cell receptors (TCR) which make pivotal interactions with both the MHC and the proteins displayed on the infected cells. The TCR unlike the soluble B-cell receptor (immunoglobulin) is not secreted, its activation results in the proliferation and release of inflammatory cytokines which heavily influence the direction, magnitude and outcome of effector functions (23). The cytokine storm in particular, is responsible for the resultant fever which can last up to 10 days. Acute symptoms such as rashes, headache, retro-orbital pain, leucopenia and myalgia are also experienced during high viral titres. When the cumulative responses are excessive, vascular permeability and coagulation abnormalities cause severe disease (DHF/DSS) through mechanisms that are not fully elucidated.

Dengue viruses utilize evasion tactics such as error prone RNA polymerases that generate variants of the viruses that are less recognizable by B and T cell receptors (27). These inhibit some of the immune responses but the combined innate and adaptive responses clear the self-limiting infection. The primary infection results in lifelong immunity to the infective DENV serotype and transient immunity to the other three serotypes. This means that asymptomatic reinfections with homotypic serotypes of DENV are common in the presence of neutralizing antibodies. The response to

secondary infections with heterotypic serotypes of DENV is not as straight forward as the response to primary infections. Previous, cross-reactive responses that are only partially neutralizing in heterotypic DENV challenge facilitate faster viral replication and faster spread of the virus by mediating infection and replication in Fc-γ receptor bearing cells and therefore increase the chances of development of DHF/DSS.

The immunological storm that occurs during infection is important for the resolution of infection but also poses significant challenges to DENV diagnosis. To mitigate morbidity and mortality associated with DENV infections, acute phase diagnosis needs to differentiate DENV from other febrile disorders such as malaria, typhoid fever, scrub typhus, influenza and leptospirosis. Timely diagnosis in the absence sufficient of clear clinical signs can aid effective clinical approaches.

1.6 DIAGNOSIS OF DENGUE VIRUS INFECTIONS

Current protocols for the diagnosis of dengue infections include; serological detection of IgM and IgG responses to the major antigenic determining regions of the envelope protein, virus isolation by culture followed by detection with immune-fluorescence, nucleic acid amplification of the DENV genome or detection of viral antigenic polypeptides such as DENV NS1 (40, 50, 100).

Diagnosis based on serology is used for diagnosis of dengue virus infections in endemic countries such as Singapore. The ratio between IgM and IgG responses is used to indicate either a primary or secondary infection. Furthermore, IgM and IgG responses are measured on two separate occasions (paired sample) from each individual to show an increase in antibody titre that is expected with progression of infection. The disadvantages of this method is that paired samples cannot always be obtained, there is a lag phase in detection of IgG and IgM antibodies and some patients fail to seroconvert (90). Additionally, there can be low specificity associated with IgM/IgG assays as the E protein epitopes that are targeted by the antibodies are found on other flaviviruses.

Dengue virus culture is highly specific and indicative of the presence of virus. Virus detection in circulation is optimal for approximately two to seven days after the onset of illness and corresponds to the period of fever (94). The attainment of a virus culture result is unfortunately slow making this diagnostic method of little value in terms of early patient management (100).

Nucleic acid amplification of the viral genome particularly of capsid and prM genes is highly sensitive in the acute phases of infection which have an associated high viral titre (24). In most instances this method uses reverse transcription-polymerase chain reaction (RT-PCR) to amplify and detect the viral genes followed by a secondary semi-nested PCR amplification to identify the

infective serotype. Unfortunately amplification processes are prone to contamination leading to false positives (82). The amplification protocols can also be complex requiring costly machinery in often resource-poor settings where much of the dengue virus burden is felt.

Detection of DENV NS1 an antigen produced by DENV has become increasingly popular. Indonesia, another DENV endemic country and also the largest archipelago country inhabited by around 240 million people has clinicians increasingly using commercial NS1 antigen detection assays as the tool of choice to confirm DENV infection (4). DENV NS1 is detected from the onset of fever, up to approximately 12 days post the presentation of symptoms (111). This method of diagnosis is quick but does not provide any information on the infective serotype. Additionally, this method suffers from sensitivity issues particularly in secondary infections which are the bulk of infections seen in endemic countries.

Detection of DENV NS1 can be carried out using multiplex polymerase chain reaction (PCR). SYBR green real-time PCR is preceded by viral RNA extraction and reverse transcription of the NS1 gene. The cycling steps of the PCR use serotype-specific primers to amplify the NS1 gene resulting in measurable signals to identify the infective DENV serotype.

NS1 detection can also be carried out using antibodies in assay formats such as ELISA or by using rapid diagnostic test (RDT) kits that employ immunochromatographic techniques. In a sandwich ELISA, at least two antibodies that bind mutually exclusive sites are used to capture and detect the antigen. Immunochromatographic assays such as lateral flow devices utilize the same concept where membrane-immobilized antibodies and a reporter antibody conjugated to a coloured microsphere provide a test result. Because both assays are antibody based, conceptually, the sensitivity of the assays will rely on the availability of the epitopes that are recognized by the antibodies and the antibody affinity for those epitopes in the test matrix. The specificities and sensitivities of the DENV NS1 detection assay would need to be evaluated in local settings to assess their utility for varied populations. In a recent comparison of a DENV NS1 detection ELISA and a DENV NS1 detection lateral flow test in Belo Horizonte, Brazil, the lateral flow devices were found to be marginally (not significantly) more sensitive than the ELISA (38). The RDT kits are advantageous in their ability to be taken into the field and their reduced assay time to obtaining a result but in scenarios where there are DENV epidemics, ELISA allows for high-throughput testing at low cost.

Of the methods that have been mentioned, multiplexed PCR is the most sensitive method to detect DENV NS1 very early during infection (14, 61). The multiplex PCR as previously stated requires strict control measures to minimize cross-contamination of samples and expensive equipment that is

generally reserved for specialized laboratories. In routine laboratory testing, patient serum is assayed for the presence of NS1 antigen using sandwich ELISA and RDTs. While the specificity of these routine testing assays can be very high, the sensitivity can be affected by the infective serotype (37, 74, 93) and secondary infections with heterotypic serotypes of DENV.

The diagnosis of acute primary and secondary dengue virus infection cannot be achieved at required levels of sensitivity with a single marker of DENV infection (40) as each method of detection is hampered at different time points by the DENV factors controlling infection and the host immune response to the infection (Figure 1.6). Notably, there is a lag phase that is associated with immune responses (IgM/IgG) to detectable viraemia and the presence of DENV NS1. While virus detection is high quite early on during acute illness, the rise in antibody titre quickly decreases it to non-detectable levels. The levels of DENV NS1 are not shown as these vary amongst individuals but its detection is possible up to 12 days after the onset of acute illness. Not shown in Figure 1.6 is the IgA immunological response to the presence of virus. The IgA class of antibody is recruited in DENV infections and its levels have been to shown to be high in the acute phase of severe disease (DHF/DSS) (63).

Diagnosis of DENV infections requires the aforementioned cognizance of the detection kinetics of the viral genome, antigenic NS1 and IgG/IgM antibodies against DENV. A study by Moi *et al.* (74) comparing the usefulness of viral genome and antigenic NS1 detection found that the sensitivity of NS1 detection was high from the onset of acute symptoms up to 10 days thereafter while the detection of the viral genome waned after just 5 days post the onset of acute symptoms. Antibody detection on the other hand, is linked closely with the convalescent phase of infection which begins at about 5 to 6 days post the onset of acute symptoms (18, 59, 82). It is therefore not surprising that the combination of DENV NS1 detection and IgM/IgG ELISA increases the DENV diagnostic window as has been reported in literature. Critically, in situations where there is a manifestation dengue hemorrhagic fever, its timing is concurrent with the decrease in fever which occurs when the antibody response peaks and starts to resolve the infection (82, 89). From a clinical perspective therefore, the diagnostic method that provides lengthy diagnosis of infection from the onset would be most beneficial in helping to plan appropriate courses of clinical action. It is for this reason that research input into improving the diagnostic sensitivity of DENV NS1 detection is crucial.

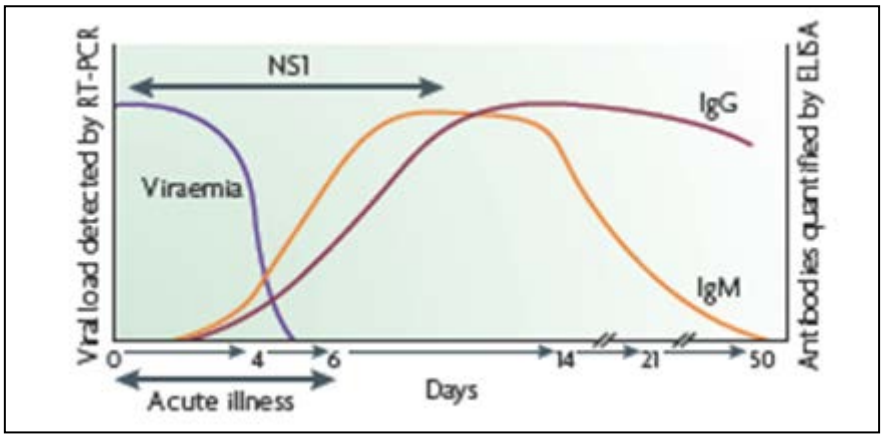

Figure 1.6 Detection kinetics of dengue virus, NS1, IgM and IgG in DENV infections (48). Shown are short lived viremea which is followed by either and IgM or IgG response depending on the presence of either a primary or secondary response. The presence of NS1 is also indicated from quite early on in infection but the levels of NS1 which are variable are not shown.

1.7 EVALUATION AND APPLICATION OF DENV NS1 AS A DIAGNOSTIC MARKER

NS1 is a 46 - 55 kDa glycoprotein (96) produced by DENV but is absent from the virion. This protein has been shown to be a good surrogate marker for acute DENV infection (2, 66, 111). The recently resolved dimeric structure of NS1 (1) shown in Figure 1.6, indicates three main domains that make up each monomer; (i) a β-roll domain with a highly hydrophobic face and a free cysteine that allows dimerization on the interior side, (ii) a wing-like domain which includes an unresolved, highly disordered loop at residues 108 – 128 which have previously been reported to be immune-dominant (35) and (iii) a C-terminal, rung-like, continuous β sheet that forms the plane of the dimer.

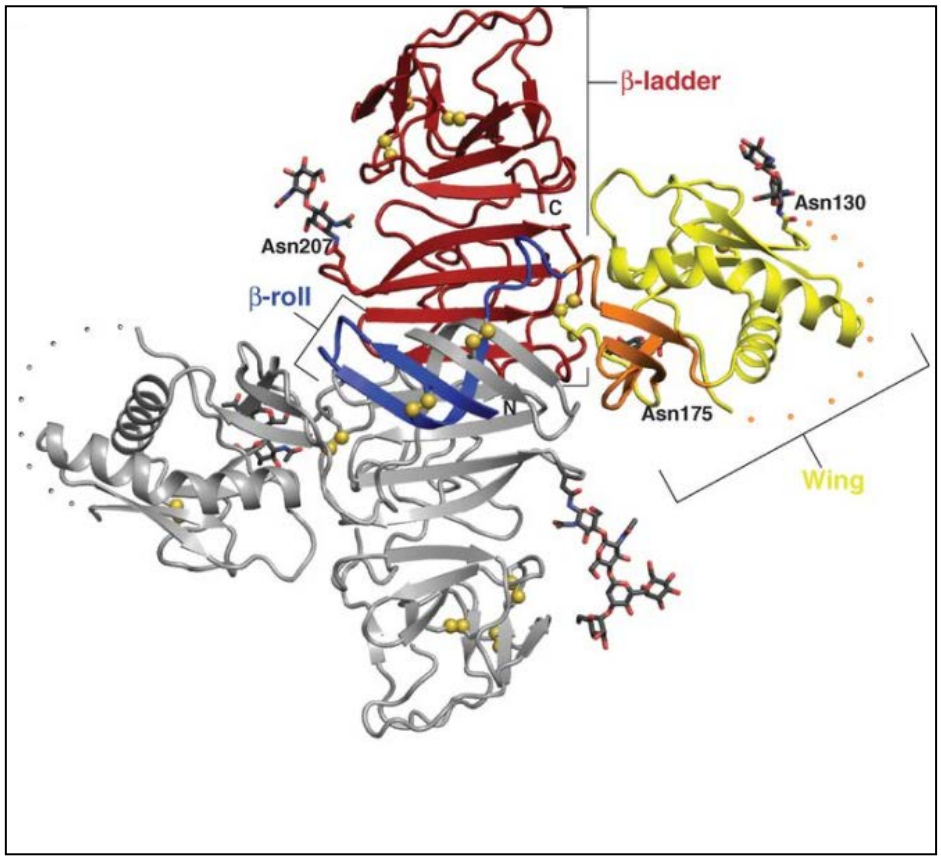

Figure 1.7 Structural domains of dimeric NS1 (1). The monomer shows a β–roll domain in blue, β-ladder domain in red and a wing domain in yellow.

NS1 is produced as a monomer in infected cells. Following post-translational modification in the ER lumen, NS1 associates with the membranes of organelles in its dimeric form, held together by a disulfide bridge. The membrane-associated dimer plays a role in assisting replication of the virus. Dimeric NS1 is then transported to the surface of infected cells where it is secreted into circulation as a hexamer. The hexamer which is detergent sensitive (25, 39), associates by hydrophobic interaction of its β rolls (5, 11). The hexameric structure of about 310 kDa has been reported by Gutsche et al. (47) to carry a lipid cargo. The lipids were found to be similar to those involved in vascular hemostasis and endothelium function indicating that NS1 could potentially mimic or hijack lipid metabolic systems to mediate plasma leakage which is characteristic of severe disease. It is the extracellular accumulation of secreted NS1 however which permits its use as a marker of infection.

Detection of DENV NS1 can precede onset of symptoms and persist up to day 12 post infection (2, 30, 66). DENV NS1 detection coincides with detectable viremia before an antibody response is mounted. Concentrations in serum vary and can reach up to 50 µg/mL (2, 111). Alcon et al. (2), in their work with polyclonal antibodies, showed that concentrations of DENV NS1 do not

significantly differ between primary and secondary infections but the duration of antigen detection is shorter in secondary infections (103). The anamnestic B-cell response to flaviviral infection also differs from the initial response not only in swifter clearance of NS1 but also in a higher representation of memory B-cells that produce antibodies against immune-dominant regions of NS1 (34). Despite the shorter duration of DENV NS1 in secondary infections, high titres of antigen have been found to be predictive of presentation with DHF/DSS (66).

Different commercial DENV NS1 capture assays (Panbio-Alere, Standard Diagnostics, Bio-Rad Platelia) are available in the market for diagnosis of DENV and these have been the subject of many utility evaluations (4, 8, 31, 37, 49, 64, 67, 68, 72, 105, 112). Results generally showed that specificity of DENV diagnosis with no cross-reactivity to NS1 from othe flaviviruses was high (upwards of 80% and in some cases 100%) but there were clear deficits in sensitivity of DENV NS1 detection. The highest sensitivity of NS1 detection was early during the course of infection and in primary infections. Sensitivity was particularly poor however in cases of secondary infection. Unexplainable geography-variable sensitivity was also reported with the Platelia Dengue NS1 (Bio-Rad) (49). Some evaluations have compared the utility of NS1 detection to serological detection of IgG/IgM (3, 10, 40, 45, 82) and the results indicated that the two assays are complementary and improve specificity and sensitivity when used in combination to offset the weaknesses of each individual assay. Algorithms have also been proposed for how different diagnostic assays such as real-time RT- PCR, IgM antibody capture ELISA, and DENV NS1 antigen capture can be combined to improve sensitivity and the window of DENV infection diagnosis as each of these assays have utilities in different phases of DENV infection (8, 40).

Combining different infection markers for simultaneous detection in multiplexed assays is an attractive strategy to achieve validated sensitivity and specificity of at least 99.5% required for inclusion of a DENV diagnostic assay in blood screening programs (78). Transfusion of blood is a life-saving intervention with an invaluable role in certain cases of patient management. The mandate of national blood programs therefore, is to establish approaches that ensure screening for transfusion-transmissible infections. One of the challenges however, lies in the unavailability of screening assays for some transfusion-transmitted infections. DENV in particular has been shown to be transfusion-transmitted (21, 26, 99). The degree of transfusion transmission in endemic regions is difficult to ascertain without an appropriately specific and sensitive screening assay. This poses a risk to blood safety in endemic regions. Current mitigation of DENV transfusion transmission by the Australian Red Cross Blood Service (ARCBS) relies on exclusion of fresh component manufacture of blood products (platelets and red blood cells) from people that are identified from questionnaires and interviews as having travelled to areas that put them at risk of infection. When

there are DENV outbreaks, the repercussions are a decline in available stocks of fresh components and a substantial cost implication associated with discarding the fresh components. There are unfortunately no cost-benefit analyses available to determine the cost of the development of a DENV screening assay – cost per infection averted - and the risk of DENV transfusion transmission. DENV prevalence and incidence rates in endemic regions of the Americas and Asia-Pacific however, justify the development of a DENV screening assay as has been done with West Nile Virus in the USA where it poses a significant threat to blood safety (15).

1.8 PROJECT RATIONALE

The significant deficiencies in sensitivity of DENV infection diagnosis by NS1 antigen detection indicate that there is scope of improvement of the antigen detection assay. The DENV NS1 detection assays rely upon the use of at least two antibodies for capture and detection of the antigen. Presumably, commercial companies would develop assays with high affinity antibodies and therefore the shortfall is not due to antibody-antigen kinetic interactions. The sensitivity deficits that are seen in antigen detection particularly in secondary infections would point to an unavailability of a B-cell epitope recognized by either the capture or detection antibody during the secondary immune responses. Major immune-dominant antigens are shared between dengue and other flaviviruses (16) and antibody responses to these antigens can interfere with accurate detection of analytes such as DENV NS1 (34) in the absence of an immune-complex dissociation step (63).

The project described herein endeavors to develop best in class reagents for DENV NS1 detection. The work focuses on using different phage libraries displaying human antibody fragments to isolate (i) antibodies that target discreet antigenic differences amongst NS1 from all four DENV serotypes and (ii) a pairing antibody that recognizes NS1 from all four DENV serotypes but avoids the immune-dominant region. We hypothesize that a serotyping assay of this nature can improve diagnostic sensitivity in secondary DENV infections as the pan-reactive binder used in the assay will target an alternate epitope, distinct from the immune-dominant epitope which is often bound by circulating endogenous antibodies that are clonally produced as a consequence of a previous, primary DENV infection. The assay would also lend itself well to epidemiological surveillance which is critical for predictions of epidemics and planning for responses to epidemics. Additionally, the reagents could be incorporated into a multiplexed assay with other markers of infection that could screen donated blood for active viraemia by using DENV NS1 as a proxy.

1.9 REFERENCES

1. **Akey, D. L., W. C. Brown, S. Dutta, J. Konwerski, J. Jose, T. J. Jurkiw, J. DelProposto, C. M. Ogata, G. Skiniotis, R. J. Kuhn, and J. L. Smith.** 2014. Flavivirus NS1 Structures Reveal Surfaces for Associations with Membranes and the Immune System. Science **343:**881-885.
2. **Alcon, S., A. Talarmin, M. Debruyne, A. Falconar, V. Deubel, and M. Flamand.** 2002. Enzyme-Linked Immunosorbent Assay Specific to Dengue Virus Type 1 Nonstructural Protein NS1 Reveals Circulation of the Antigen in the Blood during the Acute Phase of Disease in Patients Experiencing Primary or Secondary Infections. Journal of Clinical Microbiology **40:**376-381.
3. **Andries, A. C., V. Duong, C. Ngan, S. Ong, R. Huy, K. K. Sroin, V. Te, B. Y, P. L. Try, and P. Buchy.** 2012. Field Evaluation and Impact on Clinical Management of a Rapid Diagnostic Kit That Detects Dengue NS1, IgM and IgG. PLoS Neglected Tropical Diseases **6**.
4. **Aryati, A., H. Trimarsanto, B. Yohan, P. Wardhani, S. Fahri, and R. T. Sasmono.** 2013. Performance of commercial dengue NS1 ELISA and molecular analysis of NS1 gene of dengue viruses obtained during surveillance in Indonesia. BMC Infect Dis **13:**611.
5. **Avirutnan, P., R. E. Hauhart, P. Somnuke, A. M. Blom, M. S. Diamond, and J. P. Atkinson.** 2011. Binding of Flavivirus Nonstructural Protein NS1 to C4b Binding Protein Modulates Complement Activation. The Journal of Immunology **187:**424-433.
6. **Barbas, C. F.** 2001. Phage display : a laboratory manual. Cold Spring Harbor Laboratory Press, Cold Spring Harbor, NY.
7. **Bennett, S. N., E. C. Holmes, M. Chirivella, D. M. Rodriguez, M. Beltran, V. Vorndam, D. J. Gubler, and W. O. McMillan.** 2003. Selection-Driven Evolution of Emergent Dengue Virus. MOLECULAR BIOLOGY AND EVOLUTION **20:**1650-1658.
8. **Bessoff, K., E. Phoutrides, M. Delorey, L. N. Acosta, and E. Hunsperger.** 2010. Utility of a Commercial Nonstructural Protein 1 Antigen Capture Kit as a Dengue Virus Diagnostic Tool. Clinical and Vaccine Immunology **17:**949-953.
9. **Bhatt, S., P. W. Gething, O. J. Brady, J. P. Messina, A. W. Farlow, C. L. Moyes, J. M. Drake, J. S. Brownstein, A. G. Hoen, O. Sankoh, M. F. Myers, D. B. George, T. Jaenisch, G. R. W. Wint, C. P. Simmons, T. W. Scott, J. J. Farrar, and S. I. Hay.** 2013. The global distribution and burden of dengue. Nature **496:**504-507.
10. **Blacksell, S. D., R. G. Jarman, M. S. Bailey, A. Tanganuchitcharnchai, K. Jenjaroen, R. V. Gibbons, D. H. Paris, R. Premaratna, H. J. De Silva, D. G. Lalloo, and N. P. J. Day.** 2011. Evaluation of six commercial point-of-care tests for diagnosis of acute dengue infections: The need for combining NS1 antigen and IgM/IgG antibody detection to achieve acceptable levels of accuracy. Clinical and Vaccine Immunology **18:**2095-2101.
11. **Bock, G. R., J. Goode, N. Foundation., and N. I. f. T. Diseases.** 2006. New treatment strategies for dengue and other flaviviral diseases. John Wiley & Sons, Chichester :.
12. **Borrebaeck, C. A. K.** 2000. Antibodies in diagnostics – from immunoassays to protein chips. Immunology Today **21:**379-382.
13. **Bratkovič, T.** 2010. Progress in phage display: evolution of the technique and its applications. Cellular and Molecular Life Sciences **67:**749-767.
14. **Buerano, C. C., F. F. Natividad, R. C. Contreras, I. N. Ibrahim, M. N. Mangada, F. Hasebe, S. Inoue, R. R. Matias, and A. Igarashi.** 2008. Antigen sandwich ELISA predicts RT-PCR detection of dengue virus genome in infected culture fluids of Aedes albopictus C6/36 cells. Southeast Asian J Trop Med Public Health **39:**817-21.
15. **Busch, M. P., S. Caglioti, E. F. Robertson, J. D. McAuley, L. H. Tobler, H. Kamel, J. M. Linnen, V. Shyamala, P. Tomasulo, and S. H. Kleinman.** 2005. Screening the blood supply for West Nile virus RNA by nucleic acid amplification testing. N Engl J Med **353:**460-7.

16. **Calisher, C. H., N. Karabatsos, J. M. Dalrymple, R. E. Shope, J. S. Porterfield, E. G. Westaway, and W. E. Brandt.** 1989. Antigenic Relationships between Flaviviruses as Determined by Cross-neutralization Tests with Polyclonal Antisera. Journal of General Virology **70:**37-43.
17. **Carter, P. J.** 2006. Potent antibody therapeutics by design. Nature Reviews Immunology **6:**343-357.
18. **Castro-Jorge, L. A., P. R. L. Machado, C. A. Fávero, M. C. Borges, L. M. R. Passos, R. M. de Oliveira, and B. A. L. Fonseca.** 2010. Clinical evaluation of the NS1 antigen-capture ELISA for early diagnosis of dengue virus infection in Brazil. Journal of Medical Virology **82:**1400-1405.
19. **Cesareni, G.** 1992. Peptide Display on Filamentous Phage Capsids - a New Powerful Tool to Study Protein Ligand Interaction. Febs Letters **307:**66-70.
20. **Chambers, T. J., C. S. Hahn, R. Galler, and C. M. Rice.** 1990. Flavivirus genome organization, expression, and replication. Annu Rev Microbiol **44:**649-88.
21. **Chen, L. H., and M. E. Wilson.** 2004. Transmission of Dengue Virus without a Mosquito Vector: Nosocomial Mucocutaneous Transmission and Other Routes of Transmission. Clinical Infectious Diseases **39:**e56-e60.
22. **Chen, Y.-C., and S.-Y. Wang.** 2002. Activation of Terminally Differentiated Human Monocytes/Macrophages by Dengue Virus: Productive Infection, Hierarchical Production of Innate Cytokines and Chemokines, and the Synergistic Effect of Lipopolysaccharide. Journal of Virology **76:**9877-9887.
23. **Coico, R., and G. H. Sunshine.** 2009. Immunology: a short course. Wiley-Blackwell, Hoboken, N.J.
24. **Cordeiro, M. T.** 2012. Laboratory diagnosis for dengue. Revista do Instituto de Medicina Tropical de São Paulo **54:**10-12.
25. **Crooks, A. J., J. M. Lee, L. M. Easterbrook, A. V. Timofeev, and J. R. Stephenson.** 1994. The NS1 protein of tick-borne encephalitis virus forms multimeric species upon secretion from the host cell. J Gen Virol **75 (Pt 12):**3453-60.
26. **de Wazieres, B., H. Gil, D. A. Vuitton, and J. L. Dupond.** 1998. Nosocomial transmission of dengue from a needlestick injury. Lancet **351:**498.
27. **Diamond, M. S.** 2003. Evasion of innate and adaptive immunity by flaviviruses. Immunol Cell Biol **81:**196-206.
28. **Diamond, M. S., D. Edgil, T. G. Roberts, B. Lu, and E. Harris.** 2000. Infection of Human Cells by Dengue Virus Is Modulated by Different Cell Types and Viral Strains. J. Virol. **74:**7814-7823.
29. **Duane J, G.** 2002. Epidemic dengue/dengue hemorrhagic fever as a public health, social and economic problem in the 21st century. Trends in Microbiology **10:**100-103.
30. **Dussart, P., L. Chartier, A. Diop, O. Sivuth, V. Duong, C. M. Thang, M. Jacobs, A. Sakuntabhai, M. R. T. Nunes, V. T. Q. Huong, P. Buchy, L. Baril, P. F. d. C. Vasconcelos, L. Petit, L. Beniguel, L. C. Quang, S. Ly, R. d. S. S. Azevedo, J.-B. Meynard, and S. Vong.** 2012. Clinical and virological study of dengue cases and the members of their households: the multinational DENFRAME Project. PLoS Neglected Tropical Diseases **6:**e1482.
31. **Dussart, P., L. Petit, D. Moua, S. Matheus, B. Labeau, L. Baril, A. Leduc, and L. Bremand.** 2008. Evaluation of Two New Commercial Tests for the Diagnosis of Acute Dengue Virus Infection Using NS1 Antigen Detection in Human Serum. PLoS Neglected Tropical Diseases **2:**e280.
32. **Edelman, R.** 2011. Unique challenges faced by the clinical evaluation of dengue vaccines. Expert Review of Vaccines **10:**133-136.
33. **Fagerlund, A., A. H. Myrset, and M. A. Kulseth.** 2008. Construction and characterization of a 9-mer phage display pVIII-library with regulated peptide density. Applied Microbiology and Biotechnology **80:**925-36.

34. **Falconar, A. K. I.** 2007. Antibody responses are generated to immunodominant ELK/KLE-type motifs on the nonstructural-1 glycoprotein during live dengue virus infections in mice and humans: Implications for diagnosis, pathogenesis, and vaccine design. Clinical and Vaccine Immunology **14:**493-504.
35. **Falconar, A. K. I., P. R. Young, and M. A. Miles.** 1994. Precise location of sequential dengue virus subcomplex and complex B cell epitopes on the nonstructural-1 glycoprotein. Archives of Virology **137:**315-326.
36. **Falgout, B., M. Bray, J. Schlesinger, and C. Lai.** 1990. Immunization of mice with recombinant vaccinia virus expressing authentic dengue virus nonstructural protein NS1 protects against lethal dengue virus encephalitis. Journal of Virology **64:**4356-4363.
37. **Felix, A. C., C. M. Romano, C. De Campos Centrone, C. L. Rodrigues, L. Villas-Boas, E. S. Araújo, A. M. De Matos, K. I. Carvalho, C. M. T. Martelli, È. G. Kallas, C. S. Pannuti, and J. E. Levi.** 2012. Low sensitivity of NS1 protein tests evidenced during a dengue type 2 virus outbreak in Santos, Brazil, in 2010. Clinical and Vaccine Immunology **19:**1972-1976.
38. **Ferraz, F. O., M. R. Q. Bomfim, A. H. Totola, T. V. Ávila, D. Cisalpino, J. E. M. Pessanha, D. d. G. de Souza, A. L. Teixeira Júnior, M. L. Nogueira, O. Bruna-Romero, and M. M. Teixeira.** 2013. Evaluation of laboratory tests for dengue diagnosis in clinical specimens from consecutive patients with suspected dengue in Belo Horizonte, Brazil. Journal of Clinical Virology **58:**41-46.
39. **Flamand, M., F. Megret, M. Mathieu, J. Lepault, F. A. Rey, and V. Deubel.** 1999. Dengue Virus Type 1 Nonstructural Glycoprotein NS1 Is Secreted from Mammalian Cells as a Soluble Hexamer in a Glycosylation-Dependent Fashion. J. Virol. **73:**6104-6110.
40. **Fry, S. R., M. Meyer, M. G. Semple, C. P. Simmons, S. D. Sekaran, J. X. Huang, C. McElnea, C.-Y. Huang, A. Valks, P. R. Young, and M. A. Cooper.** 2011. The Diagnostic Sensitivity of Dengue Rapid Test Assays Is Significantly Enhanced by Using a Combined Antigen and Antibody Testing Approach. PLoS Negl Trop Dis **5:**e1199.
41. **Galli, S. J., and M. Tsai.** 2012. IgE and mast cells in allergic disease. Nat Med **18:**693-704.
42. **Gitlin, A. D., Z. Shulman, and M. C. Nussenzweig.** 2014. Clonal selection in the germinal centre by regulated proliferation and hypermutation. Nature **509:**637-640.
43. **Gómez Román, V. R., J. C. Murray, and L. M. Weiner.** 2014. Chapter 1 - Antibody-Dependent Cellular Cytotoxicity (ADCC), p. 1-27. *In* M. E. A. Nimmerjahn (ed.), Antibody Fc. Academic Press, Boston.
44. **Gould, E., A. Buckley, A. Barrett, and N. Cammack.** 1986. Neutralizing (54K) and non-neutralizing (54K and 48K) monoclonal antibodies against structural and non-structural yellow fever virus proteins confer immunity in mice. Journal of General Virology **67:**591-595.
45. **Gowri Sankar, S., K. J. Dhananjeyan, R. Paramasivan, V. Thenmozhi, B. K. Tyagi, and S. John Vennison.** 2012. Evaluation and use of NS1 IgM antibody detection for acute dengue virus diagnosis: Report from an outbreak investigation. Clinical Microbiology and Infection **18:**E8-E10.
46. **Gupta, S., H. R. Ansari, A. Gautam, G. P. S. Raghava, and C. Open Source Drug Discovery.** 2013. Identification of B-cell epitopes in an antigen for inducing specific class of antibodies. Biology direct **8:**27.
47. **Gutsche, I., F. Coulibaly, J. E. Voss, J. Salmon, J. d'Alayer, M. Ermonval, E. Larquet, P. Charneau, T. Krey, F. Mégret, E. Guittet, F. A. Rey, and M. Flamand.** 2011. Secreted dengue virus nonstructural protein NS1 is an atypical barrel-shaped high-density lipoprotein. Proceedings of the National Academy of Sciences.
48. **Guzman, M. G., S. B. Halstead, H. Artsob, P. Buchy, J. Farrar, D. J. Gubler, E. Hunsperger, A. Kroeger, H. S. Margolis, E. Martinez, M. B. Nathan, J. L. Pelegrino, C. Simmons, S. Yoksan, and R. W. Peeling.** 2010. Dengue: a continuing global threat. Nat Rev Microbiol **8:**S7-16.

49. **Guzman, M. G., T. Jaenisch, R. Gaczkowski, V. T. Ty Hang, S. D. Sekaran, A. Kroeger, S. Vazquez, D. Ruiz, E. Martinez, J. C. Mercado, A. Balmaseda, E. Harris, E. Dimano, P. S. A. Leano, S. Yoksan, E. Villegas, H. Benduzu, I. Villalobos, J. Farrar, and C. P. Simmons.** 2010. Multi-Country Evaluation of the Sensitivity and Specificity of Two Commercially-Available NS1 ELISA Assays for Dengue Diagnosis. PLoS Negl Trop Dis **4:**e811.
50. **Guzmán, M. G., and G. Kourí.** 2004. Dengue diagnosis, advances and challenges. International Journal of Infectious Diseases **8:**69-80.
51. **Hall, R. A., A. K. Broom, D. W. Smith, and J. S. Mackenzie.** 2002. The Ecology and Epidemiology of Kunjin Virus, p. 253-269. *In* J. Mackenzie, A. T. Barrett, and V. Deubel (ed.), Japanese Encephalitis and West Nile Viruses, vol. 267. Springer Berlin Heidelberg.
52. **Halstead, S. B.** 2008. Dengue, vol. 5. Imperial College Press, London.
53. **Halstead, S. B.** 1982. Immune enhancement of viral infection. Prog Allergy **31:**301-64.
54. **Halstead, S. B.** 1988. Pathogenesis of Dengue: Challenges to Molecular Biology. Science **239:**476-481.
55. **Halstead, S. B., and P. Simasthien.** 1970. Observations related to the pathogenesis of dengue hemorrhagic fever. II. Antigenic and biologic properties of dengue viruses and their association with disease response in the host. Yale J Biol Med **42:**276-92.
56. **Hanley, K. A., and S. C. Weaver.** 2010. Frontiers in dengue virus research. Caister Academic, Wymondham :.
57. **Hoogenboom, H. R., A. D. Griffiths, K. S. Johnson, D. J. Chiswell, P. Hudson, and G. Winter.** 1991. Multisubunit Proteins on the Surface of Filamentous Phage - Methodologies for Displaying Antibody (Fab) Heavy and Light-Chains. Nucleic Acids Research **19:**4133-4137.
58. **Hufton, S. E., P. T. Moerkerk, E. V. Meulemans, A. de Bruine, J. W. Arends, and H. R. Hoogenboom.** 1999. Phage display of cDNA repertoires: the pVI display system and its applications for the selection of immunogenic ligands. J Immunol Methods **231:**39-51.
59. **Innis, B., A. Nisalak, S. Nimmannitya, S. Kusalerdchariya, V. Chongswasdi, S. Suntayakorn, P. Puttisri, and C. Hoke.** 1989. An enzyme-linked immunosorbent assay to characterize dengue infections where dengue and Japanese encephalitis co-circulate. Am J Trop Med Hyg **40:**418 - 427.
60. **Jerne, N. K.** 1985. The generative grammar of the immune system. Bioscience Reports **5:**439-451.
61. **Khan, E., V. Mehraj, A. Nasir, N. A. Khan, B. Billoo, T. Moatter, and R. Hasan.** 2009. Evaluation of two ELISA Assay Kits against RT-PCR for diagnosis of Dengue Virus Infection in a Hospital Setting in Karachi, Pakistan. Journal of the Pakistan Medical Association **59:**390-394.
62. **Kohler, G., and C. Milstein.** 1976. Derivation of specific antibody-producing tissue culture and tumor lines by cell fusion. Eur J Immunol **6:**511-9.
63. **Koraka, P., C. P. Burghoorn-Maas, A. Falconar, T. E. Setiati, K. Djamiatun, J. Groen, and A. D. M. E. Osterhaus.** 2003. Detection of Immune-Complex-Dissociated Nonstructural-1 Antigen in Patients with Acute Dengue Virus Infections. Journal of Clinical Microbiology **41:**4154-4159.
64. **Kumarasamy, V., A. H. Wahab, S. K. Chua, Z. Hassan, Y. K. Chem, M. Mohamad, and K. B. Chua.** 2007. Evaluation of a commercial dengue NS1 antigen-capture ELISA for laboratory diagnosis of acute dengue virus infection. J Virol Methods **140:**75-9.
65. **Lee, P. D., S. Mukherjee, M. A. Edeling, K. A. Dowd, S. K. Austin, C. J. Manhart, M. S. Diamond, D. H. Fremont, and T. C. Pierson.** 2013. The Fc region of an antibody impacts the neutralization of West Nile viruses in different maturation states. J Virol **87:**13729-40.
66. **Libraty, D. H., P. R. Young, D. Pickering, T. P. Endy, S. Kalayanarooj, S. Green, D. W. Vaughn, A. Nisalak, F. A. Ennis, and A. L. Rothman.** 2002. High Circulating Levels

of the Dengue Virus Nonstructural Protein NS1 Early in Dengue Illness Correlate with the Development of Dengue Hemorrhagic Fever. Journal of Infectious Diseases **186:**1165-1168.

67. **Lima, M. d. R. Q., R. M. R. Nogueira, A. M. Bispo de Filippis, and F. B. dos Santos.** 2011. Comparison of Two Generations of the Panbio Dengue NS1 Capture Enzyme-Linked Immunosorbent Assay. Clin. Vaccine Immunol. **18:**1031-1033.
68. **Lima, M. d. R. Q., R. M. R. Nogueira, H. G. Schatzmayr, and F. B. d. Santos.** 2010. Comparison of Three Commercially Available Dengue NS1 Antigen Capture Assays for Acute Diagnosis of Dengue in Brazil. PLoS Negl Trop Dis **4:**e738.
69. **Lindorfer, M. A., J. Köhl, and R. P. Taylor.** 2014. Chapter 3 - Interactions Between the Complement System and Fcγ Receptors, p. 49-74. *In* M. E. A. Nimmerjahn (ed.), Antibody Fc. Academic Press, Boston.
70. **Loset, G. A., and I. Sandlie.** 2012. Next generation phage display by use of pVII and pIX as display scaffolds. Methods **58:**40-6.
71. **Matsuda, F., K. Ishii, P. Bourvagnet, K. Kuma, H. Hayashida, T. Miyata, and T. Honjo.** 1998. The complete nucleotide sequence of the human immunoglobulin heavy chain variable region locus. J Exp Med **188:**2151-62.
72. **McBride, W. J. H.** 2009. Evaluation of dengue NS1 test kits for the diagnosis of dengue fever. Diagnostic Microbiology and Infectious Disease **64:**31-36.
73. **Mitchell, T. J., P. W. Andrew, F. K. Saunders, A. N. Smith, and G. J. Boulnois.** 1991. Complement activation and antibody binding by pneumolysin via a region of the toxin homologous to a human acute-phase protein. Mol Microbiol **5:**1883-8.
74. **Moi, M. L., T. Omatsu, S. Tajima, C.-K. Lim, A. Kotaki, M. Ikeda, F. Harada, M. Ito, M. Saijo, I. Kurane, and T. Takasaki.** 2013. Detection of Dengue Virus Nonstructural Protein 1 (NS1) by Using ELISA as a Useful Laboratory Diagnostic Method for Dengue Virus Infection of International Travelers. Journal of Travel Medicine **20:**185-193.
75. **Mukhopadhyay, S., R. J. Kuhn, and M. G. Rossmann.** 2005. A structural perspective of the flavivirus life cycle. Nature Reviews Microbiology **3:**13-22.
76. **Mullen, L. M., S. P. Nair, J. M. Ward, A. N. Rycroft, and B. Henderson.** 2006. Phage display in the study of infectious diseases. Trends in Microbiology **14:**141-147.
77. **Muller, D. A., and P. R. Young.** 2013. The flavivirus NS1 protein: Molecular and structural biology, immunology, role in pathogenesis and application as a diagnostic biomarker. Antiviral Research **98:**192-208.
78. **Organization, W. H.** 2010. Screening donated blood for transfusion-transmissible infections: recommendations. World Health Organization.
79. **Papavasiliou, F., R. Casellas, H. Suh, X.-F. Qin, E. Besmer, R. Pelanda, D. Nemazee, K. Rajewsky, and M. C. Nussenzweig.** 1997. V(D)J Recombination in Mature B Cells: A Mechanism for Altering Antibody Responses. Science **278:**298-301.
80. **Park, S. J., and J. R. Cochran.** 2010. Protein engineering and design. CRC Press, Boca Raton.
81. **Paschke, M.** 2006. Phage display systems and their applications. Applied Microbiology and Biotechnology **70:**2-11.
82. **Peeling, R. W., H. Artsob, J. L. Pelegrino, P. Buchy, M. J. Cardosa, S. Devi, D. A. Enria, J. Farrar, D. J. Gubler, and M. G. Guzman.** 2010. Evaluation of diagnostic tests: dengue. Nature Reviews Microbiology **8:**S30-S37.
83. **Peeling, R. W., P. G. Smith, and P. M. M. Bossuyt.** 2006. A guide for diagnostic evaluations. Nature Reviews. Microbiology **4:**2-S6.
84. **Perelson, A. S., and G. F. Oster.** 1979. Theoretical studies of clonal selection: minimal antibody repertoire size and reliability of self-non-self discrimination. Journal of Theoretical Biology **81:**645-670.
85. **Petty, N. K., T. J. Evans, P. C. Fineran, and G. P. C. Salmond.** 2007. Biotechnological exploitation of bacteriophage research. Trends in Biotechnology **25:**7-15.

86. **Phillpotts, R. J., J. R. Stephenson, and J. S. Porterfield.** 1985. Antibody-dependent Enhancement of Tick-borne Encephalitis Virus Infectivity. Journal of General Virology **66:**1831-1837.
87. **Ponomarenko, J. V., and M. H. Van Regenmortel.** 2009. B cell epitope prediction. Structural Bioinformatics**:**849-879.
88. **Porterfield, J. S.** 1986. Antibody-Dependent Enhancement of Viral Infectivity, p. 335-355. *In* F. A. M. Karl Maramorosch and J. S. Aaron (ed.), Advances in Virus Research, vol. Volume 31. Academic Press.
89. **Ranjit, S., and N. Kissoon.** 2011. Dengue hemorrhagic fever and shock syndromes*. Pediatric Critical Care Medicine **12:**90-100.
90. **Rathakrishnan, A., and S. D. Sekaran.** 2013. New development in the diagnosis of dengue infections. Expert Opinion on Medical Diagnostics **7:**99-112.
91. **Rojas, R., and G. Apodaca.** 2002. Immunoglobulin transport across polarized epithelial cells. Nat Rev Mol Cell Biol **3:**944-956.
92. **Roos, A., L. H. Bouwman, D. J. van Gijlswijk-Janssen, M. C. Faber-Krol, G. L. Stahl, and M. R. Daha.** 2001. Human IgA activates the complement system via the mannan-binding lectin pathway. J Immunol **167:**2861-8.
93. **Sea, V. R. F., A. C. R. Cruz, R. Q. Gurgel, B. T. D. Nunes, E. V. P. Silva, S. S. Dolabella, and R. L. C. d. Santos.** 2013. Underreporting of Dengue-4 in Brazil Due to Low Sensitivity of the NS1 Ag Test in Routine Control Programs. PLoS One **8**.
94. **Shu, P.-Y., and J.-H. Huang.** 2004. Current Advances in Dengue Diagnosis. CLINICAL AND DIAGNOSTIC LABORATORY IMMUNOLOGY **11:**642-650.
95. **Smith, G.** 1985. Filamentous fusion phage: novel expression vectors that display cloned antigens on the virion surface. Science **228:**1315-1317.
96. **Smith, G. W., and P. J. Wright.** 1985. Synthesis of proteins and glycoproteins in dengue type 2 virus-infected vero and Aedes albopictus cells. J Gen Virol **66 (Pt 3):**559-71.
97. **Stephenson, J. R.** 2005. Understanding dengue pathogenesis: implications for vaccine design. Bulletin of the World Health Organization **83:**308-314.
98. **Suaya, J. A., D. S. Shepard, J. B. Siqueira, C. T. Martelli, L. C. S. Lum, L. H. Tan, S. Kongsin, S. Jiamton, F. Garrido, R. Montoya, B. Armien, R. Huy, L. Castillo, M. Caram, B. K. Sah, R. Sughayyar, K. R. Tyo, and S. B. Halstead.** 2009. Cost of Dengue Cases in Eight Countries in the Americas and Asia: A Prospective Study. The American Journal of Tropical Medicine and Hygiene **80:**846-855.
99. **Tambyah, P. A., E. S. C. Koay, M. L. M. Poon, R. V. T. P. Lin, and B. K. C. Ong.** 2008. Dengue Hemorrhagic Fever Transmitted by Blood Transfusion. New England Journal of Medicine **359:**1526-1527.
100. **Teles, F. R. R., D. M. F. Prazeres, and J. L. Lima-Filho.** 2005. Trends in dengue diagnosis. Reviews in Medical Virology **15:**287-302.
101. **Twiddy, S. S., C. H. Woelk, and E. C. Holmes.** 2002. Phylogenetic evidence for adaptive evolution of dengue viruses in nature. Journal of General Virology **83:**1679-1689.
102. **Vaughn, D. W., S. Green, S. Kalayanarooj, B. L. Innis, S. Nimmannitya, S. Suntayakorn, T. P. Endy, B. Raengsakulrach, A. L. Rothman, F. A. Ennis, and A. Nisalak.** 2000. Dengue Viremia Titer, Antibody Response Pattern, and Virus Serotype Correlate with Disease Severity. Journal of Infectious Diseases **181:**2-9.
103. **Vazquez, S., D. Ruiz, R. Barrero, R. Ramirez, N. Calzada, B. del Rosario Peña, S. Reyes, and M. G. Guzman.** 2010. Kinetics of dengue virus NS1 protein in dengue 4-confirmed adult patients. Diagnostic Microbiology and Infectious Disease **68:**46-49.
104. **Wang, S.** 2011. Advances in the production of human monoclonal antibodies. Antibody Technol J **1:**1-4.
105. **Wang, S. M., and S. D. Sekaran.** 2010. Evaluation of a Commercial SD Dengue Virus NS1 Antigen Capture Enzyme-Linked Immunosorbent Assay Kit for Early Diagnosis of Dengue Virus Infection. Journal of Clinical Microbiology **48:**2793-2797.

106. **Watts, D. M., K. R. Porter, P. Putvatana, B. Vasquez, C. Calampa, C. G. Hayes, and S. B. Halstead.** 1999. Failure of secondary infection with American genotype dengue 2 to cause dengue haemorrhagic fever. The Lancet **354:**1431-1434.
107. **Weber, S. S., and A. Oxenius.** 2014. Chapter 2 - Antibody-Dependent Cellular Phagocytosis and Its Impact on Pathogen Control, p. 29-47. *In* M. E. A. Nimmerjahn (ed.), Antibody Fc. Academic Press, Boston.
108. **Webster, S. D., M. D. Galvan, E. Ferran, W. Garzon-Rodriguez, C. G. Glabe, and A. J. Tenner.** 2001. Antibody-mediated phagocytosis of the amyloid beta-peptide in microglia is differentially modulated by C1q. J Immunol **166:**7496-503.
109. **Wilson, D. R., and B. B. Finlay.** 1998. Phage display: applications, innovations, and issues in phage and host biology. Can J Microbiol **44:**313-29.
110. **Wu, S.-J. L., G. Grouard-Vogel, W. Sun, J. R. Mascola, E. Brachtel, R. Putvatana, M. K. Louder, L. Filgueira, M. A. Marovich, H. K. Wong, A. Blauvelt, G. S. Murphy, M. L. Robb, B. L. Innes, D. L. Birx, C. G. Hayes, and S. S. Frankel.** 2000. Human skin Langerhans cells are targets of dengue virus infection. Nat Med **6:**816-820.
111. **Young, P. R., P. A. Hilditch, C. Bletchly, and W. Halloran.** 2000. An Antigen Capture Enzyme-Linked Immunosorbent Assay Reveals High Levels of the Dengue Virus Protein NS1 in the Sera of Infected Patients. J. Clin. Microbiol. **38:**1053-1057.
112. **Zainah, S., A. H. A. Wahab, M. Mariam, M. K. Fauziah, A. H. Khairul, I. Roslina, A. Sairulakhma, S. S. Kadimon, M. S. M. Jais, and K. B. Chua.** 2009. Performance of a commercial rapid dengue NS1 antigen immunochromatography test with reference to dengue NS1 antigen-capture ELISA. Journal of Virological Methods **155:**157-160.
113. **Zhang, W., P. R. Chipman, J. Corver, P. R. Johnson, Y. Zhang, S. Mukhopadhyay, T. S. Baker, J. H. Strauss, M. G. Rossmann, and R. J. Kuhn.** 2003. Visualization of membrane protein domains by cryo-electron microscopy of dengue virus. Nat Struct Biol **10:**907-12.

Chapter 2

ISOLATION OF SEROTYPE-SPECIFIC AND PAN-REACTIVE BINDERS AGAINST DENV NS1

2.1 INTRODUCTION

Non-structural protein 1 (NS1) is antigenic glycoprotein that is produced by dengue viruses and other flaviviruses. NS1 like other non-structural proteins produced by flaviviruses is not part of the virion. Its post translational processing and trafficking however, allows for its detection in circulation, making it an attractive diagnostic target (23). In DENV infections, the duration of NS1 detection in circulation is longer than that of detectable viremea (9, 11). Furthermore NS1 detection precedes and overlaps with detectable antibody responses in acute infections (11). The kinetics of DENV NS1 secretion and detection therefore offer a widened window of diagnostic utility when compared with virus isolation, genome detection and serology.

There is approximately 70% sequence homology amongst the four NS1 polypeptide sequences of each DENV serotype. The variation amongst DENV NS1 serotypes is not concentrated in any mutational hotspots but rather interspersed along the length of the polypeptide (Figure 2.1). This variation can be taken advantage of by isolating monoclonal antibodies that target serotype-specific regions. This is important because an ability to distinguish the infective serotype is regarded as an attractive characteristic of a DENV diagnostic assay (6, 12, 18) as the serotyping capability increases the specificity of the assay by distinguishing DENV infections from other flaviviral infections. The serotyping nature of the antibodies would also add novelty with a potentially cost cutting element in comparison to the current commercial DENV NS1 capture assays which require a subsequent test to reveal the infective DENV serotype. The targeting of distinct epitopes on NS1 from each DENV serotype also allows for balanced diagnostic sensitivity across all four DENV serotypes. The use of antibodies with reactivity to NS1 from two or more DENV serotypes in current commercial assays results in varying affinities because of inevitably varied epitope conformations caused by NS1 sequence differences. By targeting NS1 from each DENV serotype individually, the desired affinities of the isolated antibodies for the antigen can subsequently be adjusted using affinity maturation strategies.

Serotyping antibodies against DENV NS1 also have the potential to improve diagnostic sensitivity if paired with a pan-reactive antibody that avoids the immune-dominant region of DENV NS1. There exists a core immune-dominant epitope (YSWKTWG) that lies between residues 113-125 on NS1 from all four serotypes of DENV (10). Antibodies against this region are present in high proportions during secondary DENV infections. These antibodies sequester DENV NS1 in immune complexes and their binding to the immune dominant epitope can interfere with the ability of assay antibodies used in capture and detection of DENV NS1 to bind to their relevant epitopes. Improved

diagnostic sensitivity therefore relies on targeting two mutually exclusive epitopes on DENV NS1 that are spatially distinct to the immune-dominant epitope.

In seeking to isolate antibody binders against non immune-dominant epitopes, the preferred source of potential antibodies would minimize any antigen driven aspect. Phage display offers a technology that can be used to isolate such antibody fragments. Two different types of antibody display libraries exist, directed and naïve. Directed immune repertoires are constructed from mRNA that is enriched for target antigen-specific V_H and V_L genes through infection or immunization. A high proportion of the immunoglobulin mRNA encodes V genes with fine-tuned antigen binding properties. Conversely, naïve immune repertoires are assembled from pooled, existing V genes which are rearranged *in vitro* to offer varied antigen binding specificities of equally varying affinities. Naive libraries therefore offer an unshaped immune repertoire against a very large number of antigens. These libraries have been shown to have better utility in isolating binders to highly conserved proteins (16, 17). The premise behind this is that antibodies that are first produced in response to a previously un-encountered antigen will be varied and not optimized for antigen recognition. The epitopes to which these antibodies bind will therefore hypothetically vary from the epitopes for the fewer antibodies that are optimized for recognition on a subsequent encounter. The requirement for successful selection of antibodies that recognize the non-conserved regions however, depends on having a large and diverse library.

Three different biopanning strategies were used to isolate binders against recombinant DENV NS1 from three human, naïve phage libraries displaying V_H domain antibody (dAb), scFv or Fab. The first strategy involved a subtractive biopanning protocol using NS1 from other DENV serotypes to isolate serotype-specific antibodies from scFv and Fab libraries. Five serotype-specific antibody fragments were isolated. Three serotype-specific antibody fragments were isolated from the scFv library (9H2 anti DENV-1 NS1, 6A5 anti DENV-4 NS1 and 6A7 anti DENV-4 NS1) while two were isolated from the Fab library (4C11 anti DENV-2 NS1 and 7G11 anti DENV-3 NS1). This panning strategy also isolated 11 unique pan-reactive antibodies, nine of which were from the Fab library. The scFv library was interrogated again in a non-subtractive manner for high-affinity pan-reactive binders against DENV NS1. Two unique binders A1 and A2 were dominant in the panel of clones that were screened for binding to NS1 from all four DENV serotypes. The final strategy, using the V_H dAb library, involved biopanning for pan-reactive binders against DENV NS1 in which the immune-dominant epitope had been masked by a bound murine antibody. This strategy yielded a single unique antibody D1C2. The different biopanning strategies therefore collectively yielded five serotype-specific antibody fragments and 14 pan-reactive antibody fragments.

2.2.1 GENERAL RECIPES, STOCK REAGENTS AND EQUIPMENT

2.2.1.1 Culture Media

2YT – per litre; 10 g yeast extract, 16 g tryptone and 5 g NaCl

Media was autoclaved at 121°C for 20 minutes.

Variations

2YT agar – per litre add 15g agar (added prior to autoclaving)

The following supplements were added individually as required after autoclaving and cooling:

Ampicillin (A) – 1/1000 dilution of a 100 mg/mL working stock

Kanamycin (K) – 1/1000 dilution of a 30 mg/mL working stock

Tetracycline (T) – 1/1000 dilution of a 3 mg/mL working stock

Glucose (G) – to a total concentration of 2%

Lysogeny broth (LB) – per litre; 5 g yeast extract, 10 g tryptone and 10 g NaCl

Media was autoclaved at 121°C for 20 minutes.

Variations

LB agar – per litre add 15g agar (added prior to autoclaving)

The following supplements were added individually as required after autoclaving and cooling:
Ampicillin (A) – add 1/1000 dilution of a 100 mg/mL working stock

Kanamycin (K) – add 1/1000 dilution of a 30 mg/mL working stock

Glucose (G) – add to a total concentration of 2%

Sucrose (S) – add to achieve 0.4 M in final volume

2.2.1.2 Solutions

Phosphate Buffered Saline (PBS) prepared using 10 X Dulbecco's PBS (Lonza) or tablets (Amresco)

Solution autoclaved at 121°C for 20 minutes

Variations

M-PBS – add skim milk powder to varying weight/volume percentage concentrations.

PBS-Glycerol – add to 20% final concentration

PBS-T – add 0.1% Tween-20

PEG-NaCl – 20% polyethylene glycol-6000 and 2.5 M NaCl

Solution autoclaved at 121°C for 20 minutes

Elution Solution – 200 mM glycine, pH 2.5

Sterilized using vacuum-assisted filtration with a 0.45 μm HAWP membrane (Millipore)

Neutralization Buffer – 1 M Trizma, pH 7.4

Sterilized using vacuum-assisted filtration with a 0.45 μm HAWP membrane (Millipore)

2.2.1.3 Phage Display Libraries

Phage libraries displayed antibody fragments in fusion with the head capsid protein gIIIp of filamentous bacteriophage M13, achieved by cloning human antibody genes into specialised phagemid vectors. The following human naïve libraries were sources: The 'Sheets' **scFv** library, in pHEN1 phagemid vector, was obtained from Prof James Marks (UCSF) (20), a **Fab** library, in pCES1 phagemid vector (7), was obtained from the Australian Red Cross Blood Service (unpublished); and an aggregation-resistant $\mathbf{V_H}$ library, in pR2 phagemid vector, was purchased from Geneservice (UK) (5). The phagemid vectors include an inducible bacterial promoter and a periplasmic signal sequence upstream of the antibody fragment sequence. Downstream are a c-myc and/or VSV and/or histidine tag, an amber stop codon and then the gIIIp sequence (22). Transformation of suppressor XL1-Blue bacteria (Strategene) with the phagemid vector followed

by rescue of the phage with M13KO7 helper phage allows the production of phage particles that express and display antibody fragments on the tips of the gene III protein.

Diversity of the Libraries

V_H – 3.0 x 10^9

scFv – 6.7 x 10^9

Fab – 1.0 x 10^{10}

Helper Phage - M13KO7 (NEB)

2.2.1.4 Bacterial Strains

Amber codon suppressor strain XL1-Blue (Agilent - Stratagene)

Genotype: *recA1 endA1 gyrA96 thi-1 hsdR17 supE44 relA1 lac* [F´ *proAB lacI*qZΔ*M15* Tn*10* (Tetr)]

Amber codon non- suppressor strain HB2151 (GE Healthcare)

Genotype: *K12 alr ara Δ(lac-proAB) thi-1/F' proA+B lacI^q lacZΔM15*

2.2.1.5 Recombinant Antigen

Recombinant DENV-1, DENV-2, DENV-3 and DENV-4 NS1 were obtained from Professor Matthew Cooper (Institute for Molecular Bioscience, The University of Queensland). Unless where specified, all DENV NS1 used in this work was of a recombinant nature. The antigens were prepared by Alere Inc. (San Diego, U.S.A) using the NS1 sequences of clinical isolates from Western Pacific/1974 for DENV-1, Puerto Rico/1969 for DENV-2, Martinique/1999 for DENV-3 and Singapore/1995 for DENV-4. The antigens were expressed in CHO-DG44 cells and their N-terminal 7 x histidine tag was used for purification. The DENV NS1 sequences and relational homology are shown in Figure 2.1 and Figure 2.2 respectively. DENV NS1 was provided at different concentrations in a formulation buffer made up of PBS pH 7.4, 0.02% NaN_3 and 10% glycerol.

```
DENV-1          DSGCVINWKGRELKCGSGIFVTNEVHTWTEQYKFQADSPKRLSAAIGKAWEEGVCGIRSA 60
DENV-3          DMGCVINWKGKELKCGSGIFVTNEVHTWTEQYKFQADSPKRLATAIAGAWENGVCGIRST 60
DENV-2          DSGCVVSWKNKELKCGSGIFVTDNVHTRTEQYKFQPESPSKLASAIQKAHEEGICGIRSV 60
DENV-4          DMGCVVSWSGKELKCGSGIFVADNVHTWTEQYKFQPESPARLASAILNAHKDGVCGIRST 60
                * ***:.*..:**********:::*** *******.:** :*::**  * ::*:*****.

DENV-1          TRLENIMWKQISNELNHILLENDMKFTVVVGDVSGILAQGKKMIRPQPMEHKYSWKSWGK 120
DENV-3          TRMENLLWKQIANELNYILWENNIKLTVVVGDIIGVLEQGKRTLTPQPMELKYSWKTWGK 120
DENV-2          TRLENLMWKQITSELNHILSENEVKLTIMTGDIKGIMQVGKRSLRPQPTELRYSWKTWGK 120
DENV-4          TRLENVMWKQITNELNYVLWEGGHDLTVVAGDVKGVLTKGKRALTPPVNDLKYSWKTWGK 120
                **:**::****:.***::* *.  .:*::.**: *::  **: : *   : :****:***

DENV-1          AKIIGADVQNTTFIIDGPNTPECPDNQRAWNIWEVEDYGFGIFTTNIWLKLRDSYTQVCD 180
DENV-3          AKIVTAETQNSSFIIDGPNTPECPSASRAWNVWEVEDYGFGVFTTNIWLKLREVYTQLCD 180
DENV-2          AKMLSTELHNQTFLIDGPETAECPNTNRAWNSLEVEDYGFGVFTTNIWLRLREKQDAFCD 180
DENV-4          AKIFTPEARNSTFLIDGPDTSECPNERRAWNFLEVEDYGFGMFTTNIWMKFREGSSEVCD 180
                **:. .: :* :*:****:*.***.  ****  ********:******:::*:    .**

DENV-1          HRLMSAAIKDSKAVHADMGYWIESEKNETWKLARASFIEVKTCIWPKSHTLWSNGVLESE 240
DENV-3          HRLMSAAVKDERAVHADMGYWIESQKNGSWKLEKASLIEVKTCTWPKSHTLWSNGVLESD 240
DENV-2          SKLMSAAIKDNRAVHADMGYWIESALNDTWKIEKASFIEVKSCHWPKSHTLWSNGVLESE 240
DENV-4          HRLMSAAIKDQKAVHADMGYWIESSKNQTWQIEKASLIEVKTCLWPKTHTLWSNGVLESQ 240
                 :*****:**.:***********  * :*:: :**:****:* ***:**********:

DENV-1          MIIPKIYGGPISQHNYRPGYFTQTAGPWHLGKLELDFDLCEGTTVVVDEHCGNRGPSLRT 300
DENV-3          MIIPKSLAGPISQHNHRPGYHTQTAGPWHLGKLELDFNYCEGTTVVITENCGTRGPSLRT 300
DENV-2          MVIPKNFAGPKSQHNNRPGYHTQTAGPWHLGKLEMDFDFCEGTTVVVTEDCGNRGPSLRT 300
DENV-4          MLIPKSYAGPFSQHNYRQGYATQTVGPWHLGKLEIDFGECPGTTVTIQEDCDHRGPSLRT 300
                *:***  .** **** * ** ***.*********:**. * ****.: *.*. *******

DENV-1          TTVTGKTIHEWCCRSCTLPPLRFKGEDGCWYGMEIRPVKEKEENLVKSMVSA 352
DENV-3          TTVSGKLIHEWCCRSCTLPPLRYMGEDGCWYGMEIRPISEKEENMVKSLVSA 352
DENV-2          TTASGKLITEWCCRSCTLPPLRYRGEDGCWYGMEIRPLKEKEENLVSSLVTA 352
DENV-4          TTASGKLVTQWCCRSCTMPPLRFLGEDGCWYGMEIRPLSEKEENMVKSQVTA 352
                **.:** : :*******:****: *************:.*****:*.* *:*
```

Figure 2.1 Alignment of clinical isolate sequences of DENV NS1. These sequences were used for recombinant expression of DENV NS1. '*****' denotes positions with fully conserved residues, '**:**' denotes conservation of residues with similar properties '**.**' denotes weakly similar amino acid residues while no symbol denotes no homology. The amino differences amongst NS1 from all four DENV serotypes are scattered along the length of the sequences.

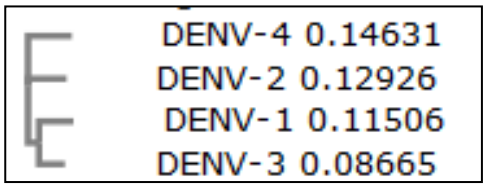

Figure 2.2 Cladogram of the inferred homology amongst DENV NS1. DENV-4 NS1 is shown as the ancestral sequence that is most closely related to DENV-2 NS1. A divergence is then shown with both DENV-1 and DENV-3 NS1 which are more closely related to each other.

2.2.1.6 Murine Antibodies

Murine antibody GUS2 which recognizes an immune dominant epitope on NS1 from all four DENV serotypes was obtained from the laboratory of Professor Paul R. Young (School of Chemistry and Molecular Biosciences, The University of Queensland)

2.2.1.7 Equipment

OD_{600} measurements were performed using the BioPhotometer (Eppendorf)

Absorbance values of chromogenic signals in plate formats were measured using the Spectramax (Molecular Devices) or the PowerWave XS2 (Biotek – Millenium Science).

Protein and nucleic acid concentrations were measured using the NanoDrop™ 1000 Spectrophotometer (Thermo Scientific).

Thermal cycling reactions were performed using the Veriti® 96-Well Thermal Cycler (Applied Biosystems).

2.2.2 BIOPANNING USING PURIFIED ANTIGEN

Three different panning strategies were employed to isolate binders depending on whether serotype-specific or pan-reactive binders were sought.

i. For isolation of serotype-specific antibodies, a subtractive panning strategy was employed. 1 mL of NS1 at 45 µg/mL from all four DENV serotypes was diluted in PBS and added to an immunotube (Nunc). The tubes were incubated overnight at room temperature on a rotating

wheel to allow for antigen immobilisation to the walls of the tube. On day two, only one of the tubes was used as the positive antigen for that selection while the other three tubes were used as the negative antigens. The negative antigens were used in a subtractive manner to deplete any binders that recognize NS1 from any other DENV serotype. In instances where binders to DENV-1 NS1 were sought for example, the phage library was first added to an immunotube coated with DENV-2 NS1. Unbound phage were decanted from that immunotube and added to another immunotube coated with DENV-3 NS1 and then a DENV-4 NS1 coated immunotube, before finally being exposed to a DENV-1 NS1 coated on the last immunotube. The unbound phage were then discarded.

ii. For isolation of pan-reactive binders, 1 mL of NS1 (45 μg/mL) from a single DENV serotype was diluted in PBS and added to an immunotube. NS1 from a different DENV serotype was used in each round of biopanning in order to isolate binders to NS1 from all four DENV serotypes. The tube with antigen was incubated overnight at room temperature on a rotating wheel to allow for antigen immobilisation. On day two, the phage library was added to the immunotubes. Unbound phage were discarded.

iii. To isolate pan-reactive binders which recognize epitopes that are removed from the immune-dominant epitope, a pan-reactive antibody (GUS2) that binds that epitope was utilized. GUS2 was diluted in PBS and immobilized on an immunotube at a concentration of 1 mg/mL. The tube was incubated overnight at room temperature on a rotating wheel. On day two, the immobilised antibody was used to capture NS1 (45 μg/mL) from a single DENV serotype. Excess DENV NS1 that was not captured was discarded. The phage library was then added to the tube with antibody-bound antigen. Unbound phage were discarded.

Day 1

DENV NS1 or GUS2 was diluted at an appropriate concentration in PBS and added to a 5 mL immunotube (Nunc). The tube(s) was/were capped and placed on a rotating wheel overnight at room temperature.

5 ml 2YT broth with tetracycline was inoculated with a single colony of XL1-Blue from a streak plate and incubated overnight at 37 ˚C whilst shaking at 220 rpm.

Day 2

The contents of the immunotubes were discarded and the tubes were washed three times with PBS. The surface of the tubes was then saturated with 10% M-PBS to block any remaining binding sites on the immunotubes. The blocking proceeded for 1 hour on the rotating wheel at room temperature. Meanwhile, an appropriate concentration of DENV NS1 and/or phage library in a 1 mL volume was made in 2% M-PBS. The blocking solution was discarded and DENV NS1 in M-PBS or the phage library in M-PBS was added to the tube and incubated on the rotating wheel for 1 hour. In the first round of biopanning, 1 000-fold representation of the phage library was added. The input titre of phage recovered from each round, was decreased ten-fold with each subsequent iteration of biopanning. Biopanning was carried out as described for each strategy above and all incubations proceeded for 1 hour on the rotating wheel.

In the final step of all three strategies, unbound non-specific phage particles were discarded. The tubes were washed three times with PBS and then three times with PBS-T. The number of washes with each buffer was increased by one for each biopanning iteration. The bound phage particles were pH eluted and then neutralized. Elution was performed by adding 1 mL of Elution Solution to the tube and incubating it for 8 minutes on a rotating wheel. The phage eluate was added to 1 mL of Neutralisation Buffer. Glycerol to a final concentration of 20% was added to half of the neutralized eluate for storage at -80 ˚C. The other half was used to infect XL1-Blue cells for amplification of the isolated binders.

375 µL of the overnight culture from day one was added to a fresh 15 mL volume of 2YT broth with tetracycline. The culture was incubated at 37 ˚C whilst shaking at 220 rpm until OD_{600} between 0.6 and 0.8. 10 mL of the log phase culture was infected with 1 mL of neutralized eluate during a 30 minute incubation at 37 ˚C.

150 µL of the infected culture was sampled and five, serial 10-fold dilutions were made to determine the output titre. 10 µL of each dilution was spotted on a 2YTAG plate. The plate was incubated overnight at 37 ˚C.

Meanwhile, the rest of the infected cells were pelleted by centrifugation at 2 000 x g for 15 minutes. The cells were resuspended in 0.5 mL 2YT broth and spread evenly over two 150 mm 2YTAG agar plates. The plates were incubated overnight at 30 ˚C to ensure propagation of most clones.

Day 3

The output titre was calculated from dilutions of infected cells with countable colonies. An enrichment in the output (the number of cells infected with the eluted phage) relative to the input (the number of phage particles used for biopanning) should occur with each round of biopanning.

Output titre/10 mL volume = number of colonies x dilution factor x 1000 (volume adjustment)

Glycerol stocks of infected cells were made by scraping the bacterial cells from both overnight plates using 10 mL total volume of 2YTAG broth. Glycerol was added to the recovered bacterial slurry at a final concentration of 20%. Some of the glycerol stock was used for phage rescue while the rest was aliquoted and stored at -80 ˚C.

Phage particles were prepared by sub-culturing a volume of the glycerol stock in 50 mL 2YTAG broth to achieve a starting OD_{600} between 0.05 and 0.1. The culture was incubated at 37 ˚C whilst shaking at 220 rpm until it reached OD_{600} between 0.4 and 0.6. 1 x 10^{11} M13KO7 helper phage particles were added to the culture. Infection with the helper phage occurred during a 30 minute incubation 37 ˚C. The culture was incubated for a further 30 minutes at 37 ˚C whilst shaking at 220 rpm. Co-infected cells were recovered by centrifugation at 2 000 x g for 20 minutes. The cells were resuspended in 100 mL 2YTAK and incubated overnight at 30 ˚C whilst shaking at 220 rpm.

2.2.3 PHAGE PRECIPITATION

Phage particles secreted into the culture media were harvested by centrifugation of the overnight culture at 2000 x g for 30 minutes. Phage particles were precipitated from the culture supernatant by addition of 1/5 volume of PEG-NaCl and incubation on ice for 1 hour. The precipitate was pelleted by centrifugation at 10 000 x g at 4 ˚C for 20 minutes. The supernatant was discarded and the pellet resuspended in 10 mL cold PBS. The suspension was subjected to a second round of precipitation on ice using 1/5 volume of PEG-NaCl and centrifugation at 10 000 x g at 4 ˚C for 20 minutes. The final pellet was resuspended in 3 mL cold PBS-glycerol and the purified phage particles were titred and stored in aliquots at -80 ˚C.

2.2.4 PHAGE TITRE

Day 1

A single colony of XL1-Blue was picked from a streak plate and used to inoculate 5 mL 2YT with tetracycline. The culture was incubated overnight at 37 ˚C whilst shaking at 220 rpm.

Day 2

50 µL of the overnight culture was sub-cultured into a fresh 5 mL volume of 2YT with tetracycline. The culture was incubated at 37 ˚C whilst shaking at 220 rpm until OD_{600} between 0.6 and 0.8 as measured by the BioPhotometer (Eppendorf). Ten, ten-fold dilutions of purified phage in PBS were made in 1.5 mL tubes. 1 µL was removed from each dilution and transferred to a new corresponding 1.5 mL tube. 100 µL of the log-phase culture was added to each tube. Bacterial infection with phage occurred during a 30 minute incubation at 37 ˚C. 10 µL of each dilution was spotted on a 2YTAG agar plate which was incubated overnight at 37 ˚C

Day 3

The number of countable colonies that corresponded to the relevant phage dilution was used to calculate the phage titre.

cfu/mL = number of colonies x dilution factor x 10 000 (volume adjustment)

2.2.5 MONOCLONAL PHAGE ELISA

To determine the binding reactivity of isolated antibody fragments displayed on phage particles, direct binding ELISA against DENV NS1 was performed.

Day 1

Round 3 biopanning glycerol stock were 16-streaked onto multiple 2YTAG agar plates. The plates were incubated overnight at 37 ˚C.

Day 2

90 single colonies were picked and inoculated into a 96 well microtitre plate with 150 µL of 2YTAG in each well. Wells H7 to H12 were kept as sterile technique controls. The plate was incubated overnight at 37 ˚C whilst shaking at 180 rpm.

Day 3

A new plate with 150 µL of 2YTAG in each well was used to sub-culture 5 µL of the overnight culture in corresponding wells. Glycerol was added at 20% final concentration to the overnight culture plate and was stored at -80 ˚C. The new sub-cultured plate was incubated for 3 hours at 37 ˚C whilst shaking at 180 rpm. To rescue the phage, a 50 µL 2YT broth volume containing 4 x 10^8 pfu of M13KO7 helper phage was added to each well. The plate was incubated at 37 ˚C for 30 minutes and then a further 30 minutes at 37 ˚C whilst shaking at 180 rpm. The plate was spun at 3 200 x g for 20 minutes and the supernatant was discarded. The bacterial pellets were resuspended in 200 µL 2YTAK and incubated overnight at 30 ˚C whilst shaking at 180 rpm.

200 µL of purified DENV1-4 NS1 was diluted to 3 µg/mL in PBS (Lonza), and used to coat the wells of a MaxiSorp plate (NUNC). The plate was incubated overnight at 4 ˚C.

Day 4

Soluble phage particles were harvested by centrifugation of the overnight culture plate at 3 200 x g for 10 minutes. The supernatants were transferred into a new microtitre plate in corresponding wells.

The unbound DENV NS1 was discarded. This was followed by three consecutive washes with PBS-T. The plate was blocked for 1 hour using 10% M-PBS and then the blocking buffer was discarded.

100 µL of the phage supernatants, diluted 1:1 in the blocking buffer, was added to relevant wells. Following a 1 hour incubation, three washes with PBS-T were performed. Probing for phage binding was performed with 200 µL of HRP-conjugated anti-M13 (GE Healthcare) diluted to 0.1 µg/mL in 10% M-PBS. Three final washes with PBS-T were performed, then 100 µL TMB substrate (Sigma Aldrich) was added to develop the chromogenic signal. The reaction was stopped with 2N sulphuric acid and the absorbance at 450 nm was measured.

2.2.6 SEQUENCING OF PHAGEMIDS

Glycerol stocks of relevant clones were streaked out on a 2YTAG agar plate and incubated overnight at 37 ˚C. The next day, a single colony was picked with a sterile loop and used to inoculate 5 mL 2YTAG broth. The culture was incubated at 37 ˚C overnight while shaking at 220 rpm. The next day, phagemid DNA was extracted using HiYield™ Plasmid Mini Kit (Real Biotech Corporation) as per the manufacturer's instructions. The concentration of the phagemid DNA was determined using the NanoDrop 1000 (Thermo Scientific). 12 µL total volume reactions with 600 ng of phagemid DNA and 1 µL of 10 µM working stock concentration of the appropriate phagemid-specific forward or reverse primers (Table 2.1 Primers for sequencing of pahgemid-encoded antibody fragments) were sent for Sanger Sequencing by the Australian Genome Research Facility (Brisbane).

Table 2.1 Primers for sequencing of phagemid-encoded antibody fragments

Phagemid Vector	Primer
pR2	For 5'-CAGGAAACAGCTATGAC-3'
pR2	Rev 3'-CCTCATACAGAAAATTC-5'
pHEN1	For 5'-CAGGAAACAGCTATGAC-3'
pHEN1	Rev 3'-CCTCATACAGAAAATTC-5'
pCES1	V_L For 5'-TTATTCGCAATTCCTTTAGTTGTTCC-3'
pCES1	C_L Rev 3'-GGCTGCCGTAGGCAATAGG-5'
pCES1	V_H For 5'-GGCGCGCCAATTCTATTTCAAGG-3'
pCES1	C_H Rev 3'-CCCATTCAGATCCTCTTCTGAGATGAG-5'

2.2.7 QUIKCHANGE SITE DIRECTED MUTAGENESIS

Clone D1C2 V_H dAb sequence included within its sequence, a T-A-G amber stop codon. To avoid expression of a truncated polypeptide in non-suppresor expression hosts, a single point mutation was performed to allow coding for a glutamine residue (C-A-G) instead. This change was performed using the QuikChange Site-Directed Mutagenesis Kit (Agilent Technologies) according to manufacturer's instructions. Two primers were designed to effect the relevant mutation.

QuikChange Mutagenesis
20 ng DNA template
125 ng forward primer
125 ng reverse primer
1μL dNTP mix (Bioline)
25U *Pfu Turbo* DNA polymerase
10 x reaction buffer
H2O to 50 μL total volume

Forward primer 5' – GAGTGGGTATCAGGCATT**CAG**GTGCAAAACGGTAGC – 3'

Reverse primer 3' – GCTACCGTTTTGCAC**CTG**AATGCCTGATACCCACTC – 5'

PCR Cycling Conditions
95 ˚C – 30 seconds
12 cycles of: **95 ˚C – 30 seconds** **55˚C – 30 seconds** **68˚C – 5.5 minutes**
4˚C – hold

DpnI digestion of parental phagemid was performed by gently mixing 10 units of DpnI restriction endonuclease with the PCR amplification reaction. The mixture was centrifuged briefly and then incubated for 1 hour at 37 ˚C.

The DpnI digested plasmid was transformed into XL1-Blue Supercompetent Cells (Stratagene). 50 μL of the cells were incubated on ice for 30 minutes with 5 μL of DpnI treated DNA. The cells

were heat pulsed at 42 ˚C for 45 seconds and then returned to ice for 2 minutes. 500 µL of SOC medium was added to the cells which were incubated at 37 ˚C for 1 hour while shaking at 220 rpm. 100 µL of the transformation reaction was spread on a lysogeny broth agar plate supplemented with ampicillin and incubated overnight at 37 ˚C.

Confirmation of the incorporation of the desired mutation was performed by sequencing of the phagemid DNA from a few colonies picked from the overnight agar plate.

2.2.8 PERIPLASMIC EXPRESSION OF SOLUBLE ANTIBODY FRAGMENTS

Day 1

A scraping of HB2151 non-supressor strain glycerol stock was 16-streaked onto a LB agar plate. The plate was incubated for 10 hours at 37 ˚C.

Day 2

10 mL of LB was inoculated with a single colony of HB2151. The culture was incubated overnight at 37 ˚C while shaking at 220 rpm.

Day 3

250 µL of the overnight culture was added to 10 mL of LB and incubated at 37 ˚C whilst shaking at 220 rpm until OD_{600} of between 0.6 and 0.8 is reached as measured on the BioPhotometer (Eppendorf). Ten, ten-fold serial dilutions of purified phage from the relevant clone were made in PBS. 100 µL of the HB2151 culture was added to each dilution. To infect the bacteria with phage, the mixtures were incubated at 37 ˚C for 30 minutes. 20 µL of the mixtures that correspond with phage dilutions 10^{-5} up to 10^{-10} were spread on LBAG plates and incubated overnight at 37 ˚C.

Day 4

A single colony of infected HB2151 was picked from a plate with an appropriate dilution of phage that yielded separate single colonies. The colony was used to inoculate 10 mL LBAG and incubated overnight at 37 ˚C.

Day 5

1 mL of the overnight culture was stocked by adding glycerol to a final concentration of 20%. The glycerol stocks were stored at - 80 ˚C.

3.5 mL of the overnight culture was also added to 350 mL LBAG and incubated at 37 ˚C whilst shaking at 220 rpm until OD_{600} of between 0.8 and 0.9. The bacterial cells were harvested by centrifugation at 1 500 x g for 10 minutes. The supernatant was discarded and the pellet resuspended in the same volume of LBSA with isopropyl-beta-D-thiogalactopyranoside (IPTG) at a final concentration of 0.2 mM. The culture was incubated for 16 hours at room temperature whilst shaking at 180 rpm.

Day 6

The bacterial cells were collected from the culture by centrifugation at 3 200 x g for 20 minutes. The supernatant was decanted and kept at 4 ˚C. The cells in the bacterial pellet were gently lysed with cold TES buffer (200 mM Tris HCl, 20% sucrose, 1 mM EDTA, pH 8.0) by resuspending and shaking at 180 rpm whilst on ice for 1 hour. The cell suspension was then centrifuged at 10 000 x g for 40 minutes at 4 ˚C. The supernatant, made up of the soluble periplasmic extract was then pooled with the cell culture supernatant and then subjected to appropriate Affinity Chromatography Purification 2.2.12.

2.2.9 REFORMATTING OF ANTIBODY FRAGMENTS INTO HUMAN IGG1

The In-Fusion® HD Cloning Kit (Clontech) was used to enable ligation-free insertion of variable regions of the isolated antibody fragments into separate mAbXpress vectors (15) that code for human constant regions of either the κ/λ light chains or the IgG1 heavy chain.

Variable gene-specific (V_H and V_L) primers (Geneworks) with 15 bp extensions complementary to the expression vector ends were used to PCR amplify the variable genes from the phagemid vectors.

PCR
DNA Template 0.1 pg – 20 ng
200 nM Forward Primer
200 nM Reverse Primer
10 x AccuPrime™ PCR Buffer (Life Technologies) 5 µL
AccuPrime™ Taq High Fidelity (Life Technologies) 0.2 µL
Nuclease-Free Water to 50 µL

PCR Cycling Conditions
95 ˚C – 2 minutes
30 cycles of: **95 ˚C – 15 seconds** **55 ˚C – 15 seconds** 68 ˚C – 30 seconds
68 ˚C – 7 minutes
4 ˚C – hold

Part of the PCR reaction volume was used to analyze the amplification products by agarose gel electrophoresis.

5 µL of the PCR reaction was treated with 2 µL of Cloning Enhancer (Clontech). The mixture was incubated at 37 ˚C for 15 minutes and then 80 ˚C for 15 minutes in a thermal cycler.

κ light chain (NBF304) Figure 2.1, λ light chain (NBF326) Figure 2.4 and IgG1 heavy chain vectors (NBF305) Figure 2.5 were linearized using a single endonuclease restriction enzyme: SacI (NEB).

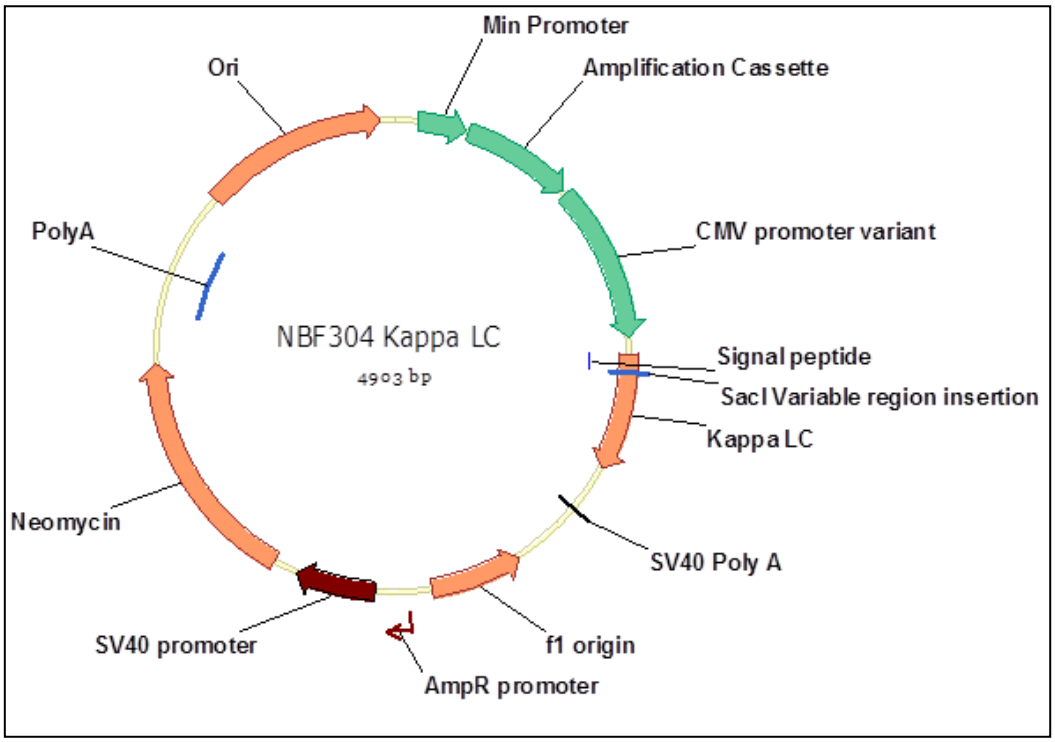

Figure 2.3 Plasmid map of κ light chain vector (NBF304). SacI linearization site used for In-Fusion® cloning is shown between the signal peptide and the kappa light chain constant gene sequence.

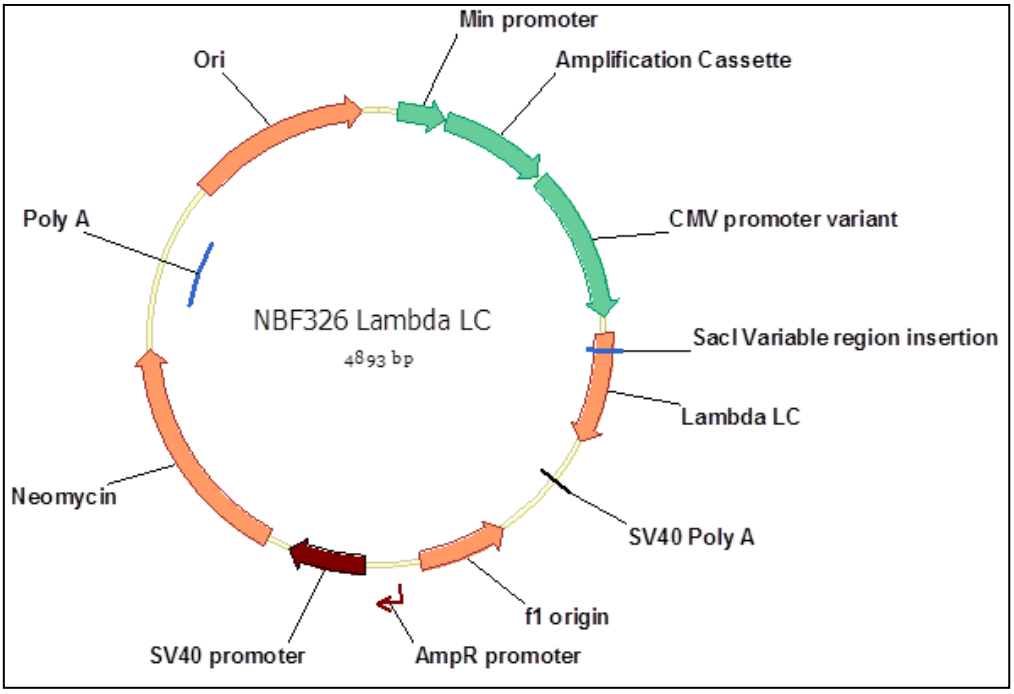

Figure 2.4 Plasmid map of λ light chain vector (NBF326). SacI linearization site used for In-Fusion® cloning is shown upstream of the lambda light chain constant gene sequence.

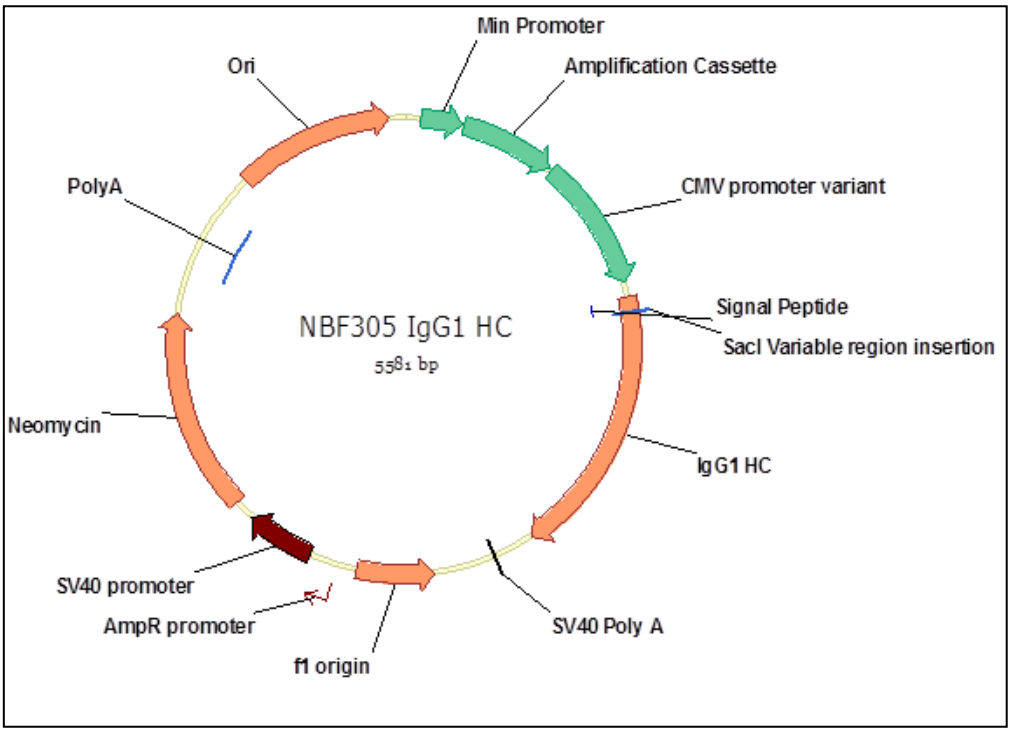

Figure 2.5 Plasmid map of IgG1 heavy chain vector (NBF305). SacI linearization site used for In-Fusion® cloning is shown between the signal peptide and the IgG1 constant gene sequence.

Restriction Endonuclease Digest
1 µg DNA Vector
10 x Buffer 4 (NEB) 2 µL
10 x BSA 2 µL
SacI (NEB) 10 units
Nuclease-Free Water to 20 µL Volume
Incubate 37 C for 4hours

The linearized vector was electrophoresed on a 1% agarose gel and the appropriate band was excised and purified using the QIAEX II Gel Extraction Kit (Qiagen) according to manufacturer's instructions.

Cloning enhancer-treated PCR products were cloned into the linearized vectors using In-Fusion® HD Enzyme (Clontech).

In-Fusion® Cloning
Linearized Vector 50-200 ng
Cloning enhancer-treated PCR product 4 µL
5 x In-Fusion® HD Enzyme Premix
Nuclease-Free Water to 10 µL Volume

All components were incubated at 50 ˚C for 15 minutes and then used for transformation of Gold efficiency, α-Select Chemically Competent Cells (Bioline) according to manufacturer's instructions.

100 µL of the transformation reaction was spread on LB-Kanamycin agar plates and incubated overnight at 37 ˚C.

Colonies that grew overnight were screened by colony PCR.

Colony PCR
Bacterial Colony – DNA Template
100 nM Forward Primer
100 nM Reverse Primer
Platinum PCR SuperMix High Fidelity (Life Technologies) 10 µL

In all instances the forward primer was mAbX Seq For. The reverse primers were mAbX Seq hG1 Rev, mAbX Seq hκ Rev or mAbX Seq hλ Rev.

PCR Cycling Conditions
95 ˚C – 2 minutes
25 cycles of: **95 ˚C – 15 seconds** **55 ˚C – 15 seconds** **68 ˚C – 45 seconds**
68 ˚C – 1 minute
4 ˚C – hold

The presence of an insert of an appropriate size during colony PCR screening was confirmed by agarose gel electrophoresis. Relevant colonies were grown overnight in 5 mL LB broth supplemented with kanamycin. The cultures were grown at 37 ˚C whilst shaking at 220 rpm. The PureLink™ Quick Plasmid Miniprep Kit (Life technologies) was used to purify plasmid DNA for

Sanger sequencing at AGRF (Sequencing of Plasmids 2.2.6) The primers used for colony PCR screening were also utilized for sequencing.

Following correct sequence confirmation, PureLink™ HiPure Plasmid Filter Maxiprep Kits (Life Technologies) were used for DNA purification from a 400 mL LB broth and kanamycin culture. The DNA was used for mammalian cell expression of IgG1 antibodies.

2.2.10 REFORMATTING OF ANTIBODY FRAGMENTS INTO HUMAN DAB FC

V_H dAb D1C2 was sub-cloned into a proprietary dAb Fc mammalian expression vector (NBF218) using endonuclease restriction sites BamHI and NheI. This vector contains an immunoglobulin kappa leader sequence, followed by BamHI and NheI sites for insertion of a gene of interest, followed by a human Fc coding region. The vector carries the β–lactamase gene that confers ampicillin resistance for propagation in *E. coli*.

PCR amplification of the V_H dAb from phagemid DNA utilized primers that introduced the BamHI and NheI restriction endonuclease sites.

V_H dAb D1C2 For 5'- GTGCCCGGATCCACCGGCGAGGTGCAGCTGTTGGAGTC – 3'

V_H dAb D1C2 Rev 3' – GGGACCAGTGGCAGAGCTCGCGATCGTGGGTG – 5'

PCR
50 ng Phagemid DNA Template
200 nM Forward Primer
200 nM Reverse Primer
Platinum PCR SuperMix High Fidelity (Life Technologies) 50 µL

PCR Cycling Conditions
95 ˚C – 2 minutes
25 cycles of: **95 ˚C – 15 seconds** **55 ˚C – 15 seconds** **68 ˚C – 45 seconds**
68 ˚C – 1 minute
4 ˚C – hold

The PCR products and the NBF218 vector were both subjected to restriction endonuclease digestion with BamHI and NheI. Digested insert and vector were both run on a 1% agarose gel at 90 V for 25 minutes. The appropriate bands were excised and purified using the Wizard SV Gel and PCR Clean-Up System (Promega)

Restriction Endonuclease Digest
3 µg NBF218 Vector OR 0.5 µg V_H dAb D1C2 insert
10 x CutSmart™ buffer (NEB) 5 µL
BamHI (NEB) 20 units
NheI (NEB) 20 units
Nuclease-Free Water to 50 µL Volume
Incubate 37 C for 8h

Ligation of the NBF218 vector and V_H dAb D1C2 insert was performed using Rapid DNA Ligation Kit (Roche).

Ligation Conditions
150 ng digested insert V_H dAb D1C2
50 ng digested and gel purified NBF218 Vector
1uL 5x DNA Dilution Buffer
5uL 2X DNA Ligation Buffer
0.5uL DNA Ligase

10 µL total volume reaction was incubated at room temperature for 15 minutes and then 2 µL used for transformation of Gold efficiency, α-Select Chemically Competent Cells (Bioline) according to manufacturer's instructions.

100 µL of the transformation reaction was spread on LB-Ampicillin agar plates and incubated overnight at 37 ˚C.

Colonies that grew overnight were screened by colony PCR as previously outlined for Reformatting of Antibody Fragments into Human IgG1 2.2.9. The same clone-specific primers were used for both PCR amplification and sequencing to ascertain that the correct dAb sequence was integrated into the NBF218 vector.

Following correct sequence confirmation, PureLink™ HiPure Plasmid Filter Maxiprep Kits (Life Technologies) were used for DNA purification from a 400 mL LB broth and ampicillin culture. The DNA was used for mammalian cell expression of V_H dAb Fc.

2.2.11 MAMMALIAN CELL EXPRESSION OF ANTIBODIES

For expression of fully assembled IgG1, a κ or λ light chain plasmid and a IgG1 heavy chain plasmid were co-transfected into Chinese hamster ovary cells adapted for suspension culture (CHO-S). For expression of VH dAb Fc, the NBF218 vector was singly transfected into CHO-S cells.

A cell density of 3.0 x 10^6 CHO-S cells per mL cultured in CD-CHO medium (Life Technologies) supplemented with 8 mM GlutaMAX™ (Life Technologies) was used for transfection. Transfection complexes were prepared using serum-free complex medium OptiPRO™ (Life Technologies), transfection reagent PEIpro™ (Polyplus transfection) and plasmid DNA.

Transfection Complexes for 1 L Total Culture Volume
267 mL of 3.0 x 10^6 CHO-S cells/mL
67 mL OptiPRO™
2.1 mL PEIpro™
533 µg plasmid DNA (266 µg per LC/HC plasmid)

Complexes were prepared in sterile 50 mL tubes (BD) by adding plasmid DNA into half the required OptiPRO™ (33.5 mL) and adding PEIpro™ to the other half the required volume of OptiPRO™ (33.5 mL). The two volumes of OptiPRO™ with both DNA and PEIpro™ were gently combined and incubated at room temperature for 15 minutes. The complexes were then added to the CHO-S cells and incubated at 37 ˚C for 4 hours in a humidified 7.5% CO_2 incubator whilst shaking at 130 rpm.

After the 4 hour incubation, the transfected CHO-S cells were subjected to a 1 : 2 dilution post-transfection feed. 512 mL of fresh CD-CHO with 8 mM GlutaMAX™ (Life Technologies) was supplemented with 75 mL Efficient Feed A (Life Technologies), 75 mL Efficient Feed B (Life Technologies), and 4 mL Anti-Clumping Agent (Gibco).

The fed culture was incubated at a hypothermic 32 ˚C in a humidified, 7.5% CO_2 incubator whilst shaking at 130 rpm. Antibodies were secreted into the culture media during the continuous culture which was maintained for up to 14 days or until cell viability dropped to 70%.

2.2.12 AFFINITY CHROMATOGRAPHY PURIFICATION

Affinity chromatography purification was performed using the AKTA Explorer chromatography system (GE Healthcare). Either a 5 mL HiTrap® MabSelect™ SuRe column (GE Healthcare) or a 5 mL HisTrap™ Excel column (GE Healthcare) was used for purification depending on the affinity tags that were present. The system and columns were cleaned by flushing with 0.5 M NaOH followed by neutralization with 1 M Tris HCl pH 8.3.

HisTrap™ Excel column (GE Healthcare)

The system and column were equilibrated using a pH 7.4 basic buffer made with 20 mM Na_2HPO_4 and 500 mM NaCl. Clarified supernatant [ultra-centrifugation or double filtration with Sartobran P300, 0.45/0.2 µm capsule filters (Sartorium Stedim)] was pH adjusted to 7.1 and loaded onto the

column at a flow rate of 1 mL per minute. Elution was performed using basic buffer that had been supplemented with a gradient of imidazole concentrations (50 mM, 300 mM and 500 mM). The eluted product was desalted, buffer-exchanged and concentrated using Macrosep Advance Centrifugal Devices (Pall) of an appropriate molecular weight cut-off.

HiTrap® MabSelect™ SuRe (GE Healthcare)

Packed recombinant Protein A Sepharose Fast Flow (GE Healthcare)

The system and column were equilibrated using 1 x PBS (Lonza). Clarified supernatant [ultra-centrifugation or double filtration with Sartobran P300, 0.45/0.2 µm capsule filters (Sartorium Stedim)] was pH adjusted to 7.1 and was loaded onto the column at a flow rate of 1 mL per minute. Elution was performed using 0.1 M glycine pH 2.7 followed by neutralization with 1/10 total elution volume of 1 M Tris HCl pH 8.3. The neutralized product was desalted, buffer-exchanged and concentrated using Macrosep Advance Centrifugal Devices (Pall) of an appropriate molecular weight cut-off.

2.2.13 DIRECT ELISA

To determine the binding reactivity of soluble antibody fragments produced by periplasmic expression in HB2151 bacterial cells or antibodies expressed in CHO-S culture, a direct binding ELISA against DENV NS1 was performed. 200 µL of purified recombinant DENV1-4 NS1 was diluted to 3 µg/mL in PBS. The diluted antigen was coated on a MaxiSorp plate (Nunc) overnight at 4˚C. The unbound protein was discarded and followed by 3 consecutive washes with PBS-T. The plate was blocked using 400 µL of 2% M-PBS. The blocking buffer was discarded after incubation for 1 hour at room temperature. 200 µL of 3 µg/mL soluble antibody fragments or reformatted antibodies diluted in 2% M-PBS were added to relevant wells. Following one hour incubation, three washes with PBS-T were performed. The plate was probed with 200 µL of HRP-conjugated anti-human lambda/anti-human kappa (The Binding Site) or HRP-conjugated anti human c-Myc (Miltenyi Biotec) or HRP-conjugated anti human IgG [γ chain specific] (Sigma Aldrich) diluted to 0.1 µg/mL in 2% M-PBS. The plate was incubated for an hour at room temperature. Three final washes with PBS-T were performed and then 100 µL TMB substrate (Sigma Aldrich) was added to develop the chromogenic signal. The reaction was stopped with 2N sulphuric acid and the absorbance at 450 nm was measured.

2.3 RESULTS

The success of a biopanning campaign is determined by the enrichment of target-specific binders from the phage displayed antibody library in iterative biopanning cycles as well as the isolation of unique monoclonal antibody fragments. A comparison of the number of titred phage particles input into the biopanning process versus the number of cells that were infected by the eluted phage particles (output) was performed to determine enrichment between each successive biopanning round. A monoclonal phage ELISA was performed with up to 90 clones displaying varying antibody fragments that were randomly screened for their ability to recognize their target antigen. Linkage of phenotype and genotype in phage display systems allowed for the phagemid DNA of the identified clones to be sequenced in order to deduce the amino acid sequence of the antibody fragments that bind the target antigen. Clustal Omega (EMBL-EBI) was used to determine the uniqueness of each isolated clone by performing amino acid sequence alignments. IMGT/V-QUEST online software was used to facilitate the identification of the complementarity determining regions (CDRs), and variable gene families of each heavy and/or light chain by using the clones' nucleotide sequences.

In the phage display system the antibody fragment is tethered to the bacteriophage as a fusion protein with gIIIp. To determine the ability of the antibody fragment to recognize the target antigen on its own, periplasmic expression of the soluble antibody fragments was performed using non-suppressor *E. coli* strain HB2151. Furthermore, the scFv and Fab were reformatted into fully assembled IgG1 and V_H dAb into V_H dAb Fc. The reformatted antibodies were expressed in CHO-S cells. The reactivity of all three formats per clone was evaluated.

2.3.1 SUBTRACTIVE BIOPANNING FOR ISOLATION OF SEROTYPE-SPECIFIC BINDERS OF DENV NS1

Two phage libraries displaying scFv or Fab antibody fragments were interrogated for binders to DENV NS1. A subtractive biopanning strategy with up to four iterative rounds of biopanning of each library employed to isolate serotype-specific binders against DENV NS1. Between rounds of biopanning, an enrichment of target specific phage is expected. The number of target-specific phage generally showed a positive enrichment trend through iterative rounds of biopanning for serotype-specific binders (Table 1). Only three rounds of subtractive biopanning were performed for target antigens DENV-2, DENV-3 and DENV-4 NS1. Meanwhile, four rounds of biopanning were required to sufficiently enrich for DENV-1 NS1 binders.

Table 2.2 Enrichment of serotype-specific phage. A specific amount of library phage particles were exposed to the target antigen in the first round (rnd) of biopanning. The amount of phage particles bound to the antigen were enumerated by infecting and titering bacterial cells. The infected bacterial cells were amplified and phage particles produced and purified. 10-fold less phage was input into the next round of biopanning and the output determined. The product of ratios before and after selection was used to calculate the enrichment factor between sequential rounds of biopanning.

Serotype-Specific DENV-1 NS1(scFv)	Input	Output	Fold Enrichment
Rnd 1	1.0×10^{12}	7.2×10^{5}	-
Rnd 2	1.0×10^{11}	2.0×10^{6}	30
Rnd3	1.0×10^{10}	1.3×10^{4}	0.063
Rnd 4	1.0×10^{9}	1.6×10^{4}	12.5
Serotype-Specific DENV-1 NS1(Fab)	**Input**	**Output**	**Fold Enrichment**
Rnd 1	1.0×10^{12}	3.2×10^{5}	-
Rnd 2	1.0×10^{11}	1.8×10^{6}	54
Rnd3	1.0×10^{10}	1.2×10^{5}	0.70
Rnd 4	1.0×10^{9}	9.7×10^{3}	0.79
Serotype-Specific DENV-2 NS1(scFv)	**Input**	**Output**	**Fold Enrichment**
Rnd 1	2.05×10^{12}	1.9×10^{8}	-
Rnd 2	4.2×10^{11}	8.0×10^{6}	0.21
Rnd3	1.1×10^{10}	1.4×10^{6}	6.68
Serotype-Specific DENV-2 NS1(Fab)	**Input**	**Output**	**Fold Enrichment**
Rnd 1	1.8×10^{12}	8.0×10^{7}	-
Rnd 2	1.7×10^{11}	2.1×10^{5}	0.02
Rnd3	8.6×10^{9}	9.8×10^{6}	922
Serotype-Specific DENV-3 NS1(scFv)	**Input**	**Output**	**Fold Enrichment**
Rnd 1	2.1×10^{12}	3.3×10^{8}	-
Rnd 2	9.4×10^{11}	1.6×10^{7}	0.11
Rnd3	1.0×10^{10}	1.5×10^{6}	8.8
Serotype-Specific DENV-3 NS1(Fab)	**Input**	**Output**	**Fold Enrichment**
Rnd 1	1.8×10^{12}	7.8×10^{7}	-
Rnd 2	1.5×10^{11}	9.5×10^{5}	0.15
Rnd3	6.9×10^{10}	5.0×10^{6}	11
Serotype-Specific DENV-4 NS1(scFv)	**Input**	**Output**	**Fold Enrichment**
Rnd 1	2.1×10^{12}	1.3×10^{8}	-
Rnd 2	6.0×10^{11}	2.5×10^{5}	6.6×10^{-3}
Rnd3	9.8×10^{10}	9.1×10^{5}	22
Serotype-Specific DENV-4 NS1(Fab)	**Input**	**Output**	**Fold Enrichment**
Rnd 1	1.8×10^{12}	1.2×10^{8}	-
Rnd 2	1.3×10^{11}	4.0×10^{5}	0.05
Rnd3	2.0×10^{10}	1.0×10^{6}	16.3

Because two different libraries were biopanned for binders against NS1 from each DENV serotype, the different subtractive biopanning protocols were designated campaign numbers which were used to denote clone prefixes for easy identification of the source of the clones. The glycerol stocks containing phage particles that were rescued from the last rounds of each subtractive biopanning campaign were streaked out on agar plates and up to 90 individual clones were randomly picked and screened for their ability to recognize NS1 from the target DENV serotype in a monoclonal phage ELISA. There was a dominance of target-specific clones isolated from the scFv library that was biopanned for serotype-specific binders against DENV-1 NS1 (Figure 2.6). Serotype-specific binders against DENV-2 NS1 [2C3, 4A1, 4B8, 4C11] (Figure 2.9), DENV-3 NS1 [7G11] (Figure 2.11) and DENV-4 NS1 [6A5, 6A7, 6G8] (Figure 2.12) however, were in much less abundance. Both scFv and Fab libraries yielded an assortment of binders with varied reactivities. For example, binders against DENV-1 and DENV-2 NS1 (8B5, 8B7 and H2) were isolated from the Fab library when binders against DENV-1 NS1 were sought (Figure 2.7). Pan-reactive binders 1A1, 1D4, 1D12 (Figure 2.10), 3A10, 3B6, 3D3, 3D12, 3E6, 3F10 (Figure 2.13), 4A5 (Figure 2.9), 6H2 (Figure 2.12), 7B5, 7C2 and 7E5 (Figure 2.11) were also isolated despite using a subtractive strategy to deplete binders against homologous regions on NS1 from all four DENV serotypes.

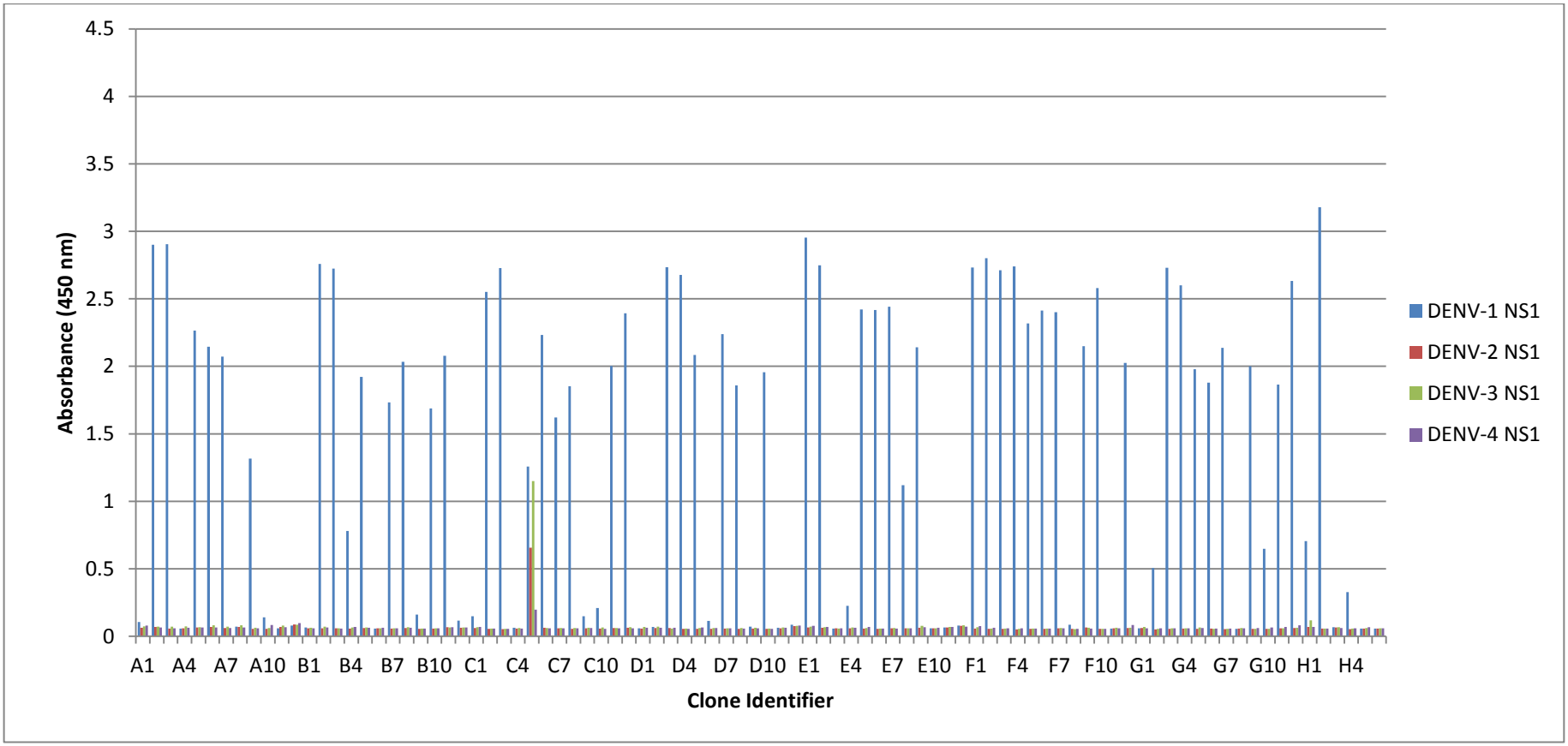

Figure 2.6 Recognition of DENV-1 NS1 by phage displayed fragments from the scFv library in a direct ELISA (Campaign 9). NS1 from each DENV serotype was immobilized onto four 96-well polystyrene plates. 90 single clone-derived phage particles from the fourth round of subtractive biopanning against DENV-1 NS1 were added to respective wells on all four plates. An HRP-conjugated antibody against M13 bacteriophage was used for detection of binding. Binding was determined by measuring the chromogenic signal produced by addition of TMB.

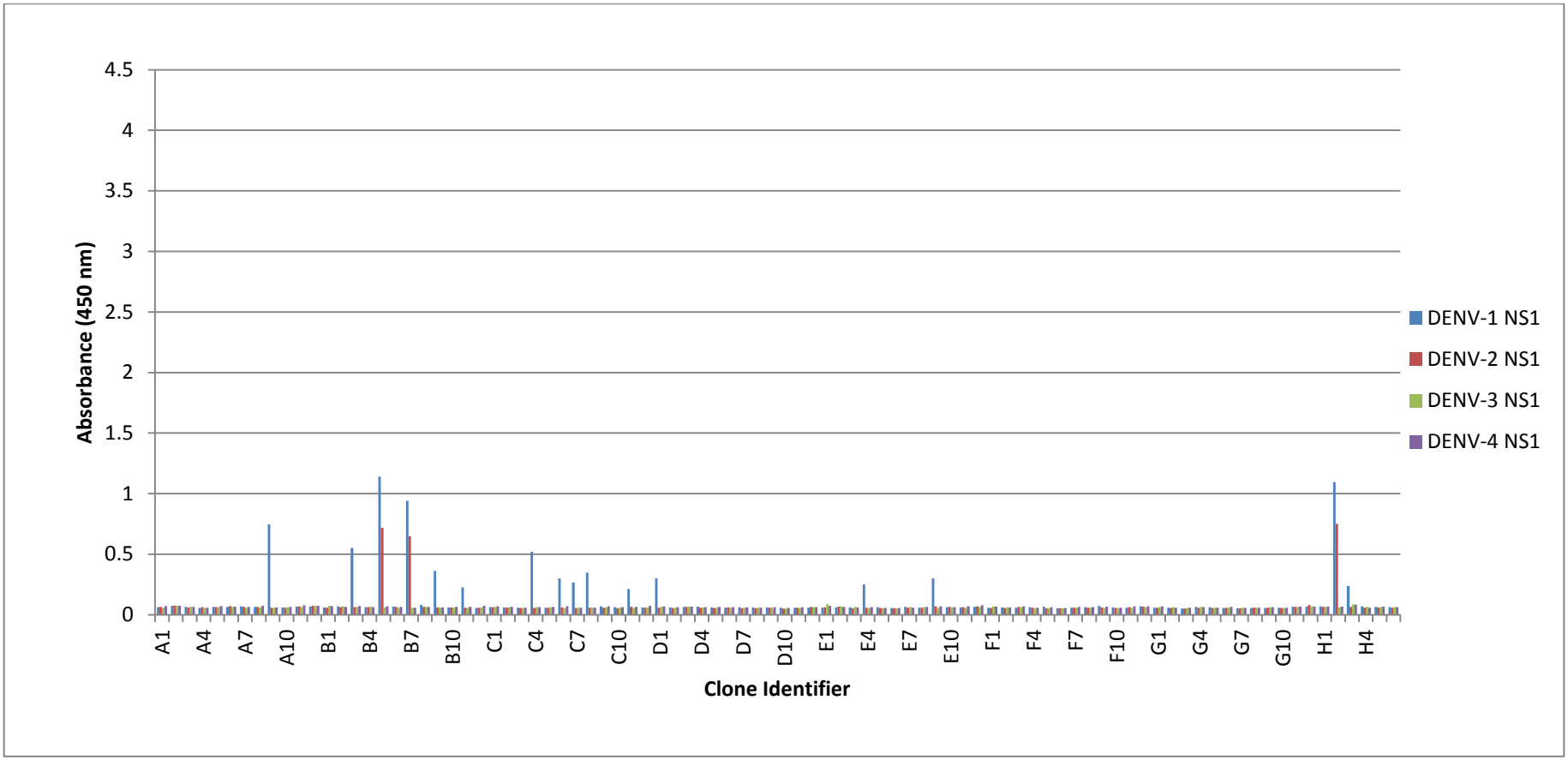

Figure 2.7 Recognition of DENV-1 NS1 by phage displayed fragments from the Fab library in a direct ELISA (Campaign 8). NS1 from each DENV serotype was immobilized onto four 96-well polystyrene plates. 90 single clone-derived phage particles from the fourth round of subtractive biopanning against DENV-1 NS1 were added to respective wells on all four plates. An HRP-conjugated antibody against M13 bacteriophage was used for detection of binding. Binding was determined by measuring the chromogenic signal produced by addition of TMB.

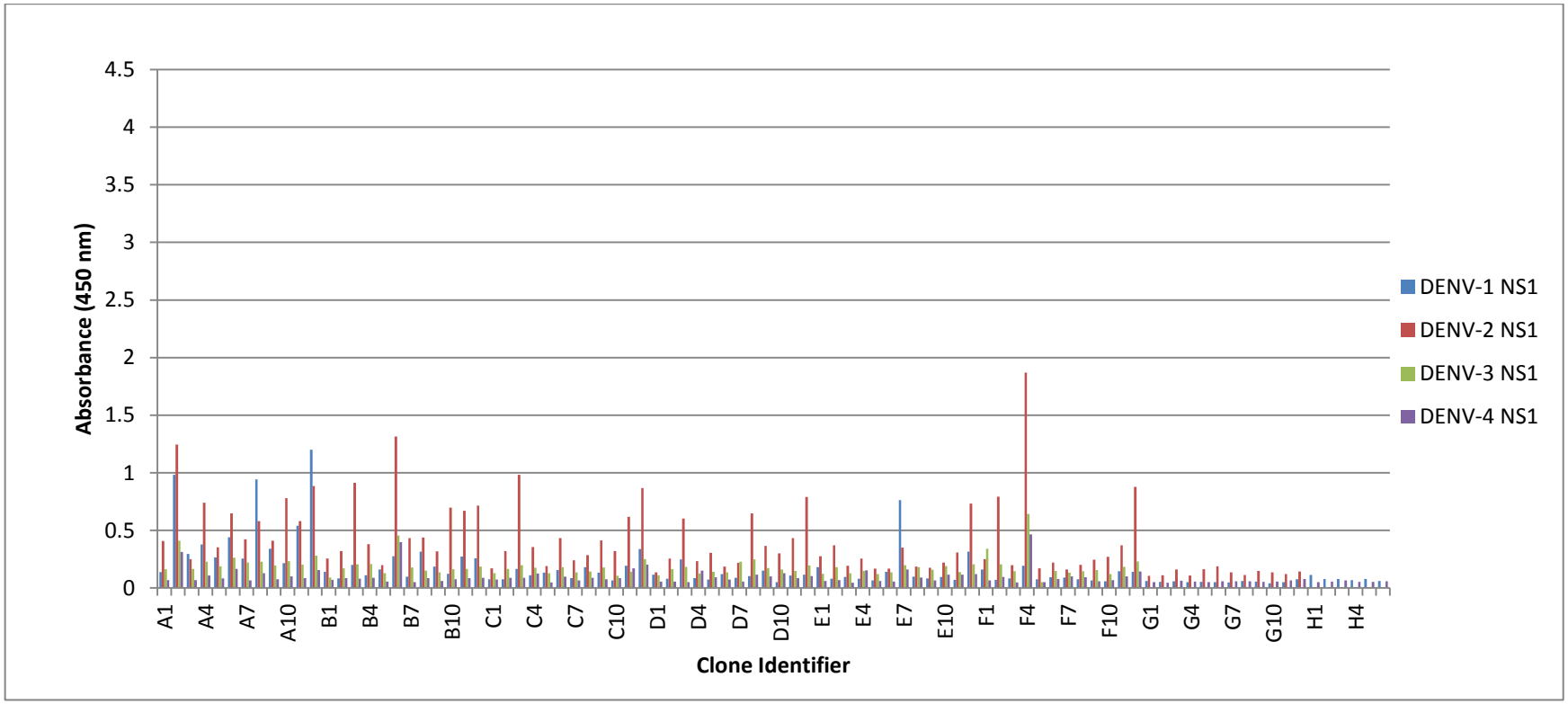

Figure 2.8 Recognition of DENV-2 NS1 by phage displayed fragments from the scFv library in a direct ELISA (Campaign 2). NS1 from each DENV serotype was immobilized onto four 96-well polystyrene plates. 90 single clone-derived phage particles from the third round of subtractive biopanning against DENV-2 NS1 were added to respective wells on all four plates. An HRP-conjugated antibody against M13 bacteriophage was used for detection of binding. Binding was determined by measuring the chromogenic signal produced by addition of TMB.

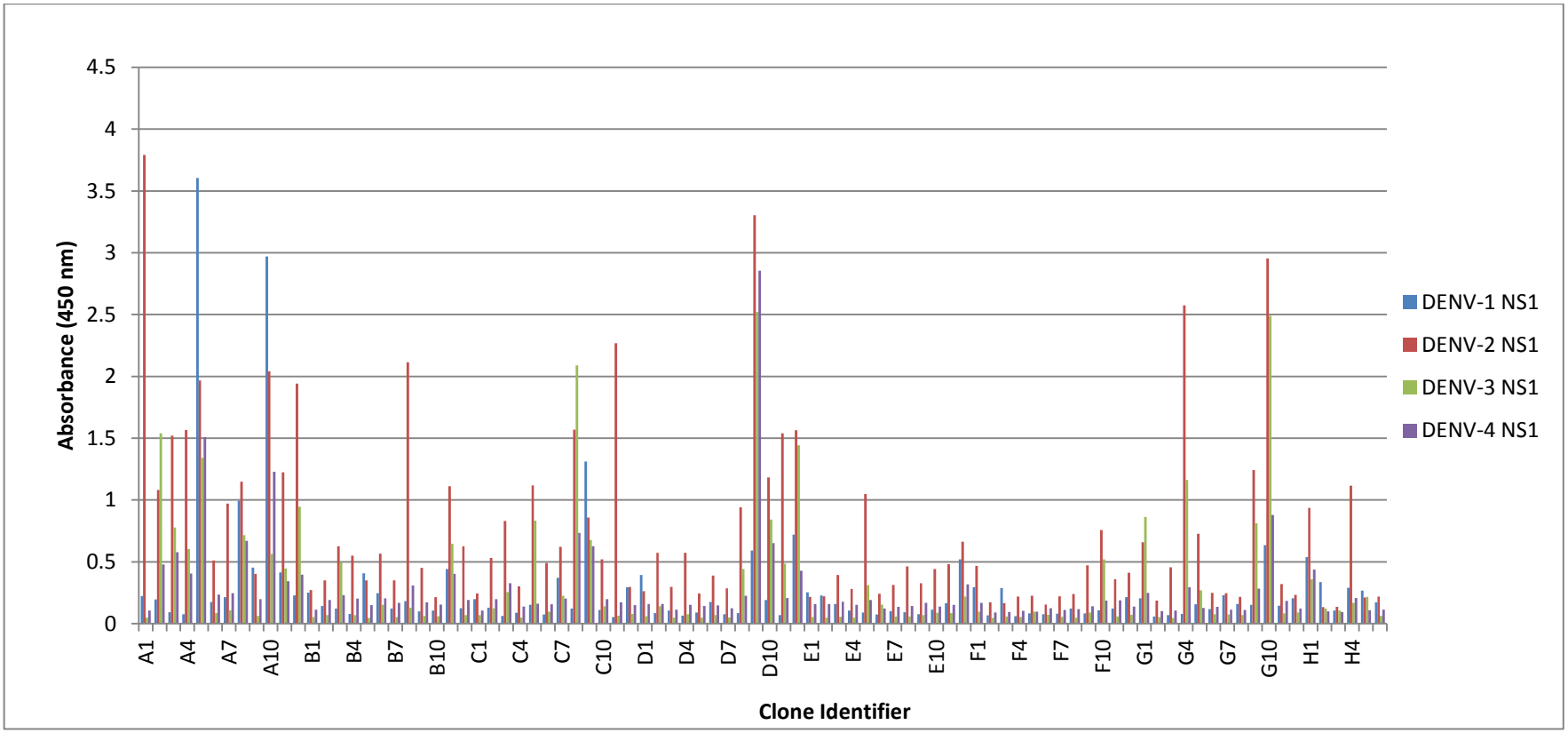

Figure 2.9 Recognition of DENV-2 NS1 by phage displayed fragments from the Fab library in a direct ELISA (Campaign 4). NS1 from each DENV serotype was immobilized onto four 96-well polystyrene plates. 90 single clone-derived phage particles from the third round of subtractive biopanning against DENV-2 NS1 were added to respective wells on all four plates. An HRP-conjugated antibody against M13 bacteriophage was used for detection of binding. Binding was determined by measuring the chromogenic signal produced by addition of TMB.

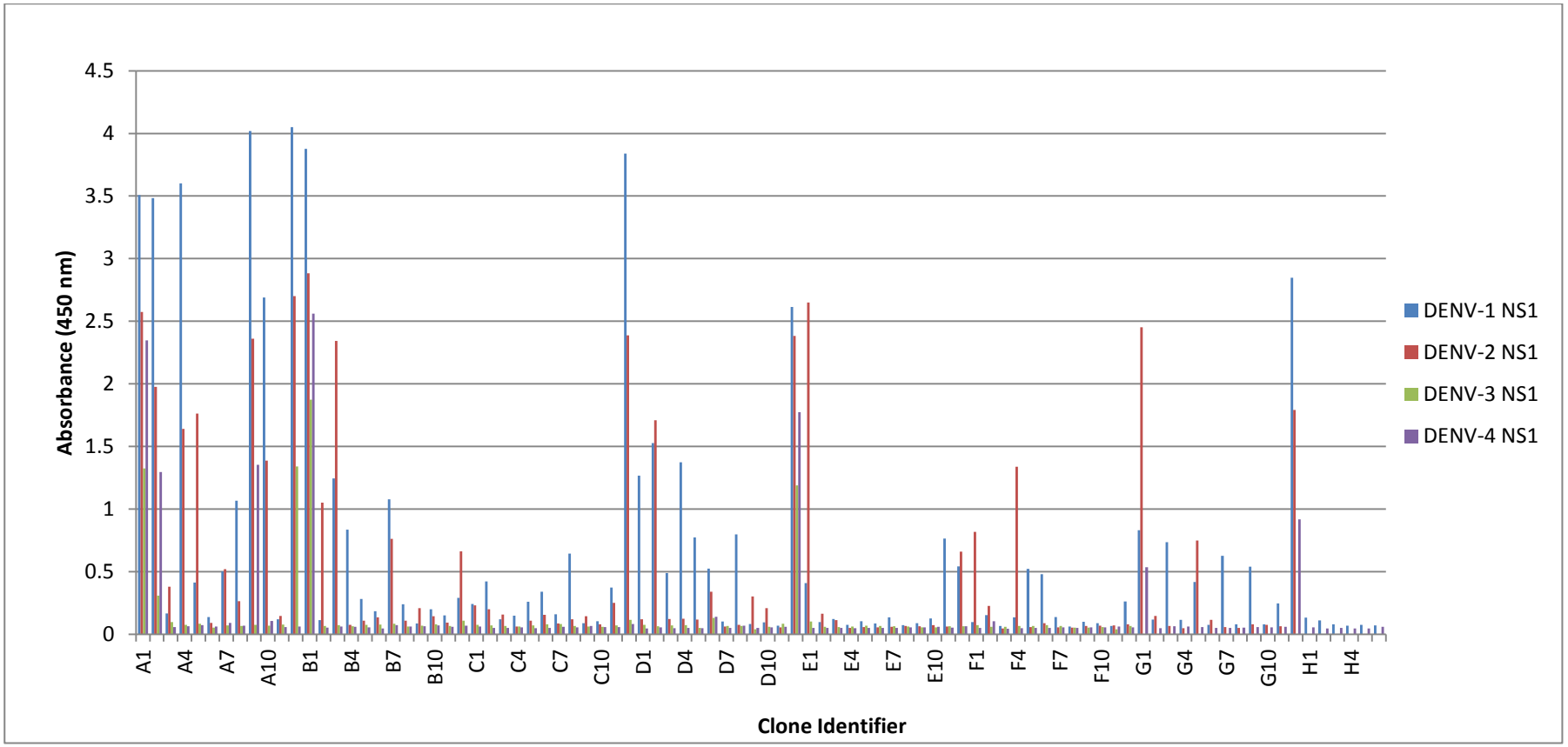

Figure 2.10 Recognition of DENV-3 NS1 by phage displayed fragments from the scFv library in a direct ELISA (Campaign 1). NS1 from each DENV serotype was immobilized onto four 96-well polystyrene plates. 90 single clone-derived phage particles from the third round of subtractive biopanning against DENV-3 NS1 were added to respective wells on all four plates. An HRP-conjugated antibody against M13 bacteriophage was used for detection of binding. Binding was determined by measuring the chromogenic signal produced by addition of TMB.

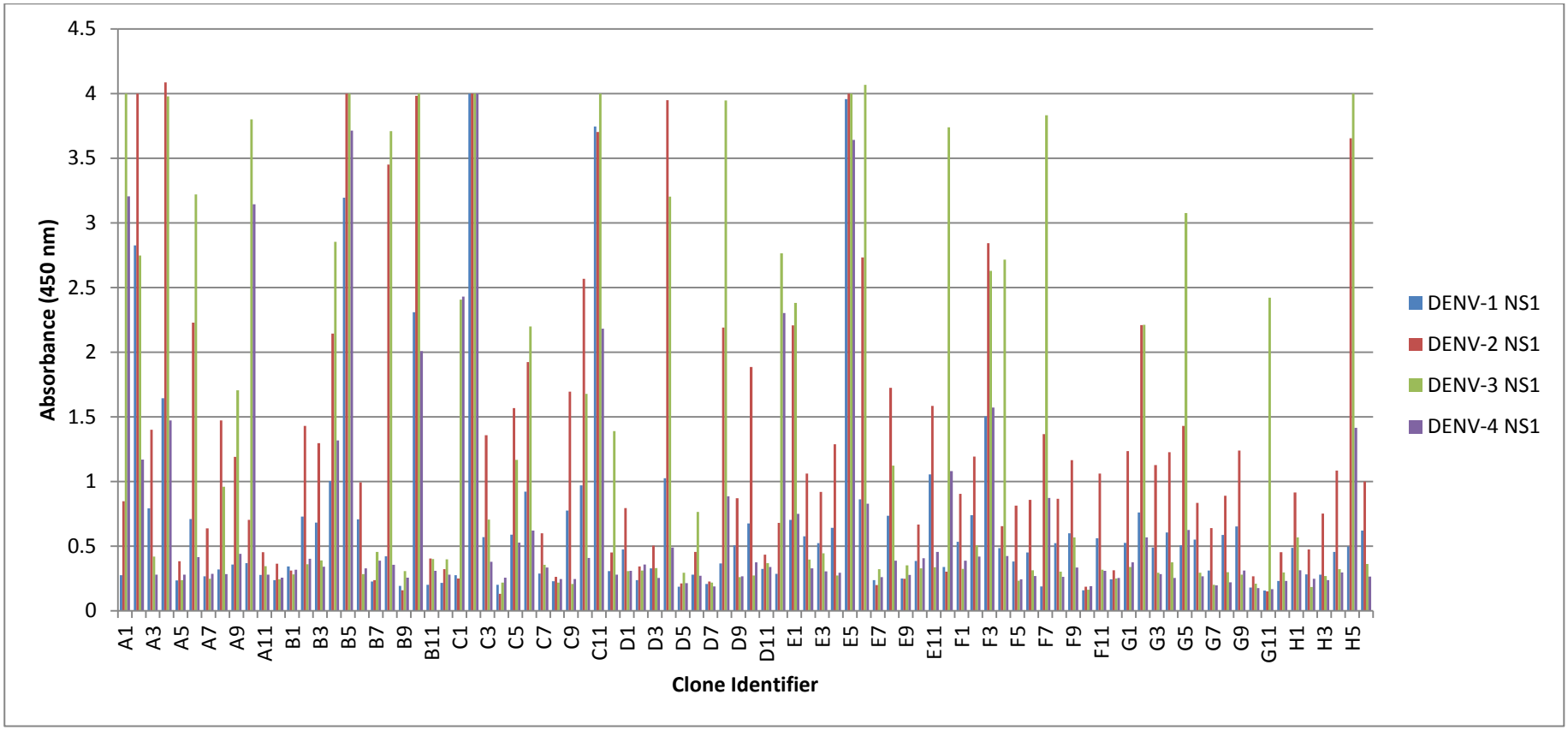

Figure 2.11 Recognition of DENV-3 NS1 by phage displayed fragments from the Fab library in a direct ELISA (Campaign 7). NS1 from each DENV serotype was immobilized onto four 96-well polystyrene plates. 90 single clone-derived phage particles from the third round of subtractive biopanning against DENV-3 NS1 were added to respective wells on all four plates. An HRP-conjugated antibody against M13 bacteriophage was used for detection of binding. Binding was determined by measuring the chromogenic signal produced by addition of TMB.

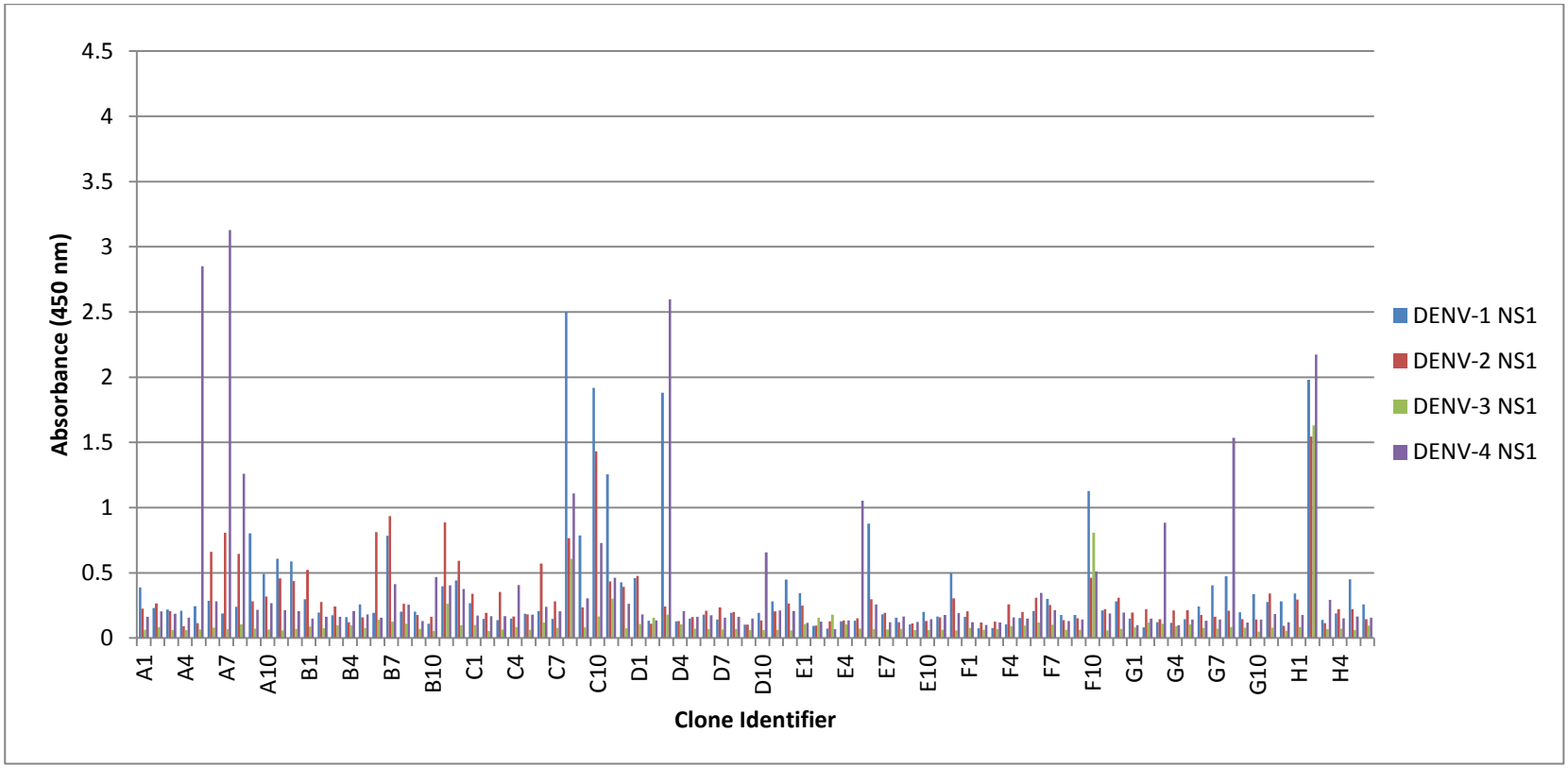

Figure 2.12 Recognition of DENV-4 NS1 by phage displayed fragments from the scFv library in a direct ELISA (Campaign 6). NS1 from each DENV serotype was immobilized onto four 96-well polystyrene plates. 90 single clone-derived phage particles from the third round of subtractive biopanning against DENV-4 NS1 were added to respective wells on all four plates. An HRP-conjugated antibody against M13 bacteriophage was used for detection of binding. Binding was determined by measuring the chromogenic signal produced by addition of TMB.

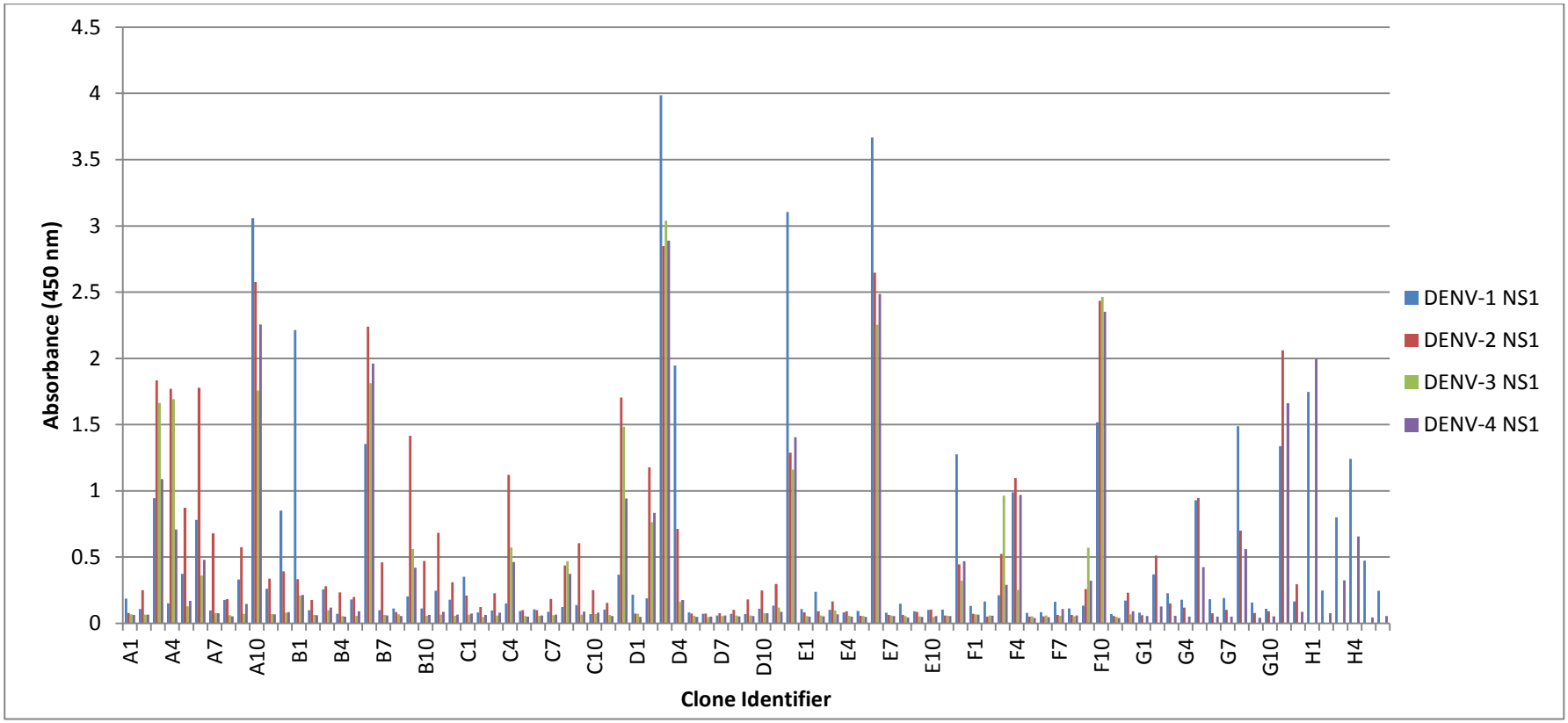

Figure 2.13 Recognition of DENV-4 NS1 by phage displayed fragments from the Fab library in a direct ELISA (Campaign 3). NS1 from each DENV serotype was immobilized onto four 96-well polystyrene plates. 90 single clone-derived phage particles from the third round of subtractive biopanning against DENV-4 NS1 were added to respective wells on all four plates. An HRP-conjugated antibody against M13 bacteriophage was used for detection of binding. Binding was determined by measuring the chromogenic signal produced by addition of TMB.

Serotype-specific and pan-reactive binders that were isolated from the different biopanning campaigns using both scFv and Fab libraries were sequenced to determine the uniqueness of the clones. 5 unique serotype-specific (9H2 α DENV-NS1, 4C11 α DENV-2 NS1, 7G11 α DENV-3, 6A5 α DENV NS1 and 6A7 α DENV-4 NS1) and 11 pan-reactive antibodies were identified. The V_H and V_L CDR3 regions as well as the variable gene families of the unique clones were determined (Table 2). The heavy and light chain CDR sequences of the serotype-specific binders showed diversity in length and composition. On the contrary, the V_H CDR3 sequence ARGRDDFWSGYYFDDAFDI from the Fab library dominated pan-reactive recognition regardless of variations in the light chain CDR sequences. This indicated that the pan-reactive interaction between the antigen and the antibody may not be dependent on cooperation between both variable domains. The variable regions of the isolated binders were derived from mostly V_H1 and V_H3 gene families and six V_L gene families of both kappa and lambda light chains (Vκ1, Vκ3, Vλ1, Vλ2, Vλ3 and Vλ6).

Table 2.3 Variable gene families and V_H CDR3 and V_L CDR3 sequences of unique antibody fragments from subtractive biopanning against DENV NS1. The variable gene families and CDRs were determined by inputting the clone nucleotide sequences into the Immunogenetics (IMGT)-V-QUEST software [http://imgt.org/IMGT_vquest/share/textes/]. (f) and (s) following clone identifiers denote isolation from either the Fab or scFv library. Clone 9 H2 is DENV-1 NS1 specific, clone 4 C11 is DENV-2 NS1 specific, clone 7 G11 is DENV-3 NS1 specific, and clones 6 A5 and 6 A7 are DENV-4 NS1 specific. Clones 1 A1, 1 D4, 3 B6, 3 D12, 3 E6, 4 A5, 5 A3, 6 H2, 7 C2 and 7 E5 recognize NS1 of all four DENV serotypes.

CLONE	**V_H Family**	**V_H CDR3**																						**V_L Family**	**V_L CDR3**											
1A1 (s)	VH1	G	S	-	-	-	-	Y	G	G	N	S	G	-	-	F	D	Y	-	-	-	-	-	Vλ3	S	S	R	D	N	R	G	T	H	R	W	V
1D4 (s)	VH1	G	F	R	-	A	T	V	D	Y	Y	G	-	-	-	M	D	V	-	-	-	-	-	Vκ1	Q	K	L	S	S	Y	P	L	T	-	-	-
3B6 (f)	VH1	A	R	G	R	D	D	F	W	S	G	-	-	-	Y	Y	F	D	D	A	F	D	I	Vκ1	Q	-	-	-	Q	S	Y	S	T	P	W	T
3D12 (f)	VH1	A	R	G	R	D	D	F	W	S	G	-	-	-	Y	Y	F	D	D	A	F	D	I	Vλ1	G	T	W	D	S	S	L	R	G	-	-	V
3E6 (f)	VH3	A	R	D	H	G	D	F	W	S	G	Y	F	V	N	Y	Y	Y	Y	G	M	D	V	Vλ6	Q	S	Y	D	S	S	G	Q	-	-	-	V
4A5 (f)	VH1	A	R	G	R	D	D	F	W	S	G	-	-	-	Y	Y	F	D	D	A	F	D	I	Vκ1	Q	-	-	-	Q	S	H	S	S	P	Y	T
4C11 (f)	VH3	A	R	D	T	-	-	-	-	-	-	-	-	-	-	-	A	M	V	I	L	D	Y	Vλ1	Q	S	Y	D	S	S	L	G	G	F	Y	V
5A3 (f)	VH1	A	R	G	R	D	D	F	W	S	G	-	-	-	Y	Y	F	D	D	A	F	D	I	Vκ1	Q	-	-	-	Q	S	Y	S	T	P	R	T
6A5 (s)	VH3	G	F	R	K	D	S	S	G	W	Y	E	I	T	P	I	D	Y	-	-	-	-	-	Vκ1	Q	K	L	S	S	Y	P	L	T	-	-	-
6A7 (s)	VH3	-	-	-	-	-	-	G	G	G	L	E	L	R	T	F	Q	H	-	-	-	-	-	Vλ3	K	S	R	D	S	S	G	N	Y	-	-	V
6H2 (s)	VH3	D	S	N	D	F	W	S	G	Y	F	D	P	G	E	F	D	Y	-	-	-	-	-	Vλ2	S	S	Y	A	G	N	R	N	L	-	-	V
7C2 (f)	VH1	A	R	G	R	D	D	F	W	S	G	-	-	-	Y	Y	F	D	D	A	F	D	I	Vκ1	Q	-	-	-	Q	S	Y	S	T	-	R	T
7E5 (f)	VH1	A	R	G	R	D	D	F	W	S	G	-	-	-	Y	Y	F	D	D	A	F	D	I	Vκ3	Q	-	-	-	Q	Y	G	N	S	-	R	T
7G11 (f)	VH4	A	R	G	R	G	-	-	-	-	-	-	-	-	-	-	-	-	-	G	S	Y	Y	Vλ1	E	T	W	D	D	N	L	S	-	A	V	V
9H2 (s)	VH1	A	S	S	-	-	S	S	S	F	Y	Y	Y	Y	G	M	D	V	-	-	-	-	-	Vλ3	Q	V	W	-	D	S	S	S	D	H	Q	V

Evaluation of the binding reactivities of phage displayed antibody fragments, soluble scFv/Fab or reformatted IgG1 antibodies showed that phage displayed antibody fragments and IgG1 had identical immune-reactivity to DENV NS1 (Figure 2.14). Soluble antibody fragments produced by periplasmic expression in HB2151 cells did not always yield a binding response due to variability in expression; however when expression was sufficient the expected response to the target antigen was observed.

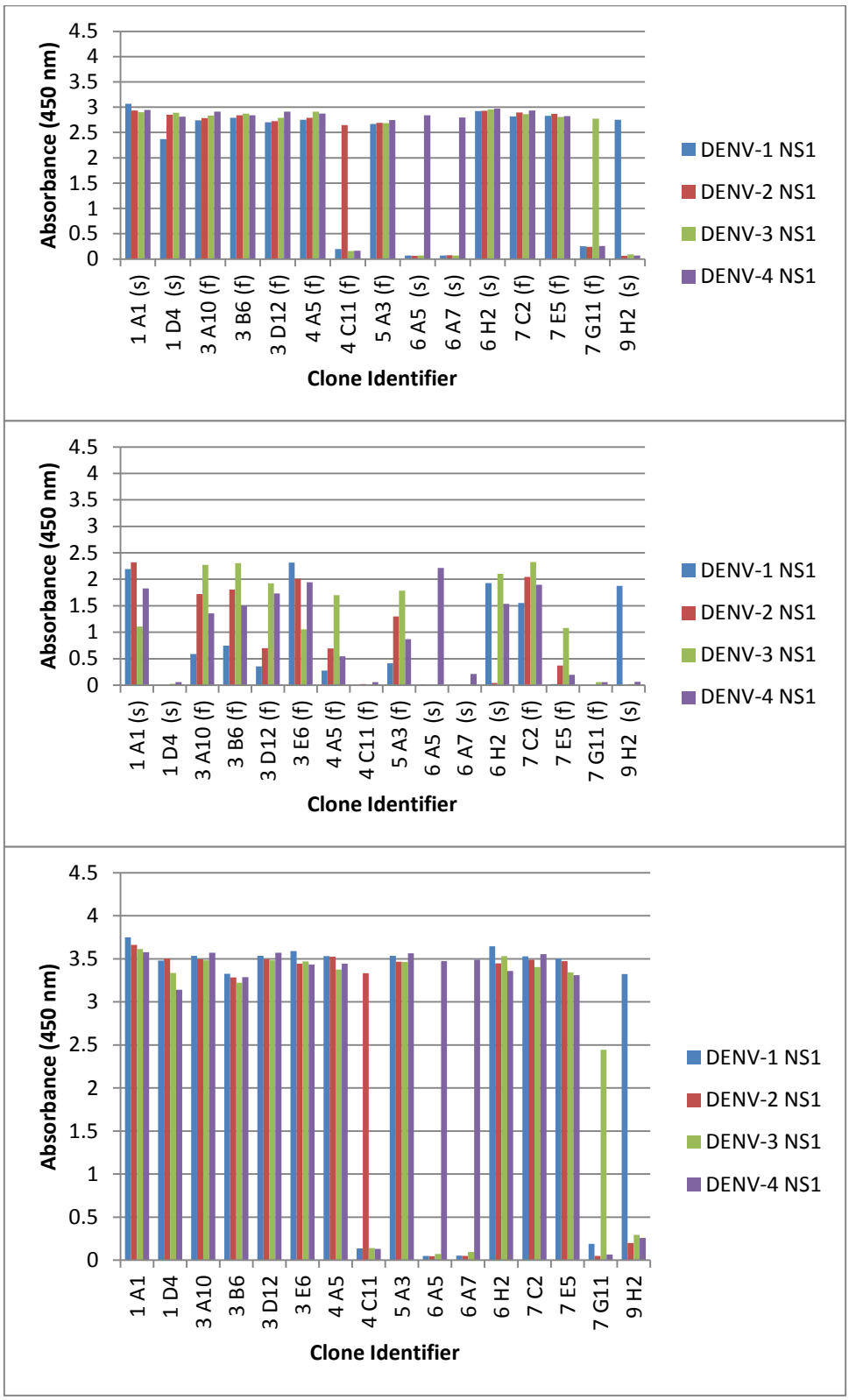

Figure 2.14 Immunoreactivity of a panel of serotype-specific and pan-reactive phage particles, scFv (s)/Fab (f) and IgG1 to DENV NS1. NS1 from all four DENV serotypes was immobilized on a polystyrene plate. Phage particles (top panel), scFv/Fab (middle panel) or IgG (bottom panel) isolated from a subtractive biopanning strategy that sought serotype-reactive binders to DENV NS1 were added to the immobilized antigen. The

reactivity of the clones in their different formats was determined by the absorbance value measured after probing with HRP-conjugated α–M13 (top panel), HRP-conjugated α-human κ/λ (middle panel) or HRP-conjugated α-human γ-Fc (bottom panel). The serotype-specific antibodies acted as negative controls for NS1 from other DENV serotypes.

2.3.2 DIRECT BIOPANNING ON IMMOBILIZED ANTIGEN FOR ISOLATION OF PAN-REACTIVE DENV NS1 BINDERS

Despite being designed for the isolation of serotype-specific antibody fragments, many pan-reactive binders against DENV-NS1 were still isolated in the subtractive biopanning strategy described above (Figure 2.14). However, due to the design of the panning strategy, it was resolved that these pan-reactive antibodies would likely have low affinity, as high affinity binders would be lost in the subtractive steps. The scFv library was therefore specifically interrogated for pan-reactive binders against DENV NS1. The Fab library was excluded from this biopanning campaign because of the previous dominance of a single V_H chain in the pan-reactive clones isolated from the subtractive biopanning strategy. It was posited that the high frequency of that V_H chain originating from a common B-cell clone, could perhaps be predictive of an immune-dominant response in the library repertoire which would still remain apparent.

NS1 from a single serotype of DENV was immobilized on polystyrene tubes in each round of biopanning. 1.0×10^{13} purified phage particles from the scFv library were used for the first round of biopanning. Ten-fold less phage were used in each subsequent round of biopanning. Enumeration of eluted phage from each iteration of biopanning showed high enrichment of pan-reactive binders against DENV NS1 (Table 2.4).

Table 2.4 Enrichment of pan-reactive phage. A specific amount of library phage particles were exposed to the target antigen in the first round of biopanning. The amount of phage particles bound to the antigen were enumerated by infecting and titering bacterial cells. The infected bacterial cells were amplified and phage particles produced and purified. 10-fold less phage was input into the next round of biopanning and the output determined. The product of ratios before and after selection was used to calculate the enrichment factor between sequential rounds of biopanning.

Pan-Reactive DENV-1, 2, 3 and 4 NS1 (scFv)	**Input**	**Output**	**Fold Enrichment**
Rnd 1	1.0×10^{13}	9.0×10^{5}	-
Rnd 2	1.0×10^{12}	9.0×10^{5}	10
Rnd3	1.0×10^{11}	9.9×10^{5}	110
Rnd 4	1.0×10^{10}	1.20×10^{6}	12

90 scFv binders that were rescued from the fourth round of biopanning were screened for their ability to recognize NS1 from all four DENV serotypes (Figure 2.15). A significant proportion of the isolated binders recognized DENV NS1. Sequencing of the clones revealed two dominant clones – A1 and A2 (Table 2.5). The heavy and light chain usage of the two clones was analyzed and showed use of VH3 and Vλ3 gene families for clone A1 while clone A2 utilized VH1 and Vλ1 gene families. The V_H CDR3 regions of the two clones showed sequence diversity while some modest homology of residues in the V_L CDR3 regions was noted.

An evaluation of the ability of A1 and A2 phage particles, soluble scFv or reformatted IgG to recognize DENV NS1 (Figure 2.16) showed a deficit in the ability of A1 soluble scFv to recognize DENV-3 NS1. A slight reduction in the ability of A2 soluble scFv to recognize DENV-1 and DENV-3 NS1 was also noted. Pan-reactive recognition of DENV NS1 by phage particles and reformatted IgG1 was again identical in this instance.

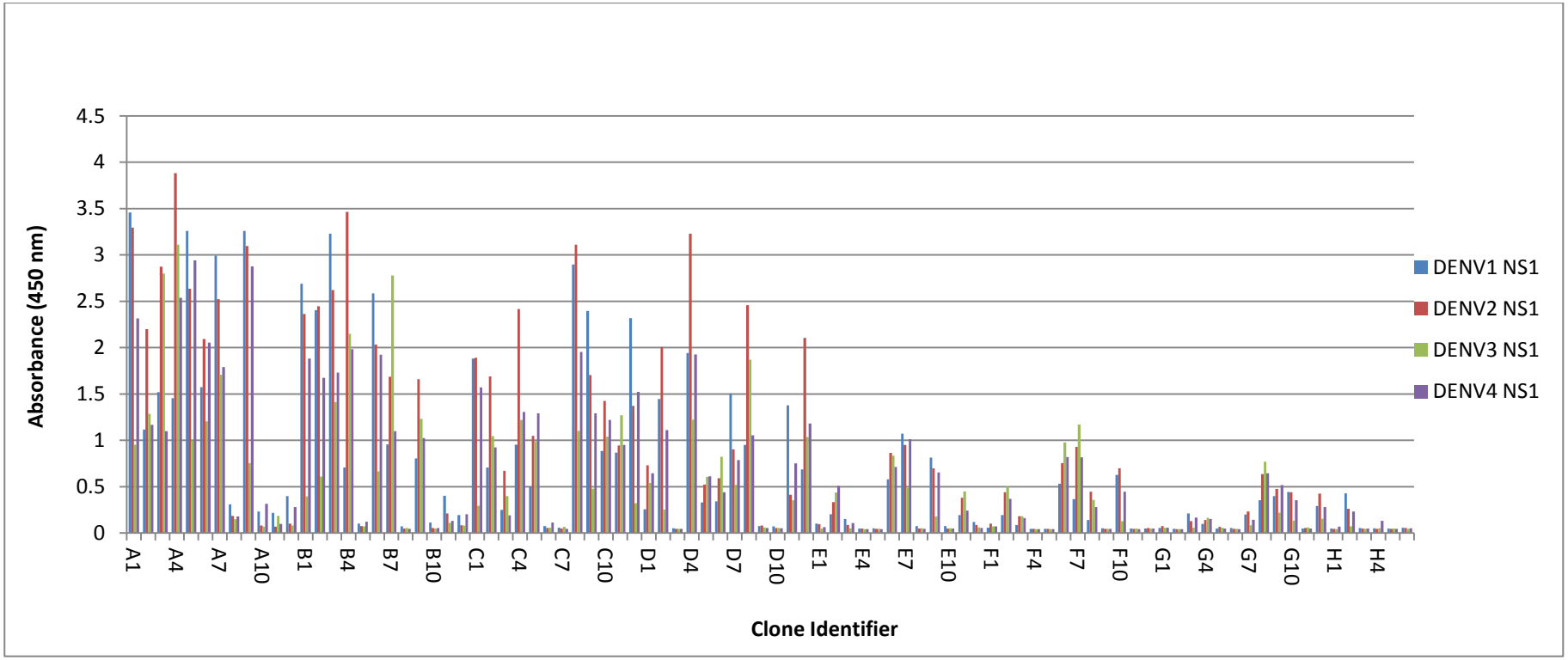

Figure 2.15 Recognition of DENV NS1 by phage displayed fragments from the scFv library in a direct ELISA. NS1 from each DENV serotype was immobilized onto four 96-well polystyrene plates. 90 single clone-derived phage particles from the fourth round of biopanning against DENV NS1 were added to respective wells on all four plates. An HRP-conjugated antibody against M13 bacteriophage was used for detection of binding. Binding was determined by measuring the chromogenic signal produced by addition of TMB.

Table 2.5 Variable gene families and V_H CDR3 and V_L CDR3 sequences of isolated pan-reactive antibody fragments against DENV-NS1. The variable gene families and CDRs were determined by inputting the clone nucleotide sequences into the Immunogenetics (IMGT)-V-QUEST software [http://imgt.org/IMGT_vquest/share/textes/]. (s), following the clone identifiers denotes isolation from the scFv library.

Clone	**V_H Family**					**V_H CDR3**															**V_L Family**	**V_L CDR3**									
A1 (s)	VH3	A	K	D	S	G	D	Y	D	F	W	S	G	Y	Y	T	R	W	F	D	P	Vλ3	N	S	R	D	S	S	G	N	H	L	V
A2 (s)	VH1	A	S	G	D	F	W	S	G	H	Y	Y	Y	Y	G	M	D	V	-	-	-	Vλ1	G	T	W	D	S	S	L	S	V	V	V

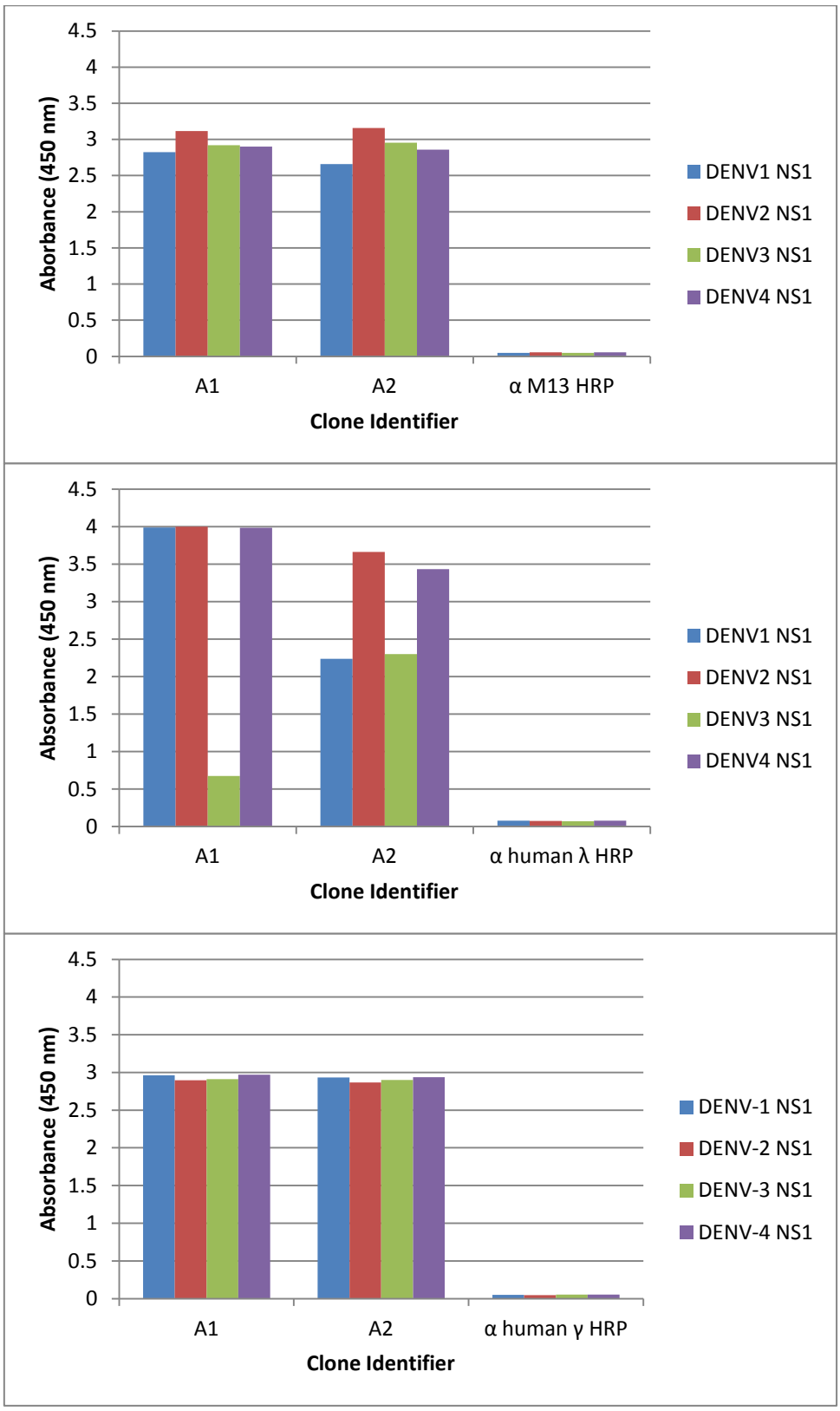

Figure 2.16 Immunoreactivity of A1 and A2 phage particles, scFv and IgG1 to DENV NS1. NS1 from all four DENV serotypes was immobilized on a polystyrene plate. A1 and A2 phage particles (top panel), scFv (middle panel) or IgG (bottom panel) isolated from a biopanning strategy that sought pan-reactive binders to DENV NS1 were added to the immobilized antigen. The reactivity of the A1 and A2 clones in their different formats was

determined by the absorbance value measured after probing with an appropriate HRP-conjugated secondary antibody. HRP-conjugated secondary antibody added to wells with just the immobilized antigen was used as the negative control.

2.3.3 TANDEM BINDING BIOPANNING USING AN IMMUNE-DOMINANT ANTIBODY FOR ISOLATION OF PAN-REACTIVE DENV NS1 BINDERS

Having isolated pan-reactive binders against DENV-NS1 from the scFv library, it was conceived that these antibodies may bind to the immune-dominant epitope which we sought to avoid in the DENV NS1 capture assay. To this end, a biopanning strategy was devised to first immobilize GUS-2 on an immunotube. GUS-2 antibody binds the immune-dominant epitope and would be used to capture DENV NS1 in four biopanning campaigns against NS1 from each DENV serotype (designated campaign D1, D2, D3 and D4). A phage library displaying aggregation-resistant V_H domains was the exposed to the GUS-2 captured DENV NS1. Three rounds of biopanning were performed and the enrichment of binders between sequential round of biopanning as measured by the ratio of phage input and phage output titre. The ratios in this instance were generally low (Table 2.6).

Table 2.6 Enrichment of pan-reactive phage that bind non immune-dominant epitopes. A specific amount of library phage particles were exposed to the target antigen in the first round (rnd) of biopanning. The amount of phage particles bound to the antigen were enumerated by infection and then obtaining a titre of the infected bacterial cells. The infected bacterial cells were amplified and phage particles produced and purified. 10-fold less phage was input into the next round of biopanning and the output determined. The product of ratios before and after selection was used to calculate the enrichment factor between sequential rounds of biopanning.

Pan-Reactive GUS2 → DENV-1 NS1 (V_H dAb)	**Input**	**Output**	**Fold Enrichment**
Rnd 1	3.0×10^{11}	2.8×10^{5}	-
Rnd 2	3.0×10^{10}	3.5×10^{4}	1.3
Rnd3	3.0×10^{9}	2.1×10^{3}	0.6
Pan-Reactive GUS2 → DENV-2 NS1 (V_H dAb)	**Input**	**Output**	**Fold Enrichment**
Rnd 1	3.0×10^{11}	2.7×10^{5}	-
Rnd 2	3.0×10^{10}	2.3×10^{4}	0.9
Rnd3	3.0×10^{9}	5.0×10^{3}	2.2
Pan-Reactive GUS2 → DENV-3 NS1 (V_H dAb)	**Input**	**Output**	**Fold Enrichment**
Rnd 1	3.0×10^{11}	2.3×10^{5}	-
Rnd 2	3.0×10^{10}	7.0×10^{3}	0.3
Rnd3	3.0×10^{9}	6.5×10^{3}	9.3
Pan-Reactive GUS2 → DENV-4 NS1 (V_H dAb)	**Input**	**Output**	**Fold Enrichment**
Rnd 1	3.0×10^{11}	2.1×10^{5}	-
Rnd 2	3.0×10^{10}	3.9×10^{4}	1.9
Rnd3	3.0×10^{9}	6.0×10^{2}	0.2

Low enrichment notwithstanding, the output phage particles from the third round of biopanning in all four separate campaigns were screened for their ability to recognize DENV NS1 in monoclonal phage ELISAs. The monoclonal phage were also screened against GUS-2 in order to confirm that the isolated binders were not interacting with the murine antibody used for DENV NS1 capture. Pan-reactive antibodies against DENV NS1 were mainly isolated in the biopanning campaign that used GUS-2 to capture DENV-1 NS1 (Figure 2.17). Monoclonal phage isolated from the biopanning campaigns that captured DENV-3 NS1 (Figure 2.19) and DENV-4 NS1 (Figure 2.20) dominantly had cross-reactivity with GUS-2.

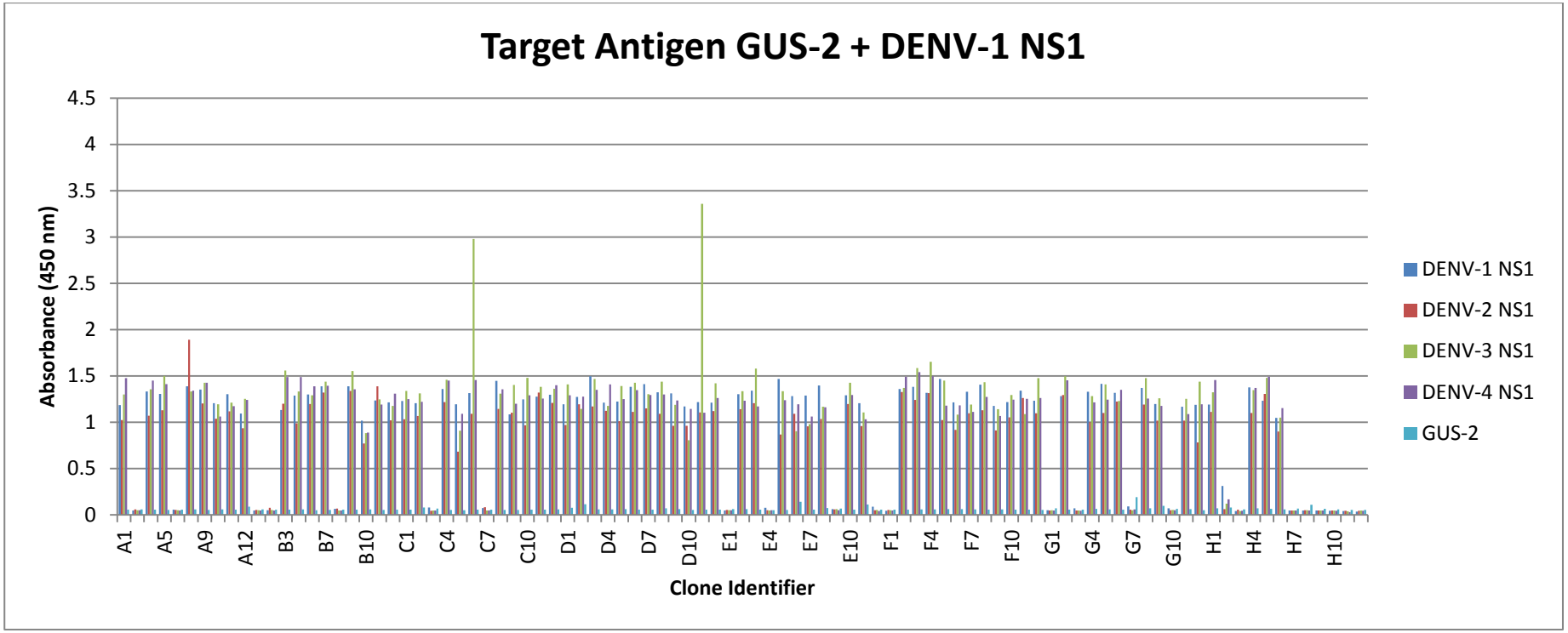

Figure 2.17 Recognition of DENV NS1 by phage displayed fragments from the V_H dAb library in a direct ELISA (Campaign D1). Five 96-well polystyrene plates had their wells coated with one of DENV-1 NS1, DENV-2 NS1, DENV-3 NS1, DENV-4 NS1or GUS-2 (an antibody that was used for capture of DENV NS1 in the biopanning strategy). 90 single clone-derived phage particles from the third round of biopanning against DENV-1 NS1 were added to respective wells on all five plates. An HRP-conjugated antibody against M13 bacteriophage was used for detection of binding. Binding was determined by measuring the chromogenic signal produced by addition of TMB.

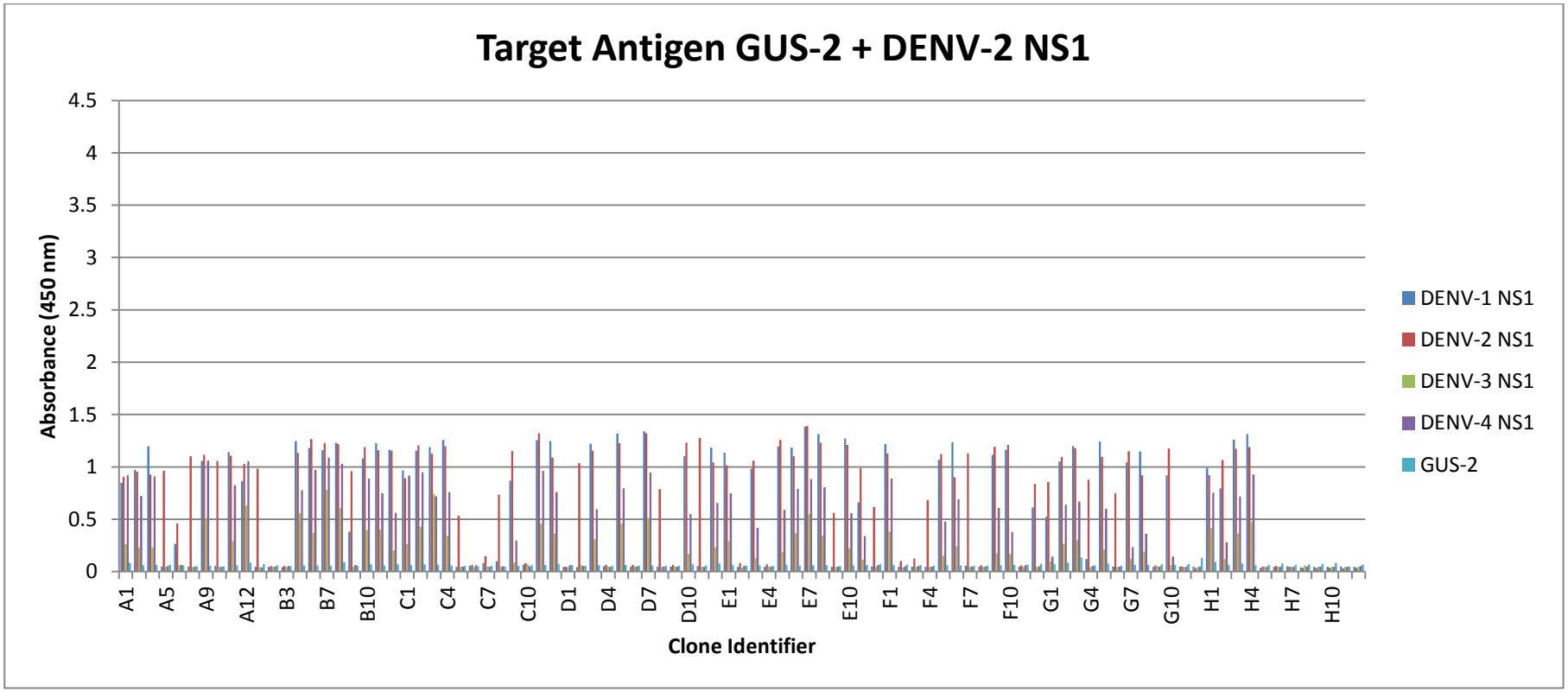

Figure 2.18 Recognition of DENV NS1 by phage displayed fragments from the V_H dAb library in a direct ELISA (Campaign D2). Five 96-well polystyrene plates had their wells coated with one of DENV-1 NS1, DENV-2 NS1, DENV-3 NS1, DENV-4 NS1or GUS-2 (an antibody that was used for capture of DENV NS1 in the biopanning strategy). 90 single clone-derived phage particles from the third round of biopanning against DENV-2 NS1 were added to respective wells on all five plates. An HRP-conjugated antibody against M13 bacteriophage was used for detection of binding. Binding was determined by measuring the chromogenic signal produced by addition of TMB.

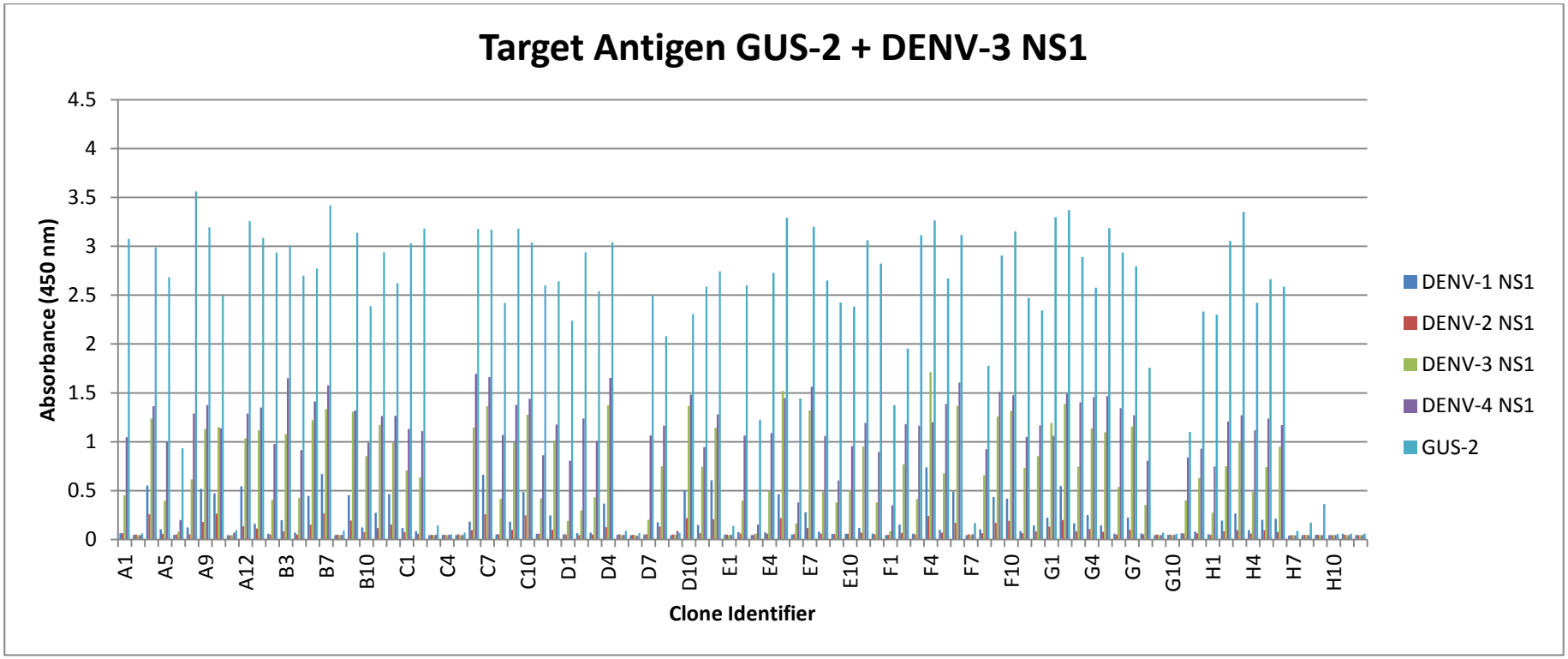

Figure 2.19 Recognition of DENV NS1 by phage displayed fragments from the V_H dAb library in a direct ELISA (Campaign D3). Five 96-well polystyrene plates had their wells coated with one of DENV-1 NS1, DENV-2 NS1, DENV-3 NS1, DENV-4 NS1or GUS-2 (an antibody that was used for capture of DENV NS1 in the biopanning strategy). 90 single clone-derived phage particles from the third round of biopanning against DENV-3 NS1 were added to respective wells on all five plates. An HRP-conjugated antibody against M13 bacteriophage was used for detection of binding. Binding was determined by measuring the chromogenic signal produced by addition of TMB.

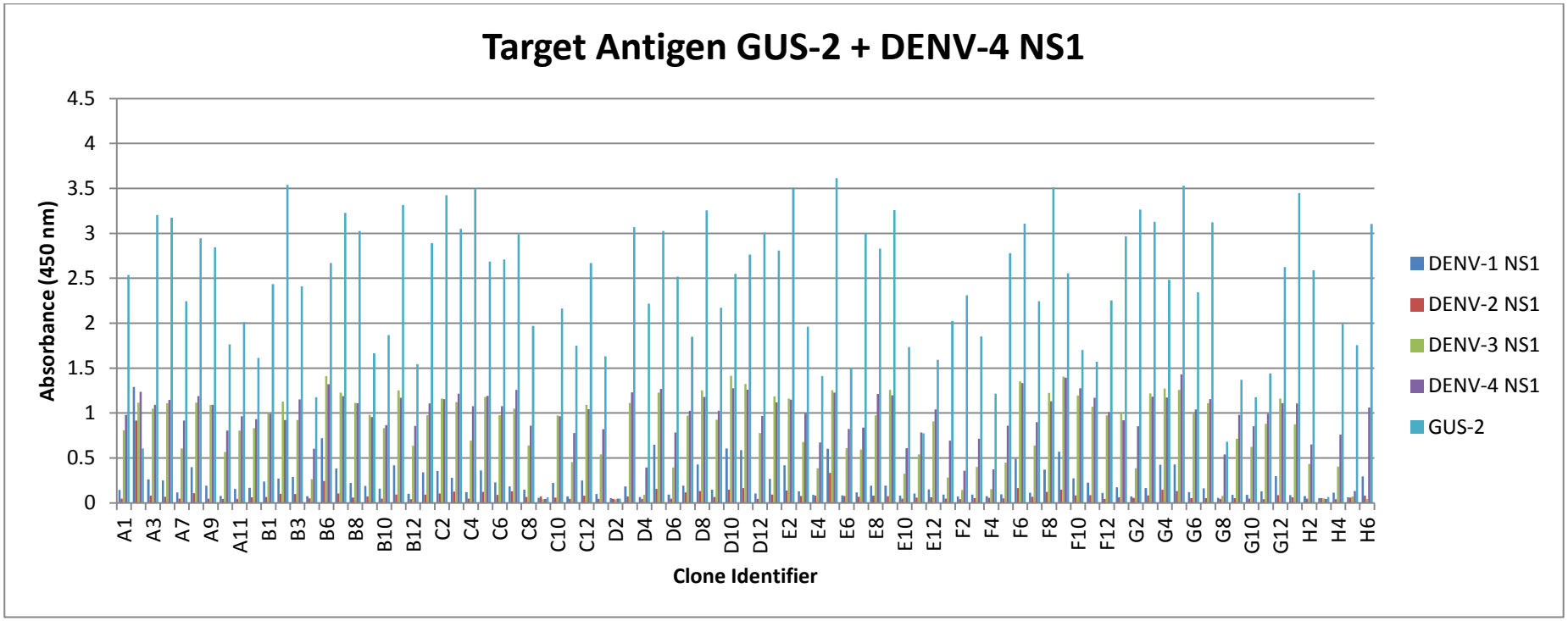

Figure 2.20 Recognition of DENV NS1 by phage displayed fragments from the V_H dAb library in a direct ELISA (Campaign D4). Five 96-well polystyrene plates had their wells coated with one of DENV-1 NS1, DENV-2 NS1, DENV-3 NS1, DENV-4 NS1or GUS-2 (an antibody that was used for capture of DENV NS1 in the biopanning strategy). 90 single clone-derived phage particles from the third round of biopanning against DENV-4 NS1 were added to respective wells on all five plates. An HRP-conjugated antibody against M13 bacteriophage was used for detection of binding. Binding was determined by measuring the chromogenic signal produced by addition of TMB.

Sequencing of the pan-reactive binders against DENV NS1 yielded a single dominant clone: D1C2 V_H dAb that binds an epitope that is spatially removed from that of GUS-2. The clone was derived from the VH3 gene family and its V_H CDR3 sequence (Table 2.7) varied from the V_H CDR3 sequences of the pan-reactive binders isolated from the scFv library (Table 2.5).

Table 2.7 Variable gene family and V_H CDR3 sequence of the isolated pan-reactive antibody fragment that binds a non immune-dominant epitope on DENV NS1. The variable gene familiy and V_H CDR3 were determined by inputting the clone nucleotide sequences into the immunogenetics (IMGT)-V-QUEST software [http://imgt.org/IMGT_vquest/share/textes/]. The clone was isolated from a V_H dAb phage library

Clone	**V_H Family**	**V_H CDR3**													
D1C2 V_H dAb	VH3	V	F	K	W	C	E	T	L	G	A	H	P	L	D	F

An evaluation of the recognition of DENV NS1 by D1C2 phage particles, soluble V_H dAb and reformatted V_H dAb Fc once again indicated correlating recognition of DENV NS1 by the phage particles and V_H dAb Fc (Figure 2.21). The soluble V_H dAb however, had low reactivity to DENV-2 NS1.

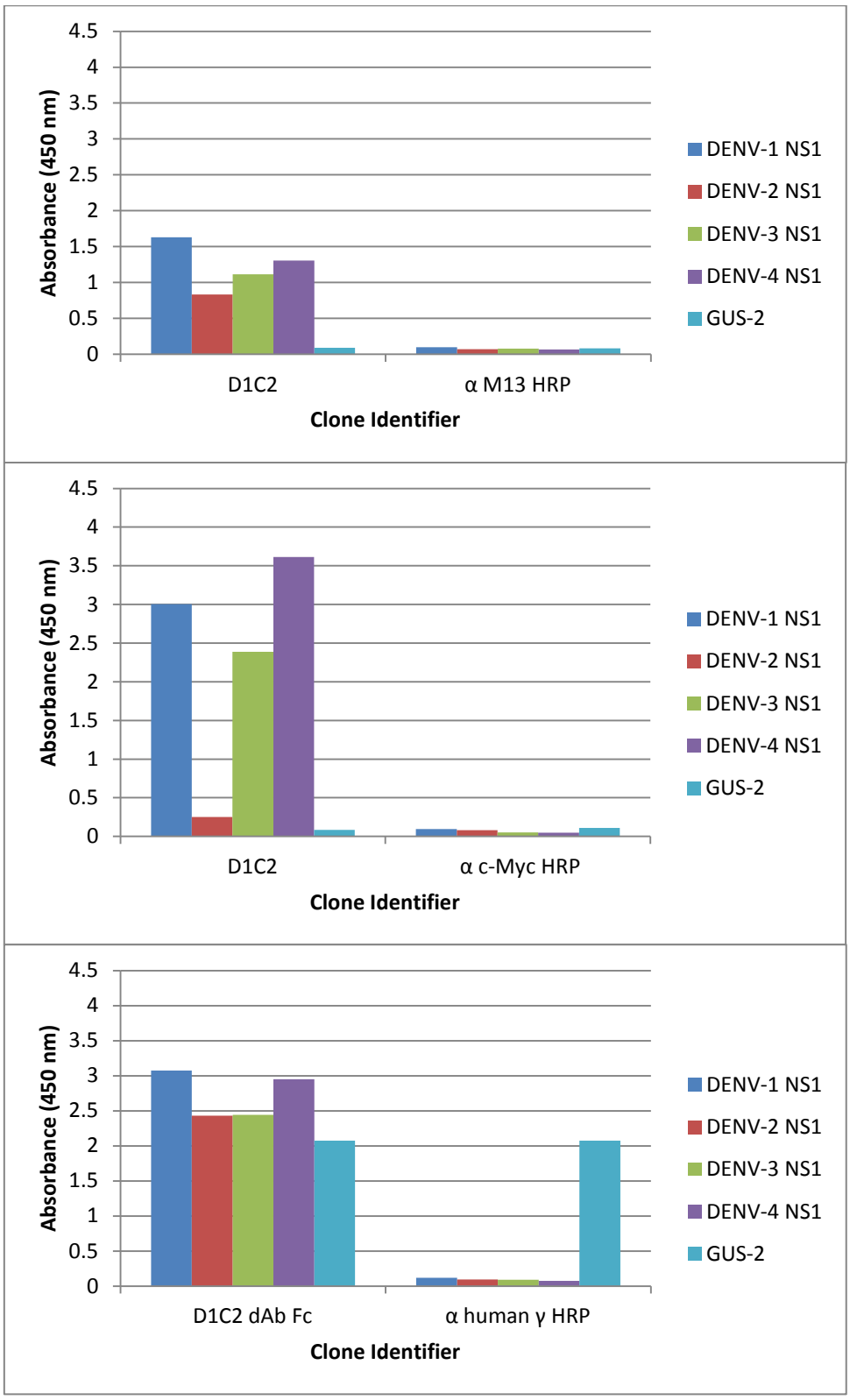

Figure 2.21 Immunoreactivity of D1C2 phage particles, V_H dAb and dAb Fc to DENV NS1. NS1 from all four DENV serotypes and GUS-2 a murine antibody against an immune-dominant epitope on DENV NS1 were immobilized on a polystyrene plate. D1C2 phage particles (top panel), V_H dAb (middle panel) or dAb Fc (bottom panel) isolated from a biopanning strategy that masked the GUS-2 epitope of DENV NS1 were added to the

immobilized antigen. The reactivity of the clone in its different formats to DENV NS1 and GUS2 was determined by the absorbance value measured after probing with an appropriate HRP-conjugated secondary antibody. HRP-conjugated secondary antibody added to wells with just the immobilized antigen or GUS-2 was used as the negative control.

2.4 DISCUSSION

Biopanning for binders against a target antigen is not always straight forward. The nature of the antigen, presentation of the antigen and the biopanning strategy that is used can determine whether relevant binders against an antigen are isolated. Despite these challenges, we successfully isolated serotype-specific antibodies against NS1 from each of the four DENV serotypes and at least one pan-reactive antibody against a non immune-dominant epitope on DENV NS1.

High homology amongst polypeptides can result in isolation of cross-reactive binders (1, 17). In this work, high homology amongst the polypeptide sequences of DENV NS1 affected the ability to solely isolate binders to serotype-specific regions even when a subtractive protocol was used to deplete binders to homologous regions. Although serotype-specific binders were successfully isolated from the scFv and Fab libraries, these were proportionally low in representation compared to the isolated pan-reactive binders. The nature of naïve libraries are such that the frequency of antigen-specific binders is low but it does not preclude the entire library from containing target-specific binders. When using a subtractive biopanning strategy, high affinity pan-reactive antibodies would be depleted in negative selection while moderate to low affinity pan-reactive antibodies may be inadvertently isolated during positive selection. This rationale was the basis for separately interrogating the phage-displayed antibody fragment libraries again for pan-reactive binders against DENV NS1. One strategy utilized immobilized NS1 from a different DENV serotype in each round of biopanning and yielded two unique scFv binders. The other strategy utilized a murine antibody (GUS-2) that masked an immune-dominant epitope that is implicated in reducing diagnostic sensitivity of NS1 capture assays in secondary DENV infections (10). This strategy separately used immobilized GUS-2 as bait for NS1 from all four DENV serotypes before exposure to the V_H dAb phage library. A single V_H dAb was isolated using this strategy. What was starkly evident about this strategy was the dominant isolation of antibodies against GUS-2. This was not the intended outcome but it arose because equi-molar concentrations of immobilized GUS-2 and captured DENV NS1 were not used. Furthermore, the stability of the interaction (affinity) between the GUS-2 and each DENV NS1 differs. Any free antibody either from excess immobilization or from antibody-antigen dissociation would have therefore presented itself as a potential target for isolation of binders from the V_H dAb library.

Variable levels of enrichment were noted during sequential rounds of biopanning. This enrichment did not however always translate to a high frequency of target-specific binders when a monoclonal phage ELISA was performed. The ratio of input to output is an indication of the number of phage that are carried through in each round, not necessarily a reflection of antigen-specific phage. Non-

specific or aberrant phage particles with growth advantages can increase background binding. Propagation can be aided by the absence of the functional insert or the presence of a non-toxic sequence therefore impacting on assembly of bacteriophage particles and their potential for infectivity (13, 21). A resolution that has been suggested to minimize this problem is to use eluted phage from the first round of panning in the next round without employing an amplification step (14). Furthermore, stringent washing conditions and more rounds of biopanning could be employed to improve the frequency of unique binders with desired properties.

Regardless of apparent levels of enrichment, the true determinant of successful biopanning is isolation of unique monoclonal binders which are subjected to physico-chemical and immunological characterization. Characterization of antibody fragments whilst tethered to phage particles is limited, as the actual concentration of binding sites cannot be controlled. Incorporation of the antibody fragment-gIIIp fusion protein into the phage particle is inefficient compared with incorporation of the wildtype gIIIp. As a result, the majority of phage particles contain no displayed binding fragment, some contain one binding fragment, whilst some may contain many (4). Periplasmic expression of soluble antibody fragments in *E.coli* can therefore be useful for characterization work during the early stages of antibody discovery. The disadvantage however is that while Fabs are monovalent and the V_H dAb phage library used in this work is aggregation resistant, scFvs can form dimers, trimers and higher aggregates (2, 4). Some eukaryotic protein sequences can also adversely affect their levels of expression and their stability when produced using prokaryotic host systems (8). Furthermore, work by Cabezas et al. (3) previously showed that phage-displayed antibody fragments do not always retain their binding activity when they are expressed as soluble antibody fragments. This therefore impacts on the utility of such fragments as was observed in some instances in this work. This problem was circumvented by reformatting the antibody fragments to include stabilizing Fc regions. It has been previously been reported that reformatted IgG can sometimes impede target recognition (19) but in this current work, all instances of IgG reformation led to identical reactivity between phage-displayed antibody fragments and phage antibodies with the antigen.

To conclude, we have been successful in isolating antibodies that bind NS1 from all four serotypes of DENV and at least one pan-reactive binder that recognizes a non immune-dominant epitope on DENV NS1. This is a challenging task because NS1 of DENV serotypes 1, 2, 3 and 4 share structure and 70% sequence homology and thus isolating antibodies that bind to serotype-specific epitopes is dependent on the extent of surface exposure of the variations that are interspersed throughout the NS1 sequence. Using hybridoma technology would require rigorous screening to identify the appropriate antibodies as antibodies against immune-dominant epitopes would

dominate the induced immune response. High quality and diverse naïve libraries, together with perceptive biopanning strategies of phage-displayed antibody fragment libraries are required to isolate binders against serotype-specific epitopes and pan-reactive non immune-dominant epitopes. These binders were isolated due to the sheer size of the libraries, the diversity of the libraries, and the creation of new specificities inherent in the V_H and V_L chain shuffling process that occurs upon library creation. Furthermore subtractive biopanning strategies and tandem binding biopanning strategies are pre-emptive of the possible challenges of isolating appropriate antibodies and were thus used to deplete the libraries of antibodies that we did not desire.

In the next chapter, the ability of the generated serotype-specific antibodies; 9H2 α DENV-1 NS1, 4C11 α DENV-2 NS1, 7G11 α DENV-3 NS1, 6A5 α DENV-4 NS1 and 6A7 α DENV-4 NS1, to be used in a sandwich ELISA for capture of DENV NS1 and its detection through pairing with all the isolated pan-reactive antibodies shall be evaluated.

2.5 REFERENCES

1. **Bradbury, A. R., S. Sidhu, S. Dübel, and J. McCafferty.** 2011. Beyond natural antibodies: the power of in vitro display technologies. Nature Biotechnology **29:**245-254.
2. **Brichta, J., M. Hnilova, and T. Viskovic.** 2005. Generation of hapten-specific recombinant antibodies: antibody phage display technology: a review. Vet Med Czech **50:**231-252.
3. **Cabezas, S., G. Rojas, A. Pavon, M. Alvarez, M. Pupo, G. Guillen, and M. G. Guzman.** 2008. Selection of phage-displayed human antibody fragments on Dengue virus particles captured by a monoclonal antibody: Application to the four serotypes. Journal of Virological Methods **147:**235-243.
4. **Carmen, S., and L. Jermutus.** 2002. Concepts in antibody phage display. Briefings in Functional Genomics and Proteomics **1:**189-203.
5. **Christ, D., K. Famm, and G. Winter.** 2007. Repertoires of aggregation-resistant human antibody domains. Protein Engineering Design and Selection **20:**413-416.
6. **Cordeiro, M. T.** 2012. Laboratory diagnosis for dengue. Revista do Instituto de Medicina Tropical de São Paulo **54:**10-12.
7. **de Haard, H. J., N. van Neer, A. Reurs, S. E. Hufton, R. C. Roovers, P. Henderikx, A. P. de Bruine, J. W. Arends, and H. R. Hoogenboom.** 1999. A large non-immunized human Fab fragment phage library that permits rapid isolation and kinetic analysis of high affinity antibodies. Journal of Biological Chemistry **274:**18218-18230.
8. **Duenas, M., M. Ayala, J. Vazquez, M. Ohlin, E. Söderlind, C. Borrebaeck, and J. Gavilondo.** 1995. A point mutation in a murine immunoglobulin V-region strongly influences the antibody yield in Escherichia coli. Gene **158:**61-66.
9. **Erra, E. O., E. M. Korhonen, L. Voutilainen, E. Huhtamo, O. Vapalahti, and A. Kantele.** 2013. Dengue in travelers: kinetics of viremia and NS1 antigenemia and their associations with clinical parameters. PLoS One **8:**e65900.
10. **Falconar, A. K. I.** 2007. Antibody responses are generated to immunodominant ELK/KLE-type motifs on the nonstructural-1 glycoprotein during live dengue virus infections in mice and humans: Implications for diagnosis, pathogenesis, and vaccine design. Clinical and Vaccine Immunology **14:**493-504.
11. **Guzman, M. G., S. B. Halstead, H. Artsob, P. Buchy, J. Farrar, D. J. Gubler, E. Hunsperger, A. Kroeger, H. S. Margolis, E. Martinez, M. B. Nathan, J. L. Pelegrino, C. Simmons, S. Yoksan, and R. W. Peeling.** 2010. Dengue: a continuing global threat. Nat Rev Microbiol **8:**S7-16.

12. **Guzmán, M. G., and G. Kourí.** 2004. Dengue diagnosis, advances and challenges. International Journal of Infectious Diseases **8:**69-80.
13. **Hammers, C. M., and J. R. Stanley.** 2014. Antibody Phage Display: Technique and Applications. J Invest Dermatol **134:**e17.
14. **Hoogenboom, H. R., A. P. de Bruïne, S. E. Hufton, R. M. Hoet, J.-W. Arends, and R. C. Roovers.** 1998. Antibody phage display technology and its applications. Immunotechnology **4:**1-20.
15. **Jones, M. L., T. Seldon, M. Smede, A. Linville, D. Y. Chin, R. Barnard, S. M. Mahler, D. Munster, D. Hart, P. P. Gray, and T. P. Munro.** 2010. A method for rapid, ligation-independent reformatting of recombinant monoclonal antibodies. J Immunol Methods **354:**85-90.
16. **Meyer, T., J. Stratmann-Selke, J. Meens, T. Schirrmann, G. F. Gerlach, R. Frank, S. Dubel, K. Strutzberg-Minder, and M. Hust.** 2011. Isolation of scFv fragments specific to OmpD of Salmonella Typhimurium. Vet Microbiol **147:**162-9.
17. **Nissim, A., H. R. Hoogenboom, I. M. Tomlinson, G. Flynn, C. Midgley, D. Lane, and G. Winter.** 1994. Antibody fragments from a 'single pot' phage display library as immunochemical reagents. EMBO J **13:**692-8.
18. **Peeling, R. W., H. Artsob, J. L. Pelegrino, P. Buchy, M. J. Cardosa, S. Devi, D. A. Enria, J. Farrar, D. J. Gubler, and M. G. Guzman.** 2010. Evaluation of diagnostic tests: dengue. Nature Reviews Microbiology **8:**S30-S37.
19. **Rouet, R., D. Lowe, K. Dudgeon, B. Roome, P. Schofield, D. Langley, J. Andrews, P. Whitfeld, L. Jermutus, and D. Christ.** 2012. Expression of high-affinity human antibody fragments in bacteria. nature protocols **7:**364-373.
20. **Sheets, M. D., P. Amersdorfer, R. Finnern, P. Sargent, E. Lindqvist, R. Schier, G. Hemingsen, C. Wong, J. C. Gerhart, and J. D. Marks.** 1998. Efficient construction of a large nonimmune phage antibody library: The production of high-affinity human single-chain antibodies to protein antigens. Proceedings of the National Academy of Sciences **95:**6157-6162.
21. **Thomas, W. D., M. Golomb, and G. P. Smith.** 2010. Corruption of phage display libraries by target-unrelated clones: Diagnosis and countermeasures. Analytical Biochemistry **407:**237-240.
22. **Wesolowski, J., V. Alzogaray, J. Reyelt, M. Unger, K. Juarez, M. Urrutia, A. Cauerhff, W. Danquah, B. Rissiek, F. Scheuplein, N. Schwarz, S. Adriouch, O. Boyer, M. Seman, A. Licea, D. V. Serreze, F. A. Goldbaum, F. Haag, and F. Koch-Nolte.** 2009. Single

domain antibodies: promising experimental and therapeutic tools in infection and immunity. Medical Microbiology and Immunology **198:**157-174.

23. **Young, P. R., P. A. Hilditch, C. Bletchly, and W. Halloran.** 2000. An Antigen Capture Enzyme-Linked Immunosorbent Assay Reveals High Levels of the Dengue Virus Protein NS1 in the Sera of Infected Patients. J. Clin. Microbiol. **38:**1053-1057.

Chapter 3

DEVELOPMENT OF A SEROTYPING DENV NS1 CAPTURE ASSAY

3.1 INTRODUCTION

The hallmark of antibody-based diagnostic assays (immunoassays) is the formation of specific and stable interactions between antibodies and antigens. The enzyme-linked immunosorbent assay (ELISA) is the most common immunoassay format. Lateral flow assays, bead assays based on the Luminex system and flow cytometry-based assays have gained popularity as diagnostic immunoassay formats but the ELISA remains the gold standard of *in vitro* analysis of biomarkers and analytes in healthcare (13). The ELISA has proven to be a reliable and sensitive immunoassay particularly in a sandwich format (8, 17) which was developed by Wide (15). The sandwich ELISA involves the use of one or more antibodies for solid-phase capture of antigen. The capture antibodies recognize sites on the antigen, which are different to the site that is recognized by another antibody that is used for detection. The detection antibody has an enzyme conjugate that provides a signal for detection of antigen recognition.

The molecular determinants of antigen recognition are applied to the artificial pairing of antibodies used to capture and detect a soluble analyte in a diagnostic assay. Successful antibody pairing is governed by principles of valency, steric hinderance and cooperativity (5). IgG are regarded as bivalent molecules because a single paratope appears once in each arm of the antibody and thus a maximum of two binding sites can simultaneously bind antigen. The number of epitopes that can concurrently be bound by antibodies on the other hand represents the valency of the antigen. It is not always possible for different combinations of antibodies to maximally bind the epitopes on a single antigen because antigens have many overlapping epitopes which lead to spatial limitation of antibody binding referred to as steric hinderance. Furthermore, binding of one antibody can distort or enhance the epitope for another antibody leading to a negative or positive cooperativity between the antibody pair (4, 11).

Characterization and optimization of antibody pairs is central to the development of antibody assays. Determination of epitopes bound by the antibodies is one of the characterization studies that are often undertaken. The epitopes can be of either a contiguous or conformational nature. Contiguous epitopes are a specified linear peptide length recognized by antibodies while conformational epitopes rely on the juxtaposition of non-contiguous regions within spatial proximity, to constitute the antigenic determinant. The boundaries of either type of epitope can be difficult to determine. Contiguous epitopes however are somewhat easier to determine experimentally using synthesized, overlapping peptides that span the length of the antigen. Determination of conformational epitopes on the contrary is a much more involved undertaking. Conformational epitopes can only be defined in structural terms and therefore require knowledge of

the detailed crystal structure of antibody-antigen complexes through techniques such as X-ray diffraction or information regading structure in solution by nuclear magnetic resonance spectroscopy.

Optimally paired antibodies are pivotal for immunoassays because the aim is to either qualitatively detect a soluble analyte or quantitatively measure a soluble analyte with high reliability. The strength and stability of the antibody-antigen interaction is critical to the detection or quantification of the macromolecular complex. The kinetics of the interaction as signified by association and dissociation phases are influenced by the concentration of antibody ligand, the concentration of the antigen analyte, and the rate constants of the intrinsic association and dissociation of the antibody with the antigen (k_a and $k_{d,}$ respectively) (12). Measured k_a and $k_{d,}$ are used to calculate the affinity or the strength of the antibody-antigen interaction. At optimized concentrations of capture and detection antibodies, antigen affinity and/or positive cooperativity of the antibodies can be exploited in a sandwich ELISA to detect antigen at varying concentrations dependent on individuals' responses to disease. NS1 concentrations in serum vary in DENV infections. DENV NS1 levels can reach upwards of 15 μg/mL (2, 16). Using polyclonal mouse and rabbit antibodies against DENV-1 NS1, Alcon et al. (2) determined that DENV-1 NS1 concentrations in primary infections ranged between 0.04 and 2 μg/mL while a slightly lower concentration range between 0.01 and 2 μg/mL was measured in secondary infections (2). Diagnostically relevant immunoassays therefore need to be able to sensitively detect the lower limits of DENV NS1 in the sera of infected patients.

This chapter focuses on using generated IgG antibodies against DENV NS1 to develop a qualitative assay that serotypes DENV infections. The utility of individual serotype-specific and pan-reactive antibodies in a sandwich ELISA assay was evaluated. Pan-reactive antibodies were used for antigen capture followed by detection with serotype-specific antibodies. Pan-reactive antigen capture was unsuccessful except in the instance where a control murine antibody GUS-2 which binds the immune dominant epitope was used for DENV NS1 capture. The assay was inverted to capture DENV NS1 with serotype-specific antibodies, and detect with pan-reactive phage particles. The inversion still failed to yield a detectable pan-reactive signal except where GUS-2 antibody was again used for detection. The serotype-specific antibodies were taken forward for further characterization. The antibodies showed an ability to bind native NS1 antigen in a serotype-specific manner. The serotype-specific antibodies were found to recognize spatially clustered conformational epitopes. The calculated equilibrium dissociation constants of the interactions of the serotype-specific antibodies with DENV NS1 ranged from 2.9×10^{-7} to 3.5×10^{-9} M. Serotype-specific antibodies were paired with GUS-2 for proof-of-principle serotyping capability and limit of

DENV NS1 detection sandwich ELISA assay. The results showed that DENV NS1 could be detected in the ng/mL range with DENV-1 NS1 being able to be detected at 0.04 ng/mL using GUS-2 antibody capture and 9H2 antibody detection.

3.2 MATERIALS AND METHODS

3.2.1 MURINE ANTIBODIES

Murine antibodies 1G5, 1H7, 3D1 and GUS-2 used in this research were kindly provided by Professor Paul Young (School of Chemistry and Molecular Biosciences, The University of Queensland).

3.2.2 HRP CONJUGATION OF ANTIBODIES

1 mg of each antibody was buffer exchanged into 500 µL of bicarbonate buffer (Thermo Scientific) using Zeba Spin Desalting Columns, 7K MWCO (Thermo Scientific). Amine conjugation of antibody with horseradish peroxidase (HRP) was performed using the EZ-Link Plus Activated Peroxidase Kit (Thermo Scientific) according to manufaturer's instructions. Removal of excess unconjugated HRP was performed using the Zeba Spin Desalting Columns, 7K MWCO. Concentration of each antibody following desalting and conjugation was determined on the NanoDrop™ 1000 Spectrophotometer (Thermo Scientific).

3.2.3 SANDWICH ELISA

3 µg/mL of capture antibody was prepared in phosphate buffered saline (PBS) and used to coat a MaxiSorp™ plate (Nunc) overnight at 4 ˚C. Any unbound antibody was discarded and followed by three consecutive washes with a wash buffer made with 1 x phosphate buffered saline (PBS) and 0.01% Tween20. Excess binding sites on the plate were blocked using a blocking buffer made with PBS supplemented with 2.5% skim milk powder (M-PBS). The blocking buffer was discarded and 1 µg/mL of DENV NS1 made in 2.5% M-PBS was added and incubated for an hour. The incubation was followed by three washes with wash buffer. 3 µg/mL of detection antibody or phage diluted in blocking buffer was added to the wells. Following one hour incubation, three washes with the wash buffer were performed and the plate was probed with 200 µL of HRP-conjugated anti-M13 (GE Healthcare) or HRP-conjugated goat anti mouse [H+L] IgG (Life Technologies) or HRP-conjugated goat anti human IgG [γ chain specific] (Sigma) diluted to 0.1 µg/mL in M-PBS. Three final washes with the wash buffer were performed then 100 µL TMB substrate (Sigma Aldrich) was added to develop the chromogenic signal. The reaction was stopped with 2N sulphuric acid and the absorbance at 450 nm was read using the Spectramax (Molecular Devices) or the PowerWave XS2 (Biotek – Millenium Science).

3.2.4 ELISA WITH IMMOBILIZED PEPTIDES

A peptide corresponding to amino acid residues 111-125 of DENV-1 NS1 (CGGHK**YSWK**S**WGKAK**IIG) and a control unrelated peptide (CGGSKGTPMYSVDL), both with cysteine-glycine-glycine leader residues were synthesised by the Australian Biobest Biotechnology Service. The underlined residues are conserved on NS1 across all four serotypes. The peptides were reconstituted to 5 mg/mL using 1 x PBS. The cysteine residue was used to immobilize and orientate 10 µg/mL of the peptide diluted in binding buffer, on maleimide activated clear 8-well strips (Thermo Scientific) as per manufacturer's instructions. A blocking step with PBS supplemented with 2% skim milk powder (M-PBS) was included after inactivating excess maleimide groups using a cysteine solution. GUS-2, 3D1, 9H2, 4C11, 7G11 and 6A5 test antibodies were used at a concentration of 10 µg/mL in M-PBS. HRP-conjugated anti mouse IgG (H+L) (Life Technologies) or HRP-conjugated anti human IgG [γ chain specific] (Sigma Aldrich) were used at concentration of 0.1 µg/mL in M-PBS. TMB substrate was used to develop the chromogenic signal and absorbances were measured using the Spectramax (Molecular Devices).

3.2.5 VERO CELL INFECTION

Vero (African green monkey kidney) cells were adapted and grown using Opti-MEM (Gibco) supplemented with 3% fetal calf serum (Bovogen) in T25 vented flasks (Greiner Bio-One) in a humidified, 37 ˚C incubator with 5% $C0_2$. Cells were split using 0.5% Trypsin versene (Gibco) and seeded at 50% confluence in either T25 vented flasks or in 96-well cell culture plates (Corning® Costar®). Cells were infected with DENV-1, DENV-2, DENV-3, DENV-4 (all East Timor strains corresponding to GenBank entries 440432.1, 440433.1, 440434.1 and 440435.1 respectively) or Kunjin virus (KUNV, a highly attenuated, Australasian variant of West Nile virus) at 0.1 multiplicity of infection in serum-free Opti-MEM for 2 hours at 37 ˚C. After infection, the infection medium was replaced with Opti-MEM supplemented with 2% fetal calf serum. DENV infected cells were cultured for three days while KUNV infected cells were cultured for two days. Cell culture supernatants from T25 flasks were harvested and concentrated (Macrosep Advance Centrifugal Devices, Pall) then used in a sandwich ELISA to detect secreted NS1 while infected cells in 96-well cell culture plates were fixed and used in immunofluorescence assays.

3.2.6 IMMUNOFLUORESCENCE ASSAYS

Immunofluorescence assays were performed on cells fixed with paraformaldehyde and permeabilised with 0.1% Triton x100. Wells were blocked with 2% casein in PBS with 0.01%

Tween 20 (PBS-T). Serotype-specific antibodies against DENV NS1 were used at a concentration of 10 µg/mL in blocking solution, while the mouse antibody against the flaviviral envelope protein was used at a concentration of 1 µg/mL also in blocking solution. Following one hour incubation, three washes were performed using PBS-T. Anti mouse Alexa Fluor 546 (Life Technologies), anti-human Alexa Fluor 488 (Jackson ImmunoResearch) and Hoescht (Thermo Scientific) in blocking buffer were added to the wells and incubated for a further hour before another 3 washes with PBS-T. Immuno-fluorescence imaging was performed at 40 x magnification using the InCell Analyzer (GE Healthcare).

3.2.7 WESTERN BLOTTING

Determination of antibody binding to linear epitopes was performed by Western blot. 5 µg/mL of DENV NS1 and 15 µg/mL of bi-specific antibody NBF 736 (scFv – human Fc – scFv) were denatured at 90 ˚C for 7 minutes in a reaction with 4 x LDS buffer (NuPAGE), 10 X reducing agent (NuPage). 20 µL reactions of reduced proteins were loaded into single wells of a Mini Protean® TGX Stain-Free™ Gel. 10 µL of SeeBlue Plus 2 marker was used as a standard to determine the molecular mass of sample proteins. The proteins were electrophoresed at 200 volts for 30 minutes using the Tris/Glycine/SDS Buffer (BioRad) in a Mini Protean® Tetra System (BioRad). The proteins from the gel were turbo-blotted for 7 minutes onto a 0.2 µm PVDF membrane from the Trans-Blot® Turbo™ Mini PVDF Transfer Packs using the Trans-Blot® Turbo™ Transfer System. Each membrane was blocked for 30 minutes in a tray with 25 mL blotting buffer (25 mM Trizma base, 0.15 M NaCl and 0.1% Tween-20) supplemented with 2% skim milk powder. 5 µg of test antibody in 25 mL blocking buffer was added to each membrane and incubated for an hour. The blocking buffer was discarded and rinsed once with blotting buffer. 1 µg of HRP-conjugated goat anti mouse [H+L] IgG (Life Technologies) or HRP-conjugated goat anti human IgG [γ chain specific] (Sigma) in 25 mL blocking buffer was added to each membrane and incubated for another hour. The membranes were washed three times with blotting buffer. The signal from the HRP conjugate was developed using the Clarity™ Western ECL Substrate (Bio-Rad) for 5 minutes and exposed to UV light for 3 minutes using the ChemiDoc MP System (Bio-Rad).

3.2.8 SURFACE PLASMON RESONANCE

Antigen–antibody interaction kinetics and affinity were determined by Surface Plasmon Resonance (SPR) using the Biacore T100 (GE Healthcare). About 9 000 resonance units (RU) of anti human Fc (GE Healthcare, Human Antibody Capture Kit) or anti mouse Fc (GE Healthcare, Mouse Antibody Capture Kit) were immobilized on CM5 sensor chips. One flow cell acted as the reference

surface for the assay and did not have any antibody captured on its surface. The other flow cell acted as the active surface for the assay where the captured anti-DENV NS1 was used to assess interaction with the recombinant DENV NS1 analyte. Two-fold, serial dilutions of NS1 were made from 1 µM to 62.5 nM using the instrument running buffer (1 X HBS EP^+) with a final 300 mM NaCl concentration. Single cycle kinetics assays or high performance multi-cycle kinetics assays were performed. The flow rate used for injection of the capture antibody and the analyte was 30 µL/minute. Variable anti DENV NS1 capture times were used to allow approximately 140 RU of capture, then association with different concentrations of analyte proceeded for 3 minutes. Dissociation of the antigen from the antibody was measured over 10 or 15 minutes. Regeneration of the anti human Fc surface with 3M $MgCl_2$ was performed after each capture and analyte binding while regeneration of the anti mouse Fc surface was performed with 10 mM Glycine.HCl at pH 1.7 after each single cycle. The flow rate used for regeneration was 10 µL/minute for 30 seconds. The evaluation software generated sensorgrams of the antigen-antibody interactions yielding association and dissociation rate constants, from which the equilibrium dissociation constant was calculated assuming a 1:1 model of interaction.

3.2.9 LIMIT OF DETECTION ELISA

Checkerboard titration of capture and detection antibodies was performed in a sandwich ELISA format by immobilizing capture antigen in two-fold serial dilutions across the plate ranging in concentration from 10 µg/mL to 4.9 ng/mL. A single concentration of DENV NS1 (200 ng/mL) was captured in all the wells. Detection of capture was carried out using HRP-conjugated antibody that was titrated two-fold, down the plate starting at concentrations that ranged from 625 ng/mL to 4.9 ng/mL. Absorbance signals were measured at 450 nm after addition of TMB and 2N sulphuric acid. The concentrations of capture and detection antibodies that yielded the highest absorbance signal with minimal background noise were chosen to perform a titration of DENV NS1 in a sandwich ELISA to determine the limit of DENV NS1 detection by the antibody pair.

To determine the limit of DENV NS1 detection, a sandwich ELISA was performed using capture antibodies at 10 µg/mL and HRP-conjugated detection antibody at 625 ng/mL. The antigen to be detected by the antibody sandwich was prepared in PBS as two-fold serial dilutions of DENV NS1 ranging from 1.6 µg/mL to 49 pg/mL. The signal from the HRP-conjugated detection antibody was developed using TMB and an end-point absorbance signal was measured at 450 nm after stopping the reaction with 2N sulphuric acid.

3.3.1 SELECTION OF CAPTURE AND DETECTION ANTIBODY PAIRS

Characterization of the tandem binding potential of antibody pairs is important for determination of their prospective diagnostic utility in an antigen capture assay. The ability of pan-reactive and serotype-specific binders to detect DENV NS1 in a sandwich ELISA was therefore evaluated.

In the first instance, pan-reactive antibodies (including GUS-2) were used in solid-phase capture of DENV NS1. HRP-conjugated, serotype-specific antibodies were used for detection of captured antigen. The results showed that only GUS-2 was able to bind NS1 from all four dengue serotypes for detection by the serotype-specific antibodies (Figure 3.1).

The assay was also reversed where serotype-specific antibodies were used for capture of DENV NS1 and pan-reactive, phage-displayed antibody fragments were used for detection of the captured antigen. We previously showed in Chapter 2 that isolated phage-displayed antibody fragments and reformatted IgG1 antibodies have matched reactivity with DENV NS1. Murine GUS-2 antibody was included in pan-reactive detection as we did not have a phage-displayed antibody fragment that corresponded to the hybridoma-derived antibody. The results once again showed that the serotype-specific antibodies were only able to capture DENV NS1 and bind in-tandem with pan-reactive GUS-2 for detection of NS1 capture from all four DENV serotypes (Figure 3.2).

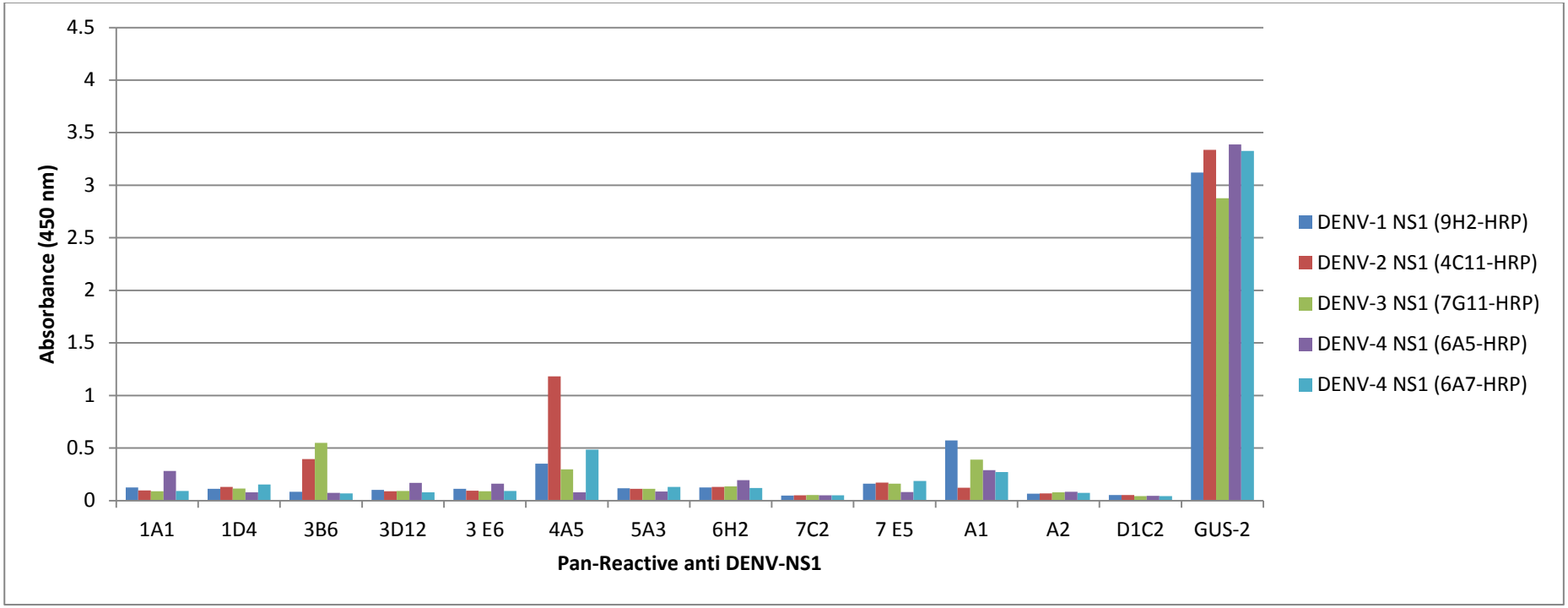

Figure 3.1 Tandem binding of pan-reactive antibodies and serotype-specific antibodies to DENV NS1. Fourteen pan-reactive antibodies were each immobilized to four wells in a 96-well polystyrene plate. NS1 from each DENV serotype was added to the four wells for each pan-reactive antibody. HRP-conjugated, serotype specific antibodies against DENV NS1 were used for detection of binding for the corresponding DENV serotype. Binding was determined by measuring the chromogenic signal produced by addition of TMB.

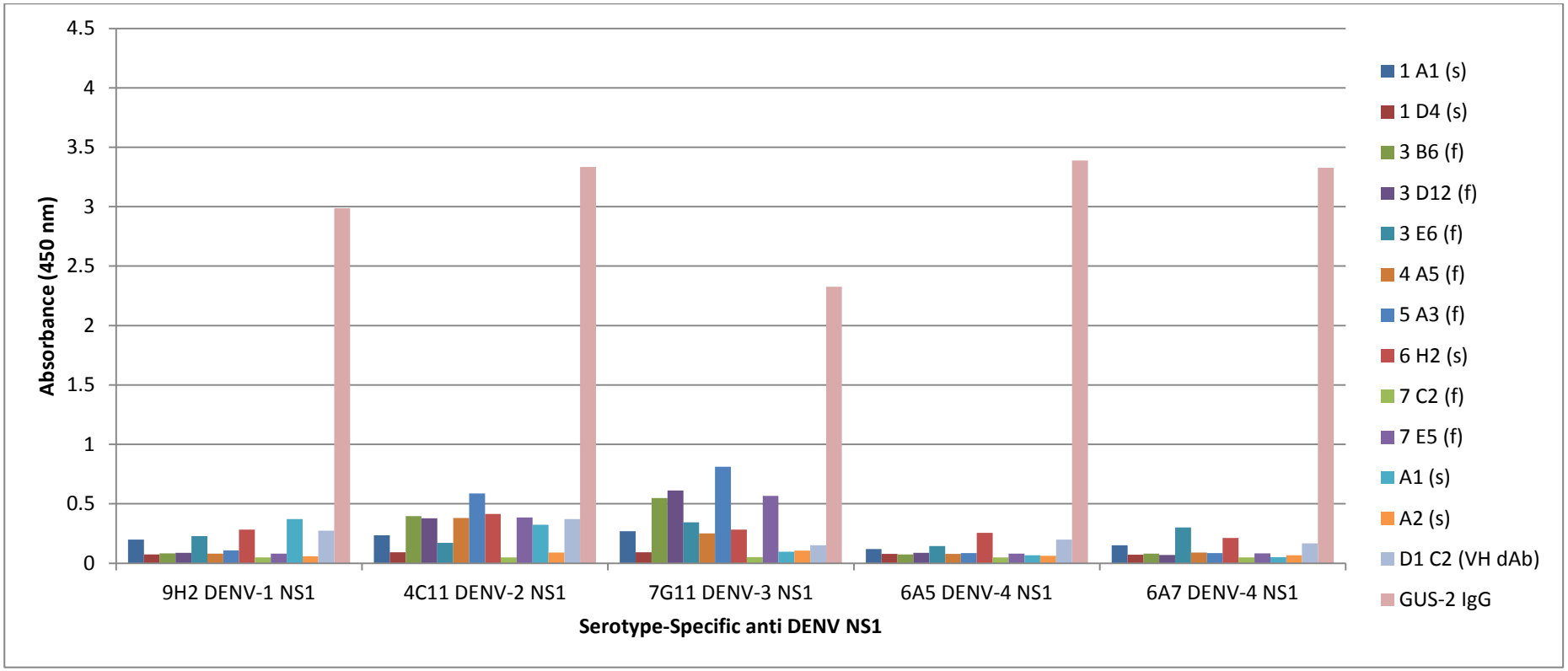

Figure 3.2 Tandem binding of serotype-specific antibodies and pan-reactive phage particles to DENV NS1. Five serotype-specific antibodies were immobilized to 14 wells each in a 96-well polystyrene plate. DENV NS1 was added to the 14 wells corresponding to the relevant serotype-specific antibody. Pan-reactive phage particles displaying scFv (s), Fab (f), V_H dAb, or GUS-2 antibody were added to the five wells corresponding to each serotype-specific antibody. An HRP-conjugated antibody against M13 bacteriophage was used for detection of binding by phage particles. HRP-conjugated antibody against murine Fc γ was used for detection of binding by GUS-2 antibody. Binding was determined by measuring the chromogenic signal produced by addition of TMB.

The inability for tandem binding of DENV NS1 by both serotype-specific and pan-reactive antibodies raised possibilities of the capture antibodies binding epitopes which sterically hinder the binding of the detection antibodies. To investigate this, the pan-reactive antibodies were used to capture DENV NS1 and GUS-2 was used for detection of capture. The rationale here was that the ability of the serotype-specific antibodies to bind DENV NS1 in tandem with GUS-2 meant that they bound spatially disparate epitopes. If the serotype-specific antibodies were sterically hindering the binding of the other pan-reactive antibodies, then using GUS-2 as the capture antibody would off-set that hindrance. The results of this assay showed that none of the pan-reactive antibodies, except D1C2, could bind NS1 from all four serotypes in tandem with GUS-2 (Figure 3.3). The ability of D1C2 antibody to bind DENV NS1 in tandem with GUS-2 is a logical finding, as D1C2 was isolated using a biopanning strategy which involved using Gus-2 to mask the immune-dominant epitope to isolate a pan-reactive binder from the V_H dAb library. D1C2 antibody therefore, must be binding a different epitope to GUS-2 but unfortunately binding an epitope which spatially competes with all four serotype-specific antibodies. Figure 3.3 also shows that antibodies 1A1, 3B6, 3E6 and 6H2 were only able to recognize DENV-1 NS1 in a sandwich with GUS-2 but not NS1 from the other three DENV serotypes. Because all pan-reactive antibodies except D1C2 were isolated from biopanning strategies that involved immobilized DENV NS1 it is likely that the antibodies recognize cryptic epitopes that are better exposed when the NS1 antigen was adsorbed on plastic.

Taken summatively, the data indicated positive binding reactivity with serotype-specific antibodies 9H2, 4C11, 7G11, 6A5 and 6A7 as well as pan-reactive antibody D1C2. Because D1C2 could not bind DENV NS1 in tandem with the serotype-specific antibodies, only the serotype-specific antibodies were taken forward for further characterization.

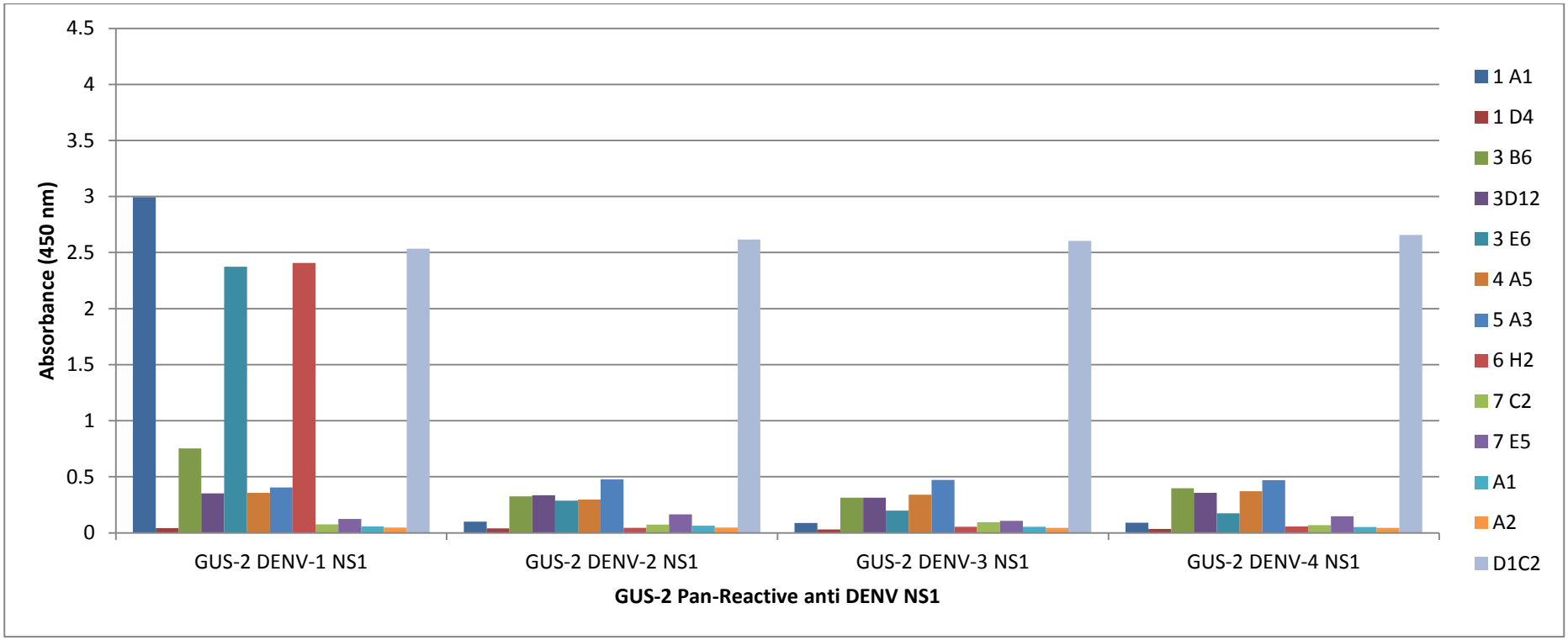

Figure 3.3 Tandem binding of GUS-2 and pan-reactive antibodies to DENV NS1. GUS-2 antibody was immobilized to 52 wells in a 96-well polystyrene plate. NS1 from each DENV serotype was added to 13 of these wells each. 13 pan-reactive antibodies against DENV NS1 were added to the plate. Binding was detected using a HRP-conjugated antibody against human Fc γ. Binding was determined by measuring the chromogenic signal produced by addition of TMB.

3.3.2 REACTIVITY OF SEROTYPE-SPECIFIC ANTIBODIES WITH NATIVE DENV NS1

Recombinant antigens often have tags that can be useful for expression and/or purification. One of the disadvantages of biopanning using these antigens that have not had the tags removed is that binders that recognize antigen-tag junctions can be isolated. DENV NS1 used in this work included an N-terminal hepta-histidine tag. To ascertain that the generated serotype-specific antibodies only recognized DENV NS1, immunoassays using native DENV NS1 were performed.

Vero cells were mock 'infected' or infected with clinical isolates of each DENV or KUNV. Infection with virus leads to accumulation of intracellular, membrane-associated NS1 and extracellular accumulation of secreted NS1. Serotype-specific antibodies were used to capture secreted NS1 from concentrated culture media in an ELISA format. HRP-conjugated GUS-2 was used to detect binding. Antibodies 9H2, 4C11, 7G11 and 6A5 were able to capture DENV NS1 in a serotype-specific manner while antibody 6A7 failed to recognize native DENV-4 NS1 (Figure 3.4). The Vero cells infected with KUNV were used to test for cross-reactivity with other flaviviral NS1 and no cross-reactivity was noted. Differences in the observed absorbance values are mainly because of differences in NS1 concentration. Dengue viruses are variably virulent resulting in production of different amounts of NS1. The amount of NS1 added to the assays was not standardized.

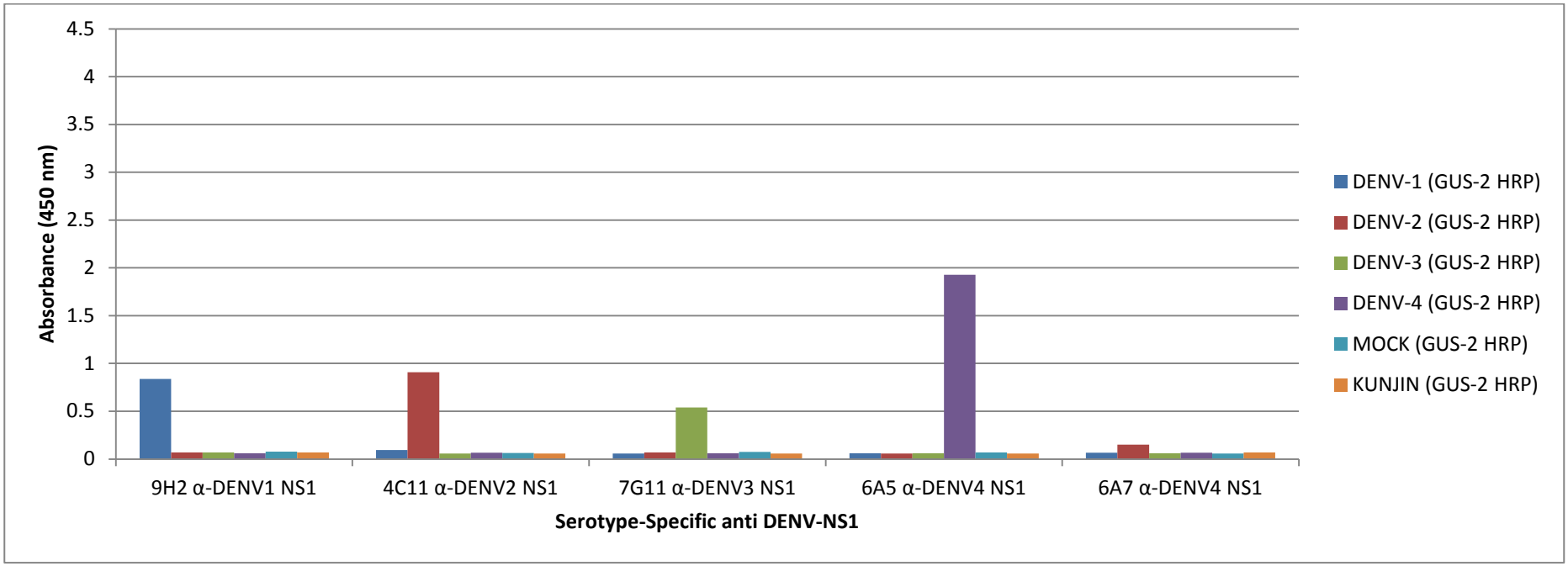

Figure 3.4 Serotype-specific recognition of native secreted DENV NS1. Each serotype-specific antibody was immobilized to six wells on a 96-well polystyrene plate. Concentrated culture supernatants from DENV, mock or Kunjin infected Vero cells were each added to five wells corresponding to each serotype-specific antibody. HRP-conjugated GUS-2 was added to detect binding of NS1 to the capture antibodies. Binding was determined by measuring the chromogenic signal produced by addition of TMB.

The reactivity of the reformatted, serotype-specific antibodies 9H2, 4C11, 7G11 and 6A5 with native, membrane-associated DENV NS1 was investigated by immunofluorescence assays using DENV, mock and kunjin infected Vero cells. 4G2 is an antibody against flaviviral envelope protein and it was used as a positive control to show that the cells were infected with flavivirus. The mock 'infected' Vero cells were used as a negative control. The results as shown in Figure 3.5, indicate that all four serotype-specific antibodies were again able to discern NS1 from each DENV serotype with no flaviviral cross reactivity noted.

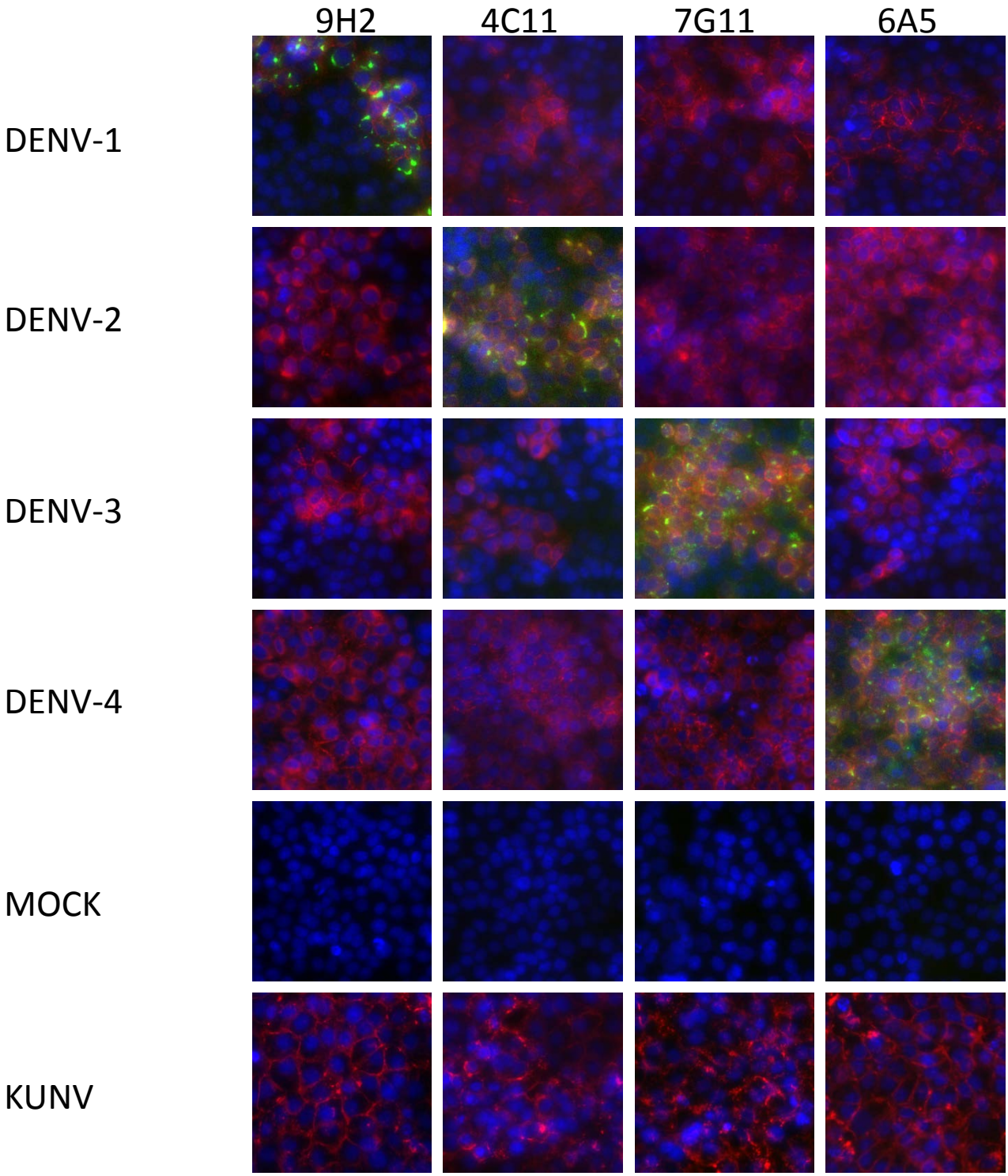

Figure 3.5 Serotype-specific recognition of native membrane-associated DENV NS1. Immunofluorescence assay micrographs showing binding of serotype-specific anti DENV NS1 to DENV, mock and KUNV infected Vero cells. Following 3 days of DENV infection or 2 days of KUNV virus infection, cells were paraformaldehyde treated and then permeabilised prior to addition of human antibodies against DENV NS1 (9H2, 4C11, 7G11 and 6A5). A control mouse antibody against flavivirus envelope protein (4G2) was added to each well to ensure flaviviral infection of cell. Anti-human IgG-488 (Green) and anti-

mouse IgG-Alexa Fluor546 (Red) were added to all wells in a dual stain to ascertain binding of antibodies to native antigen and confirm infection of Vero cells. All wells also had a nuclear stain (Hoescht) (Blue) added to them to determine the relative localisation of binding. Antibodies against DENV NS1 and the envelope protein showed peri-nuclear binding and diffuse cytoplasmic binding respectively.

3.3.3 PREDICTION OF EPITOPES BOUND BY SEROTYPE-SPECIFIC ANTIBODIES

Sandwich ELISA relies on mutual exclusivity of the epitopes recognized by capture and detection antibodies. The epitopes of the serotype-specific antibodies which can be used for either antigen capture or antigen detection therefore need to be determined to aid the isolation of a potential pan-reactive pairing antibody.

To evaluate whether contiguous or conformational epitopes were recognized by the serotype-specific antibodies, a Western blot was performed. Denatured DENV NS1 and a control bi-specific antibody with a human Fc linker were probed using the serotype-specific antibodies and an HRP-conjugated antibody against human Fc γ. GUS-2 and an HRP-conjugated antibody against mouse Fc γ were used as pan-reactive positive probes for detection of the contiguous immune-dominant epitope on NS1 from all four DENV serotypes. Positive control GUS-2 was able to detect contiguous epitopes on denatured antigen while serotype-specific antibodies did not bind denatured antigen (Figure 3.6). The binding of serotype-specific antibodies therefore, relies on structural integrity of the antigen pointing to recognition of conformational epitopes.

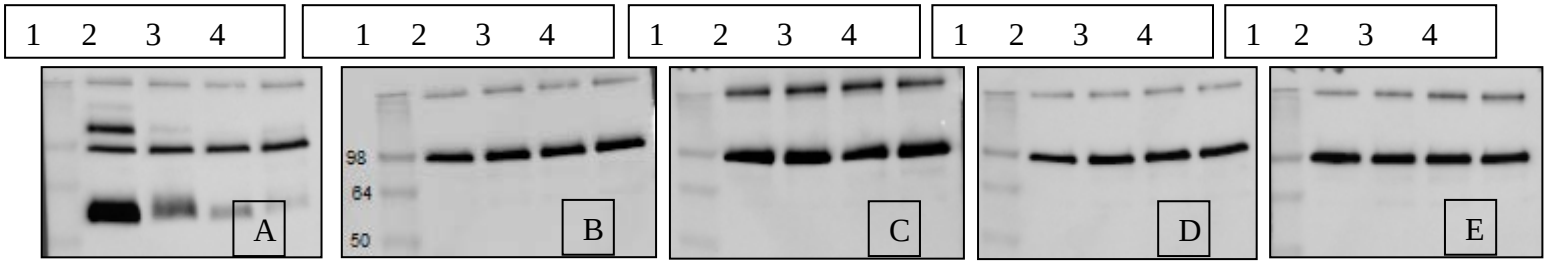

Figure 3.6 Western blotting of denatured DENV NS1. 5 x 20 µL reactions made up of NS1 from each DENV serotype at concentration of 5 µg/mL as well as a bi-specific antibody NBF736 with a human Fc γ linker at a concentration of 15 µg/mL were linearized using SDS and reducing agent and heated at 90 ˚C for 7 minutes. The 20 µL reactions of reduced proteins were loaded onto a Mini Protean® TGX Stain-Free™ Gel. 10 µL of SeeBlus Plus 2 marker was added to lane 1, DENV-1 NS1 + bispecific NBF736 was added to lane 2, DENV-2 NS1 + bispecific NBF736 was added to lane 3, DENV-3 NS1 + bispecific NBF736 was added to lane 4 and DENV-4 NS1 + bispecific NBF736 was added to lane 5. The proteins were electrophoresed at 200 volts for 30 minutes, turbo-blotted onto a PVDF membrane and probed with antibodies GUS-2 (panel A), 9H2 (panel B), 4C11 (panel C), 7G11 (panel D), (panel E) and an HRP-conjugated antibody against mouse and/or human Fc γ. The signal was developed with an ECL substrate and exposed to UV light for 3 minutes. Using the molecular mass marker (kDa) indicated in panel B, the DENV NS1 band was seen at about 55 kDa with a dimer seen as 110 kDa. Bi-specific NBF736 an 83 kDa protein was detected at about 95 kDa with a forced dimer detected at >148 kDa.

Determination of conformational epitopes requires complex and time consuming techniques which were beyond the scope of this project. A small of panel of murine antibodies were used in a sandwich ELISA with serotype-specific antibodies to potentially determine the relative epitopes of the serotype-specific antibodies. The motivation for this assay was to evaluate if any of the murine antibodies hindered binding of the serotype-specific antibodies. The panel of murine antibodies included 1G5, 1H7, 3D1 and GUS-2. Antibody **1G5** binds amino acid residues 299-307 on **DENV-2, 3 and 4 NS1**, antibody **1H7** binds amino acid residues 25-33 on **DENV-2 NS1** and antibody **3D1** binds amino acid residues 111-119 on **DENV-1, 2, 3 and 4 NS1** (6). Antibody GUS-2 also binds the same epitope as 3D1 and this was demonstrated in a direct ELISA using a peptide corresponding to amino acid residues 111-125 of DENV-1 NS1 in Figure 3.7. In the sandwich ELISA, murine antibodies against DENV NS1 were used to capture the antigen and HRP-conjugated, serotype-specific antibodies were used to detect capture. It was determined as shown in Figure 3.8, that the serotype-specific antibodies are unaffected by the binding of 1G5, 1H7 and GUS2. 3D1; however, another pan-reactive antibody which binds the same epitope as GUS 2 perturbed binding of all four serotype-specific antibodies.

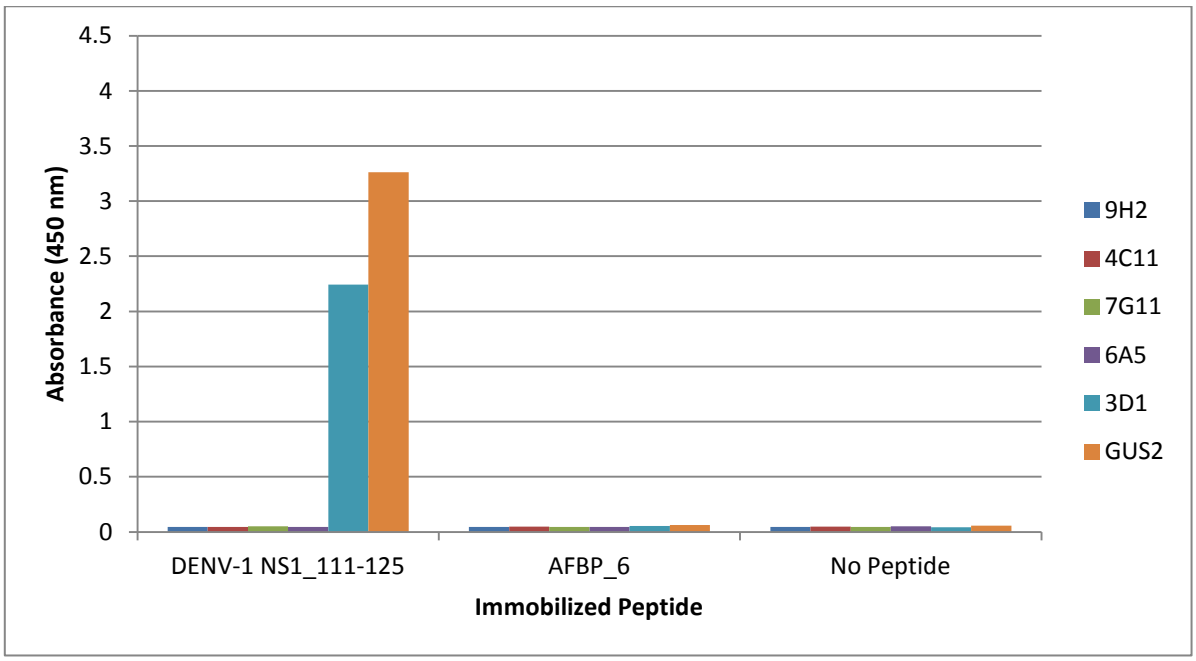

Figure 3.7 Binding of serotype-specific human antibodies and pan-reactive murine antibodies to a DENV NS1 immune-dominant linear peptide. A peptide that includes the sequence of the DENV-1 NS1 immune-dominant epitope (DENV-1 NS1_111-125: CGG**HKYSWKSWGKAKIIG**) and an unrelated peptide (AFBP_6: CGG**SKGTPMYSVDL**) were each immobilised to six wells in 96-well maleimide plate using the N-terminal cysteines of the peptides. Serotype-specific antibodies (used as negative controls) and pan-reactive antibodies were added to wells coated with each peptide. The binding of serotype-specific and pan-reactive antibodies to those peptides was determined by detection with an HRP-conjugated antibody against mouse or human Fc γ. Binding was determined by measuring the chromogenic signal produced by addition of TMB.

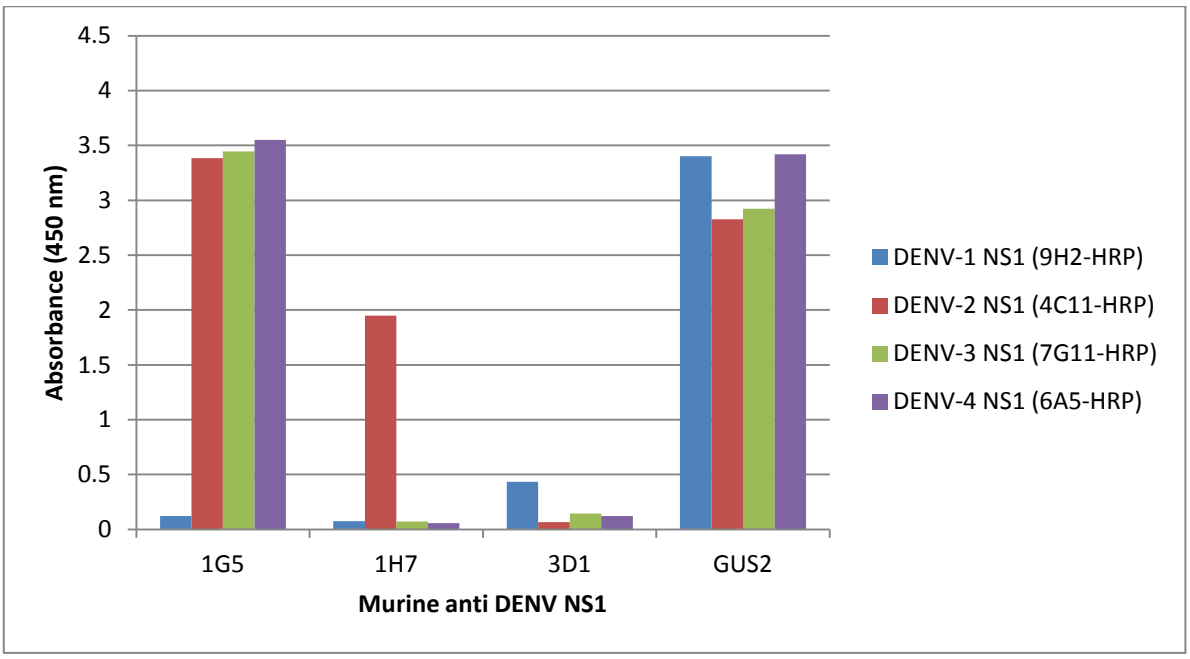

Figure 3.8 Mapping of serotype-specific DENV NS1 epitopes (murine antibody capture). Four murine antibodies against DENV NS1 were used as immobilized solid capture of DENV NS1 in a sandwich ELISA. NS1 from each DENV serotype was added to polystyrene wells coated with each murine antibody. HRP-conjugated, serotype-specific antibodies were used to detect tandem antigen binding for identification of shared epitopes between capture and detection antibodies. Binding was determined by measuring the chromogenic signal produced by addition of TMB.

The perturbation of serotype-specific antibody binding to DENV NS1 that was observed when using 3D1 as a capture antibody could have been be due to; (i) 3D1 binding the immune-dominant epitope with a footprint that sterically hindered the binding of the serotype-specific antibodies or (ii) negative cooperativity and distortion of the epitopes recognized by serotype-specific antibodies following binding 3D1. To determine which factor was at play, the sandwich ELISA assay was reversed. Capture reversal using human serotype-specific antibody capture and murine antibody detection resulted in comparable signals between 3D1 and GUS-2 detection antibodies (Figure 3.9). This indicates that pairing of 3D1 and serotype-specific antibodies leads to negative cooperativity when 3D1 is used as the capture antibody.

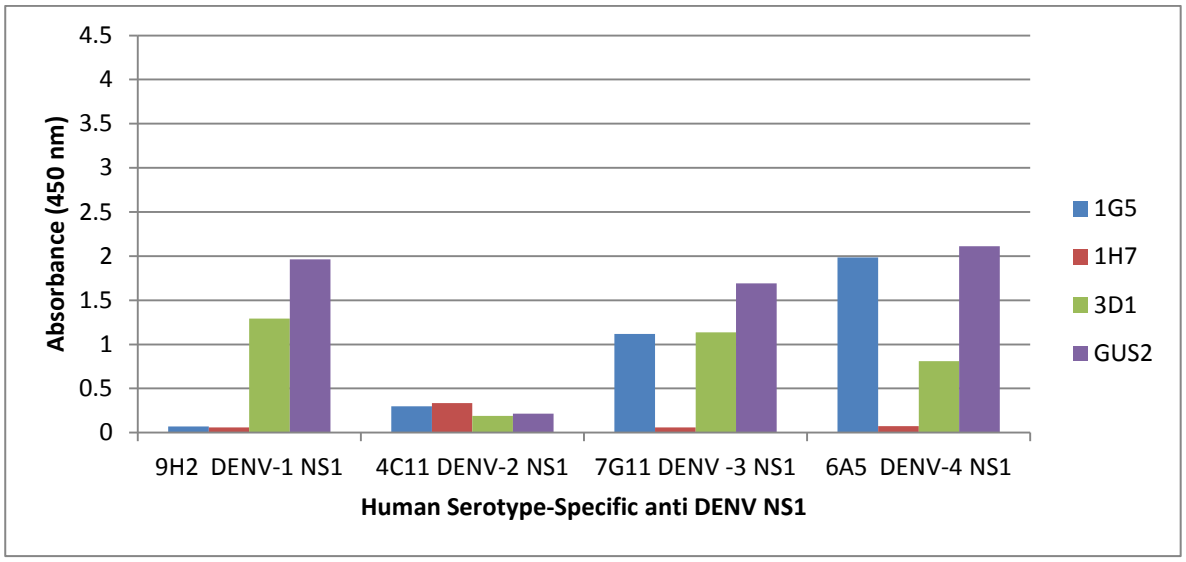

Figure 3.9 Mapping of serotype-specific DENV NS1 epitopes (human antibody capture). Four human, serotype-specific antibodies against DENV NS1 were used as immobilized solid capture of DENV NS1 in a sandwich ELISA. NS1 from each DENV serotype was added to polystyrene wells coated with each human antibody. Murine antibodies and a secondary HRP-conjugated antibody against mouse Fc γ were used to detect tandem antigen binding for identification of shared epitopes between capture and detection antibodies. Binding was determined by measuring the chromogenic signal produced by addition of TMB

Collectively, the negative cooperativity of 3D1 with all four serotype-specific antibodies and the inability of all four serotype-specific antibodies to pair with reformatted antibody D1C2 (V_H Fc) suggested that the epitopes of the serotype-specific antibodies are spatially clustered on DENV NS1. Relative localization of the epitopes however, will require additional experimental work.

3.3.4 INTERACTION KINETICS OF SEROTYPE-SPECIFIC ANTIBODIES AND DENV NS1

Quantitative determinations of the interaction kinetics of the serotype-specific antibodies and pan-reactive GUS-2 with DENV NS1 were performed to evaluate the potential utility of the antibodies in a DENV NS1 capture assay. Association and dissociation phases of the complexes that resulted from the interaction of the antibodies with their antigens were investigated using SPR.

The sensorgrams that are relevant to the k_a and k_d of GUS-2 with DENV NS1 are shown in Figure 3.10. The sensorgrams that are relevant to the k_a and k_d of the serotype-specific antibodies with DENV NS1 are shown in Figure 3.11. The K_D were extrapolated from measurements of k_a and k_d as shown in Table 3.1. GUS-2 showed the highest affinity for DENV-1 NS1 (5.4 x 10^{-9} M) and DENV-2 NS1 (1.8 x 10^{-9} M) constituted by a slower k_d and a faster k_a respectively, when compared to the interactions kinetics of GUS-2 with DENV-3 NS1 and DENV-4 NS1. The K_D for the serotype-specific antibody interaction with DENV NS1 ranged from 2.9 x 10^{-7} M between 4C11 and DENV-2 NS1 to almost 100-fold increased interaction between 6A5 and DENV-4 NS1(3.5 x 10^{-9} M) . 4C11 and DENV-2 NS1 in particular had a lower K_D because of a faster k_d. Figure 3.11 (panel B) also showed a lower response during the association phase of the kinetics measurements with only 20 RU measured when the highest concentration of DENV-2 NS1 (1 μM) was streamed over the captured 4C11 antibody surface. Interaction kinetics and affinities between 9H2 and DENV-1 NS1 as well as between 7G11 and DENV-3 NS1 were comparable as seen on the sensorgrams (Figure 3.11 panel A and B) and the calculated affinities on Table 1. The highest affinity of the serotype-specific antibodies was between antibody 6A5 and DENV-4 NS1 (3.5 x 10^{-9} M). A two-fold higher association rate and an almost 3-fold slower dissociation rate between 6A5 and DENV-4 NS1 when compared to 9H2 and DENV-1 NS1 as well as 7G11 and DENV-3 NS1was responsible for the observed higher affinity.

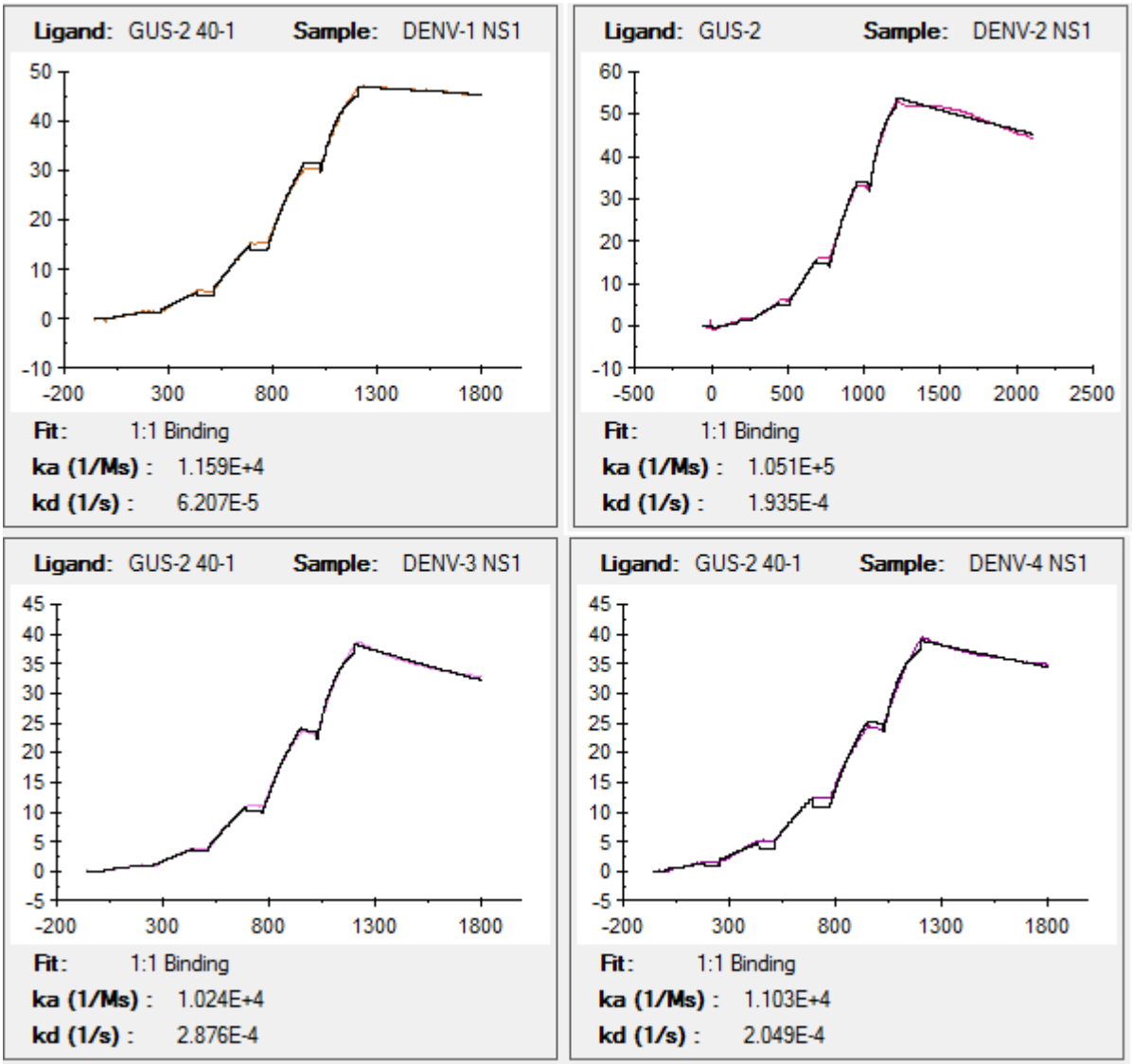

Figure 3.10 SPR sensorgrams for the interaction of GUS-2 antibody and NS1 from each DENV serotype. Analysis was performed on the Biacore T100 using single cycle kinetics. The antibody was immobilized on a CM5 sensor chip at a density that was measured at 140 resonance units (RU). Serial two-fold increasing concentrations of antigen from 62.5 nM to 1 µM were injected over the surface in a single cycle. The association phase proceeded for 180 seconds and the dissociation phase proceeded for 600 seconds (900 seconds for GUS-2 and DENV-2 NS1). The sensorgrams from these injections are shown as coloured lines. A 1:1 model of binding was fitted to the data (black lines) and the association rate (k_a), dissociation rate (k_d) and equilibrium dissociation constant (K_D) were determined for these interactions using the evaluation software.

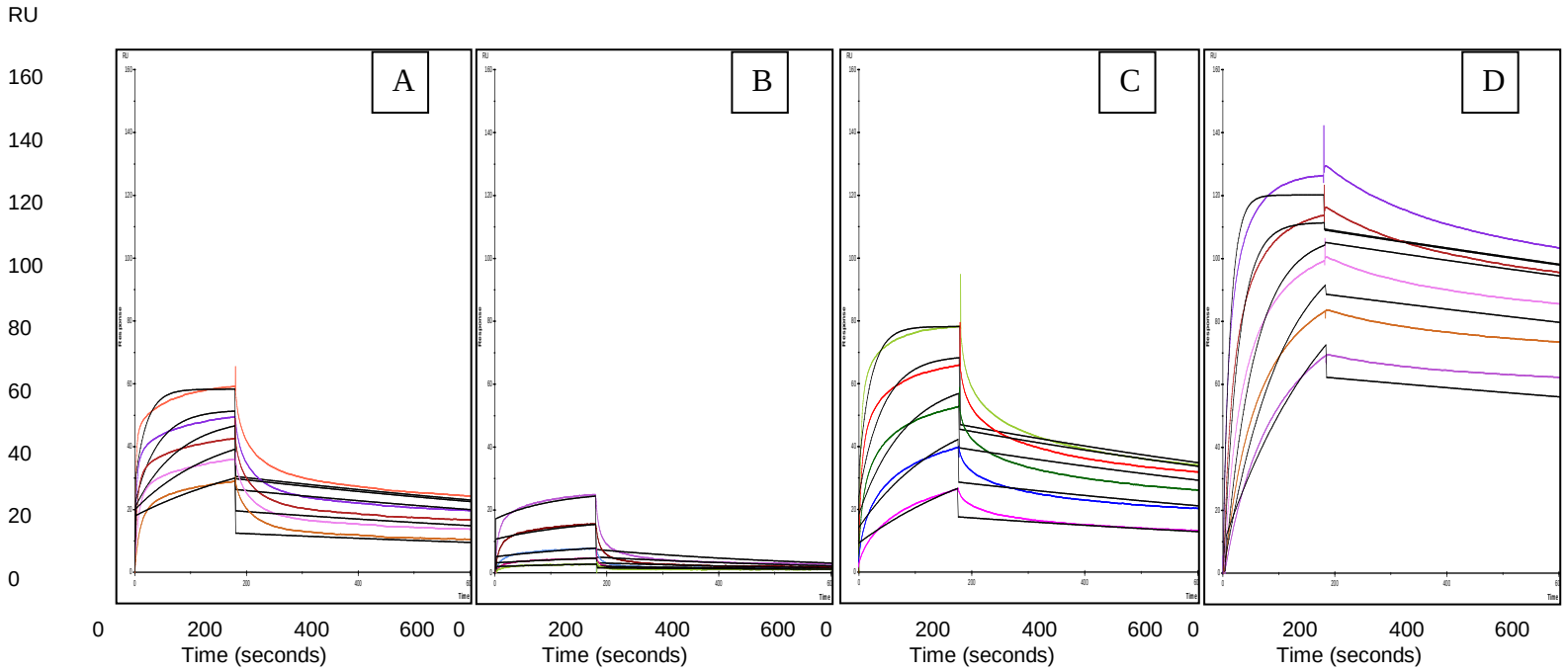

Figure 3.11 SPR sensorgrams for the interaction of 9H2 (A), 4C11 (B), 7G11 (C) and 6A5 (D) antibodies and NS1 from each DENV serotype. Analysis was performed on the Biacore T100 using high performance multi cycle kinetics. The antibodies were immobilized on a CM5 sensor chip at a density that was measured at 140 resonance units (RU). Serial two-fold increasing concentrations of antigen from 62.5 nM to 1 µM were singly injected over the surface in multiple cycles that included surface regeneration between different concentrations of antigen. The association phase proceeded for 180 seconds while the dissociation phase proceeded for 900 seconds (only 420 seconds of the dissociation phase is shown). The sensorgrams from these injections are shown as coloured lines. A 1:1 model of binding was fitted to the data (black lines) and the association rate (k_a), dissociation rate (k_d) and equilibrium dissociation constant (K_D) were determined for these interactions using the evaluation software.

Table 3.1 Kinetics and affinities of antibody-antigen interaction. SPR data from single cycle and high performance multi-cycle analysis runs indicating association rates (k_a) [M-1 s-1], dissociation rate (k_d) [s-1] ± standard error as well as the equilibrium dissociation constants (KD) k_d/k_a [M]. X denotes that no measurable interaction was detected by the assay.

	ANALYTE			
ANTIBODY	**DENV-1 NS1**	**DENV-2 NS1**	**DENV-3 NS1**	**DENV-4 NS1**
9H2	k_a $4.7x10^{4}$ ± 150 k_d $6.7x10^{-4}$ ± $2.9x10^{-6}$ K_D $1.4x10^{-8}$	X	X	X
4C11	X	k_a $7.5x10^{3}$± 140 k_d $2.1x10^{-3}$ ± $1.5x10^{-5}$ K_D $2.9x10^{-7}$	X	X
7G11	X	X	k_a $4.5x10^{4}$ ± 89 k_d $7.1x10^{-4}$ ± $1.8x10^{-6}$ K_D $1.5x10^{-8}$	X
6A5	X	X	X	k_a $7.5x10^{4}$±57 k_d 2.6 x 10^{-4} ±$2.2x10^{-7}$ K_D 3.5 x 10^{-9}
GUS-2	k_a $1.2x10^{4}$± 12 k_d $6.2x10^{-5}$ ± $7.9x10^{-7}$ K_D $5.4x10^{-9}$	k_a $1.1x10^{5}$± 140 k_d $1.9x10^{-4}$ ± $5.6x10^{-7}$ K_D $1.8x10^{-9}$	k_a $1.0x10^{4}$± 11 k_d $2.9x10^{-4}$ ± $7.5x10^{-7}$ K_D $2.8x10^{-8}$	k_a $1.1x10^{4}$± 17 k_d $2.0x10^{-4}$ ± $1.1x10^{-6}$ K_D $1.9x10^{-8}$

3.3.5 LIMIT OF DETECTION OF DENV NS1 IN A SEROTYPING SANDWICH ELISA

Knowledge of the affinities of antibodies for their relevant antigen allows for predictions of the stability of the antibody pair and sandwiched antigen complex. The stability of that complex influences the minimum amount of antigen that can be detected by the antibody sandwich. Minimum amounts of antigen that can be detected by a diagnostic assay lend themselves to determining the sensitivity of the assay. To be able to ascertain the limits of antigen detection, one needs to first establish the optimal concentrations of capture and detection antibodies that are required for positive detection of the antigen with minimal noise:signal ratios. Optimized conditions yield the best antigen binding and the best precision of antigen detection.

Checkerboard titrations of the coating antibody and HRP-conjugated detection antibody were performed to detect a set amount of DENV NS1 (200 ng/mL) in a sandwich ELISA. 10 μg/mL of serotype-specific capture antibodies and 625 ng/mL of HRP-conjugated GUS-2 were shown to provide the best signal for detection of 200 ng/mL of DENV NS1 (Figure 3.12). Figure 3.12 also shows that the highest concentration of HRP-conjugated GUS-2 (625 ng/mL) had negligible background noise when used with the lowest concentration of capture antibody (4.9 ng/mL). When GUS-2 was used as the capture antibody for DENV NS1 in a reversal of the assay, 10 μg/mL of GUS-2 and 625 ng/mL of HRP-conjugated serotype-specific antibodies again proved to be the optimal concentrations required by the assay (Figure 3.13). In this instance however, lower concentrations of GUS-2 (down to 2.5 μg/mL) could produce the same signal when paired with 6A5 anti DENV-4 NS1.

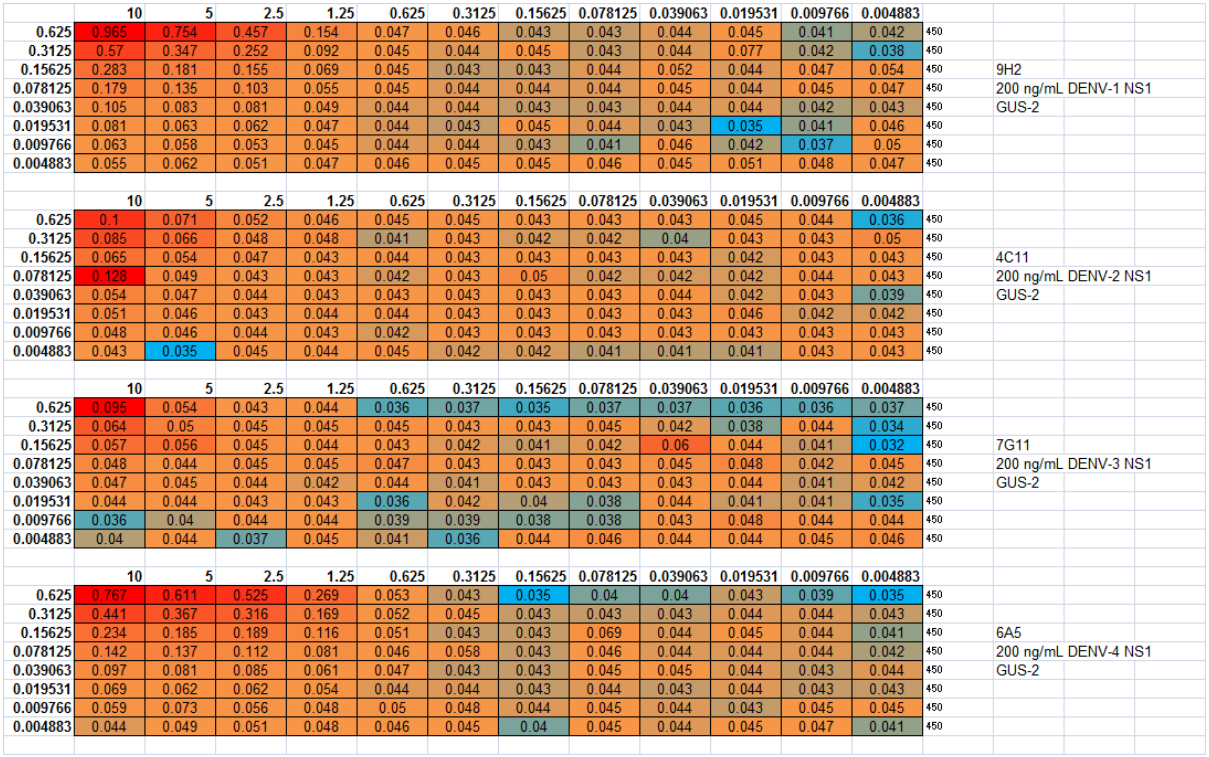

	10	5	2.5	1.25	0.625	0.3125	0.15625	0.078125	0.039063	0.019531	0.009766	0.004883			
0.625	0.965	0.754	0.457	0.154	0.047	0.046	0.043	0.043	0.044	0.045	0.041	0.042	450		
0.3125	0.57	0.347	0.252	0.092	0.045	0.044	0.045	0.043	0.044	0.077	0.042	0.038	450		
0.15625	0.283	0.181	0.155	0.069	0.045	0.043	0.043	0.044	0.052	0.044	0.047	0.054	450	9H2	
0.078125	0.179	0.135	0.103	0.055	0.045	0.044	0.044	0.044	0.045	0.044	0.045	0.047	450	200 ng/mL DENV-1 NS1	
0.039063	0.105	0.083	0.081	0.049	0.044	0.044	0.043	0.043	0.044	0.044	0.042	0.043	450	GUS-2	
0.019531	0.081	0.063	0.062	0.047	0.044	0.043	0.045	0.044	0.043	0.035	0.041	0.046	450		
0.009766	0.063	0.058	0.053	0.045	0.044	0.044	0.043	0.041	0.046	0.042	0.037	0.05	450		
0.004883	0.055	0.062	0.051	0.047	0.046	0.045	0.045	0.046	0.045	0.051	0.048	0.047	450		

	10	5	2.5	1.25	0.625	0.3125	0.15625	0.078125	0.039063	0.019531	0.009766	0.004883			
0.625	0.1	0.071	0.052	0.046	0.045	0.045	0.043	0.043	0.043	0.045	0.044	0.036	450		
0.3125	0.085	0.066	0.048	0.048	0.041	0.043	0.042	0.042	0.04	0.043	0.043	0.05	450		
0.15625	0.065	0.054	0.047	0.043	0.044	0.043	0.043	0.043	0.043	0.042	0.043	0.043	450	4C11	
0.078125	0.128	0.049	0.043	0.043	0.042	0.043	0.05	0.042	0.042	0.042	0.044	0.043	450	200 ng/mL DENV-2 NS1	
0.039063	0.054	0.047	0.044	0.043	0.043	0.043	0.043	0.043	0.044	0.042	0.043	0.039	450	GUS-2	
0.019531	0.051	0.046	0.043	0.044	0.044	0.043	0.043	0.043	0.043	0.046	0.042	0.042	450		
0.009766	0.048	0.046	0.044	0.043	0.042	0.043	0.043	0.043	0.043	0.043	0.043	0.043	450		
0.004883	0.043	0.035	0.045	0.044	0.045	0.042	0.042	0.041	0.041	0.041	0.043	0.043	450		

	10	5	2.5	1.25	0.625	0.3125	0.15625	0.078125	0.039063	0.019531	0.009766	0.004883			
0.625	0.095	0.054	0.043	0.044	0.036	0.037	0.035	0.037	0.037	0.036	0.036	0.037	450		
0.3125	0.064	0.05	0.045	0.045	0.045	0.043	0.043	0.045	0.042	0.038	0.044	0.034	450		
0.15625	0.057	0.056	0.045	0.044	0.043	0.042	0.041	0.042	0.06	0.044	0.041	0.032	450	7G11	
0.078125	0.048	0.044	0.045	0.045	0.047	0.043	0.043	0.043	0.045	0.048	0.042	0.045	450	200 ng/mL DENV-3 NS1	
0.039063	0.047	0.045	0.044	0.042	0.044	0.041	0.043	0.043	0.043	0.044	0.041	0.042	450	GUS-2	
0.019531	0.044	0.044	0.043	0.043	0.036	0.042	0.04	0.038	0.044	0.041	0.041	0.035	450		
0.009766	0.036	0.04	0.044	0.044	0.039	0.039	0.038	0.038	0.043	0.048	0.044	0.044	450		
0.004883	0.04	0.044	0.037	0.045	0.041	0.036	0.044	0.046	0.044	0.044	0.045	0.046	450		

	10	5	2.5	1.25	0.625	0.3125	0.15625	0.078125	0.039063	0.019531	0.009766	0.004883			
0.625	0.767	0.611	0.525	0.269	0.053	0.043	0.035	0.04	0.04	0.043	0.039	0.035	450		
0.3125	0.441	0.367	0.316	0.169	0.052	0.045	0.043	0.043	0.043	0.044	0.044	0.043	450		
0.15625	0.234	0.185	0.189	0.116	0.051	0.043	0.043	0.069	0.044	0.045	0.044	0.041	450	6A5	
0.078125	0.142	0.137	0.112	0.081	0.046	0.058	0.043	0.046	0.044	0.044	0.044	0.042	450	200 ng/mL DENV-4 NS1	
0.039063	0.097	0.081	0.085	0.061	0.047	0.043	0.043	0.045	0.045	0.044	0.043	0.044	450	GUS-2	
0.019531	0.069	0.062	0.062	0.054	0.044	0.044	0.043	0.044	0.043	0.044	0.043	0.043	450		
0.009766	0.059	0.073	0.056	0.048	0.05	0.048	0.044	0.045	0.044	0.043	0.045	0.045	450		
0.004883	0.044	0.049	0.051	0.048	0.046	0.045	0.04	0.045	0.044	0.045	0.047	0.041	450		

Figure 3.12 Antibody titration for serotype-specific antibody capture and GUS-2 antibody detection of DENV NS1. Two-fold dilutions of capture antibody were immobilized across a 96-well polystyrene plate, starting at 10 µg/mL until 4.9 ng/mL. 200 ng/mL of NS1 from a single DENV serotype was added to all the wells. Detection was carried out using a range of HRP-conjugated detection antibody that was titrated two-fold down the plate starting at a concentration of 625 ng/mL until 4.9 ng/mL. Binding was determined by measuring the chromogenic signal produced by addition of TMB. A 3 colour scale heat-map ranging from blue for lowest absorbance values, orange for mid absorbance values and red for the highest absorbance values was used to determine the optimal capture and detection antibody concentrations.

	10	5	2.5	1.25	0.625	0.3125	0.15625	0.078125	0.039063	0.019531	0.009766	0.004883			
0.625	4.2	3.067	3.382	3.236	1.033	0.117	0.052	0.045	0.044	0.054	0.048	0.036	450		
0.3125	3.799	3.383	2.58	2.165	0.854	0.078	0.048	0.044	0.044	0.044	0.044	0.044	450		
0.15625	3.21	2.855	2.067	1.572	0.519	0.084	0.062	0.045	0.045	0.044	0.055	0.045	450	GUS-2	
0.078125	2.062	1.937	1.399	1.005	0.292	0.056	0.047	0.044	0.043	0.044	0.044	0.045	450	200 ng/mL DENV-1 NS1	
0.039063	1.439	1.136	0.919	0.669	0.205	0.052	0.045	0.045	0.044	0.046	0.045	0.044	450	9H2	
0.019531	0.901	0.755	0.476	0.358	0.13	0.048	0.045	0.045	0.045	0.046	0.045	0.046	450		
0.009766	0.48	0.365	0.312	0.223	0.091	0.046	0.044	0.045	0.044	0.045	0.045	0.046	450		
0.004883	0.311	0.24	0.2	0.136	0.055	0.045	0.044	0.045	0.051	0.044	0.045	0.045	450		

	10	5	2.5	1.25	0.625	0.3125	0.15625	0.078125	0.039063	0.019531	0.009766	0.004883			
0.625	2.676	1.934	1.178	0.625	0.13	0.049	0.044	0.052	0.044	0.043	0.045	0.042	450		
0.3125	1.712	1.126	0.586	0.262	0.064	0.044	0.044	0.043	0.043	0.043	0.044	0.044	450		
0.15625	0.946	0.611	0.337	0.167	0.057	0.045	0.045	0.045	0.045	0.05	0.046	0.057	450	GUS-2	
0.078125	0.514	0.341	0.192	0.096	0.049	0.051	0.045	0.043	0.046	0.044	0.046	0.047	450	200 ng/mL DENV-2 NS1	
0.039063	0.298	0.191	0.119	0.069	0.047	0.052	0.044	0.045	0.045	0.045	0.046	0.047	450	4C11	
0.019531	0.16	0.116	0.079	0.058	0.052	0.046	0.051	0.047	0.045	0.045	0.046	0.048	450		
0.009766	0.1	0.077	0.06	0.051	0.045	0.046	0.044	0.045	0.044	0.043	0.045	0.048	450		
0.004883	0.078	0.066	0.054	0.048	0.045	0.044	0.045	0.044	0.045	0.044	0.046	0.04	450		

	10	5	2.5	1.25	0.625	0.3125	0.15625	0.078125	0.039063	0.019531	0.009766	0.004883			
0.625	0.507	0.373	0.231	0.161	0.062	0.045	0.044	0.043	0.042	0.038	0.04	0.039	450		
0.3125	0.258	0.178	0.12	0.081	0.051	0.044	0.043	0.043	0.044	0.046	0.045	0.041	450		
0.15625	0.133	0.102	0.078	0.061	0.046	0.044	0.045	0.045	0.046	0.046	0.045	0.035	450	GUS-2	
0.078125	0.091	0.072	0.065	0.05	0.054	0.044	0.046	0.053	0.044	0.045	0.043	0.06	450	200 ng/mL DENV-3 NS1	
0.039063	0.068	0.06	0.052	0.048	0.045	0.044	0.044	0.045	0.046	0.045	0.045	0.044	450	7G11	
0.019531	0.054	0.05	0.05	0.046	0.046	0.045	0.046	0.045	0.045	0.045	0.045	0.045	450		
0.009766	0.047	0.046	0.08	0.07	0.044	0.044	0.046	0.044	0.044	0.044	0.045	0.048	450		
0.004883	0.041	0.039	0.039	0.04	0.045	0.046	0.046	0.046	0.07	0.043	0.044	0.04	450		

	10	5	2.5	1.25	0.625	0.3125	0.15625	0.078125	0.039063	0.019531	0.009766	0.004883			
0.625	4.2	4.2	4.2	4.007	2.042	0.196	0.054	0.047	0.045	0.045	0.046	0.045	450		
0.3125	3.953	3.568	3.578	2.716	1.169	0.108	0.05	0.045	0.044	0.047	0.044	0.045	450		
0.15625	3.593	3.564	2.822	2.006	0.708	0.087	0.05	0.045	0.045	0.046	0.045	0.045	450		
0.078125	2.508	2.297	1.809	1.286	0.38	0.057	0.048	0.044	0.045	0.045	0.045	0.044	450	GUS-2	
0.039063	1.647	1.339	1.192	0.672	0.26	0.052	0.044	0.047	0.044	0.047	0.046	0.047	450	200 ng/mL DENV-4 NS1	
0.019531	1.041	0.802	0.58	0.399	0.145	0.049	0.047	0.047	0.045	0.046	0.045	0.046	450	6A5	
0.009766	0.567	0.457	0.365	0.261	0.081	0.048	0.043	0.05	0.046	0.045	0.046	0.046	450		
0.004883	0.398	0.288	0.236	0.183	0.074	0.048	0.046	0.047	0.044	0.047	0.047	0.046	450		

Figure 3.13 Antibody titration for GUS-2 antibody capture and serotype-specific antibody detection of DENV NS1. Two-fold dilutions of capture antibody were immobilized across a 96-well polystyrene plate, starting at 10 µg/mL until 4.9 ng/mL. 200 ng/mL of NS1 from a single DENV serotype was added to all the wells. Detection was carried out using a range of HRP-conjugated detection antibody that was titrated two-fold down the plate starting at a concentration of 625 ng/mL until 4.9 ng/mL. Binding was determined by measuring the chromogenic signal produced by addition of TMB. A 3 colour scale heat-map ranging from blue for lowest absorbance values, orange for mid absorbance values and red for the highest absorbance values was used to determine the optimal capture and detection antibody concentrations.

For ease of standardization, 10 μg/mL of capture antibodies and 625 ng/mL of HRP-conjugated detection antibodies were used in sandwich ELISA formats to determine the limit of DENV NS1 detection. The concentrations of capture and detection antibodies were kept constant while DENV NS1 was titrated two-fold from 1.6 μg/mL to 49 pg/mL. The limit of detection was considered as the last diluted antigen concentration that gave a value larger than the mean absorbance of negative samples plus three standard deviations. The desired level of DENV NS1 detection was 10 ng/mL (2). Serotype-specific antibody capture of DENV NS1 with HRP-conjugated GUS-2 antibody detection resulted in minimum detection of 2.7, 48.5, 43.4 and 6.0 ng/mL of DENV-1 NS1, DENV-2 NS1, DENV-3 NS1 and DENV-4 NS1 respectively (Figure 3.14). Meanwhile GUS-2 antibody capture of DENV NS1 with HRP-conjugated serotype-specific detection resulted in minimum detection of 0.04, 11.5, 12.5 and 0.2 ng/mL of DENV-1 NS1, DENV-2 NS1, DENV-3 NS1 and DENV-4 NS1 respectively (Figure 3.15). GUS-2 pan-reactive capture of DENV NS1 therefore yielded limits of detection that were closest to fulfilling the minimum desired requirement of 10 ng/mL when NS1 from all four DENV serotypes was captured in a sandwich assay with HRP-conjugated serotype-specific antibodies.

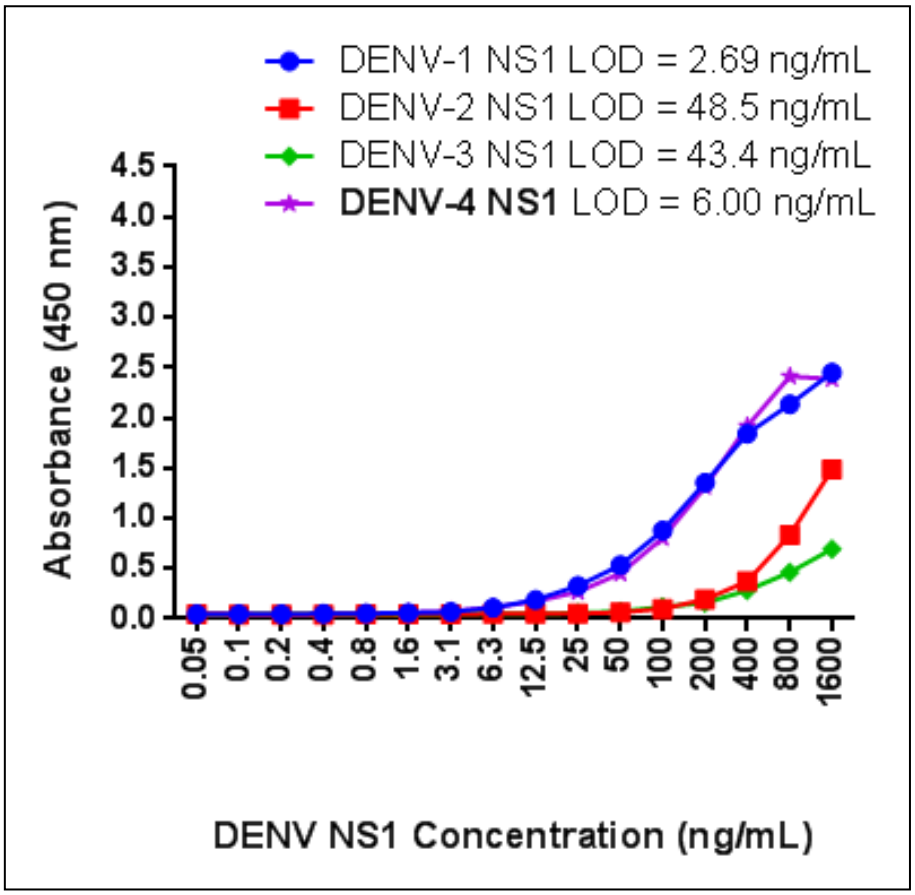

Figure 3.14 Limit of DENV NS1 detection using serotype-specific antibody capture and GUS-2 antibody detection. 10 µg/mL of immobilized antibodies were used to capture dilutions of DENV NS1 ranging from 1.6 µg/mL to 49 pg/mL. Detection of captured antigen was performed with 625 ng/mL of an HRP-conjugated antibody. Measured absorbance values are shown in the curves. The cut-off value was calculated as the mean blank value + 3 x SD of negative readings. The limits of detection (LOD) of NS1 from each DENV serotype are shown in the figure legend.

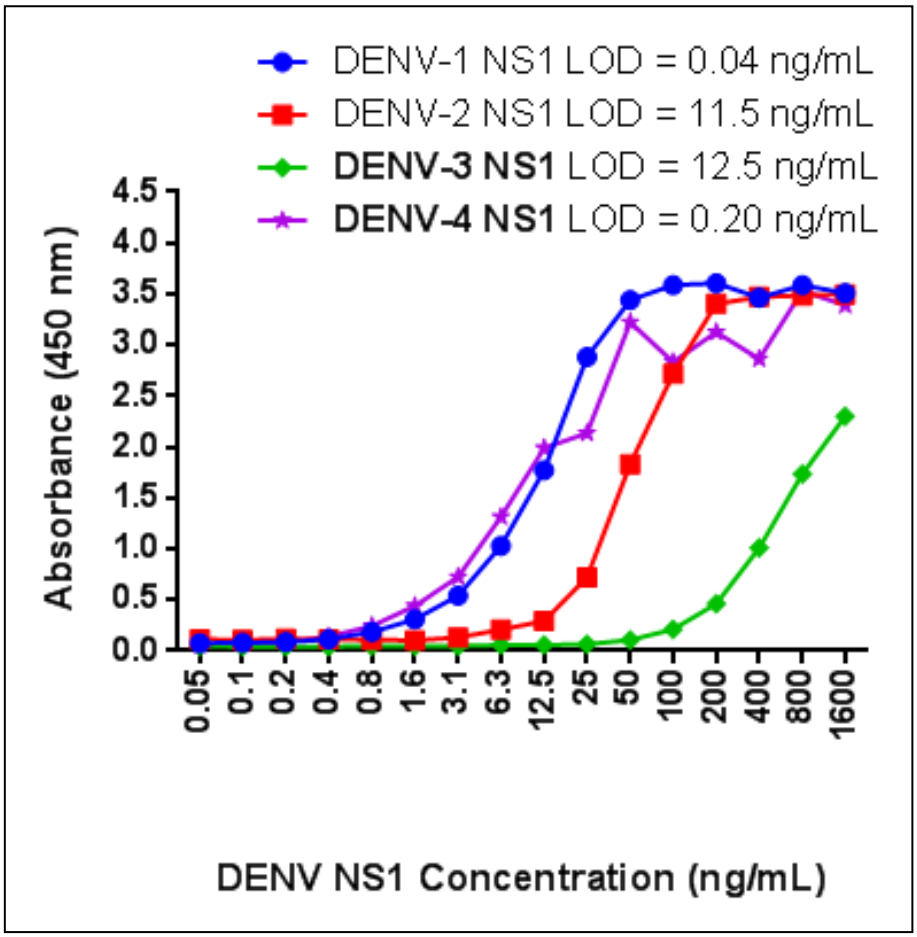

Figure 3.15 Limit of DENV NS1 detection using GUS-2 antibody capture and serotype-specific antibody detection. 10 µg/mL of immobilized antibodies were used to capture dilutions of DENV NS1 ranging from 1.6 µg/mL to 49 pg/mL. Detection of captured antigen was performed with 625 ng/mL of an HRP-conjugated antibody. Measured absorbance values are shown in the curves. The cut-off value was calculated as the mean blank value + 3 x SD of negative readings. The limits of detection of NS1 from each DENV serotype are shown in the figure legend.

3.4 DISCUSSION

Developing a diagnostic sandwich ELISA for capture and detection of antigen can be a difficult undertaking. A sufficient number of antibodies that can be used for antigen capture and antigen detection have to be trialed for an ability to sandwich the antigen. The formation of an antibody sandwich depends on both antibodies binding to spatially distinct sites without impinging each other's individual epitopes. Furthermore, the affinities of each antibody in the sandwich pair are required to be high enough to result in a stable sandwich complex that can sensitively detect antigen.

Using a sandwich ELISA format, 13 pan-reactive antibodies that bind DENV NS1 and 5 serotype-specific antibodies that each bind NS1 from a single DENV serotype were evaluated for their ability to capture and detect DENV NS1 in a serotype specific manner. None of the serotype- specific antibodies were able to bind DENV NS1 in tandem with the 13 pan-reactive antibodies. Using a control pan-reactive murine antibody (GUS-2) however, we found that serotype-specific antibody 9H2 and GUS-2 could sandwich DENV-1 NS1, serotype-specific antibody 4C11 and GUS-2 could sandwich DENV-2 NS1, serotype-specific antibody 7G11 and GUS-2 could sandwich DENV-3 NS1, serotype-specific antibody 6A5 and GUS-2 could sandwich DENV-4 NS1 and serotype-specific antibody 6A7 and GUS-2 could sandwich DENV-4 NS1. Furthermore, pan-reactive antibody D1C2 and GUS-2 could sandwich NS1 from all four DENV serotypes. In essence, we had fulfilled the aims of this project; (i) to isolate immune-reagents that could use NS1 to serotype DENV infections and (ii) to isolate a DENV pan-reactive immune-reagent that binds a non immune-dominant epitope. However these antibodies could not pair with each other as they bound to regions that competitively hindered tandem binding of the antigen.

In theory, the more antibodies one isolates, especially from animal immunization-driven strategies, the greater the chances of finding optimal pairs. When isolating binders using phage display technology however, strategies that are used to isolate the binders play a pivotal role in the level of success that is achieved. Fewer numbers of isolated clones, especially from biopanning naïve human libraries, can limit the ability to assemble a capture assay. The serotype-specificity of the isolated antibodies contributes to improvement of diagnostic assay specificity. Pan-reactive antibodies that bind a non-immune dominant epitope and are not affected by simultaneous binding to the immune-dominant epitope contribute to improvement of diagnostic assay sensitivity. Both of these aspects need to be combined to improve the specificity and sensitivity of DENV diagnosis. Knowledge of an ability to isolate binders to non immune-dominant regions of DENV NS1, means that serotype-specific antibodies could be utilized as DENV NS1 capture reagents in a biopanning

strategy to isolate appropriate pan-reactive binders. Equally pan-reactive D1C2 could be used to capture DENV NS1 in a biopanning strategy to isolate appropriate serotype-specific binders. The likelihood of isolating a single pan-reactive binder however is higher than the likelihood of isolating antibodies that recognize NS1 from each DENV serotype. It is for this reason that the serotype-specific antibodies were taken forward for further characterization.

The serotype-specific antibodies were found to have a high success rate (4/5) of native antigen recognition as all antibodies, with the exception of 6A7 anti DENV-4 NS1, could recognize native, secreted DENV NS1 from infected Vero cells. Isolating target-specific binders despite the presence of the hepta-histidine purification tag highlights good antigenicity of full length recombinant antigen, as has previously been observed in another study (9).

The epitopes recognized by serotype-specific antibodies as characterized by Western blot and ELISA suggested a conformational nature and similar localization on NS1 from all four DENV serotypes. The similar localization of serotype-specific binders of DENV NS1 could serendipitously be due to the libraries being constructed from donors who have had previous DENV infections of all serotypes, or it could suggest the presence of antibodies against NS1 of each DENV serotype in the naïve immune repertoire. Computational design of antibody-antigen interfaces may be helpful in identifying where the serotype-specific antibodies bind. Exploration of antibody-antigen models may even be beneficial in identifying a pairing pan-reactive antibody which could potentially bind one of the many linear epitopes which have previously been shown to exist on highly accessible regions along the length of DENV NS1 (1, 3, 14). Akey et al (1) identified these epitopes to exist in hotspots such as the wing-domain disordered loop and the C-terminal tip of the β-ladder on the DENV NS1 hexamer. The immune-dominant epitope of DENV-NS1 exists in the wing-domain disordered loop but there are multitudes of other linear epitopes (1) that could potentially be targeted by a suitable pan-reactive antibody.

The K_D of an affinity matured antibody derived from the natural immune system is theoretically hypothesized to be about 2.3×10^{-9} M (7, 10). Higher affinity antibodies are generally generated by way of *in vitro* affinity maturation. Pan-reactive GUS-2 which was derived from a mouse immunization driven strategy was inherently subjected to *in vivo* affinity maturation and had affinities in the expected nanomolar range. Serotype-specific antibody 6A5 which binds DENV-4 NS1 also had an affinity in the nanomolar range (3.5×10^{-9}). Serotype-specific antibodies 9H2 and 7G11 had approximately 4-fold lower affinity for their targets DENV-1NS1 and DENV-3 NS1 compared to 6A5 and DENV-4 NS1. More characteristic of the affinity of antibodies isolated from naïve libraries, was antibody 4C11 against DENV-2 NS1, which showed the lowest affinity for its

target at $2.9x10^{-7}$ M. It is evident that the sensorgrams for the interaction between GUS-2 and DENV NS1 (Figure 3.10) are different to those of the interaction between the serotype-specific antibodies and DENV NS1 (Figure 3.11). The 1:1 binding model is inadequate because the interaction of the serotype-specific antibodies does not follow simple reversible mass transport kinetics. This means that the reported association and dissociation constants are likely inaccurate. The difference in curvature of the association phase of the interaction is indicative of a heterogeneity of the serotype-specific antibody affinities for binding sites on DENV NS1 resulting in effects of homotropic cooperativity (5). This implies that while low concentrations of a serotype-specific antibody singly interact with antigen, higher concentrations affect (positively or negatively) the affinity of the antibodies to DENV NS1. The net result would be macroscopic and microscopic association constants. Employment of techniques such as isothermal titration calorimetry can provide information of the valencies of both antigen and antibody and hence analysis of cooperativity and stoichiometry of the antibody-antigen interaction to provide more accurate equilibrium dissociation rate constants.

When the serotype-specific antibodies and pan-reactive GUS-2 were used in a limit of detection ELISA, it was unsurprising to note that capture with the higher affinity GUS-2 antibody improved limits of antigen detection and hence assay sensitivity. This was because higher affinity capture antibodies are critical for stabilizing the sandwiched complex. The affinity of the detection antibody nonetheless, also plays a complementary role in influencing antigen detection. As these were proof-of-principle assays, these detection limit assays will need to be repeated with an appropriate pan-reactive antibody that binds a non immune-dominant epitope using a diagnostically applicable test matrix such as serum to determine whether the assay results in improved sensitivity of DENV NS1 detection. Furthermore, characterized sera of patients who experienced secondary infections with DENV would need to be evaluated for an improvement of diagnostic sensitivity when using a pan-reactive antibody that binds a non immune-dominant epitope is utilized in the assay.

To conclude, the current results with GUS-2 capture and serotype-specific antibody detection are promising, particularly with antibodies 9H2 and 6A5 that recognize DENV-1 NS1 and DENV-4 NS1 respectively (Figure 3.15). Comparable detection limits were obtained using 4C11 anti DENV-2 NS1 and 7G11 anti DENV-3 NS1 as detection antibodies (11.5 and 12.5 ng/mL respectively). These detection limits are close to the desired minimum detection threshold of 10 ng/mL. Further optimization of the sandwich ELISA conditions could potentially resolve this issue. Although 4C11 antibody showed exquisite specificity for DENV-2 NS1, the affinity was about 20-fold less than the affinity of 7G11 antibody for DENV-3 NS1. An improvement of the affinity of 4C11 was conceived to possibly improve the limit of detection of DENV-2 NS1. Affinity maturation of antibody 4C11 will therefore be the focus of the next chapter.

3.5 REFERENCES

1. **Akey, D. L., W. C. Brown, S. Dutta, J. Konwerski, J. Jose, T. J. Jurkiw, J. DelProposto, C. M. Ogata, G. Skiniotis, R. J. Kuhn, and J. L. Smith.** 2014. Flavivirus NS1 Structures Reveal Surfaces for Associations with Membranes and the Immune System. Science **343:**881-885.
2. **Alcon, S., A. Talarmin, M. Debruyne, A. Falconar, V. Deubel, and M. Flamand.** 2002. Enzyme-Linked Immunosorbent Assay Specific to Dengue Virus Type 1 Nonstructural Protein NS1 Reveals Circulation of the Antigen in the Blood during the Acute Phase of Disease in Patients Experiencing Primary or Secondary Infections. Journal of Clinical Microbiology **40:**376-381.
3. **AnandaRao, R., S. Swaminathan, S. Fernando, A. M. Jana, and N. Khanna.** 2005. A custom-designed recombinant multiepitope protein as a dengue diagnostic reagent. Protein expression and purification **41:**136-147.
4. **Blake, R. C., 2nd, J. B. Delehanty, M. Khosraviani, H. Yu, R. M. Jones, and D. A. Blake.** 2003. Allosteric binding properties of a monoclonal antibody and its Fab fragment. Biochemistry **42:**497-508.
5. **Cowan, R., and P. A. Underwood.** 1988. Steric effects in antibody reactions with polyvalent antigen. Journal of Theoretical Biology **132:**319-335.
6. **Falconar, A. K. I., P. R. Young, and M. A. Miles.** 1994. Precise location of sequential dengue virus subcomplex and complex B cell epitopes on the nonstructural-1 glycoprotein. Archives of Virology **137:**315-326.
7. **Foote, J., and H. N. Eisen.** 1995. Kinetic and affinity limits on antibodies produced during immune responses. Proc Natl Acad Sci U S A **92:**1254-6.
8. **Gonzalez, R. M., S. L. Seurynck-Servoss, S. A. Crowley, M. Brown, G. S. Omenn, D. F. Hayes, and R. C. Zangar.** 2008. Development and validation of sandwich ELISA microarrays with minimal assay interference. Journal of proteome research **7:**2406-2414.
9. **Huang, J. L., J. H. Huang, R. H. Shyu, C. W. Teng, Y. L. Lin, M. D. Kuo, C. W. Yao, and M. F. Shaio.** 2001. High-level expression of recombinant dengue viral NS-1 protein and its potential use as a diagnostic antigen. J Med Virol **65:**553-60.
10. **Poulsen, T. R., A. Jensen, J. S. Haurum, and P. S. Andersen.** 2011. Limits for Antibody Affinity Maturation and Repertoire Diversification in Hypervaccinated Humans. The Journal of Immunology **187:**4229-4235.
11. **Simmons, M. A.** 2005. Trends in monoclonal antibody research. Nova Biomedical Books, New York.

12. **Van Der Merwe, P. A.** 2001. Surface plasmon resonance, p. 137-170. Oxford University Press: New York, NY, USA.
13. **Vashist, S. K., E. M. Schneider, E. Lam, S. Hrapovic, and J. H. Luong.** 2014. One-step antibody immobilization-based rapid and highly-sensitive sandwich ELISA procedure for potential in vitro diagnostics. Scientific reports **4**.
14. **Vita, R., L. Zarebski, J. A. Greenbaum, H. Emami, I. Hoof, N. Salimi, R. Damle, A. Sette, and B. Peters.** 2010. The Immune Epitope Database 2.0. Nucleic Acids Research **38:**D854-D862.
15. **Wide, L.** 1969. RADIOIMMUNOASSAYS EMPLOYING IMMUNOSORBENTS. Acta Endocrinologica **62:**S207-S221.
16. **Young, P. R., P. A. Hilditch, C. Bletchly, and W. Halloran.** 2000. An Antigen Capture Enzyme-Linked Immunosorbent Assay Reveals High Levels of the Dengue Virus Protein NS1 in the Sera of Infected Patients. J. Clin. Microbiol. **38:**1053-1057.
17. **Zangar, R. C., S. M. Varnum, and N. Bollinger.** 2005. Studying cellular processes and detecting disease with protein microarrays. Drug metabolism reviews **37:**473-487.

Chapter 4

AFFINITY MATURATION OF AN ANTIBODY AGAINST DENV-2 NS1

4.1 INTRODUCTION

Primary and secondary responses of B cells to foreign antigens vary in affinity. Higher affinity to antigens is developed through a process of combinatorial rearrangement of V gene segments in the germline (4), a clonal selection process of some antibodies in the existing repertoire, and somatic hypermutation of the antigen binding regions of the antibody (3). In order to improve the affinity of antibodies isolated from naive libraries, aspects of *in vivo* maturation can be mimicked by *in vitro* affinity through variations of mutagenesis and variable chain sequence shuffling. Herein, a stochastic random mutagenesis strategy and a non-stochastic targeted mutagenesis strategy shall be discussed.

The antigen binding sites of antibodies are made up of selected elements within the variable regions known as complementarity determining regions (CDRs). There are three CDRs on each of the heavy and light chains and these form contiguous conformations unique to each antibody, varying in sequence, size, shape and charge to allow an ability to recognize and bind to different epitopes (22). The number of CDRs that participate in actual antigen recognition vary amongst antibodies and are largely influenced by the target antigen (22). Furthermore, not all residues within the CDRs participate in antigen recognition as most of them are involved in stabilizing the antibody-antigen interaction (14). The leniency in interaction allowed by the residues that determine binding to an antigen is what determines cross-reactivity with structurally related antigens. The majority of the interaction of antibodies with antigen is enabled by V_L CDR3 and V_H CDR3 (16). CDR3 of the heavy chain however is often considered the most contributory to binding as it is the longest loop and is at the centre of the antigen combining site (7).

The aim in affinity maturation is to increase the binding energy between an antibody and an antigen to improve their interaction. Because the interaction is predominantly mediated by residues in contact with each other on the antibody and antigen, targeted mutagenesis of variable regions of antibodies is often the preferred strategy for mutagenesis. The location and the chemistry of the amino acid side chains that are substituted during these mutagenesis processes are pivotal in optimizing the interaction between the antibody and the antigen. It is difficult however, to identify the exact amino acids that are involved in binding without high resolution structures of the antibody-antigen complex. Furthermore amino acid substitutions in the contact regions do not necessarily yield improved physicochemical characteristics (5). In general, amino acids with hydrophobic properties such as tryptophan for example are known to be integral in mediating antibody-antigen interaction (13) and therefore are valued in CDRs and excluded from mutagenesis. The substitutions that are desired are inclusions of large aromatic residues that can facilitate van der

Waal's and electrostatic interactions as well as small flexible residues that mediate plasticity of interaction. Parallel to, or alternate to targeted mutagenesis, random mutagenesis may be employed. Random mutagenesis introduces changes to both the variable and framework regions of the antibody fragment. Levels of random mutagenesis that are applied vary, resulting in varying mutagenic coverage and therefore variable success in identify synergetic mutations necessary for improved interaction. Some success has been had with this strategy but the improvement in binding is mainly fortuitous as opposed to rationally attained. Additional to improvements in binding kinetics, random mutagenesis has also been shown to introduce mutations adjunct to regions that directly interact with the antigen which can be seemingly neutral, but important in optimizing the stability of antibody binding (5, 20).

4C11 is a parent antibody that was generated from a Fab clone with binding specificity to DENV-2 NS1. The Fab clone was isolated from a naïve antibody library displayed on M13 phage. 4C11 binds to DENV-2 NS1 with a low affinity that compromises the potential diagnostic utility of this antibody in a DENV NS1 capture assay. Using surface plasmon resonance the equilibrium dissociation constant (K_D) of the interaction between antibody and antigen was calculated as 5.1 x 10^{-7} M. This antibody affinity required improvement to a value approaching 1.0 x 10^{-9} M in order for it to have better value in a diagnostic assay that detects capture of DENV NS1 (2). The aim of this work was to assess the effect of mutagenesis on the kinetics of 4C11 antibody interaction with recombinant DENV-2 NS1 and evaluate its impact on the sensitivity of a DENV-2 NS1 capture assay. To achieve this, two phage scFv sub-libraries displayed on the gIII protein of filamentous phage were constructed. One library used targeted mutagenesis of particular residues within Vh CDR3, which were hypothesised to be solvent-exposed based on the known structure of a homologous Vh sequence. The selected residues were then targeted for saturation mutagenesis (designed to introduce all possible nucleotide substitutions) using nucleotide doping primers to produce all possible combinations involving all 20 naturally occurring amino acids. The second library was constructed using an error-prone polymerase for moderate global mutagenesis of the scFv. Due to a high predominance of the parental sequence that was observed in the random mutagenesis library and the low ratio of mutants that actually included amino acid substitutions in the CDRs, only the targeted mutagenesis library was carried forward for affinity driven selection. Three unique binders A4, C5 and E7 were isolated from the targeted mutagenesis library using a selection method based on the equilibrium dissociation of the parental antibody. Bio layer interferometry (BLI) with reformatted IgG antibodies demonstrated variations in the interaction kinetics of the generated antibodies when compared with the parental antibody. Antibody A4 had a single neutral substitution which resulted in slightly improved affinity in comparison to 4C11

antibody. Antibodies C5 and E7 had association rate constants that were similar to that of 4C11 but unfortunately had higher dissociation rate constants resulting a net loss of affinity. Despite the actual loss of affinity for C5 and E7, all three isolated mAbs showed at least a 2-fold improvement in DENV-2 NS1 capture when evaluated in an ELISA format, showing that changes in antibody-antigen interaction kinetics does not necessarily correlate with assay performance.

4.2.1 SYNTHESIS OF 4C11 SCFV FROM 4C11 IGG1 SEQUENCE

4C11 was synthesized as a scFv by Geneart using both the heavy and light chain variable gene sequences. The heavy chain sequence preceded that of the light chain and the sequences were linked by a 3 x GGGGS linker. A SpeI restriction site was incorporated into the region immediately 3' of the V_H-CDR3, by using codons ACA-CTA-GTC to encode amino acid residues TLV. This restriction site allows for independent insertion of the PCR products yielded from targeted mutagenesis of the variable heavy chain region alone.

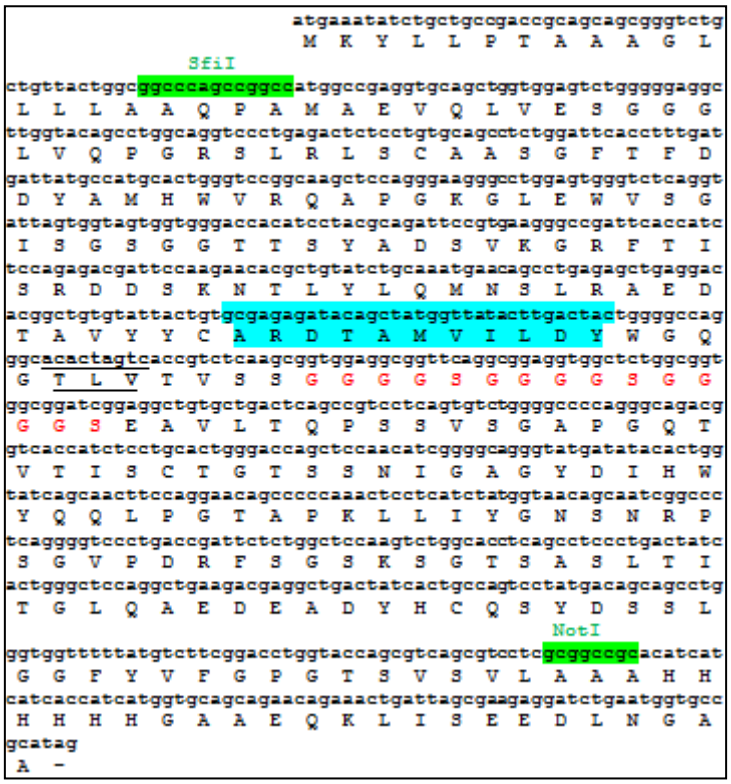

Figure 4.1 Nucleotide and amino acid sequence of Geneart synthesised 4C11 scFv sequence. Variable heavy and light chain sequences of antibody 4C11 are shown with a tri-GGGGS linker. The sequence is flanked by cloning restriction endonuclease sites for SfiI and NotI. An internal SpeI site (underlined) is also included downstream of the variable heavy chain sequence.

4.2.2 SUB-CLONING OF 4C11 SCFV INTO PHAGEMID VECTOR PNBF1603

The 4C11 scFv sequence was sub-cloned into an in-house phagemid vector pNBF1603 by using restriction endonucleases SfiI and NotI.

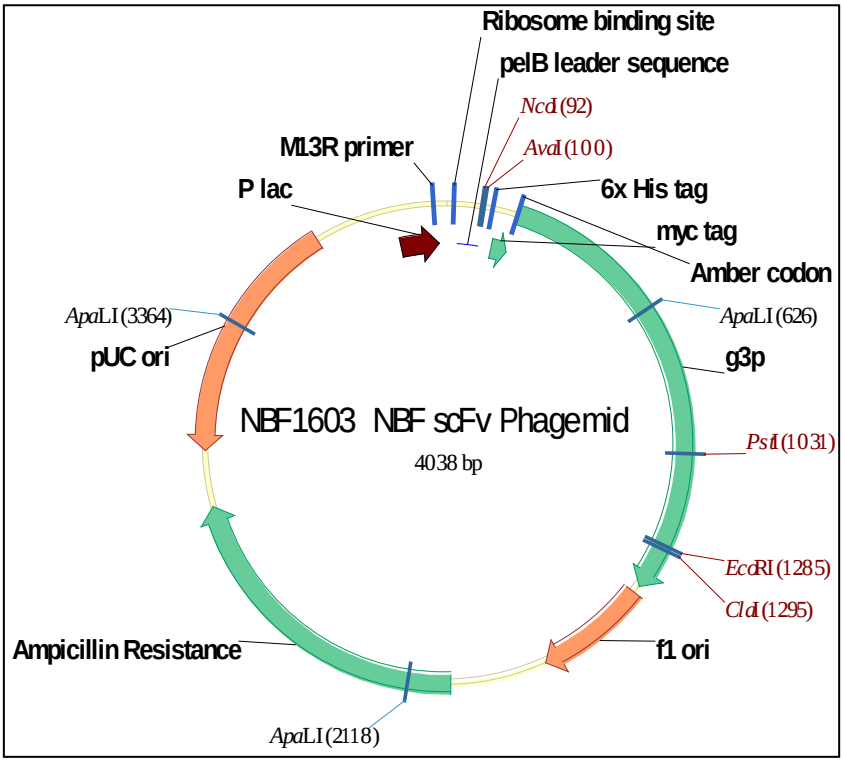

Figure 4.2 Phagemid map of expression vector NBF1603. A plasmid with a bacteriophage origin of replication (phagemid) is shown. Antibody fragment sequences are cloned in downstream of the leader periplasmic signal sequence (pelB) and in between restriction sites for SfiI and NotI endonucleases. The antibody fragment sequence is also cloned in frame with the gene III protein fusion partner.

1 µg of reconstituted vector containing the 4C11 scFv sequence and 1 µg of expression vector pNBF1603 were digested using 10 units of NotI High Fidelity (NEB) endonucleases, 1 x CutSmart™ buffer (NEB) and nuclease-free water in a 25 µL total volume reaction. The reaction was incubated at 37 ˚C for an hour. 10 units of SfiI (NEB) were then added to the reaction which was incubated at 50 ˚C for another hour.

The products of the restriction endonuclease digest were electrophoresed on a 1% agarose gel with Sbyr Safe (Life Technologies) at 90 V for 30 minutes. The DNA product bands were visualized using the Safe Imager™ 2.0 (Invitrogen) and the relevant bands excised using a blade. Gel slices with the relevant DNA products were purified using the concentrating and desalting protocol of the

QiaEXII Gel Extraction Kit (Qiagen) followed by DNA quantification on the NanoDrop 1000 (Thermo Scientific).

Ligation of the pNBF1603 vector and 4C11 scFv insert was performed using Rapid DNA Ligation Kit (Roche).

Ligation Conditions
150 ng Digested insert (4C11 scFv)
50 ng Digested pNBF1603
1uL 5x DNA Dilution Buffer
5uL 2X DNA Ligation Buffer
0.5uL DNA Ligase

10 µL total volume reaction was incubated at room temperature for 15 minutes

XL1-Blue Supercompetent cells (Agilent Technologies) were transformed with the ligation reaction. An aliquot of cells was thawed on ice and 50 µL was gently transferred into a pre-chilled 1.5 mL tube. 0.85uL of β-mercaptoethanol was added to the cells, mixed gently and incubated on ice for 10 minutes. 2 µL of the ligation reaction was then added, mixed gently and followed by a 30 minute incubation on ice. The cells were heat shocked for 45 seconds in a waterbath held at 42 ˚C then returned to ice for 2 minutes. 250uL LB was added to the transformation reaction and incubated at 37 ˚C, 220 rpm for 1 hour. 100 µL of the culture was spread on a 2YTAG agar plate and incubated overnight at 37 ˚C.

Transformant colonies were screened by colony PCR.

Colony PCR
Bacterial Colony
Platinum PCR SuperMix High Fidelity (Life Technologies)
pNBF Forward 100 nM
pNBF Reverse 100 nM
H_2O – Volume to 50 µL

pNBF1603_Forward: TCTGCTGTTACTGGC**GGCCCAGCCGGCC**ATGG

pNBF1603_Reverse: CCATGATGGTGATGATGATGT**GCGGCCGC**

PCR Cycling Conditions
94 ˚C – 2 minutes
30 cycles of: **94 ˚C – 30 seconds** **55 ˚C – 30 seconds** **68 ˚C – 1 minute**
68 ˚C – 10 minutes
4 ˚C – hold

A single clone with the appropriate 4C11 scFv insert was cultured in 5mL 2YTAG broth overnight at 37 ˚C, 220 rpm. The culture was used for DNA isolation using the PureLink® Quick Plasmid Miniprep Kit (Life Technologies) according to manufacturer's instructions.

4.2.3 PCR AMPLIFICATION OF TARGETED MUTAGENESIS INSERTS

Targeted mutagenesis of 4C11 was performed by randomization of the V_H CDR3 as outlined by Lou and Marks (11). The PDB database was used to find a homologous V_H sequence and model exposed regions that would most likely influence interaction with the antigen. The closest V_H homologue of 4C11 (86.6%) in the PDB database is a human anti-steroid Fab 5F2 in complex with testosterone (accession number 3kdm), and UCSF chimera software was used to visualise the model Figure 4.3. The 3D molecular model (SWISS MODEL) shows the surface exposed residues of this molecule, and homology with 4C11 was used to predict the exposed residues of the Vh CDR3 of 4C11. The sequence for the V_H CDR3 in clone 4C11 is **ARD**TAMVIL**DY**, with the exposed residues, highlighted in aqua to be the target residues for mutagenesis were the basis of the randomized primers to be used for mutagenesis of V_H CDR3.

Using the 4C11 scFv sequence as template, a library of inserts with mutations in the exposed residues was created by using nucleotide doped primers that have a bias to include the wild-type nucleotide in 70% of all nucleotide incorporation instances. The forward primer **5'-TCTGCTGTTACTGGCGGCCCAGCCGGCCATGG-3'** incorporates a SfiI restriction site, and the reverse primer contains the doped nucleotides and a SpeI site. **5'-GACGGTGACTAGTGTGCCCTGGCCCCAGTAGTCS13S14S12S14S32S34ATCTCTCGCACAGTAATACACAGC-3'**, where S is a 50% mix of G and C, 1 is 70%A, 2 is 70% C, 3 is 70% G and 4 is 70% T with equal amounts of the remaining nucleotides.

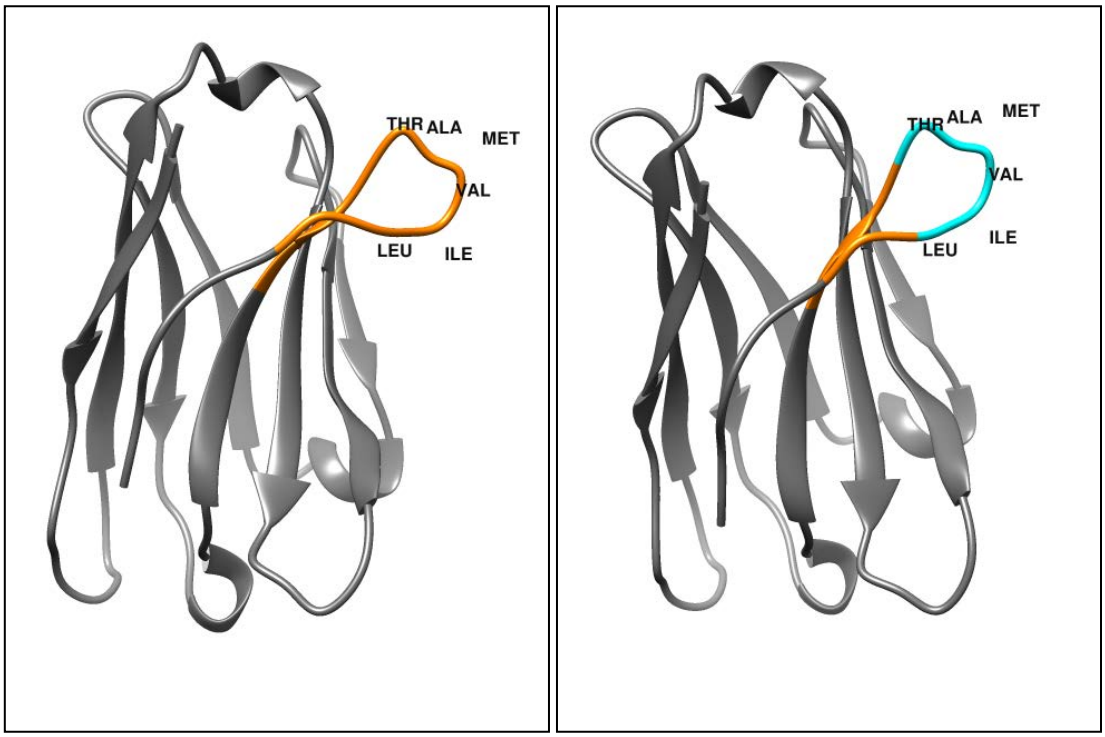

Figure 4.3 Hypothetical model of the VH region of 4C11. Shown are three hypervariable CDR loops of the heavy chain and anti-parallel β-sheets representative of the conserved framework. The complete VH CDR3 is highlighted in orange on the left and the residues targeted for mutation are shown using their three letter amino acid code and highlighted in aqua on the right.

Targeted Mutagenesis
400 ng DNA template
100 µL Top Taq Master Mix (Qiagen)
pNBF1603 Forward 200 nM
Doped Reverse Primer 200 nM
Nuclease-Free Water to 200 µL Volume

PCR Cycling Conditions
94 ˚C – 2 minutes
25 cycles of: **94 ˚C – 30 seconds** **55 ˚C – 30 seconds** **72 ˚C – 1 minute**
72 ˚C – 10 minutes
4 ˚C – hold

4.2.4 PCR AMPLIFICATION OF RANDOM MUTAGENESIS INSERTS

Moderate global mutagenesis of the entire length of 4C11 scFv was performed using an error prone polymerase (Mutazyme II) included in the Genemorph II Random Mutagenesis Kit (Agilent Technologies). The starting amount of DNA and the number of amplifcation cycles, influence mutation frequency. The input template amount has an inverse proportionality to error accumulation.

A forward primer **5'-TCTGCTGTTACTGGCGGCCCAGCCGGCCATGG-3'** which incorporates a SfiI restriction site and a reverse primer **3'-CCATGATGGTGATGATGATGTGCGGCCGC -5'** which incorporates a NotI restriction site were used in the PCR.

Random Mutagenesis
400 ng DNA Template
10 U Mutazyme II DNA Polymerase (Agilent Technologies)
1 x Mutazyme II Reaction Buffer
10 nM each dNTP
pNBF Forward 200 nM
pNBF Reverse 200 nM
Nuclease-Free Water to 200 µL Volume

PCR Cycling Conditions
94 ˚C – 2 minutes
25 cycles of: **94 ˚C – 30 seconds** **55 ˚C – 30 seconds** **72 ˚C – 1 minute**
72 ˚C – 10 minutes
4 ˚C – hold

4.2.5 CONSTRUCTION OF 4C11 MUTANT SUB-LIBRARIES

To construct the mutant libraries, restriction endonuclease digested pNBF1603 vector and restriction endonuclease digested PCR inserts derived from random or targeted mutagenesis were ligated and used to used to transform TG1 cells (Lucigen).

Restriction Endonuclease Digest	
Random Mutagenesis	Targeted Mutagenesis
20 µg DNA Vector / 5 µg PCR insert	20 µg DNA Vector / 5 µg PCR insert
1 x CutSmart™ buffer (NEB)	1 x CutSmart™ buffer (NEB))
SfiI (NEB) 30 units/5ug DNA 50 ˚C – 4 hours	SfiI (NEB) 30 units/5ug DNA 50 ˚C – 4 hours
NotI (NEB) 30 units/5ug DNA 37 ˚C – 4 hours	SpeI (NEB) 30 units/5ug DNA 37 ˚C – 4 hours

Restriction endonuclease products were analysed on a 1% agarose gel with Sybr® Safe (Life Technologies). DNA fragments were electrophoresed at 90 V for 30 minutes. The relevant DNA fragments were were visualized using the Safe Imager™ 2.0 (Invitrogen) and excised from the gel using a blade. The DNA was purified from the gel slices using the Wizard SV Gel and PCR Clean-Up System (Promega) according to manufacturer's instructions.

pNBF1603 vector backbone and mutant PCR products from both libraries were ligated using ElectroLigase (NEB). 1 µg of 4010 bp pNBF1603 backbone and approximately 3 times molar excess of insert from each library were ligated according to the reagent protocol. The volume of the reaction was concentrated to 5 µL using the Wizard SV Gel and PCR Clean-Up System (Promega).

4.2.6 TRANSFORMATION BY ELECTROPORATION AND LIBRARY RESCUE

A 1.0 mm cuvette was used per reaction in the Biorad Gene Pulser Xcell to apply an exponential decay pulse of 1800 volts to 25 µL TG1 phage display electrocompetent cells (Lucigen) to allow transformation of the cells with an appropriate amount of pUC 19 positive control DNA (10 pg), 4C11 digested negative control (100ng) and concentrated ligated library (4 µL) as per Lucigen's transformation protocol. An internal resistance value of 600 ohms and a capacitance value of 10 µF were also input into the Gene Pulser's electroporation parameters. The cells were diluted in 975 µL recovery medium (Lucigen) following electroporation. Transformants were plated out at different concentrations on YT agar (per litre 5g yeast extract, 8g tryptone, 5g NaCl, 15g agar) supplemented with 10 µg/mL ampicillin to determine transformation efficiency, background re-circularized vector proportions and library diversity. The rest of the transformation reaction was spread on ten x 150 mm YT agar plates and incubated overnight at 37 ˚C to prepare glycerol stocks of the library. Glycerol stocks were made by scraping transformants with 15 mL total volume of YT broth with 20% glycerol. The stocks were snap frozen on dry ice and stored at -80 ˚C.

To rescue the phagemid libraries, 100 mL of 2YTAG broth was inoculated with 100 µL of library glycerol stocks and incubated at 37 ˚C, 220 rpm until an OD_{600} of approximately 0.4 was reached. $4x10^{11}$ particles of M13K07 helper phage were added to the cultures and incubated at 37 °C for 30 minutes followed by another 30 minutes at 37 ˚C with shaking at 220 rpm. The cultures were then spun at 3000 x g for 10 minutes in 50 mL falcon tubes. The supernatant was discarded and the pellet resuspended in 100 mL fresh 2YTAK broth. The culture was incubated overnight at 30 ˚C, 220 rpm. PEG-NaCl (20% polyethylene glycol-6000 and 2.5 NaCl) was used to precipitate the phage as detailed in 2.2.3 on page 41 by determination of phage titre as detailed in 2.2.4 on page 41.

4.2.7 COLONY PCR AND SEQUENCING OF UNPURIFIED PCR PRODUCTS

To determine appropriate mutagenesis relevant to each sub-library, glycerol stocks were streaked out on LBAG agar and incubated overnight at 37 ˚C. Colonies were chosen at random and targeted mutagenesis PCR products were amplified with M13 reverse primer (used as the forward primer) and g3p reverse primer to yield a 2200 bp fragment. Random mutagenesis PCR products were amplified with M13 reverse primer (used as the forward primer) and f1 origin of replication reverse primer to yield a 1000 bp fragment.

Colony PCR
Bacterial Colony – DNA Template
100 nM Forward Primer
100 nM Reverse Primer
2 x MyTaq™ Mix (Bioline) 10 µL
Nuclease-Free Water to 20 µL

PCR Cycling Conditions
95 ˚C – 1 minute
25 cycles of: **95 ˚C – 15 seconds** **55 ˚C – 15 seconds** **72 ˚C – 30 seconds**
72 ˚C – 10 minutes
4 ˚C – hold

The PCR products were resolved using the E-Gel® 96 agarose gel 2% with SYBR® Safe (Life Technologies) on the Mother E-base™ device (Life Technologies). 9 µL of the PCR volume was diluted with 11 µL of nuclease-free water and added to the wells of the E-Gel®. The far right wells of the E-Gel® had 10 µL of low range quantitative DNA ladder (Life Technologies) diluted in an equal volume of nuclease-free water. The electrophoresis system was run on a 12 minute EG program and the gel was imaged on the ChemiDoc MP System (Bio-Rad).

Bidirectional sequencing of unpurified PCR products was performed by the Australian Genome Research Facility (Brisbane). 20 µL total volume reactions made up of 11 µL PCR products and 9 µL nuclease free water were submitted in a plate format along with 200 µL total volume of each sequencing primer; pNBF1603_Forward: 5’-TCTGCTGTTACTGGC**GGCCCAGCCGGCC**ATGG-3’ and gIIIp_Reverse: 3’-CCTTCATAATTTGCATAGCGATCCAGGG-5’ made up to 3.2 µM concentration.

4.2.8 RECOMBINANT DENV-2 NS1

Recombinant DENV-2 NS1 was generously provided by Professor Paul Young's research group (School of Chemistry and Molecular Biosciences, The University of Queensland. The antigen was prepared using the NS1 sequence of a clinical isolate from East Timor. The antigen was expressed in Schneider 2 cells and has an N-terminal 6 x histidine tag but immuno-affinity chromatography was used for its purification. DENV-2 NS1 was provided in PBS.

4.2.9 BIOTINYLATION OF RECOMBINANT DENV-2 NS1

Amine biotinylation of DENV-2 NS1 was performed using the EZ-Link Sulfo-NHS LC biotin kit (Thermo Scientific) according to instructions. 20 fold excess of 10 mM biotin reagent was added to a volume of recombinant DENV-2 NS1 of a known concentration determined by UV spectrophotometry at 280 nm. Unbound biotin was removed using a Zeba Spin Desalting Column, 7K MWCO (Thermo Scientific).

4.2.10 EQUILIBRIUM BIOPANNING

The sub-library comprised of mutated antibody scFv fragments displayed on filamentous phage, was biopanned against biotinylated recombinant DENV-2 NS1 using the equilibrium selection protocol described by Lou and Marks (11). Varying concentrations of biotinylated recombinant DENV-2 NS1 were captured on magnetic beads displaying tetrameric streptavidin (Streptavidin Particles Plus-DM. BD Biosciences), then exposed to the library. In the first round, the molar concentration of DENV-2 NS1 that was bound to the magnetic streptavidin beads was equivalent to $K_D/10$. This was reduced ten-fold to $K_D/100$ in the second round of biopanning and then $K_D/1000$ in the final round of biopanning. Magnetic streptavidin beads were pre-incubated with 1 x PBS with 2% casein before capture of biotinylated antigen. 10^{12} transducing units (TU) of the phage library were also pre-incubated with 1 x PBS with 2% casein before addition to the first concentration of biotinylated recombinant antigen. 10^{11} TU of the first round binders were used in the second round of biopanning while 10^{10} TU of the second round binders were used the last round of biopanning. The IMagnet (BD Biosciences) was used to pull down the fragments that had bound to the biotinylated antigen on the streptavidin magnetic beads. This allowed for washing away of non-binders and weak binders firstly with 1 x PBS with 2% casein (x2), then 1 x PBS with 0.1% Tween-20 (x7) and 1 x PBS (x1). Non-specific elution of phage binders was performed with an acidic buffer (200 mM glycine pH 2.7) and neutralised with 1M Tris-HCl pH 7.4. A phage rescue

was performed and the titre of the phage was determined (see sections 2.2.3 and 2.2.4 for detailed methods on page 41)

4.2.11 MONOCLONAL PHAGE ELISA

Method details can be found in section 2.2.5 on page 42.

4.2.12 REFORMATTING OF ANTIBODY FRAGMENTS

Unique, antigen specific antibody fragments were reformatted to fully human IgG1. The IgG1 were constructed by In-Fusion® cloning (Clontech) of the variable light and heavy chains into mAb expression vectors containing the human IgG1 framework (10) as outlined in section 2.2.9 on page 46.

4.2.13 EXPRESSION AND PURIFICATION OF IGG1

The vectors expressing the introduced variable regions were co-transfected into CHO cells adapted for suspension culture using PEIpro (Polyplus transfection) and maintained using the method outlined in section 2.2.11 on page 53. The expressed antibodies were secreted into the medium enabling harvesting by centrifugation followed by double filtration with Sartobran P300, 0.45/0.2 µm capsule filters (Sartorium Stedim) on day 10 post-transfection. The antibodies were purified on the AKTA Explorer chromatography system (GE Healthcare) using a 5 mL HiTrap mAbSelect SuRe column (GE Healthcare). The antibodies were eluted using 0.1 M glycine pH 2.7 and neutralized with 1/10 total elution volume of 1 M Tris pH 7.4. The neutralized antibodies were desalted and concentrated using Macrosep Advance Centrifugal Devices (Pall). The concentrated protein was diluted in 1 x PBS to a concentration of 1 mg/mL and stored at -20 ˚C.

4.2.14 BIO LAYER INTERFEROMETRY

Interaction kinetics were measured using the Octet RED96 System (fortéBIO - Pall). A series of hydrated Anti-Human IgG Fc Capture Biosensors (fortéBIO - Pall) were equilibrated for 180 seconds in 1 x PBS before 200 µL of monoclonal antibody diluted to 25 µg/mL was used to coat the biosensors over 3 minutes at a low immobilization level with the response units not exceeding 2.0 nm. Serial 1 in 2 dilutions of DENV-2 NS1 from 500 nM to 15.6 nM were made. The antibody coated sensors were immersed into 200 µL of recombinant antigen diluted to different concentrations. The interaction of each antibody and each antigen dilution proceeded for 3 minutes, followed by a 5 minute dissociation phase in 1 x PBS. Measurements of association and dissociation rate constants were used to derive the equilibrium dissociation rate constants.

4.2.15 LIMIT OF DETECTION ELISA

Method is as outlined in 3.2.9 on page 100

Variation – Detection antibody was 100 µL of a pan-reactive, HRP-conjugated antibody from the commercial Panbio® Dengue Early ELISA Kit.

4.3.1 CONSTRUCTION OF THE 4C11 SCFV MUTANT SUB-LIBRARIES

In this work we sought to mutate residues within the variable regions of the original 4C11 Fab binder without any variation to the constant regions. For ease of global mutagenesis in particular, the variable regions of 4C11 Fab were synthesised as 4C11 scFv and cloned into an in-house phagemid vector (pNBF1603) using restriction endonucleases SfiI and NotI. Targeted mutagenesis of the CDR3 regions of the variable heavy domain was performed by PCR using nucleotide doping primers. The forward primer for the PCR incorporated a SfiI restriction endonuclease site while the reverse nucleotide doping primers incorporated a SpeI restriction endonuclease site. The primer pair yielded fragments that were 370 basepairs in length with some proportion of the PCR products showing a tendency to produce a non-specific product. Random mutagenesis was performed using forward and reverse primers that incorporated an upstream SfiI and downstream NotI restriction endonuclease sites that flank the scFv sequence respectively, to yield fragments with a length of 765 basepairs. Restriction endonuclease treated PCR products of the appropriate fragment size for each sub-library construction (Figure 4.4), were gel purified and cloned into a similarly digested and gel purified pNBF1603 vector (Figure 4.5). The purified products were treated with an electroligase before transformation into TG1 cells.

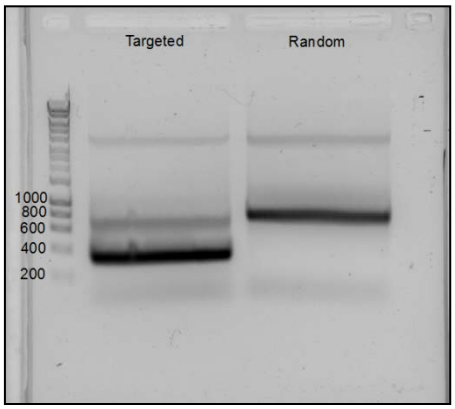

Figure 4.4 Agarose gel electrophoresis analysis of restriction enzyme treated PCR products. Primers for targeted and random mutagenesis yielded PCR fragments of different basepair lengths. The fragments were digested with restriction endonuclease pairs SfiI-SpeI and SfiI-NotI, electrophoresed and the appropriate fragments were ligated with a relevantly digested NBF1603 backbone vector.

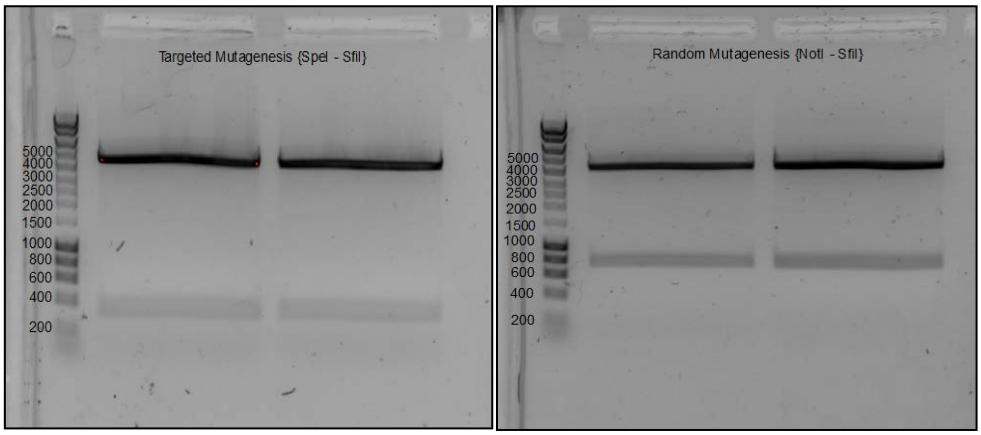

Figure 4.5 Agarose gel electrophoresis analysis of restriction endonuclease treated pNBF1603-4C11 scFv. The 4C11 variable heavy sequence (left) and the 4C11 scFv sequence (right) were excised from the pNBF1603 vector using restriction endonuclease pairs SfiI-SpeI and SfiI-NotI respectively to create a backbone for PCR mutant inserts.

4.3.2 DNA LIBRARY SIZE

Phage scFv sub-libraries derived from targeted and random mutagenesis yielded 2.08 x 10^8 and 3.88 x 10^8 transformants as shown in Table 4.1. For the targeted mutagenesis sub-library, maximal mutation coverage of the 6 exposed amino acid residues to include substitutions with all 20 natural amino acids would require a diversity of 20^6 (6.4 x 10^7) individual clones. The library diversity that was attained was 2.08 x 10^8. Cells transformed with digested vector only were used as a negative control to determine the background bias of the 4C11 parent vector. The background was approximately 9.5 x 10^5 transformants resulting in the true diversity of the targeted mutagenesis sub-library being 2.07 x 10^8. Each possible mutant combination would have therefore been theoretically represented at least once in this library. For the random mutagenesis sub-library, the attained library diversity was 3.88 x 10^8 with a background bias of 1.50 x 10^6 resulting in a true diversity of 3.865 x 10^8. This diversity brought about by moderate global mutagenesis is important as high mutation frequencies are associated with an accumulation of template sequence errors and insufficient representation of all generated mutant fragments on a phage display platform.

Table 4.1 Summary of library sizes attained from targeted and random mutagenesis. The calculated library titre is shown, including the transformation efficiency of the electroporation protocol using a control pUC19 vector. Digested parental vector (pNBF1603) was also used to transform TG1 cells to quantify the proportion of the library that included undigested parental 4C11 scFv.

	4C11 scFv TM	**4C11 scFv RM**
Transformation efficiency pUC19 (cfu/µg)	6.1×10^{10}	5.4×10^{10}
Library Titre	2.08×10^{8}	3.88×10^{8}
Negative Control Digested Parental Vector Only	9.5×10^{5}	1.5×10^{6}
Ratio of parental : mutants	1: 218	1: 258

4.3.3 LIBRARY DIVERSITY

To ascertain the amino acid variation of mutants within the generated sub-libraries and determine library quality in terms of redundancy, inclusion of stop codons and out-of frame mutations, sequence analysis of random clones from each sub-library was performed. Glycerol stocks of each sub-library were streaked out on LB agar supplemented with ampicillin and glucose. Clones chosen at random were subjected to colony PCR to amplify DNA segments. The products were resolved by E-Gel® electrophoresis (Figure 4.6) and also submitted to the Australian Genome Research Facility (Brisbane) for bidirectional Sanger sequencing of unpurified PCR products.

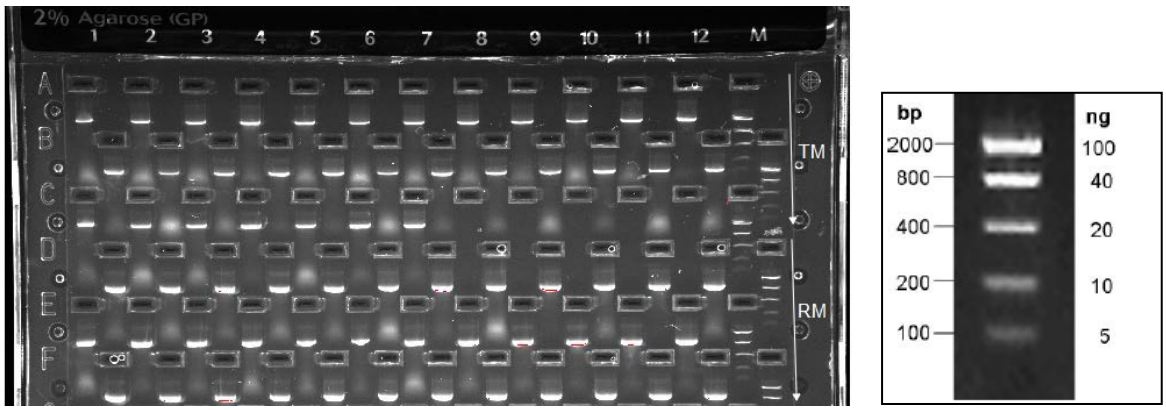

Figure 4.6 Agarose gel electrophoresis of colony PCR products. Rows A – C had targeted mutagenesis (TM) PCR products amplified with M13 reverse primer (used as the forward primer) and gIIIp reverse primer. Rows D – F had random mutagenesis (RM) PCR products amplified with M13 reverse primer (used as the forward primer) and f1 origin of replication reverse primer. E-Gel low range quantitative DNA ladder shown on the right was added to column M.

Both sub-library sequences were derived from dual sequencing with the pNBF1603 forward and gIIIp reverse primers. Contiguous sequences with the primer pair did not cover the upstream 4C11 scFv sequence up to and including V_H CDR1. Good quality sequences from 20 clones in each sub-library were selected for multiple sequence alignment using the European Bioinformatic Institute's Clustal Omega program to determine appropriate mutagenesis and sequence diversity. For the targeted mutagenesis library, the amino acid sequences show that within the 20 clone sample size, mutagenesis was confined to the targeted V_H CDR3 region. There were no wild type 4C11 V_H CDR3 sequences that were isolated and each of the 20 clones had unique V_H CDR3 sequences (Figure 4.7). This indicated a likelihood of a highly diverse library within the region that was targeted for mutagenesis. For the random mutagenesis library, amino acid substitutions were noted along the length of the 4C11 scFv sequence (Figure 4.8). 10 of the 20 clones that were included in the sequence alignment were parental 4C11 scFv. Alignments were made using amino acid sequences and not nucleotide sequences thus some mutations which take advantange of the redundancy of the genetic code may have resulted in silent mutations. Of the 10 clones that were mutated the substitutions were mostly within the framework regions of the scFv. Mutant 6 had a single amino acid substitution from an alanine to a threonine at the beginning of V_H CDR3 while mutant 18 had two changes in V_L CDR3 which included glycine to tryptophan and tyrosine to phenylalanine amino acid substitutions. Mutant 18 was also the only clone that had an amino acid insertion which was seen downstream of V_L CDR3. No amino acid deletions or incorporation of stop codons were noted. Due to the high representation of parental 4C11 scFv in the random

mutagenesis library and limited availability of recombinant DENV-2 NS1 for both biopanning and isolated binder characterization, the highly diverse, targeted mutagenesis library was carried forward to be interrogated for affinity matured binders.

```
4C11M17      MHWVRQAPGKGLEWVSGISGSGGTTSYADSVKGRFTISRDDSKNTLYLQMNSLRAEDTAV

4C11M11      MHWVRQAPGKGLEWVSGISGSGGTTSYADSVKGRFTISRDDSKNTLYLQMNSLRAEDTAV

4C11M12      MHWVRQAPGKGLEWVSGISGSGGTTSYADSVKGRFTISRDDSKNTLYLQMNSLRAEDTAV
4C11M9       MHWVRQAPGKGLEWVSGISGSGGTTSYADSVKGRFTISRDDSKNTLYLQMNSLRAEDTAV
4C11M4       MHWVRQAPGKGLEWVSGISGSGGTTSYADSVKGRFTISRDDSKNTLYLQMNSLRAEDTAV
4C11M18      MHWVRQAPGKGLEWVSGISGSGGTTSYADSVKGRFTISRDDSKNTLYLQMNSLRAEDTAV
4C11M16      MHWVRQAPGKGLEWVSGISGSGGTTSYADSVKGRFTISRDDSKNTLYLQMNSLRAEDTAV
4C11M15      MHWVRQAPGKGLEWVSGISGSGGTTSYADSVKGRFTISRDDSKNTLYLQMNSLRAEDTAV
4C11M13      MHWVRQAPGKGLEWVSGISGSGGTTSYADSVKGRFTISRDDSKNTLYLQMNSLRAEDTAV
4C11M10      MHWVRQAPGKGLEWVSGISGSGGTTSYADSVKGRFTISRDDSKNTLYLQMNSLRAEDTAV
4C11M7       MHWVRQAPGKGLEWVSGISGSGGTTSYADSVKGRFTISRDDSKNTLYLQMNSLRAEDTAV
4C11M2       MHWVRQAPGKGLEWVSGISGSGGTTSYADSVKGRFTISRDDSKNTLYLQMNSLRAEDTAV
4C11M1       MHWVRQAPGKGLEWVSGISGSGGTTSYADSVKGRFTISRDDSKNTLYLQMNSLRAEDTAV
4C11M3       MHWVRQAPGKGLEWVSGISGSGGTTSYADSVKGRFTISRDDSKNTLYLQMNSLRAEDTAV
4C11M8       MHWVRQAPGKGLEWVSGISGSGGTTSYADSVKGRFTISRDDSKNTLYLQMNSLRAEDTAV
4C11M20      MHWVRQAPGKGLEWVSGISGSGGTTSYADSVKGRFTISRDDSKNTLYLQMNSLRAEDTAV
4C11M19      MHWVRQAPGKGLEWVSGISGSGGTTSYADSVKGRFTISRDDSKNTLYLQMNSLRAEDTAV
4C11M14      MHWVRQAPGKGLEWVSGISGSGGTTSYADSVKGRFTISRDDSKNTLYLQMNSLRAEDTAV
4C11M6       MHWVRQAPGKGLEWVSGISGSGGTTSYADSVKGRFTISRDDSKNTLYLQMNSLRAEDTAV
4C11O        MHWVRQAPGKGLEWVSGISGSGGTTSYADSVKGRFTISRDDSKNTLYLQMNSLRAEDTAV
4C11M5       MHWVRQAPGKGLEWVSGISGSGGTTSYADSVKGRFTISRDDSKNTLYLQMNSLRAEDTAV
             ************************************************************

4C11M17      YYCARDIMSLRMDYWGQGTLVTVSSGGGGSGGGGSGGGGSEAVLTQPSSVSGAPGQTVTI
4C11M11      YYCARDMEMMKLDYWGQGTLVTVSSGGGGSGGGGSGGGGSEAVLTQPSSVSGAPGQTVTI
4C11M12      YYCARDPAMMRLDYWGQGTLVTVSSGGGGSGGGGSGGGGSEAVLTQPSSVSGAPGQTVTI
4C11M9       YYCARDTWMMHMDYWGQGTLVTVSSGGGGSGGGGSGGGGSEAVLTQPSSVSGAPGQTVTI
4C11M4       YYCARDKFVDKKDYWGQGTLVTVSSGGGGSGGGGSGGGGSEAVLTQPSSVSGAPGQTVTI
4C11M18      YYCARDTVLVKYDYWGQGTLVTVSSGGGGSGGGGSGGGGSEAVLTQPSSVSGAPGQTVTI
4C11M16      YYCARDTAVMNQDYWGQGTLVTVSSGGGGSGGGGSGGGGSEAVLTQPSSVSGAPGQTVTI
4C11M15      YYCARDTALLIIDYWGQGTLVTVSSGGGGSGGGGSGGGGSEAVLTQPSSVSGAPGQTVTI
4C11M13      YYCARDTGIVTLDYWGQGTLVTVSSGGGGSGGGGSGGGGSEAVLTQPSSVSGAPGQTVTI
4C11M10      YYCARDMATDILDYWGQGTLVTVSSGGGGSGGGGSGGGGSEAVLTQPSSVSGAPGQTVTI
4C11M7       YYCARDTPVDILDYWGQGTLVTVSSGGGGSGGGGSGGGGSEAVLTQPSSVSGAPGQTVTI
4C11M2       YYCARDSADVNLDYWGQGTLVTVSSGGGGSGGGGSGGGGSEAVLTQPSSVSGAPGQTVTI
4C11M1       YYCARDNAMVLVDYWGQGTLVTVSSGGGGSGGGGSGGGGSEAVLTQPSSVSGAPGQTVTI
4C11M3       YYCARDTAKVNFDYWGQGTLVTVSSGGGGSGGGGSGGGGSEAVLTQPSSVSGAPGQTVTI
4C11M8       YYCARDTAIVNIDYWGQGTLVTVSSGGGGSGGGGSGGGGSEAVLTQPSSVSGAPGQTVTI
4C11M20      YYCARDTALAMLDYWGQGTLVTVSSGGGGSGGGGSGGGGSEAVLTQPSSVSGAPGQTVTI
4C11M19      YYCARDTAWVMYDYWGQGTLVTVSSGGGGSGGGGSGGGGSEAVLTQPSSVSGAPGQTVTI
4C11M14      YYCARDIAMVIHDYWGQGTLVTVSSGGGGSGGGGSGGGGSEAVLTQPSSVSGAPGQTVTI
4C11M6       YYCARDTAPVMIDYWGQGTLVTVSSGGGGSGGGGSGGGGSEAVLTQPSSVSGAPGQTVTI
4C11O        YYCARDTAMVILDYWGQGTLVTVSSGGGGSGGGGSGGGGSEAVLTQPSSVSGAPGQTVTI
4C11M5       YYCARDTATVMLDYWGQGTLVTVSSGGGGSGGGGSGGGGSEAVLTQPSSVSGAPGQTVTI
             ******      ********************************************
```

```
4C11M17      SCTGTSSNIGAGYDIHWYQQLPGTAPKLLIYGNSNRPSGVPDRFSGSKSGTSASLTITGL
4C11M11      SCTGTSSNIGAGYDIHWYQQLPGTAPKLLIYGNSNRPSGVPDRFSGSKSGTSASLTITGL
4C11M12      SCTGTSSNIGAGYDIHWYQQLPGTAPKLLIYGNSNRPSGVPDRFSGSKSGTSASLTITGL
4C11M9       SCTGTSSNIGAGYDIHWYQQLPGTAPKLLIYGNSNRPSGVPDRFSGSKSGTSASLTITGL
4C11M4       SCTGTSSNIGAGYDIHWYQQLPGTAPKLLIYGNSNRPSGVPDRFSGSKSGTSASLTITGL
4C11M18      SCTGTSSNIGAGYDIHWYQQLPGTAPKLLIYGNSNRPSGVPDRFSGSKSGTSASLTITGL
4C11M16      SCTGTSSNIGAGYDIHWYQQLPGTAPKLLIYGNSNRPSGVPDRFSGSKSGTSASLTITGL
4C11M15      SCTGTSSNIGAGYDIHWYQQLPGTAPKLLIYGNSNRPSGVPDRFSGSKSGTSASLTITGL
4C11M13      SCTGTSSNIGAGYDIHWYQQLPGTAPKLLIYGNSNRPSGVPDRFSGSKSGTSASLTITGL
4C11M10      SCTGTSSNIGAGYDIHWYQQLPGTAPKLLIYGNSNRPSGVPDRFSGSKSGTSASLTITGL
4C11M7       SCTGTSSNIGAGYDIHWYQQLPGTAPKLLIYGNSNRPSGVPDRFSGSKSGTSASLTITGL
4C11M2       SCTGTSSNIGAGYDIHWYQQLPGTAPKLLIYGNSNRPSGVPDRFSGSKSGTSASLTITGL
4C11M1       SCTGTSSNIGAGYDIHWYQQLPGTAPKLLIYGNSNRPSGVPDRFSGSKSGTSASLTITGL
4C11M3       SCTGTSSNIGAGYDIHWYQQLPGTAPKLLIYGNSNRPSGVPDRFSGSKSGTSASLTITGL
4C11M8       SCTGTSSNIGAGYDIHWYQQLPGTAPKLLIYGNSNRPSGVPDRFSGSKSGTSASLTITGL
4C11M20      SCTGTSSNIGAGYDIHWYQQLPGTAPKLLIYGNSNRPSGVPDRFSGSKSGTSASLTITGL
4C11M19      SCTGTSSNIGAGYDIHWYQQLPGTAPKLLIYGNSNRPSGVPDRFSGSKSGTSASLTITGL
4C11M14      SCTGTSSNIGAGYDIHWYQQLPGTAPKLLIYGNSNRPSGVPDRFSGSKSGTSASLTITGL
4C11M6       SCTGTSSNIGAGYDIHWYQQLPGTAPKLLIYGNSNRPSGVPDRFSGSKSGTSASLTITGL
4C11O        SCTGTSSNIGAGYDIHWYQQLPGTAPKLLIYGNSNRPSGVPDRFSGSKSGTSASLTITGL
4C11M5       SCTGTSSNIGAGYDIHWYQQLPGTAPKLLIYGNSNRPSGVPDRFSGSKSGTSASLTITGL
             ************************************************************

4C11M17      QAEDEADYHCQSYDSSLGGFYVFGPGTSVSVLAAAHHHHHHGAAEQKLISEEDLNGAA
4C11M11      QAEDEADYHCQSYDSSLGGFYVFGPGTSVSVLAAAHHHHHHGAAEQKLISEEDLNGAA
4C11M12      QAEDEADYHCQSYDSSLGGFYVFGPGTSVSVLAAAHHHHHHGAAEQKLISEEDLNGAA
4C11M9       QAEDEADYHCQSYDSSLGGFYVFGPGTSVSVLAAAHHHHHHGAAEQKLISEEDLNGAA
4C11M4       QAEDEADYHCQSYDSSLGGFYVFGPGTSVSVLAAAHHHHHHGAAEQKLISEEDLNGAA
4C11M18      QAEDEADYHCQSYDSSLGGFYVFGPGTSVSVLAAAHHHHHHGAAEQKLISEEDLNGAA
4C11M16      QAEDEADYHCQSYDSSLGGFYVFGPGTSVSVLAAAHHHHHHGAAEQKLISEEDLNGAA
4C11M15      QAEDEADYHCQSYDSSLGGFYVFGPGTSVSVLAAAHHHHHHGAAEQKLISEEDLNGAA
4C11M13      QAEDEADYHCQSYDSSLGGFYVFGPGTSVSVLAAAHHHHHHGAAEQKLISEEDLNGAA
4C11M10      QAEDEADYHCQSYDSSLGGFYVFGPGTSVSVLAAAHHHHHHGAAEQKLISEEDLNGAA
4C11M7       QAEDEADYHCQSYDSSLGGFYVFGPGTSVSVLAAAHHHHHHGAAEQKLISEEDLNGAA
4C11M2       QAEDEADYHCQSYDSSLGGFYVFGPGTSVSVLAAAHHHHHHGAAEQKLISEEDLNGAA
4C11M1       QAEDEADYHCQSYDSSLGGFYVFGPGTSVSVLAAAHHHHHHGAAEQKLISEEDLNGAA
4C11M3       QAEDEADYHCQSYDSSLGGFYVFGPGTSVSVLAAAHHHHHHGAAEQKLISEEDLNGAA
4C11M8       QAEDEADYHCQSYDSSLGGFYVFGPGTSVSVLAAAHHHHHHGAAEQKLISEEDLNGAA
4C11M20      QAEDEADYHCQSYDSSLGGFYVFGPGTSVSVLAAAHHHHHHGAAEQKLISEEDLNGAA
4C11M19      QAEDEADYHCQSYDSSLGGFYVFGPGTSVSVLAAAHHHHHHGAAEQKLISEEDLNGAA
4C11M14      QAEDEADYHCQSYDSSLGGFYVFGPGTSVSVLAAAHHHHHHGAAEQKLISEEDLNGAA
4C11M6       QAEDEADYHCQSYDSSLGGFYVFGPGTSVSVLAAAHHHHHHGAAEQKLISEEDLNGAA
4C11O        QAEDEADYHCQSYDSSLGGFYVFGPGTSVSVLAAAHHHHHHGAAEQKLISEEDLNGAA
4C11M5       QAEDEADYHCQSYDSSLGGFYVFGPGTSVSVLAAAHHHHHHGAAEQKLISEEDLNGAA
             ************************************************************
```

Figure 4.7 Sequence alignment of targeted mutagenesis clones. Sequences of 20 clones chosen at random were compared for diversity in the VH CDR3 regions. In bold and underlined are V_H CDR2, V_H CDR3, V_L CDR1, V_L CDR2 and V_L CDR3 in order of appearance. 4C11O is the wildtype 4C11 sequence.

```
4C11M18      MHWVRQAPGKGLEWVSGISGSGGTTSYADSVKGRFTISRDDSKNTLYLQMNSLRAEDTAV
4C11M15      MHWVRLAPGKGLEWVSGISGSGGTTSYADSVKGRFTISRDDSKNTLYLQMNSLRAEDTAV
4C11M7       MHWVRQAPGKGLEWVSGISGSGGTTSYADSVKGRLTISRDDSKNTLYLQMNSLRAEDTAV
4C11M6       MHWVRQAPGKGLEWVSGISGSGGTTSYADSVKGRFTISRDDSKNTLYLQMNSLRAEDTAV
4C11M4       MHWVRQAPGKGLEWVSGISGSGGTTSYADSVKGRFTISRDDSKNTLYLQMNSLRAEDTAV
4C11M3       MHWVRQASGKGLEWVSGISGSGGTTSYADSVKGRFTISRDDSKNTPYLQMNSLRAEDTAV
4C11M1       MHWVRQAPGKGLEWVSGISGSGGTTSYADSVKGRFTISRDDSKNTLYLQMNSLRAEDTAV
4C11M20      MHWVRQAPGKGLEWVSGISGSGGTTSYADSVKGRFTISRDDSKNTLYLQMNSLRAEDMAV
4C11M16      MHWVRQAPGKGLEWVSGISGSGGTTSYADSVKGRFTISRDDSKNTLYLQMNSLRAEDTAV
4C11M11      MHWVRQAPGKGLEWVSGISGSGGTTSYADSVKGRFTISRDDSKNTLYLQMNSLRAEDTAV
4C11O        MHWVRQAPGKGLEWVSGISGSGGTTSYADSVKGRFTISRDDSKNTLYLQMNSLRAEDTAV
4C11M2       MHWVRQAPGKGLEWVSGISGSGGTTSYADSVKGRFTISRDDSKNTLYLQMNSLRAEDTAV
4C11M5       MHWVRQAPGKGLEWVSGISGSGGTTSYADSVKGRFTISRDDSKNTLYLQMNSLRAEDTAV
4C11M8       MHWVRQAPGKGLEWVSGISGSGGTTSYADSVKGRFTISRDDSKNTLYLQMNSLRAEDTAV
4C11M10      MHWVRQAPGKGLEWVSGISGSGGTTSYADSVKGRFTISRDDSKNTLYLQMNSLRAEDTAV
4C11M12      MHWVRQAPGKGLEWVSGISGSGGTTSYADSVKGRFTISRDDSKNTLYLQMNSLRAEDTAV
4C11M13      MHWVRQAPGKGLEWVSGISGSGGTTSYADSVKGRFTISRDDSKNTLYLQMNSLRAEDTAV
4C11M14      MHWVRQAPGKGLEWVSGISGSGGTTSYADSVKGRFTISRDDSKNTLYLQMNSLRAEDTAV
4C11M17      MHWVRQAPGKGLEWVSGISGSGGTTSYADSVKGRFTISRDDSKNTLYLQMNSLRAEDTAV
4C11M19      MHWVRQAPGKGLEWVSGISGSGGTTSYADSVKGRFTISRDDSKNTLYLQMNSLRAEDTAV
4C11M9       MHWVRQAPGKGLEWVSGISGSGGTTSYADSVKGRFTISRDDSKNTLYLQMNSLRAEDTAV
             ***** * *************************:********** *********** **

4C11M18      YYCARDTAMVILDYWGQGTLVTVSSGGGGSGGGGSGGGGSEAVLTQPSSVSGAPGQTVTI
4C11M15      YYCARDTAMVILDYWGQGTLVTVSSGGGGSGGGGSGGGGSEAVLTQPSSVSGAPGQTVTI
4C11M7       YYCARDTAMVILDYWGQGTLVTVSSGGGGSGGGGSGGGGSEAVLTQPSSVSGAPGQTVTI
4C11M6       YYCTRDTAMVILDYWGQGTLVTVSSGGGGSGGGGSGGGGSEAVLTQPSSVSGAPGQTVTI
4C11M4       YYCARDTAMVILDYWGQGTLVTVSSGGGGSGGGGSGGGGSEAVLTQPSSVSGAPGQTVTF
4C11M3       YYCARDTAMVILDYWGQGTLVTVSSGGGGSGGGGSGGGGSEAVLTQPSSVSGAPGQTVTI
4C11M1       YYCARDTAMVILDYWGQDTLVTVSSGGGGSGGGGSGGGGSEAVLTQSSSVSGAPGQTVTI
4C11M20      YYCARDTAMVILDYWGQGTLVTVSSGGGGSGGGGSGGGGSEAVLTQPSSVSGAPGQTVTI
4C11M16      YYCARDTAMVILDYWGQGTLVTVSSGGGGSGGGGSGGGGSEAVLTQPSSVSGAPGQTVTI
4C11M11      YYCARDTAMVILDYWGQGTLVTVSSGGGGSGGGGSGGGGSEAVLTQPSSVSGAPGQTVTI
4C11O        YYCARDTAMVILDYWGQGTLVTVSSGGGGSGGGGSGGGGSEAVLTQPSSVSGAPGQTVTI
4C11M2       YYCARDTAMVILDYWGQGTLVTVSSGGGGSGGGGSGGGGSEAVLTQPSSVSGAPGQTVTI
4C11M5       YYCARDTAMVILDYWGQGTLVTVSSGGGGSGGGGSGGGGSEAVLTQPSSVSGAPGQTVTI
4C11M8       YYCARDTAMVILDYWGQGTLVTVSSGGGGSGGGGSGGGGSEAVLTQPSSVSGAPGQTVTI
4C11M10      YYCARDTAMVILDYWGQGTLVTVSSGGGGSGGGGSGGGGSEAVLTQPSSVSGAPGQTVTI
4C11M12      YYCARDTAMVILDYWGQGTLVTVSSGGGGSGGGGSGGGGSEAVLTQPSSVSGAPGQTVTI
4C11M13      YYCARDTAMVILDYWGQGTLVTVSSGGGGSGGGGSGGGGSEAVLTQPSSVSGAPGQTVTI
4C11M14      YYCARDTAMVILDYWGQGTLVTVSSGGGGSGGGGSGGGGSEAVLTQPSSVSGAPGQTVTI
4C11M17      YYCARDTAMVILDYWGQGTLVTVSSGGGGSGGGGSGGGGSEAVLTQPSSVSGAPGQTVTI
4C11M19      YYCARDTAMVILDYWGQGTLVTVSSGGGGSGGGGSGGGGSEAVLTQPSSVSGAPGQTVTI
4C11M9       YYCARDTAMVILDYWGQGTLVTVSSGGGGSGGGGSGGGGSEAVLTQPSSVSGAPGQTVTI
             ***:************* ************************** ************:
```

```
4C11M18      SCTGTSSNIGAGYDIHWYQQLPGTAPKLLIYGNSNRPSGVPDRFSGSKSGTSASLTITGL
4C11M15      SCTGTSSNIGAGHDIHWYQQLPGTAPKLLIYGNSNRPSGVPDRFSGSKSGTSASLTITGL
4C11M7       SCTGTSSNIGTGYDIHWYQQLPGTAPKLLIYGNSNRPSGVPDRFSGSKSGTSASLTITGL
4C11M6       SCTGTSSNIGAGYDIHWYQQLPGTAPKLLIYGNSNRPSGVPDRFSGSKSGTSASLTITGL
4C11M4       SCTGTSSNIGAGYDIHWYQQLPGTAPKLLIYGNSNRPSGVPDRFSGSKSGTSASLTITGL
4C11M3       SCTGTSSNIGAGYDIHWYQQLPGTAPKLLIYGNSNRPSGVPDRFSGSKSGTSASLTITGL
4C11M1       SCTGTSSNIGAGYDIHWYQQLPGTAPKLLIYGNSNRPSGVPDRFSGSKSGTSASLTITGL
4C11M20      SCTGTSSNIGAGYDIHWYQQLPGTAPKLLIYGNSNRPSGVPDRFSGSKSGTSASLTITGL
4C11M16      SCTGTSSNIGAGYDIHWYQQLPGTAPKLLIYGNSNRPSGVPDRFSGSKSGTSASLTITGL
4C11M11      SCTGTSSNIGAGYDIHWYQQLPGTAPKLLIYGNSNRPSGVPDRFSGSKSGTSASLTITGL
4C11O        SCTGTSSNIGAGYDIHWYQQLPGTAPKLLIYGNSNRPSGVPDRFSGSKSGTSASLTITGL
4C11M2       SCTGTSSNIGAGYDIHWYQQLPGTAPKLLIYGNSNRPSGVPDRFSGSKSGTSASLTITGL
4C11M5       SCTGTSSNIGAGYDIHWYQQLPGTAPKLLIYGNSNRPSGVPDRFSGSKSGTSASLTITGL
4C11M8       SCTGTSSNIGAGYDIHWYQQLPGTAPKLLIYGNSNRPSGVPDRFSGSKSGTSASLTITGL
4C11M10      SCTGTSSNIGAGYDIHWYQQLPGTAPKLLIYGNSNRPSGVPDRFSGSKSGTSASLTITGL
4C11M12      SCTGTSSNIGAGYDIHWYQQLPGTAPKLLIYGNSNRPSGVPDRFSGSKSGTSASLTITGL
4C11M13      SCTGTSSNIGAGYDIHWYQQLPGTAPKLLIYGNSNRPSGVPDRFSGSKSGTSASLTITGL
4C11M14      SCTGTSSNIGAGYDIHWYQQLPGTAPKLLIYGNSNRPSGVPDRFSGSKSGTSASLTITGL
4C11M17      SCTGTSSNIGAGYDIHWYQQLPGTAPKLLIYGNSNRPSGVPDRFSGSKSGTSASLTITGL
4C11M19      SCTGTSSNIGAGYDIHWYQQLPGTAPKLLIYGNSNRPSGVPDRFSGSKSGTSASLTITGL
4C11M9       SCTGTSSNIGAGYDIHWYQQLPGTAPKLLIYGNNNRPSGVPDRFSGSKSGTSASLTITGL
             **********:*:********************.*************************

4C11M18      QAEDEADYHCQSYDSSLGWFFMSSDLVPAVSVLAAAHHHHHHGAAEQKLISEEDLNGAA
4C11M15      QAEDEADYHCQSYDSSLGGFYVFGPGTS-VSVLAAAHHHHHHGAAEQKLISEEDLNGAA
4C11M7       QAEDEADYHCQSYDSSLGGFYVFGPGTS-VSVLAAAHHHHHHGAAEQKLISEEDLNGAA
4C11M6       QAEDEADYHCQSYDSSLGGFYVFGPDTS-VSVLAAAHHHHHHGAAEQKLISEEDLNGAA
4C11M4       QADDEADYHCQSYDSSLGGFYVFGPGTS-VSVLAAAHHHHHHGAAEQKLISEEDLNGAA
4C11M3       QAEDEADYHCQSYDSSLGGFYVFGPGTS-VSVLAAAHHHHHHGAAEQKLISEEDLNGAA
4C11M1       QAEDEADYHCQSYDSSLGGFYVFGPGTS-VSVLAAAHHHHHHGAAEQKLISEEDLNGAA
4C11M20      QAEDEADYHCQSYDSSLGGFYVFGPGTS-VSVLAAAHHHHHHGAAEQKLISEEDLNGAA
4C11M16      QAEDEADYHCQSYDSSLGGFYVVGPGTS-VSVLAAAHHHHHHGAAEQKLISEEDLNGAA
4C11M11      QAEDEADYHCQSYDSSLGGFYVFRPGTS-VSVLAAAHHHHHHGAAEQKLISEEDLNGAA
4C11O        QAEDEADYHCQSYDSSLGGFYVFGPGTS-VSVLAAAHHHHHHGAAEQKLISEEDLNGAA
4C11M2       QAEDEADYHCQSYDSSLGGFYVFGPGTS-VSVLAAAHHHHHHGAAEQKLISEEDLNGAA
4C11M5       QAEDEADYHCQSYDSSLGGFYVFGPGTS-VSVLAAAHHHHHHGAAEQKLISEEDLNGAA
4C11M8       QAEDEADYHCQSYDSSLGGFYVFGPGTS-VSVLAAAHHHHHHGAAEQKLISEEDLNGAA
4C11M10      QAEDEADYHCQSYDSSLGGFYVFGPGTS-VSVLAAAHHHHHHGAAEQKLISEEDLNGAA
4C11M12      QAEDEADYHCQSYDSSLGGFYVFGPGTS-VSVLAAAHHHHHHGAAEQKLISEEDLNGAA
4C11M13      QAEDEADYHCQSYDSSLGGFYVFGPGTS-VSVLAAAHHHHHHGAAEQKLISEEDLNGAA
4C11M14      QAEDEADYHCQSYDSSLGGFYVFGPGTS-VSVLAAAHHHHHHGAAEQKLISEEDLNGAA
4C11M17      QAEDEADYHCQSYDSSLGGFYVFGPGTS-VSVLAAAHHHHHHGAAEQKLISEEDLNGAA
4C11M19      QAEDEADYHCQSYDSSLGGFYVFGPGTS-VSVLAAAHHHHHHGAAEQKLISEEDLNGAA
4C11M9       QAEDEADYHCQSYDSSLGGFYVFGPGTS-VSVLAAAHHHHHHGAAEQKLISEEDLNGAA
             **:*************** *::    .  ******************************
```

Figure 4.8 Sequence alignment of random mutagenesis clones. 20 randomly selected clones had their sequences compared for diversity along the length of the scFv. In bold and underlined are V_H CDR2, V_H CDR3, V_L CDR1, V_L CDR2 and V_L CDR3 in order of appearance. 4C11O is the wildtype 4C11 sequence.

4.3.4 BIOPANNING AND SCREENING OF BINDERS

The targeted mutagenesis phagemid library was rescued by superinfection with M13K07 helper phage. Phage particles were precipitated and enumerated prior to being used for biopanning. A soluble-phase based biopanning strategy which employed biotinylated antigen and streptavidin magnetic beads was used to select binders with an improved equilibrium dissociation constant K_D. Three rounds of biopanning were performed in an effort to enrich binders with an improved K_D. The equilibrium dissociation constant of antibody 4C11 was previously calculated as 5.1×10^{-7} M using surface plasmon resonance. 5.0×10^{-8}M of biotinylated recombinant antigen (ten-fold less than the calculated K_D of antibody 4C11) was displayed on streptavidin magnetic beads for biopanning. The molar concentration of biotinylated recombinant DENV-2 NS1 displayed on magnetic streptavidin beads was decreased ten-fold in subsequent rounds of biopanning; round two used K_D /100 (5.0×10^{-9} M) and the third round used K_D /1000 (5.0×10^{-10} M). The number of phage particles that were used input into each round of biopanning were also decreased ten-fold in each round, initially starting with 10^{12} transducing units. After three rounds of biopanning, a monoclonal phage ELISA was performed using the output of the third round of biopanning (Figure 4.9).

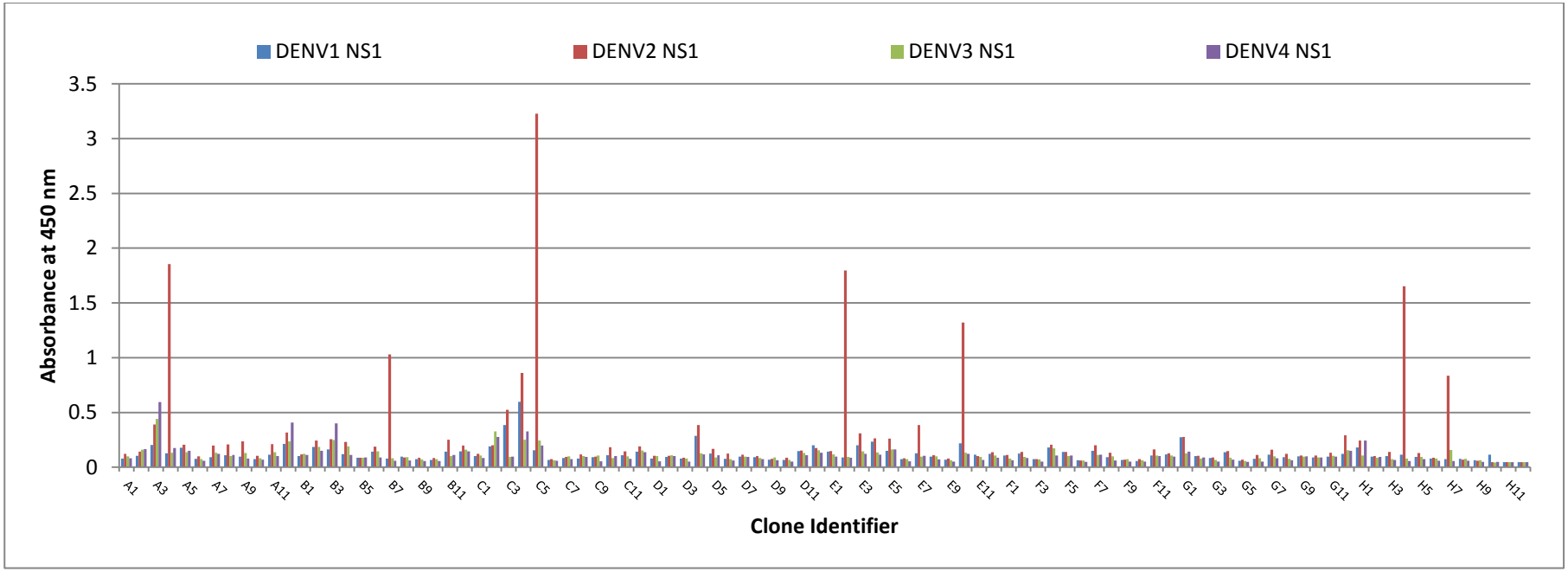

Figure 4.9 Monoclonal phage ELISA of targeted mutagenesis clones. DENV-2 NS1 specific binders were isolated by immobilizing the recombinant antigen on a polystyrene 96 well plate and adding phage particles from 90 randomly chosen clones. Wells H7-H12 had no phage added to them and acted as negative control wells. Bound phage particles were detected using an HRP-conjugated antibody against M13 filamentous phage.

90 clones chosen at random were screened for their ability to recognize recombinant DENV-2 NS1. Eight clones; A4, B7, C5, E2, E7, E10, H4 and H7 were identified as positive binders. Considering that the targeted mutagenesis sub-library was focused on a single parent clone (4C11 scFv) and the biopanning protocol enriches for binders against DENV-2 NS1, it was surprising that the number of target-unrelated clones far exceed the number of target-related clones. The eight isolated clones were sub-cultured and the phage particles propagated from that culture were used in a confirmatory monoclonal phage ELISA (Figure 4.10). All clones except H7 showed binding to DENV-2 NS1. This was expected as H7 acted as a negative control in the initial screening and its previous positive absorbance reading was likely due to some contaminating crossover.

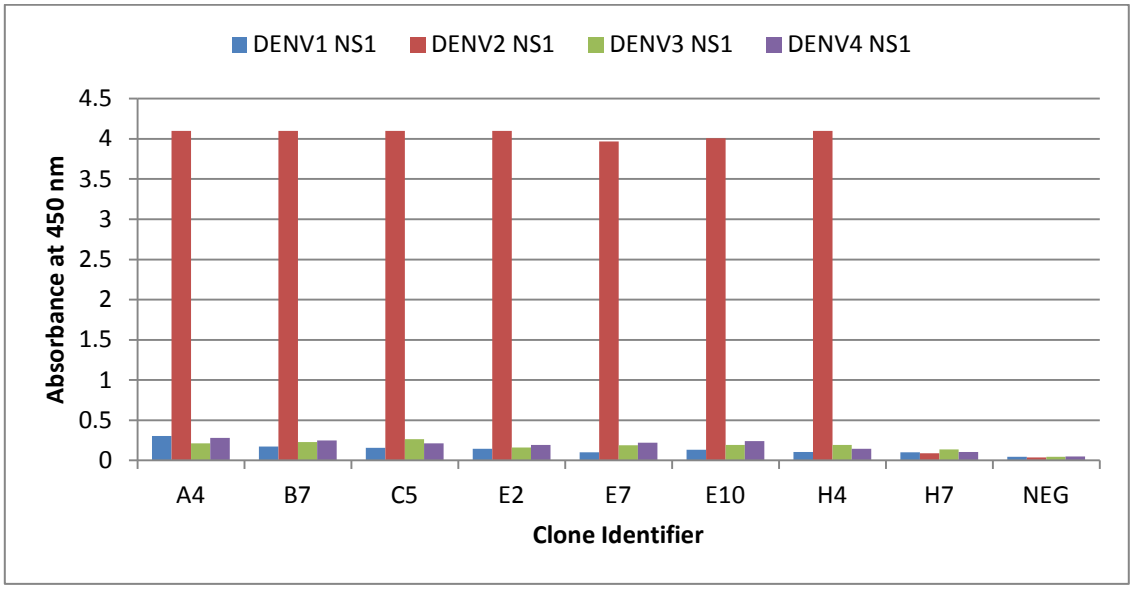

Figure 4.10 Confirmatory monoclonal phage ELISA. To confirm recombinant DENV-2 NS1 recognition, phage particles corresponding to each clone were propagated and added to polystyrene wells coated with recombinant antigen. Binders were detected with HRP-conjugated antibody against M13 filamentous phage.

All seven isolated clones were sequenced to determine their uniqueness (Figure 4.11). Four (B7, E2, E10 and H4) of the seven clones were wild type 4C11 scFv which is representative of the bias of the library towards 4C11 scFv background. The other three clones (A4, C5 and E7) showed some mutations in the targeted V_H CDR3 region on positions with high substitution priority as they are on the hypervariable loop interface

```
E7      YYCARDIGGVILDYWGQGTLVTVSSGGGGSGGGGSGGGGS
A4      YYCARDYGRVILDYWGQGTLVTVSSGGGGSGGGGSGGGGS
4C11    YYCARDTAMVILDYWGQGTLVTVSSGGGGSGGGGSGGGGS
E10     YYCARDTAMVILDYWGQGTLVTVSSGGGGSGGGGSGGGGS
B7      YYCARDTAMVILDYWGQGTLVTVSSGGGGSGGGGSGGGGS
E2      YYCARDTAMVILDYWGQGTLVTVSSGGGGSGGGGSGGGGS
H4      YYCARDTAMVILDYWGQGTLVTVSSGGGGSGGGGSGGGGS
C5      YYCARDTASVILDYWGQGTLVTVSSGGGGSGGGGSGGGGS
```

Figure 4.11. Amino acid sequences of post-selection clones. Clones B7, E2, E10 and H4 have the same V_H CDR3 sequence as the parent clone 4C11 scFv. Clone C5 has a single amino acid change from methionine to serine while clones E7 and A4 have three of the six targeted amino acid residues mutated.

The three isolated scFv clones were reformatted to full IgG1 in order to characterize alterations of the generated antibodies' kinetic profiles in comparison to the parent antibody. The characterization of interaction kinetics was carried out using bio layer interferometry. The net effect of kinetic alterations was subsequently characterized by a limit of detection ELISA to evaluate the effect of kinetic alterations on solid phase capture of recombinant DENV-2 NS1. Because of changes to the assay instrumentation for measuring interaction kinetics from surface plasmon resonance to bio layer interferometry and the change in expression hosts for recombinant DENV-2 NS1 expression from a mammalian expression system in CHO cells to a baculovirus expression system, a comparison of absolute values from previous assays could not be utilised, rather a fold change between the parent antibody and mutant variants was used to establish if there have been any beneficial gains from V_H CDR3 mutagenesis.

4.3.5 KINETICS AND AFFINITY CHARACTERIZATION – BIO LAYER INTERFEROMETRY

Antibodies 4C11, A4, C5 and E7 were captured on anti-human IgG Fc capture biosensors. The antibody-coated biosensors were dipped in separate two-fold dilutions of DENV-2 NS1 from 500 nM to 15.6 nM to determine the kinetics of the interaction between the antibodies the antigen (Figure 4.12). A molar affinity value was calculated and reported in Table 4.2 using dissociation rate constants and association rate constants with responses from concentrations with minimal error values. When compared to parental 4C11 antibody, only A4 antibody showed a slight improvement in affinity due to a marginal improvement in the dissociation rate constant. Although antibody C5 showed a similar binding response as antibody A4, antibody C5 like E7 unfortunately had a reduction in K_D because of an increased off rate (Figure 4.12).

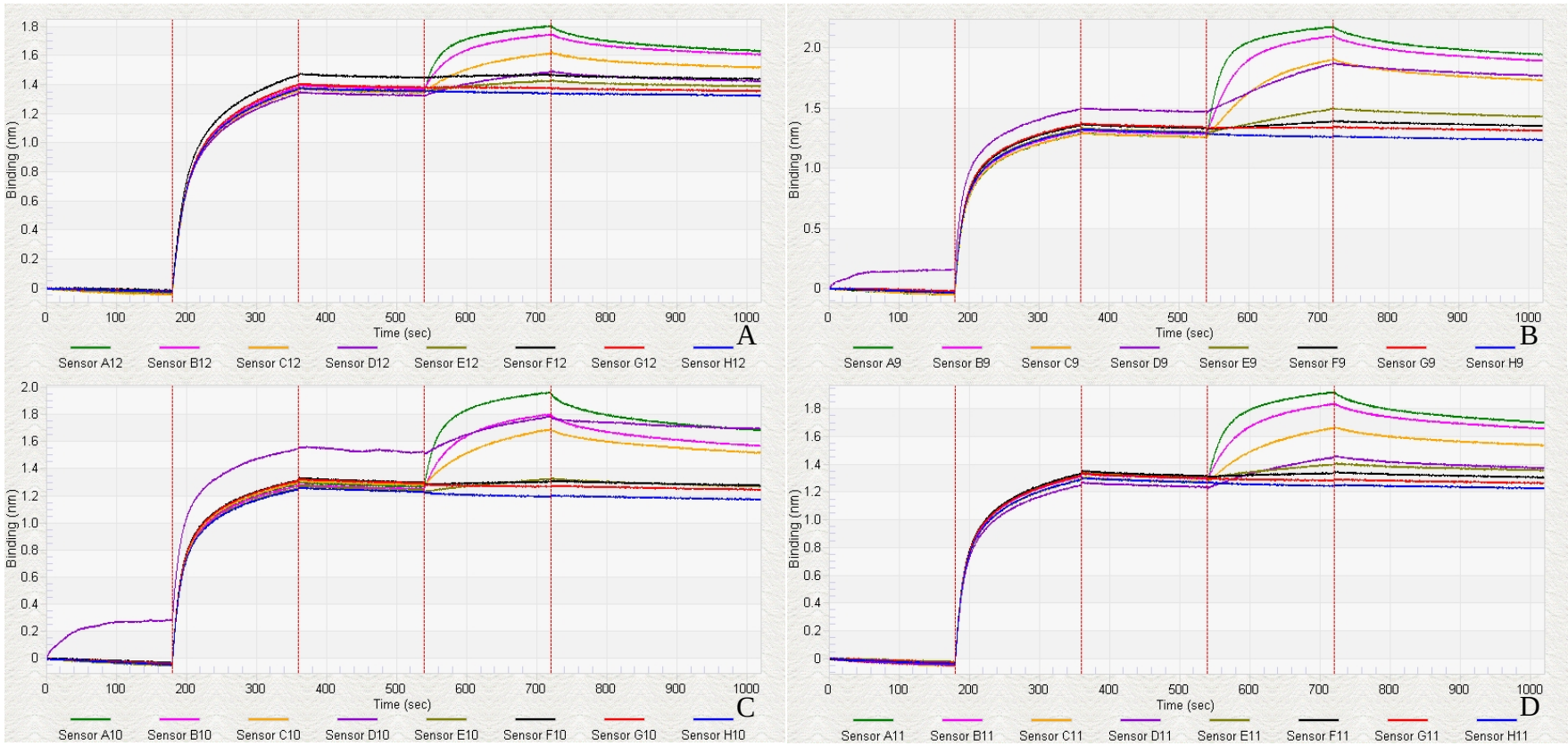

Figure 4.12 BLI sensorgrams for the interaction of antibodies 4C11 (A), A4 (B), C5 (C) and E7 (D) with DENV-2 NS1. Anti-human IgG Fc capture biosensors were coated with antibody in the first association phase (180 seconds -360 seconds). The interaction was allowed to stabilize before the antibody-coated biosensors were dipped in separate two-fold dilutions of DENV-2 NS1 from 500 nM to 15.6 nM. The highest concentration as shown on the x-axis is represented the green trace while the lowest concentration is represented by the blue trace. The response to the different concentrations of DENV-2 NS1 is measured in nm as shown on the y-axis.

Table 4.2 Kinetics and affinities of antibody-antigen interaction. Bio layer interferometry data indicating association rate constants (k_a) [M^{-1} s^{-1}] ± standard error, dissociation rate constants (k_d) [s^{-1}] ± standard error as well as the equilibrium dissociation constants (K_D) kd/ka [M] is shown. Also included is a fold change in K_D relative to the interaction of the parental 4C11 antibody with DENV-2 NS1 (K_D 4C11/ K_D mutant antibody).

Antibody	**K_a ± SE [M^{-1} s^{-1}]**	**K_d ± SE [s^{-1}]**	**K_D [M]**	**Fold change in K_D**
4C11	1.80×10^5 ± 5.30×10^3	9.82×10^{-4} ± 1.35×10^{-5}	9.34×10^{-9}	-
A4	1.08×10^5 ± 2.13×10^3	6.87×10^{-4} ± 8.35×10^{-5}	7.41×10^{-9}	1.26
C5	1.78×10^5 ± 4.20×10^3	1.12×10^{-3} ± 1.54×10^{-5}	1.03×10^{-8}	0.91
E7	2.12×10^5 ± 8.8×10^3	1.25×10^{-3} ± 1.90×10^{-5}	1.06×10^{-8}	0.88

4.3.6 EVALUATION OF ANTIBODY PERFORMANCE IN A DENV-2 NS1 CAPTURE ELISA

To evaluate the performance of recombinant DENV-2 NS1 capture by the isolated binders, reformatted antibodies were used as capture reagents in a limit of detection ELISA. An HRP-conjugated, pan-reactive antibody from a Panbio® Dengue Early ELISA Kit was used as the detection antibody in all instances. When high affinity binders are isolated, an extended attachment to the solid phase capture at low antigen concentration is expected. The results from the limit of detection ELISA (Figure 4.13) vary from those obtained by BLI. In a sandwich ELISA format, the limit of detection of recombinant DENV-2 NS1 using antibodies 4C11, A4, C5 and E7 was 7.5 ng/mL, 3.4 ng/mL, 2.4 ng/mL and 3.3 ng/mL respectively. Parental 4C11 antibody showed the poorest performance while mutant antibodies A4, C5, and E7 showed at least a 2-fold improvement in the amount of recombinant DENV-NS1 that can be accurately detected by absorbance as different from the blank.

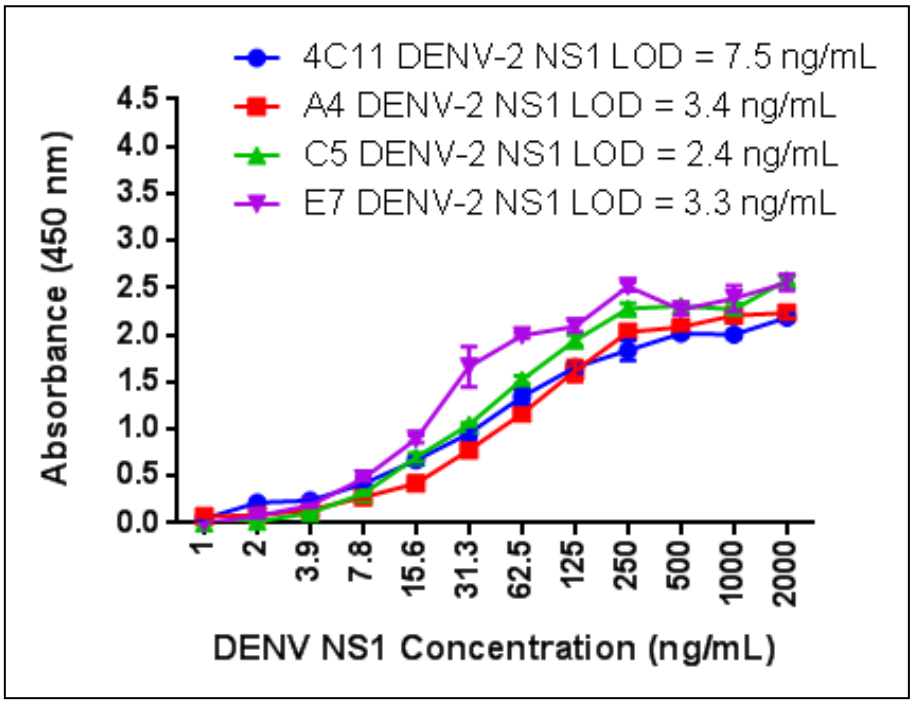

Figure 4.13 Standard curves of recombinant DENV-2 NS1 detection. Antibodies 4C11, A4, C5 and E7 were used to capture dilutions of recombinant DENV-2 NS1. Detection of captured antigen was performed with a pan-reactive, HRP-conjugated antibody from a Panbio® Dengue Early ELISA Kit. Blank subtracted absorbance data indicating the mean ± SD is shown. The cut-off value for the limit of detection was calculated as the mean blank value + 3 x SD of negative readings. The limits of detection of DENV-2 NS1 using 4C11, A4, C5 and E7 antibodies as capture reagents were 7.5 ng/mL, 3.4 ng/mL, 2.4 ng/mL and 3.3 ng/mL respectively.

4.4 DISCUSSION

The combination of phage display technology and mutagenesis in affinity maturation strategies has had considerable success but is also thwarted by pitfalls. Identifying the ideal regions to mutate to attain a significant improvement in affinity is not always straight forward. Furthermore, the creation of a phage display library presenting antibody fragments and its subsequent biopanning has multiple steps that are inherently riddled with opportunity to lose binders with optimal properties.

Ideally, an energetic map of the antibody-antigen binding site is useful in identifying the regions that need to be targeted in the affinity maturation process. Increasingly, in the absence of antibody – antigen structures, computational modeling of protein interfaces is performed to identify the amino acids that would participate in the interaction (6). Antigen structures however, such as in this case, are not always available. A partial x-ray structure of DENV NS1 was only published in February 2014 (1). As such, experimental evolution of antibodies, particularly their antigen binding regions is performed in an effort to improve affinity. Antigen binding residues do not contribute equally to the overall affinity that an antibody has to an antigen. In choosing the amino acid residues to mutate within binding regions, some consideration has to be given to the fact that the greater the number of residues that are mutated the higher the requirement of the construction of a complex library with enormous diversity not adequately feasible with current phage display systems. Generally, six or less codons are targeted when using saturated mutagenesis to allow for confident representation of all mutants in the constructed sub-library (12). Based on this a low complexity sub-library targeting the V_H CDR3 was constructed and used to biopan for binders with gain of affinity mutations. Parallel to the targeted mutagenesis sub-library, a random mutagenesis sub-library generated by an error prone polymerase was also constructed. Random mutagenesis, due to its non-discriminatory nature, results in amino acid substitutions in both the framework and CDR egions. Due to this, isolation of affinity matured binders using this strategy is often fortuitously instead of rationally derived. Unfortunately, the properties introduced by random mutagenesis can also be inadvertently detrimental not only in terms of affinity but stability and solubility as well. Based on these aforementioned factors, a high representation of parental 4C11 scFv in sequenced clones from the random mutagenesis library, and a limitation of available recombinant DENV-2 NS1, the targeted mutagenesis sub-library was selected for biopanning and characterization of isolated binders.

A selection method based on the equilibrium rate constant was chosen to identify higher affinity binders. In this method, the molar concentration of biotinylated antigen equivalent to or less than the equilibrium rate constant is bound to streptavidin coated magnetic beads and then the sub-library of mutants is added to identify binders during iterative rounds of biopanning. The premise is

that higher affinity binders will competitively displace lower affinity binders to the low concentration antigen. Rajpal et al (15) found that this method resulted in moderate improvements in affinity as was also discovered in this work. The use of low antigen concentration favours moderate to high affinity binders but may not necessarily select for lower dissociation rates. Amendments to selection conditions to include more stringent washing steps and longer incubation steps could have been considered to remove binders that have an inadequate dissociation rate. The limitation of recombinant DENV-2 NS1 antigen availability hindered the use of excess molar non-biotinylated antigen in a different strategy which relies on dissociation rate constants. In that method, low concentrations of biotinylated antigen are similarly oriented on streptavidin coated magnetic beads. The sub-library of mutants is again added to allow interaction of binders with the antigen. Excess non-biotinylated antigen is then added, the premise there being that low affinity binders will dissociate and bind to the non-biotinylated antigen which will be discarded during the washing steps. The net result would be higher affinity binders still bound to biotinylated antigen on streptavidin magnetic beads being enriched through the rounds of biopanning.

Three iterative rounds of biopanning yielded seven recombinant DENV-2 NS1 specific binders, from 90 randomly selected clones. This number is proportionally low in view of the fact that the library is based on a parent antibody which binds DENV-2 NS1. The expectation was that there would be a larger number of clones to screen. Since a targeted sub-library focused on DENV-2 NS1 was used in the biopanning procedure, there was no initial concern about biotinylation or the biotin binding pocket on streptavidin diverting selection of binders away from the intended target. It is plausible that non-specific binders to streptavidin or biotin-antigen junctions were isolated and make up some proportion of the 83 clones that do not recognize DENV-2 NS1. A more likely explanation is the low propagation of binders that hinder sufficient phage particles being produced to allow for definitive identification of binders by way of absorbance values that conclusively differ from non-binders.

Three unique binders (A4, C5 and E7) were isolated from the biopanning protocol that relied on the equilibrium dissociation constant to determine the amount of input antigen. The scFv were reformatted to human IgG1 for characterization. In comparison to parental antibody 4C11, antibody A4 showed a 1.26-fold improvement in affinity calculated from BLI kinetics measurements and a 2-fold improvement in antigen capture when used in a detection limit sandwich ELISA. A comparable improvement in antigen capture was seen with antibodies C5 and E7, but these antibodies had decreased affinity due to faster off rates. Antibody A4 had three amino acid substitutions in the targeted V_H CDR3 region from T-A-M to Y-G-R. Similarly antibody E7 had three amino acid substitutions involving a change from residues T-A-M to I-G-G. Antibody C5 meanwhile had a

single amino acid substitution from T-A-M to T-A-S. The inclusion of tyrosine (Y) and glycine (G) in V_H CDR3 in high affinity binders is common and this bias has been shown to be consequent of reading frame 1 of the heavy chain diversity gene segment (17). Glycine residues are known to mediate turns in the CDR loops which can improve antibody-antigen interaction while tyrosine residues have been found to specifically interact with antigen in a non-specific manner assisted by the interaction between the aromatic rings and positively charged residues (13). Charged arginine (R) and non-polar isoleucine (I) residues have limited utility when substituted in CDRs because they lack an ability to establish substantial non-bonded forces required to mediate an interaction with the antigen. Serine (S) on the other hand is ampipathic and has moderate hydrogen potential values that contribute to interaction with antigen in a topology-dependent manner. Summatively, the tyrosine-glycine-arginine substitution resulted in the marginal improvement in affinity of antibody A4.

On reflection, the residues that were mutated were modeled off a paratope which represents a hypothetical structure based on the most closely related existing homologue. As this structure has not been fully validated, the mutagenic changes that are introduced may not be fully maximised. Furthermore, literature has previously focused on V_H CDR3 being the main binding energy contributor in interactions with antigen (18, 23). It has been found however, that where CDR3 of both heavy and light chains are targeted, a greater number of beneficial mutations are identified in the light chain (15). This indicates an *in vivo* propensity for fine tuning in the heavy chain, mediated by VDJ recombination that is lacking in the light chain. Further iterations of this work could perhaps investigate the effect of V_L CDR3 mutagenesis on affinity maturation as it undergoes fewer *in vivo* recombination events. A strategy that involves parallel mutagenesis of heavy and light variable regions and then combining the low complexity libraries has been shown to result in the isolation of high affinity binders (21). In that strategy, identifying and targeting consensus sequences that are known to accumulate mutations on variable regions of antibodies such as A/G-G-C/T-A/T or A-G-C/T (8, 9, 19) could be explored.

The success of affinity maturation strategies can be fortuitous but the design of high quality mutagenesis libraries is also pivotal for improving the odds of isolating binders with improved properties. Furthermore, when opting for targeted mutagenesis, particularly of a single limited region such as V_H CDR3, the original properties of the parent clone and the epitope to which is binds, places constraints on the level of success that can be achieved in terms of fine tuning the interaction between the antibody and the antigenic determinant. In terms of antibody 4C11, this could suggest that the V_H CDR3 residues chosen for mutagenesis are in fact very important to binding, and relatively intolerant to amino acid substitutions. This is supported by the fact that 4

out of the 7 sequences were wildtype even though no wild type clones were detected in 20 randomly sequenced library clones.

Only antibody A4 showed an improvement in comparison to the parental antibody by both BLI characterization and limit of detection ELISA. The improvement in affinity that was attained however lacks a considerable improvement to the dissociation rate. Despite this the improvement is sufficient to stabilize the interaction with DENV-2 NS1 and translate to comparable performance in a serotyping DENV NS1 capture assay using serotype-specific antibodies 9H2 anti DENV-1 NS1, 7G11 anti DENV-3 NS1 and 6A5 anti DENV-4 NS1 which were characterized in Chapter 3. To conclude, this affinity maturation exercise has highlighted the difficulties in truly capturing the nuances associated with sequence and function as well as their subsequent influence in determining affinity.

1. **Akey, D. L., W. C. Brown, S. Dutta, J. Konwerski, J. Jose, T. J. Jurkiw, J. DelProposto, C. M. Ogata, G. Skiniotis, R. J. Kuhn, and J. L. Smith.** 2014. Flavivirus NS1 Structures Reveal Surfaces for Associations with Membranes and the Immune System. Science **343:**881-885.
2. **Alcon, S., A. Talarmin, M. Debruyne, A. Falconar, V. Deubel, and M. Flamand.** 2002. Enzyme-Linked Immunosorbent Assay Specific to Dengue Virus Type 1 Nonstructural Protein NS1 Reveals Circulation of the Antigen in the Blood during the Acute Phase of Disease in Patients Experiencing Primary or Secondary Infections. Journal of Clinical Microbiology **40:**376-381.
3. **Allen, D., A. Cumano, R. Dildrop, C. Kocks, K. Rajewsky, N. Rajewsky, J. Roes, F. Sablitzky, and M. Siekevitz.** 1987. Timing, Genetic Requirements and Functional Consequences of Somatic Hypermutation during B-Cell Development. Immunological Reviews **96:**5-22.
4. **Alt, F., T. Blackwell, and G. Yancopoulos.** 1987. Development of the primary antibody repertoire. Science **238:**1079-1087.
5. **Barderas, R., J. Desmet, P. Timmerman, R. Meloen, and J. I. Casal.** 2008. Affinity Maturation of Antibodies Assisted by in Silico Modeling. Proceedings of the National Academy of Sciences of the United States of America **105:**9029-9034.
6. **Chen, T. S., and A. E. Keating.** 2012. Designing specific protein-protein interactions using computation, experimental library screening, or integrated methods. Protein Sci **21:**949-63.
7. **Chothia, C., and A. M. Lesk.** 1987. Canonical structures for the hypervariable regions of immunoglobulins. J Mol Biol **196:**901-17.
8. **Chowdhury, P. S., and I. Pastan.** 1999. Improving antibody affinity by mimicking somatic hypermutation in vitro. Nat Biotech **17:**568-572.
9. **Goyenechea, B., and C. Milstein.** 1996. Modifying the sequence of an immunoglobulin V-gene alters the resulting pattern of hypermutation. Proc Natl Acad Sci U S A **93:**13979-84.
10. **Jones, M. L., T. Seldon, M. Smede, A. Linville, D. Y. Chin, R. Barnard, S. M. Mahler, D. Munster, D. Hart, P. P. Gray, and T. P. Munro.** 2010. A method for rapid, ligation-independent reformatting of recombinant monoclonal antibodies. J Immunol Methods **354:**85-90.
11. **Lou, J., and J. D. Marks.** 2010. Affinity Maturation by Chain Shuffling and Site Directed Mutagenesis, p. 377-396. *In* R. Kontermann and S. Dübel (ed.), Antibody Engineering. Springer Berlin Heidelberg.

12. **Lowman, H. B., and J. A. Wells.** 1993. Affinity Maturation of Human Growth Hormone by Monovalent Phage Display. Journal of Molecular Biology **234:**564-578.
13. **Mian, I. S., A. R. Bradwell, and A. J. Olson.** 1991. Structure, function and properties of antibody binding sites. J Mol Biol **217:**133-51.
14. **Padlan, E. A., C. Abergel, and J. P. Tipper.** 1995. Identification of specificity-determining residues in antibodies. FASEB J **9:**133-9.
15. **Rajpal, A., N. Beyaz, L. Haber, G. Cappuccilli, H. Yee, R. R. Bhatt, T. Takeuchi, R. A. Lerner, and R. Crea.** 2005. A general method for greatly improving the affinity of antibodies by using combinatorial libraries. Proceedings of the National Academy of Sciences of the United States of America **102:**8466-8471.
16. **Schier, R., A. McCall, G. P. Adams, K. W. Marshall, H. Merritt, M. Yim, R. S. Crawford, L. M. Weiner, C. Marks, and J. D. Marks.** 1996. Isolation of Picomolar Affinity Anti-c-erbB-2 Single-chain Fv by Molecular Evolution of the Complementarity Determining Regions in the Center of the Antibody Binding Site. Journal of Molecular Biology **263:**551-567.
17. **Schroeder, H. W., Jr., M. Zemlin, M. Khass, H. H. Nguyen, and R. L. Schelonka.** 2010. Genetic control of DH reading frame and its effect on B-cell development and antigen-specifc antibody production. Crit Rev Immunol **30:**327-44.
18. **Vandyk, L., and K. Meek.** 1992. Assembly of IgH CDR3: Mechanism, Regulation, and Influence on Antibody Diversity. International Reviews of Immunology **8:**123-133.
19. **Wagner, S. D., C. Milstein, and M. S. Neuberger.** 1995. Codon bias targets mutation. Nature **376:**732.
20. **Wang, F., S. Sen, Y. Zhang, I. Ahmad, X. Zhu, I. A. Wilson, V. V. Smider, T. J. Magliery, and P. G. Schultz.** 2013. Somatic hypermutation maintains antibody thermodynamic stability during affinity maturation. Proceedings of the National Academy of Sciences **110:**4261-4266.
21. **Wang, Y., Z.-y. Keck, A. Saha, J. Xia, F. Conrad, J. Lou, M. Eckart, J. D. Marks, and S. K. H. Foung.** 2011. Affinity Maturation to Improve Human Monoclonal Antibody Neutralization Potency and Breadth against Hepatitis C Virus. Journal of Biological Chemistry **286:**44218-44233.
22. **Wilson, I. A., and R. L. Stanfield.** 1993. Antibody-antigen interactions. Current Opinion in Structural Biology **3:**113-118.
23. **Xu, J. L., and M. M. Davis.** 2000. Diversity in the CDR3 region of V(H) is sufficient for most antibody specificities. Immunity **13:**37-45.

Chapter 5

REFLECTIONS

PROSPECTIVE WORK

AND

CONCLUSIONS

5.1 PROJECT CONTEXTUALIZATION

The project described in this thesis endeavored to improve the specificity and sensitivity of the diagnosis of DENV infections. DENV NS1 was chosen as the antigenic target for diagnosis because of its ability to act as a proxy for the presence of virus (32) and also for its ability to be pre-emptive for the development of severe disease (Dengue Hemorrhagic Fever/Dengue Shock Syndrome) (19). Many commercial antibody-based assays that capture and detect DENV NS1 are available but have consistently been shown to have deficits in specificity and even more so in sensitivity (3, 5, 11, 14, 17, 18, 20, 21, 23, 29, 33). Diminution of specificity is driven by cross-reactivity with NS1 from other flaviviruses which have high homology with DENV NS1. Compromised sensitivity meanwhile, which is mainly seen in secondary infections with DENV, is thought to be due to the formation of immune complexes made up of antibodies that target the immune-dominant epitope on DENV NS1 and DENV NS1 itself (13). The formation of the immune complexes conceivably leads to altered binding of anti-NS1 assay antibodies through steric hindrance and compromises the ability of the assay antibodies to either capture or detect DENV NS1.

Progressive nanoparticle-based assays for the capture DENV NS1 have been reported in recent research literature. One example is an SPR-based assay that detects binding of DENV NS1 to gold nanoparticles that have anti DENV NS1 immobilized to the nanoparticle (8). Another example involves immobilization of antibodies against DENV NS1 onto gold nanoparticles that are coated onto screen-printed electrodes (25). Binding of DENV NS1 to the immobilized antibodies is measured by amperometric responses. Despite these elaborate assays, the inherent deficits of the diagnostic assays unfortunately still remain. We chose to improve DENV diagnostic sensitivity by focusing on the actual immune reagents used in the diagnostic assays. Additionally, a serotyping capability of the DENV NS1 assay would increase its cost-benefit ratio.

5.2 HYPOTHESIS, METHODS & MAIN FINDINGS

We hypothesized that serotype-specific antibodies against DENV NS1 could maintain specificity of detection while pan-reactive binders against non immune-dominant epitopes on DENV NS1 could improve sensitivity of detection. This thesis describes the first study that explicitly explores the use of naive immune repertoires to isolate antibodies against DENV NS1 in an effort to use serotype-specificity to improve DENV diagnostic sensitivity.

To investigate our hypothesis, we interrogated three naive phage libraries displaying human antibody fragments. Different biopanning strategies illustrated in Figure 5.1 were used to isolate binders against DENV NS1.

To isolate serotype-specific binders, a subtractive biopanning strategy was used. This strategy yielded binders against NS1 from each DENV serotype. To isolate pan-reactive binders that recognize non immune-dominant epitopes on DENV NS1, only the strategy that involved the masking of the immune-dominant epitope with an immobilized antibody (tandem binding biopanning) was successful, isolating a single pan-reactive antibody. Unfortunately, pairing of the serotype-specific antibodies against DENV NS1 with the pan-reactive antibody that binds a non immune-dominant epitope on DENV NS1 was unsuccessful because the antibodies did not bind mutually exclusive epitopes on the antigen. Binding of any of the serotype-specific antibodies therefore sterically hindered binding of the pan-reactive antibody and vice-versa, indicating that the epitopes for serotype-specificity are spatially clustered with each other and with the pan-reactive non-immune dominant epitope.

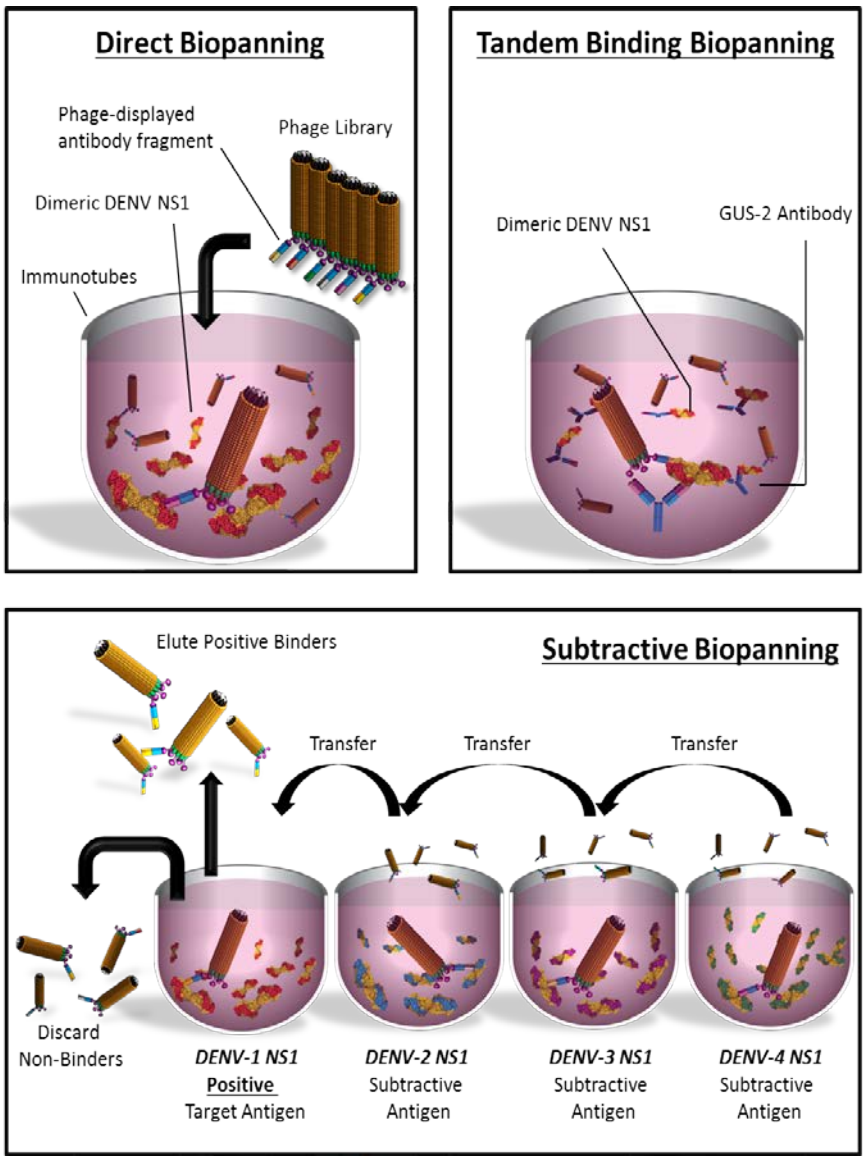

Figure 5.1 Biopanning strategies for isolation of binders against DENV NS1.Antigen that was adsorbed on a polystyrene immunotube was used to isolate pan-reactive binders from a phage-displayed antibody fragment library in a direct biopanning strategy. Pan-reactive binders were also isolated using a tandem-binding biopanning strategy in which polystyrene-immobilized GUS-2 (a pan-reactive antibody against the immune-dominant epitope on DENV NS1) was used to capture the antigen. The captured antigen was exposed to the phage-displayed library to isolate target-specific binders. Serotype-specific binders were isolated using a subtractive biopanning strategy in which adsorbed NS1 from three other DENV serotypes were used as negative controls to deplete binders against high homology regions from the phage-displayed antibody fragment library. The library was finally exposed to the target antigen and the binders were eluted.

Characterisation of serotype-specific antibodies revealed that one of the serotype-specific antibodies, (4C11, which recognizes DENV-2 NS1) had low affinity for its target. Targeted mutagenesis of the V_H CDR3, a region known to influence antibody-antigen interactions, and random mutagenesis of the entire phage-displayed antibody fragment was carried out using nucleotide doping primers and error-prone polymerase respectively. Diffuse mutagenesis along the lengths of the antibody fragments in the random mutagenesis 4C11 sub-library tended to also involve framework regions which should ideally remain conserved. The targeted mutagenesis 4C11 sub-library was therefore the only library taken forward for biopanning for a higher affinity binder. A new single binder, with a single amino-acid substitution from a serine to a methionine was isolated and it showed only a two-fold improvement in affinity. These findings indicated that V_H CDR3 in antibody 4C11 is tolerant of only small changes and these changes do not significantly affect affinity.

5.3 IMPLICATIONS OF FINDINGS & LIMITATIONS OF THE RESEARCH

Our initial hypothesis was that we could increase both the specificity and sensitivity of DENV diagnosis by adding serotyping capability, and by targeting non immune-dominant epitopes on DENV respectively. Unfortunately, we could not accept or reject this hypothesis because the serotype-specific antibodies and the pan-reactive antibody binding a non-immune dominant epitope on DENV NS1 could not simultaneously bind DENV NS1 in a sandwich ELISA. To isolate a pan-reactive antibody against DENV NS1 that can simultaneously bind the serotype-specific antibodies and be unaffected by binding of endogenous antibodies against the immune-dominant epitope of DENV NS1 requires an inventive biopanning strategy. Immobilized serotype-specific antibodies can be used as DENV NS1 capture reagents in a tandem-binding biopanning strategy as shown in Figure 5.1. The fact that the serotype-specific antibodies seem to bind spatially clustered epitopes and orient the NS1 in the same direction gives plausibility that this strategy will be capable of isolating a single pan-reactive antibody. To avoid the immune dominant epitope however, an additional antibody masking this epitope will also need to be used as an immobilized DENV NS1 capture reagent between iterations of serotype-specific driven biopanning. Isolation of an appropriate pan-reactive binder would then allow testing of the hypothesis that serotype-specific antibodies against DENV NS1 when paired with a pan-reactive binder against a non immune-dominant DENV NS1 epitope can improve diagnostic specificity and diagnostic sensitivity of DENV infections. The hypothesis would need to be tested using characterised sera from healthy individuals, individuals with acute primary and secondary DENV infections and individuals with acute and primary and secondary flaviviral infections. The mere conception of such a complex

biopanning strategy underscores the versatility of phage display in condition-controlled antibody discovery.

Isolation of the serotype-specific antibodies is the highlight of the research reported in this thesis. The DENV NS1 serotyping assay that is being proposed has superior attributes compared to competing assays in published literature. A serotyping assay that uses polyclonal human anti-DENV NS1 and serotype-specific phage-displayed scFvs from a human naive library, both targeting virus particles (presumably the E protein of DENV) have been described by Cabezas et al. (6, 7). Ding et al. (10) describe a serotyping assay that incorporates hybridoma-derived, serotype-specific antibodies and a hybridoma-derived pan-reactive antibody against DENV NS1. Meanwhile, Qiu (24) and Xu (31) both from the same group, describe serotyping assays for DENV-1 NS1 and DENV-2 NS1 using hybridoma-derived serotype-specific antibodies and hybridoma-derived pairing antibodies for each serotype-specific antibody. The aforementioned studies are a sampling of the serotyping assays that have been developed. These assays have inherent weaknesses. Targeting the envelope protein reduces the window of DENV diagnosis due to the limited duration of virus detection (16). The immunization-driven strategy for isolation of both serotype-specific and pan-reactive antibodies against DENV NS1 resulted in an expected high specificity but variable sensitivity. Also, using different pairing antibodies for each serotype-specific antibody will invariably lead to a highly complex assay unless the serotyping aspect is abandoned.

Another limitation of this work is that assumptions were made about the regions that were most likely to contribute to the interaction of low affinity antibody 4C11 and DENV-2 NS1. This led to very limited success in improving the affinity of that interaction. Firstly, only V_H CDR3 was targeted for mutagenesis undermining the possible influence of V_λ CDR3 on antibody-antigen interaction. Only one mutant was isolated with a single amino acid change in V_H and this change made only a marginal change in affinity, so changes in V_H seem not to be tolerated; possibly more variants could be isolated by mutagenesis of the light chain. A random mutagenesis library was also created, but the frequency of mutation in framework regions in randomly sequenced clones meant this library was not interrogated further. However, it is possible that high affinity binders to DENV-2 NS1 could have been fortuitously isolated from this library. Biopanning of the 4C11 random mutagenesis library could therefore be undertaken to evaluate if a higher affinity antibody against DENV-2 NS1 can be isolated before new mutagenesis strategies are explored. It would be important however to confirm that random mutagenesis does not shift the current epitope.

5.4 RECOMMENDATIONS FOR FUTURE WORK

The research presented in this thesis opens up exciting possibilities for other associated projects.

A full antibody complement for a serotyping DENV NS1 assay, i.e serotype-specific antibodies and a pairing pan-reactive antibody against a non immune-dominant epitope, would be useful for inclusion in a multiplexed assay for the development of a DENV blood screening assay. Multiplexing using technologies such as lab on chip or Luminex-based platforms can facilitate further improvement of diagnostic sensitivity (ultra-sensitivity) by incorporating assays that detect several markers of DENV infection. A point of consideration however, is the fact that DENV infections are mostly prevalent in countries with developing economies and assays should be restricted to formats that are compatible with currently existing laboratory capabilities.

There is currently no approved vaccine for DENV infections. Phase III trials of a recently successful tetravalent DENV vaccine by Sanofi Pasteur were very encouraging with regard to seroconversion rates to all four DENV serotypes (26). The Envelope protein of DENV is the target of the Sanofi Pasteur vaccine which is made up of a genetically modified recombinant virus vaccine called ChimeriVax Dengue. The vaccine employs the use of the 17D yellow fever vaccine as a scaffold in which Envelope protein genes corresponding to neutralizing determinants of the virion from the yellow fever 17D strain were substituted with those of the dengue virion. Protective immune responses can be elicited from vaccination with DENV NS1 (2). The serotype-specific antibodies that were isolated in this work target conformational epitopes. To evaluate the utility of those epitopes in inducing a protective immune response as a vaccine would involve a laborious undertaking to firstly identify the exact epitopes bound by the antibodies and then manipulate linear polypeptides to form those exact conformations when displayed on a suitable display scaffold. The recently resolved structure of NS1 (1) nonetheless opens up possibilities for more informed epitope mapping research for possible vaccine development.

Diagnostic antibodies do not need to be of human origin, and since serotype-specific antibodies isolated in this work are of human origin, it allows for their possible use in other applications. As an alternative to vaccine development, the use of therapeutic antibodies against DENV NS1 could be explored. Passive immunity can be achieved by inoculation with antibodies against NS1 following a challenge with DENV (28). Mortality-associated DHF is associated with increased levels of NS1 (19) and therefore accumulated levels of NS1 in circulation could be modulated using therapeutic antibodies. Because NS1 is not part of the virion, the effector function of the antibodies would not be in virus neutralization but rather in complement activation or increased phagocytosis to mop up excess NS1. Some antibodies against NS1 that map to the conserved wing peptide on DENV NS1

(22) and the conserved tip of the DENV NS1 β-ladder (9) have been implicated in auto-reactivity with cellular components such as platelets and endothelial cells and therefore have to be avoided as they can actually accelerate disease pathogenesis. It would be interesting to see if antibodies derived from naïve, human antibody fragment libraries would target epitopes that can elicit a therapeutic response.

The mechanisms through which DENV NS1 contributes to disease pathogenesis are not fully elucidated. It has been hypothesized that DENV NS1 contributes to endothelial dysfunction by mimicking lipid metabolic pathways (15). The isolated serotype-specific antibodies could be used as research tools to investigate pathogenesis and the immunological pathways that are inhibited by antibodies against DENV NS1.

In the presence of an appropriate pairing, pan-reactive antibody that binds a non immune-dominant epitope, the serotype-specific antibodies that have been isolated from this work could therefore lend themselves to DENV NS1 quantitation. There have been reports on the possibility of clinically exploiting the correlation of high DENV NS1 levels with the likelihood of severe disease presentation (4, 12, 19, 27). This would be a more DHF/DSS-specific predictive marker than measuring non-specific level of cytokines. Murine research by Watanabe *et al.* (30) however, suggests that presentation with DHF/DSS is dependent on the infective serotype. To conclusively tell if there is an association between high DENV NS1 levels and presentation with DHF/DSS, there is a requirement for the use of standardized monoclonal antibodies with homotypic reactivities in the quantitation assays as opposed to the pooled polyclonal antibodies with heterotypic reactivities which have been used in the cited literature.

5.5 CONCLUSION

To conclude, this thesis investigated the use of naive immune repertoires to isolate antibodies against DENV NS1 in an effort to particularly improve DENV diagnostic sensitivity. We successfully isolated serotype-specific antibodies against DENV NS1 that lend themselves to precise DENV diagnostic specificity. These antibodies are crucial for future iterations of biopanning to isolate pan-reactive, non immune-dominant epitope binders that can improve DENV diagnostic sensitivity. Furthermore we developed biopanning strategies that incorporated combinations of positive and negative biopanning utilizing NS1 derived from the four DENV serotypes. These strategies were designed to probe subtle variations in the three dimensional space/shape relationships of the serotype-specific DENV NS1 surface and this successfully translated to the isolation of antibodies against DENV NS1 with exquisite specificity for each serotype where serotype-specificity was verified by binding to both soluble, recombinant DENV NS1 and DENV NS1 expressed on membranes of DENV infected Vero cells. The techniques and methodologies developed during the course of this research could be applied to antibody isolation against other viruses and virus families, where it may be of value to generate antibodies to common viral subunits with high homology within a viral family.

1. **Akey, D. L., W. C. Brown, S. Dutta, J. Konwerski, J. Jose, T. J. Jurkiw, J. DelProposto, C. M. Ogata, G. Skiniotis, R. J. Kuhn, and J. L. Smith.** 2014. Flavivirus NS1 Structures Reveal Surfaces for Associations with Membranes and the Immune System. Science **343:**881-885.
2. **Amorim, J. H., M. O. Diniz, F. A. Cariri, J. F. Rodrigues, R. S. P. Bizerra, A. J. Gonçalves, A. M. de Barcelos Alves, and L. C. de Souza Ferreira.** 2012. Protective immunity to DENV2 after immunization with a recombinant NS1 protein using a genetically detoxified heat-labile toxin as an adjuvant. VACCINE **30:**837-845.
3. **Aryati, A., H. Trimarsanto, B. Yohan, P. Wardhani, S. Fahri, and R. T. Sasmono.** 2013. Performance of commercial dengue NS1 ELISA and molecular analysis of NS1 gene of dengue viruses obtained during surveillance in Indonesia. BMC Infect Dis **13:**611.
4. **Avirutnan, P., N. Punyadee, S. Noisakran, C. Komoltri, S. Thiemmeca, K. Auethavornanan, A. Jairungsri, R. Kanlaya, N. Tangthawornchaikul, and C. Puttikhunt.** 2006. Vascular leakage in severe dengue virus infections: a potential role for the nonstructural viral protein NS1 and complement. Journal of Infectious Diseases **193:**1078-1088.
5. **Bessoff, K., E. Phoutrides, M. Delorey, L. N. Acosta, and E. Hunsperger.** 2010. Utility of a Commercial Nonstructural Protein 1 Antigen Capture Kit as a Dengue Virus Diagnostic Tool. Clinical and Vaccine Immunology **17:**949-953.
6. **Cabezas, S., G. Rojas, A. Pavon, M. Alvarez, M. Pupo, G. Guillen, and M. G. Guzman.** 2008. Selection of phage-displayed human antibody fragments on Dengue virus particles captured by a monoclonal antibody: Application to the four serotypes. Journal of Virological Methods **147:**235-243.
7. **Cabezas, S., G. Rojas, A. Pavon, L. Bernardo, Y. Castellanos, M. Alvarez, M. Pupo, G. Guillen, and M. Guzman.** 2009. Phage-displayed antibody fragments recognizing dengue 3 and dengue 4 viruses as tools for viral serotyping in sera from infected individuals. Archives of Virology **154:**1035-1045.
8. **Camara, A. R., P. M. P. Gouvêa, A. C. M. S. Dias, A. M. B. Braga, R. F. Dutra, R. E. De Araujo, and I. C. S. Carvalho.** 2013. Dengue immunoassay with an LSPR fiber optic sensor. Optics Express **21:**27023-27031.
9. **Cheng, H.-J., H.-Y. Lei, C.-F. Lin, Y.-H. Luo, S.-W. Wan, H.-S. Liu, T.-M. Yeh, and Y.-S. Lin.** 2009. Anti-dengue virus nonstructural protein 1 antibodies recognize protein

disulfide isomerase on platelets and inhibit platelet aggregation. Molecular immunology **47:**398-406.

10. **Ding, X., D. Hu, Y. Chen, B. Di, J. Jin, Y. Pan, L. Qiu, Y. Wang, K. Wen, M. Wang, and X. Che.** 2011. Full Serotype- and Group-Specific NS1 Capture Enzyme-Linked Immunosorbent Assay for Rapid Differential Diagnosis of Dengue Virus Infection. Clin. Vaccine Immunol. **18:**430-434.
11. **Dussart, P., L. Petit, D. Moua, S. Matheus, B. Labeau, L. Baril, A. Leduc, and L. Bremand.** 2008. Evaluation of Two New Commercial Tests for the Diagnosis of Acute Dengue Virus Infection Using NS1 Antigen Detection in Human Serum. PLoS Neglected Tropical Diseases **2:**e280.
12. **Duyen, H. T., T. V. Ngoc, D. T. Ha, V. T. Hang, N. T. Kieu, P. R. Young, J. J. Farrar, C. P. Simmons, M. Wolbers, and B. A. Wills.** 2011. Kinetics of plasma viremia and soluble nonstructural protein 1 concentrations in dengue: differential effects according to serotype and immune status. Journal of Infectious Diseases**:**jir014.
13. **Falconar, A. K. I.** 2007. Antibody responses are generated to immunodominant ELK/KLE-type motifs on the nonstructural-1 glycoprotein during live dengue virus infections in mice and humans: Implications for diagnosis, pathogenesis, and vaccine design. Clinical and Vaccine Immunology **14:**493-504.
14. **Felix, A. C., C. M. Romano, C. De Campos Centrone, C. L. Rodrigues, L. Villas-Boas, E. S. Araújo, A. M. De Matos, K. I. Carvalho, C. M. T. Martelli, È. G. Kallas, C. S. Pannuti, and J. E. Levi.** 2012. Low sensitivity of NS1 protein tests evidenced during a dengue type 2 virus outbreak in Santos, Brazil, in 2010. Clinical and Vaccine Immunology **19:**1972-1976.
15. **Gutsche, I., F. Coulibaly, J. E. Voss, J. Salmon, J. d'Alayer, M. Ermonval, E. Larquet, P. Charneau, T. Krey, F. Mégret, E. Guittet, F. A. Rey, and M. Flamand.** 2011. Secreted dengue virus nonstructural protein NS1 is an atypical barrel-shaped high-density lipoprotein. Proceedings of the National Academy of Sciences.
16. **Guzman, M. G., S. B. Halstead, H. Artsob, P. Buchy, J. Farrar, D. J. Gubler, E. Hunsperger, A. Kroeger, H. S. Margolis, E. Martinez, M. B. Nathan, J. L. Pelegrino, C. Simmons, S. Yoksan, and R. W. Peeling.** 2010. Dengue: a continuing global threat. Nat Rev Microbiol **8:**S7-16.
17. **Guzman, M. G., T. Jaenisch, R. Gaczkowski, V. T. Ty Hang, S. D. Sekaran, A. Kroeger, S. Vazquez, D. Ruiz, E. Martinez, J. C. Mercado, A. Balmaseda, E. Harris, E. Dimano, P. S. A. Leano, S. Yoksan, E. Villegas, H. Benduzu, I. Villalobos, J. Farrar, and C. P. Simmons.** 2010. Multi-Country Evaluation of the Sensitivity and Specificity of

Two Commercially-Available NS1 ELISA Assays for Dengue Diagnosis. PLoS Negl Trop Dis **4:**e811.

18. **Kumarasamy, V., A. H. Wahab, S. K. Chua, Z. Hassan, Y. K. Chem, M. Mohamad, and K. B. Chua.** 2007. Evaluation of a commercial dengue NS1 antigen-capture ELISA for laboratory diagnosis of acute dengue virus infection. J Virol Methods **140:**75-9.
19. **Libraty, D. H., P. R. Young, D. Pickering, T. P. Endy, S. Kalayanarooj, S. Green, D. W. Vaughn, A. Nisalak, F. A. Ennis, and A. L. Rothman.** 2002. High Circulating Levels of the Dengue Virus Nonstructural Protein NS1 Early in Dengue Illness Correlate with the Development of Dengue Hemorrhagic Fever. Journal of Infectious Diseases **186:**1165-1168.
20. **Lima, M. d. R. Q., R. M. R. Nogueira, A. M. Bispo de Filippis, and F. B. dos Santos.** 2011. Comparison of Two Generations of the Panbio Dengue NS1 Capture Enzyme-Linked Immunosorbent Assay. Clin. Vaccine Immunol. **18:**1031-1033.
21. **Lima, M. d. R. Q., R. M. R. Nogueira, H. G. Schatzmayr, and F. B. d. Santos.** 2010. Comparison of Three Commercially Available Dengue NS1 Antigen Capture Assays for Acute Diagnosis of Dengue in Brazil. PLoS Negl Trop Dis **4:**e738.
22. **Liu, I. J., C. Y. Chiu, Y. C. Chen, and H. C. Wu.** 2011. Molecular mimicry of human endothelial cell antigen by autoantibodies to nonstructural protein 1 of dengue virus. J Biol Chem **286:**9726-36.
23. **McBride, W. J. H.** 2009. Evaluation of dengue NS1 test kits for the diagnosis of dengue fever. Diagnostic Microbiology and Infectious Disease **64:**31-36.
24. **Qiu, L. W., B. Di, K. Wen, X. S. Wang, W. H. Liang, Y. D. Wang, Y. X. Pan, M. Wang, Y. Q. Ding, and X. Y. Che.** 2009. Development of an antigen capture immunoassay based on monoclonal antibodies specific for dengue virus serotype 2 nonstructural protein 1 for early and rapid identification of dengue virus serotype 2 infections. Clin Vaccine Immunol **16:**88-95.
25. **Silva, M. M. S., A. C. M. S. Dias, M. T. Cordeiro, E. Marques, M. O. F. Goulart, and R. F. Dutra.** 2014. A thiophene-modified screen printed electrode for detection of dengue virus NS1 protein. Talanta **128:**505-510.
26. **Sinha, G.** 2014. Sanofi's dengue vaccine first to complete phase 3. Nature Biotechnology **32:**605-606.
27. **Vaughn, D. W., S. Green, S. Kalayanarooj, B. L. Innis, S. Nimmannitya, S. Suntayakorn, T. P. Endy, B. Raengsakulrach, A. L. Rothman, F. A. Ennis, and A. Nisalak.** 2000. Dengue Viremia Titer, Antibody Response Pattern, and Virus Serotype Correlate with Disease Severity. Journal of Infectious Diseases **181:**2-9.

28. **Wan, S.-W., Y.-T. Lu, C.-H. Huang, C.-F. Lin, R. Anderson, H.-S. Liu, T.-M. Yeh, Y.-T. Yen, B. A. Wu-Hsieh, and Y.-S. Lin.** 2014. Protection against Dengue Virus Infection in Mice by Administration of Antibodies against Modified Nonstructural Protein 1. PLoS One **9:**e92495.

29. **Wang, S. M., and S. D. Sekaran.** 2010. Evaluation of a Commercial SD Dengue Virus NS1 Antigen Capture Enzyme-Linked Immunosorbent Assay Kit for Early Diagnosis of Dengue Virus Infection. Journal of Clinical Microbiology **48:**2793-2797.

30. **Watanabe, S., K. H. Tan, A. P. S. Rathore, K. Rozen-Gagnon, W. Shuai, C. Ruedl, and S. G. Vasudevan.** 2012. The Magnitude of Dengue Virus NS1 Protein Secretion Is Strain Dependent and Does Not Correlate with Severe Pathologies in the Mouse Infection Model. Journal of Virology **86:**5508-5514.

31. **Xu, H., B. Di, Y.-x. Pan, L.-w. Qiu, Y.-d. Wang, W. Hao, L.-j. He, K.-y. Yuen, and X.-y. Che.** 2006. Serotype 1-Specific Monoclonal Antibody-Based Antigen Capture Immunoassay for Detection of Circulating Nonstructural Protein NS1: Implications for Early Diagnosis and Serotyping of Dengue Virus Infections. J. Clin. Microbiol. **44:**2872-2878.

32. **Young, P. R., P. A. Hilditch, C. Bletchly, and W. Halloran.** 2000. An Antigen Capture Enzyme-Linked Immunosorbent Assay Reveals High Levels of the Dengue Virus Protein NS1 in the Sera of Infected Patients. J. Clin. Microbiol. **38:**1053-1057.

33. **Zainah, S., A. H. A. Wahab, M. Mariam, M. K. Fauziah, A. H. Khairul, I. Roslina, A. Sairulakhma, S. S. Kadimon, M. S. M. Jais, and K. B. Chua.** 2009. Performance of a commercial rapid dengue NS1 antigen immunochromatography test with reference to dengue NS1 antigen-capture ELISA. Journal of Virological Methods **155:**157-160.